DISCOVERING LINEARMYCINS IN BACTERIAL COMPETITION: LYSIS, AUTOLYSIS, AND RESISTANCE

A Dissertation

by

REED MICHAEL STUBBENDIECK

Submitted to the Office of Graduate and Professional Studies of
Texas A&M University
in partial fulfillment of the requirements for the degree of

DOCTOR OF PHILOSOPHY

Chair of Committee,	Paul Straight
Committee Members,	Jennifer Herman
	Matthew Sachs
	David Threadgill
Interdisciplinary Faculty Chair,	Dorothy Shippen

May 2017

Major Subject: Genetics

ABSTRACT

Throughout history, especially beginning in the mid-twentieth century, humans have adapted numerous specialized metabolites produced by microbes as therapeutics. Since their inception, antibiotics have been a powerful tool used in science and medicine. We have uncovered a great deal about the cellular functions that antibiotics target, mechanisms of resistance, and their application in treating disease. However, there are still gaps in our understanding of the ecological function and roles of specialized metabolites. Additionally, in recent years we've begun to appreciate the importance of microbial communities in diverse environmental settings, including the human microbiome. The structure and maintenance microbial communities resulting from networks of competitive interactions and are driven by many factors including the production and response to antibiotics and other specialized metabolites. Currently, whole microbial communities are not tractable to study. To address fundamental questions relating to the fitness of members in a community I use a model competitive system with two soil bacteria: *Bacillus subtilis* and *Streptomyces* sp. Mg1 (*S.* Mg1).

On an agar surface, colonies of *B. subtilis* lyse and degrade in response to *S.* Mg1 cultured at a distance. In this dissertation, I determined that *B. subtilis* lysis is caused by the family of polyketides known as linearmycins. I obtained mutants of *B. subtilis* that were spontaneously resistant to linearmycins and formed biofilms. Each resistant mutant that I identified had a missense mutation in *yfiJK*, which encodes a previously uncharacterized two-component signaling system. In response to linearmycin exposure, I

found that the YfiJK system activates expression of the *yfiLMN* operon. This operon encodes an ATP-binding cassette transporter that is both necessary and sufficient for both the linearmycin resistance and biofilm formation phenotypes of the *yfiJK* mutants. Finally, I determined that linearmycin biosynthesis and expression of the linearmycin (*lny*) biosynthetic gene cluster are coordinated during *S.* Mg1 growth. In particular, we observe an increase in both linearmycins and extracellular vesicles during stationary phase, suggesting an autolytic origin for linearmycin-laden extracellular vesicles produced by *S.* Mg1. Together, my results demonstrate that coordinated regulation of developmental processes including autolysis, biofilm formation, and motility with specialized metabolism and antibiotic resistance promote competitive fitness of bacteria.

DEDICATION

To my mother, Cheryl, my father, James, and my brother, Aaron. Without each of you, I wouldn't have been able to reach this goal. Thank you for everything.

To Mari Pesek. I miss our conversations about life, science, and spiders. Thank you for the advice, encouragement, and laughter. You were taken from us too soon.

ACKNOWLEDGEMENTS

First and foremost, I want to acknowledge my adviser, Dr. Paul Straight. Thank you for taking the chance on me. Thank you for providing me the environment and guidance to develop as a scientist and as a better human being. Thank you for every chat, experience, and opportunity. Simply put, thank you for everything.

For serving on my dissertation committee and providing insight, I would also like to thank Drs. Tadhg Begley, Jennifer Herman, Matthew Sachs, and David Threadgill. In addition, I would also like to thank Drs. Eileen Hebets and Kasey Fowler-Finn for my first training as a scientist and steering me in the right direction. I'd also like to thank Drs. Eric Malina and Cheryl Bailey for convincing me that I could succeed in science.

I want to acknowledge all the past and present members of the Straight laboratory for their friendship and contributions to my development as a scientist. I want to thank Dr. Chris Hoefler for teaching me everything from molecular biology to natural product isolation and characterization throughout my graduate school career. In particular, I thank Chris for all of his patience, time, and effort. I would also like to thank Dr. Carol Vargas-Bautista for being my senior in the lab and introducing me to *Bacillus* genetics. Further, I thank Carol for her current role as my academic adviser. I want to thank Yongjin Liu and Chengxi Zhang for being my fellow graduate students over the past years and sharing in the experience. I've had the opportunity to work with several

excellent undergraduate students during my time: Roosheel Patel, Yifan Ma, Paolo Giovanelli, and Daniel Labuz. Thank you all.

I want to thank the members of the Genetics Graduate Student and Biochemistry Graduate Student Associations for all the fun and support. In particular, I thank Camille Duran, Erika Downey Slinker, and Ashley and Scott Mattison. You all have been the best of friends to me since we all started together. Thank you for the lifelong friendships.

Finally, I would be remiss if I didn't thank *Bacillus subtilis* and *Streptomyces* sp. Mg1. Though at times our relationship has been tenuous, overall it has been an excellent one. None of the following would have been possible without these wonderful microbes.

CONTRIBUTORS AND FUNDING SOURCES

This work was supervised by a dissertation committee consisting of Professors Paul Straight (adviser) and Jennifer Herman of the Department of Biochemistry & Biophysics, Professor Matthew Sachs of the Department of Biology, and Professor David Threadgill of the Departments of Veterinary Pathobiology and Molecular and Cellular Medicine at Texas A&M University. Professor Tadhg Begley of the Department of Chemistry at Texas A&M University also served as a member of the dissertation committee. All work for the dissertation was completed independently by Reed Stubbendieck.

Support for graduate study was provided by the National Science Foundation (http://nsf.gov/) (NSF-CAREER Award MCB-1253215) to Paul Straight, and the Robert A. Welch Foundation (http://www.welch1.org/) (Grant #A-1796) to Paul Straight. The funders had no role in study design, data collection and analysis, decision to publish, or preparation of this dissertation. The contents of this dissertation are solely the responsibility of the authors and do not necessarily represent the official views of the National Science Foundation or the Robert A. Welch Foundation.

NOMENCLATURE

ABC	ATP-binding cassette
ACN	Acetonitrile
CDI	Contact-dependent inhibition
DMSO	Dimethyl sulfoxide
ECM	Extracellular matrix
EPS	Exopolysaccharide
EV	Extracellular vesicle
HK	Histidine kinase
HPLC	High performance liquid chromatography
LB	Lysogeny broth
LDA	Lytic and degradative activity
LDA^R	LDA resistant
MeOH	Methanol
MPI	Mean pixel intensity
MYM	Maltose-yeast extract-malt extract
NH_4OAc	Ammonium acetate
OME	Outer membrane exchange
RR	Response regulator
SKF	Spore-killing factor
SM	Specialized metabolite
SPE	Solid phase extraction

T6SS	Type VI secretion system

TABLE OF CONTENTS

Page

LIST OF FIGURES

Page

LIST OF TABLES

Page

CHAPTER I

INTRODUCTION AND LITERATURE REVIEW[1]

Summary

Microbial communities span many orders of magnitude ranging in scale from hundreds of cells on a single particle of soil to billions of cells within the lumen of the gastrointestinal tract. Bacterial cells in all habitats are members of densely populated local environments that facilitate competition between neighboring cells. Accordingly, bacteria require dynamic systems to respond to the competitive challenges and the fluctuations in environmental circumstances that tax their fitness. The assemblage of bacteria into communities provides an environment where competitive mechanisms are developed into new strategies for survival. In this chapter, we will highlight a number of mechanisms used by bacteria to compete between species. We focus on recent discoveries that illustrate the dynamic and multifaceted functions used in bacterial competition, and discuss how specific mechanisms provides a foundation for understanding bacterial community development and function.

Introduction

Microbes compete to survive in naturally mixed communities and diverse environments. Microbial communities colonize niches as different as the surface of our

---

[1]Adapted with permission from "Multifaceted Interfaces of Bacterial Competition" by Stubbendieck RM, Straight PD. Copyright ©2016 American Society for Microbiology, [J. Bacteriol. 198:2145-2155. doi: 10.1128/JB.00275-16.]

teeth to the soils beneath our feet. The taxonomic diversity of organisms within these communities is a complex function of differing nutrients, niches, and interactions between species. In general, the abiotic influences on communities are identified through analysis of the chemical, spatial, and other relevant parameters that define local environments. Abiotic factors are varied and influence microbial growth in many ways, but can often be manipulated in the laboratory to understand their influence on microbial communities. The interactions between species, on the other hand, are functions of a particular community and are a greater challenge to identify and resolve. Some broad categorization provides guidelines for outcomes expected during interaction between species. Specifically, when interactions occur between species and are non-neutral, they are at times cooperative, but this appears to be the exception to the rule (1). More commonly, competition between species appears to define the interactions that may predominate in microbial communities.

Competition is categorized into two modes, exploitative and interference (2). Exploitative competition is passive in the sense that one organism depletes its surroundings of nutrients, thereby preventing competitors from gaining access to those resources. In contrast, interference competition invokes antagonistic factors produced to impede competitors (3). In microbial systems, competition is typically framed in the context of growth limitation or inhibition due to exploitation and interference. However, while species may be sensitive or resistant to growth inhibitory activities, they also may engage in antibiotic synthesis, motility, sporulation, predatory functions, and biofilm

formation in response to competition. Though not universal amongst all bacteria, these physiological changes represent the diversity of mechanisms to enhance the competitive fitness of bacterial species equipped with them. The ability of individual species to employ a spectrum of competitive mechanisms and responses to challenges may be essential to their survival in communities of diverse organisms, where competitive stress may take many forms. To better understand the forces that enable bacteria to thrive in communities, we consider numerous competitive functions that determine the relative fitness of different bacteria within a community.

Direct studies on natural communities such as those in soils or plant and animal hosts are notoriously difficult, because they are complex and variable. Also, explanting environmental isolates to the laboratory creates additional complications. For instance, many organisms do not grow under standard laboratory conditions. Recent technological advances such as the iChip (4) enable the growth of many previously uncultured bacteria, but *in situ* manipulation of whole bacterial communities remains challenging. A frequently used approach to study microbial community interactions is to culture two or more species together under defined conditions. By investigating simple microbial communities, culture-based studies can provide powerful mechanistic insights into competitive functions.

In recent years, competition studies between bacteria have contributed to a more informed view of competitive mechanisms used by different species. We focus this

chapter on mechanisms of interference and exploitation competition between species involving specialized metabolites, enzymes, and functions associated with the cell envelope, highlighting interaction outcomes that differ from growth inhibition by classical antibiotics. The cell envelope forms the barrier between a bacterial cell and its surroundings, which include competing bacteria. We will parse different competitive mechanisms into those that occur across the envelope due to exchange of diffusible factors, and those that require contact between cell envelopes, either directly or via their embedded proteins.

Interference and exploitation at a distance

Specialized metabolites

Competition between species is often mediated through bioactive metabolites synthesized by competitors. Specialized metabolites (SMs) are molecules produced by bacteria that are not involved in primary metabolism but are involved in other biological processes. Many specialized metabolites were previously called “secondary” metabolites because their presence is dispensable under laboratory conditions and their production often occurs during late stages of growth (5). However, SMs may be essential for some bacteria to persist in the environment (6) or under competitive stress. In the context of competitive interactions, SMs of primary interest are those affecting the growth and development of competing bacteria. For instance, antibiotics provide some of the clearest mechanistic insights for chemical interactions between competing species of bacteria. However, considering their measurable biological activities at subinhibitory

concentrations, even the empirical roles of antibiotics in nature are subject to debate (7–10). Overall, the biological functions of SMs are numerous and, arguably, largely unknown. We will focus, therefore, on several illuminating examples where bacteria use antibiotics and other SMs in precisely targeted mechanisms that affect competing organisms in ways other than inhibition of growth. The abilities of bacteria to respond dynamically to a range of chemical stresses may have profound effects on their fitness in competitive multi-species communities.

Exploitation competition due to SMs

In some cases, clearly self-serving functions of SMs indirectly lead to exploitation of resources, yielding a competitive advantage. Exploitation competition occurs when one organism disrupts the growth of its competitors by using a shared, limited resource (11). Exploitation often occurs when one bacterial species alters its external environment through their various metabolic functions and prohibits the growth of other bacterial species (3). This exploitation can arise from direct consumption of nutrients, buildup of toxic waste products, or the activity of SMs. An example of SM-mediated exploitation is found in siderophores, which are SMs produced for capture of iron (12). Iron is essential for cytochromes and iron-sulfur proteins, and competition for iron is driven by its availability. Siderophores are one mechanism to chelate external iron, which is then imported as a complex into the producer cells (13). Siderophore production thus increases the bioavailability of iron while simultaneously depleting the supply available to competitors. The significance of iron is underscored by the numerous

examples of siderophore-mediated competition in different environments, including competition for colonization of the light organ in Hawaiian bobtail squid by different strains of *Vibrio fischeri* (14) and between the human opportunistic pathogens *Staphylococcus aureus* and *P. aeruginosa* (15). Bacteria also acquire iron from their environment and engage in exploitation competition by using other iron uptake systems including transporters (16). However, because siderophores are extracellular SMs, they are also subject to piracy by other species, posing a competitive risk to the producing organism (e.g. 17, 18). These examples of siderophores illustrate the potential complexity of specialized metabolites and exploitative interactions that are probably pervasive in nutrient-limited environments.

Interference competition due to SMs

Antibiotic activity without antibiosis

The classic view of antibiotics and other SMs as weapons has guided their isolation and characterization since their discovery. In the process of discovery, antibiotic molecules are isolated from bacterial strains grown in the laboratory and tested for growth inhibition of target organisms (19). This approach has been effective for identifying the majority of antibiotics, but it has left gaps in our understanding of the ecological functions of these molecules. For instance, concentrations of antibiotics sufficient to inhibit growth may be rare in natural environments (20, 21). Do antibiotics at lower than inhibitory concentrations have functions relevant to competitive interactions? This question has inspired investigation into the effects of subinhibitory

concentrations of antibiotics on bacteria, where a wide range of responses has been observed among organisms exposed to different antibiotics. For example, subinhibitory concentrations of jadomycin B cause *Streptomyces coelicolor* to prematurely sporulate and produce a pigmented antibiotic prodigiosin (22), subinhibitory concentrations of kanamycin induce the expression of type VI secretion genes in *Pseudomonas aeruginosa* (23), and numerous other antibiotics induce global transcriptional responses (reviewed in depth, 24). Cellular stresses from subinhibitory antibiotic concentrations may trigger these responses as early warning systems of chemical warfare. Alternatively, the natural functions of some antibiotics and SMs may be reflected in the subinhibitory responses of competitors, independent of inhibitory activity (10). Clearly delineated mechanisms of concentration-dependent activities and responses during competition are needed to understand the roles of antibiotics and other SMs in community dynamics.

Multifunctional metabolites

Bacteria produce many SMs, representing an enormous chemical diversity with poorly understood function (20). Although antibiotic activity is the most common activity ascribed to SMs, many antibiotics also have effects on bacterial competitors that are independent of growth inhibition (see above). There are numerous reports detailing the effects of SMs on the multicellular development of a bacterial species. For example, the soil bacterium *Pseudomonas protogens* produces 2,4-diacetylphloroglucinol, a SM with antifungal activity that is used in biocontrol (25). The cellular differentiation of *B. subtilis* is inhibited by 2,4-diacetylphloroglucinol when cultured with *P. protogens* (26).

In contrast, *B. subtilis* biofilm formation is stimulated by the antifungal nystatin (27) and by peptide antibiotics (28). Bacillaene, is a *B. subtilis* produced SM that was originally identified as an antibiotic inhibitor of protein synthesis (29). Bacillaene also interferes with prodigiosin production in *Streptomyces coelicolor* and *Streptomyces lividans* without inhibiting growth (30, 31).

Another mechanism for SM interference in competitor development is to derail normal signaling processes. For example, some marine bacteria produce SMs that interfere with quorum sensing, and thus disrupt subsequent downstream processes reliant on communication between competitor cells (32, 33). One challenge is to understand the fitness benefits of such modulatory activities in competitive interactions between bacteria. However, in many cases the connection between SMs and the responses they elicit in competitors is unknown. Model systems using two or more bacteria cultured together have been developed to investigate how SMs and other factors influence competitive fitness under controlled settings.

Model systems of SM-mediated competition between species

Multi-species model systems are advantageous because they open the door to the diversity of competitive functions used by a single organism, including production of multiple SMs and different patterns of response to competitor SMs. Soil bacteria provide an illustrative example of diverse competitive functions. Species of *Streptomyces* are ubiquitous in the soil and renowned for their capacity to synthesize SMs (34).

Streptomyces species undergo developmental phases of their lifecycle, including aerial growth and sporulation (35). Sporulation of some streptomycetes depends upon the peptide SapB that acts as a surfactant and lowers surface tension, enabling aerial hyphae to expand upward (36). *Bacillus subtilis* produces its own lipopeptide surfactant, surfactin. *Bacillus subtilis* requires surfactin for biofilm development and some types of motility (27, 37, 38). Intriguingly, surfactin also antagonizes aerial development of many *Streptomyces* species (39, 40). Insight into the mechanism arose from *S. coelicolor*, which when treated with surfactin was unable to process and secrete SapB to support aerial growth (41). When compared to antibiotics that target growth, inhibition of sporulation is a subtle developmental effect that presumably prevents the spread of *Streptomyces*. Although *B. subtilis* does not likely produce multifunctional surfactin explicitly for competition, the inhibition of *Streptomyces* development may enhance competitive fitness in natural environments. Indeed, some species of *Streptomyces* have acquired enzymatic resistance to surfactin, consistent with a natural competitive function. Using imaging mass spectrometry it was demonstrated that *Streptomyces* sp. Mg1 hydrolyzes surfactin (Figure 1A-B) (40). The enzyme, surfactin hydrolase, was shown to specifically inactivate surfactin and plipastatin, another lipopeptide produced by *B. subtilis* (40). Hydrolytic inactivation is a common resistance mechanism for many antibiotics (42). Analogously to the emergence of new β-lactamases, production of surfactin hydrolase and other antibiotic degrading enzymes promotes the competitive fitness of their bacterial producers, although with surfactin the selection is against a developmental process.

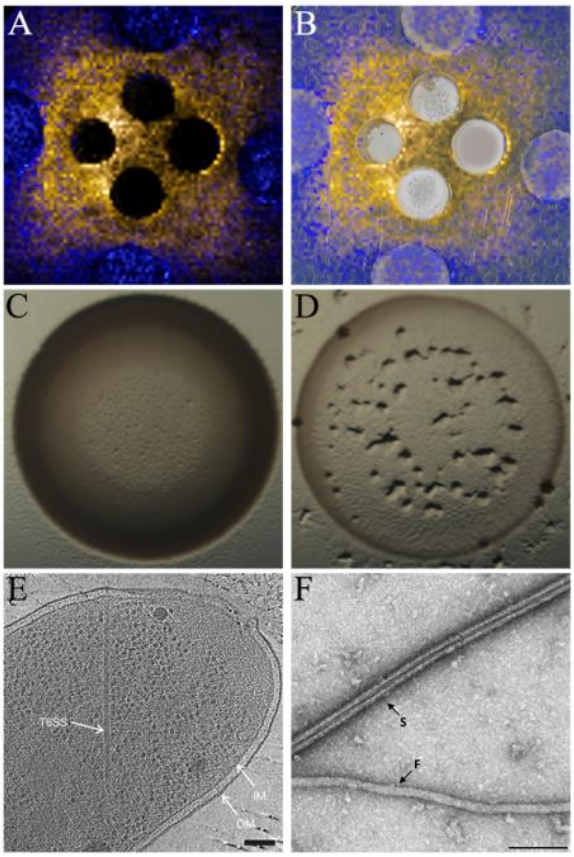

Figure 1. Mechanisms of bacterial competition

(A and B) Detecting patterns of SM production and degradation through imaging mass spectrometry. (A) False-colored extracted ion image showing the distribution of surfactin (orange) produced by *B. subtilis* and hydrolyzed surfactin (blue) caused by hydrolysis of surfactin by surfactin hydrolase produced by *Streptomyces* sp. Mg1. (B) The extracted ion image from (A) overlaid onto a photograph of a culture of *B. subtilis* and *Streptomyces* sp. Mg1 to highlight the localization patterns of each SM during competition. (C and D) Revealing essential SM functions using predator-prey interactions. (C) Photograph of *Myxococcus xanthus* spotted onto the center of a wild-type *B. subtilis* NCIB3610 colony. The colony is opaque due to intact, viable *B. subtilis*. (D) A mutant *B. subtilis* strain deficient in bacillaene production becomes transparent as it is consumed by *M. xanthus*, which forms fruiting bodies on the lysed remains of the *B. subtilis* colony. (E and F) Structural features of a contact-mediated competitive apparatus. (E) Cryo-electron micrographs of a T6SS apparatus inside an intact *Vibrio cholerae* cell. Scale Bar is 100 nm. (F) Comparison of flagellum (F) and T6SS sheath (S) isolated from *V. chloerae*. Scale bar Is 100 nm. Panels C and D were provided by John Kirby. Panels E and F were reproduced from (43) with permission.

Competitive culture models enable us to interpret the functions of SMs in new ways that enhance our view of competition dynamics. Several reports show that SMs provide defense against otherwise overwhelming forces. For instance, laboratory strains of *B. subtilis* are preyed upon by *Myxococcus xanthus,* but the undomesticated *B. subtilis* strain NCIB 3610 is resilient (44). Many domesticated laboratory strains of *B. subtilis* lack a gene, *sfp*, required for production of several SMs, including bacillaene (45, 46). This defect, which renders domesticated *B. subtilis* susceptible to *M. xanthus* predation, was subsequently shown to be specific to the loss of bacillaene production (44) (Figure 1C-D). Indeed, exogenous application of bacillaene protected sensitive strains of *B. subtilis* and *Escherichia coli* from predation. Thus, under the pressure of predation, bacillaene is essential for defense of *B. subtilis*. Intriguingly this is not the only demonstration of a defensive role for bacillaene. Strains of *B. subtilis* deficient in bacillaene production are also hypersensitive to lysis by *S.* Mg1 (47). Bacillaene was originally discovered as an antibiotic inhibitor of protein synthesis, (29) and its function dispensable for growth of *B. subtilis*. However, competition studies expand our view of bacillaene to include essential defensive functions, the precise mechanisms of which are not known. Nevertheless, examples such as bacillaene and surfactin serve to illustrate that SMs provide important competitive functions for the producer organisms.

As seen in examples from antibiotics to siderophores, SMs have varied and sometimes essential functions in competition between species. However, aside from antibiotics, little mechanistic detail is available for the targets and processes affected by

SMs (e.g. 32, 33). The identification of chemically mediated mechanisms of competition will require continued exploration of competitive dynamics between species. An important consideration is how the SMs operate along with other entities that mediate interactions between competing species.

Secreted enzymes

In addition to SMs, bacteria secrete enzymes that participate in competition. Secreted enzymes that confer antibiotic resistance have a clear competitive benefit (40). Additionally, bacteria benefit by interfering with the development of their competitors, e.g. using enzymes to degrade signaling molecules like acyl homoserine lactones (48–51). However, surprisingly little is known about how bacteria use secreted enzymes to kill or inhibit their competitors. The predatory bacteria *M. xanthus* is a prolific producer of degradative enzymes and encodes in its genome more than 300 degradative hydrolytic enzymes (52, 53). The functions of many of these enzymes are unknown, but bacteriolytic activity has been demonstrated for some (54). An example of competitive enzyme function is found where *Staphylococcus epidermidis* competes with *Staphylococcus aureus* for colonization of the human nasal cavity (55). *Staphylococcus epidermidis* secretes a serine protease, Esp, which inhibits *S. aureus* biofilm formation (56). Esp degrades *S. aureus* biofilms by inactivating autolysins and preventing release of DNA that is an essential component of the biofilm extracellular matrix (57). The presence of *Corynebacterium* spp. in the nasal cavity is often inversely correlated with pathogenic *Streptococcus pneumoniae* (58). Like *S. epidermidis*, *Corynebacterium*

accolens also utilizes a secreted enzyme, LipS1, to interfere with a competitor. LipS1 is a triacylglycerol lipase that produces oleic acid from the hydrolysis of a human-produced triglyceride, triolein (59). Oleic acid and other free fatty acids inhibit the growth of *S. pneumoniae* (59, 60). Esp and LipS1 interfere with bacterial competitors but through fundamentally different mechanisms. Thus, secreted enzymes may have many active roles at the cell surface of competitors, although this area is in need of further study.

Extracellular vesicles

Extracellular vesicles are of great interest for both bacterial and eukaryotic interaction processes. Vesicles are capable of vectoring proteins, lipids, nucleic acids, and small molecules that function in competitive and signaling processes (61). Many bacteria produce extracellular vesicles (EVs) during normal growth. The precise mechanisms of EV biogenesis and cargo loading are beginning to be identified. Gram-negative bacteria produce EVs (also called outer membrane vesicles) when the outer membrane is "pinched," and the vesicle buds from the cell surface (62). A second vesicle-release mechanism is reported to occur within biofilms of *P. aeruginosa* (63). In this system, prophage-encoded endolysins activate cellular lysis, releasing membrane fragments that form vesicles and permeate the extracellular space. The problem for Gram-positive bacteria is more complicated due to the lack of an outer membrane, and the mechanism of EV generation is currently unknown, although several models have been hypothesized (64). After formation, EVs are released into the environment. When

an EV encounters a Gram-negative cell the vesicular membrane and the outer membrane fuse, which delivers the cargo into the recipient's periplasm (65). Extracellular vesicles have been observed to adsorb to the cell wall of Gram-positive bacteria, thereby delivering their contents to target cells (65).

Extracellular vesicles are used by bacteria for diverse processes including biofilm formation (66), carbon storage (67), virulence (68), and quorum sensing (69). Bacteria also use EVs for defensive measures against several types of antimicrobial insult. For instance, the EVs of *Prochlorococcus* adsorb phages (67), and EVs from *P. aeruginosa* and *Staphylococcus aureus* protect β-lactamases from proteolytic degradation (70, 71). Though EVs are often characterized for their defensive functions (72), bacteria also use vesicles to deliver antagonistic agents to competing bacteria. These agents can be enzymes, such as the peptidoglycan-degrading hydrolases produced by *P. aeruginosa* (65) and *Lysobacter* sp. XL1 (73), or antibiotic SMs like actinorhodin or prodigiosins found in the EVs produced by *S. coelicolor* (74) and *S. lividans* (75), respectively.

The EVs of *M. xanthus* are of tour de force in regards to their competitive potential. The EVs produced by *M. xanthus* not only contain 29 predicted hydrolytic enzymes (11 of which were not found in the outer membrane) but also 16 specialized metabolites including the myxalamids, which are known antibiotics, and DKxanthene 534 (76). DKxanthene 534 and myxalamids are polyketide and hybrid polyketide-peptide molecules, respectively, both having non-polar hydrocarbon regions. Consistent

with membrane localization, both molecules are typically extracted from cell pellets and have low abundance in supernatants (77, 78). These characteristics highlight an important function of EVs to facilitate transfer of hydrophobic molecules, including antibiotics, across aqueous environments (69).

Extracellular vesicles also intersect with SMs in intriguing patterns that may affect competition between bacteria. Recently, it was shown that *B. subtilis* disrupts its own EVs by secreting surfactin (79). The targeted lysis of EVs by surfactin may serve as a defensive mechanism against antibiotic-laden vesicles produced by competing organisms or as an offensive tool to prevent non-polar signaling molecules, including quorum sensors, from reaching their intended targets. Extending on overlapping functions, bacteria reportedly become reversibly resistant to antibiotics when they swarm (80). In *B. subtilis*, swarming motility requires surfactin (81, 82). As an intriguing hypothesis for niche exploration, *B. subtilis* might produce surfactin not only to promote its movement over surfaces but also as a defense mechanism against EVs produced by other organisms.

Contact-mediated competition

Different species of bacteria physically interact at high cell densities in ways that promote information exchange, such as plasmid conjugation, or through competitive interaction mechanisms. Some competitive functions appear to have evolved to function specifically in close proximity. In particular, bacteria use membrane and cell envelope

embedded functions that are outwardly directed toward competitors. Such mechanisms are likely to be important for survival under crowded conditions through both their inhibitory functions and their contributions to community structure.

Contact-dependent inhibition

As a specific mechanism of interference competition, contact-dependent inhibition (CDI) describes a membrane protein that operates as a delivery system for a cellular toxin. The prototypical CDI system was first described in uropathogenic *E. coli* EC93 and consists of three components: CdiA, CdiB, and CdiI (83). CdiA and CdiB are homologous to the two-partner secretion system proteins TpsA and TpsB, respectively. In two-partner secretion systems, the secreted substrate TpsA is translocated across the outer membrane through its cognate beta-barrel protein TpsB (84). Likewise, in CDI systems the toxin CdiA is attached to CdiB, which is an outer membrane beta-barrel protein that extends away from the cell. This arrangement leads to CDI being referred to as a "toxin on a stick" (85). CdiI provides the producing cell with immunity towards its own toxin by specifically binding to CdiA and inhibiting its activity (86). When a CDI-producing cell (CDI^+) makes direct contact with a susceptible target cell, its CdiA toxin interacts with the outer membrane protein BamA (87). The CdiA protein is then deposited onto the target cell surface and undergoes self-cleavage, which transports the carboxy-terminal (CT) portion of CdiA into the periplasm (88). Many CdiA toxins are nucleases and require entry into the cytoplasm to exert their effects (86). Translocation of the toxin into cytoplasm requires the proton motive force (89) and interaction with

toxin-specific inner membrane protein receptors (90). The requirement for a membrane receptor protein on target cells limits CDI to a narrower range of specificity when compared to diffusible agents like antibiotics. This specificity is due to variability in extracellular loops 6 and 7 of BamA, which form the CdiA-CT-binding site (91). Due to the narrower target range, it has been speculated that CDI systems are a means to inhibit closely related species. This would allow CDI^+ bacteria to inhibit other bacteria that are more likely in direct competition for the same or very similar ecological niches (85).

Biofilms are community structures that form as a result of the concerted effort between many cells. The conditions within a biofilm are inherently stressful to cells. Resources including nutrients, oxygen, and physical space are limiting (92). These conditions breed competition between cells within the biofilm and provide strong selection for competition. For example, growth within a biofilm selects for bacteria that engage in exploitation competition by preferentially occupying biofilm surfaces and gaining access to oxygen (93). Biofilm growth has also selected for cells that are able to engage in inference competition with their neighbors. *Burkholderia thailandensis* illustrates the utility of CDI functions for promoting competitive success in a biofilm. Disruption of the CDI system (CDI^-) of *B. thailandensis* both sensitizes cells to CDI from isogenic siblings and abolishes biofilm formation (94). Both functions are tied to BcpA (homologous to CdiA), but the biofilm functions are independent of CDI activity (95). These observations suggest that CDI systems help to ensure a competitive advantage by supporting biofilm formation while excluding competitors. CDI-dependent

cell adhesion and defects in biofilm production for CDI$^-$ strains have also been reported in *E. coli* (96) and *P. aeruginosa* (97), further solidifying the link between CDI and biofilm development.

Aside from the costs of biofilm formation and the cellular challenges within a biofilm, these structures serve to protect bacteria from various external stresses (98, 99). For instance, bacteria have evolved mechanisms, including CDI, to competitively exclude non-sibling cells from biofilms (100). Developing biofilms contain three-dimensional structures called "pillars" for *B. thailandensis* (101). These structures extend outwards from the biofilm attachment site, providing cells within the pillars better access to oxygen and nutrients than the cells in the biofilm substratum (92). The CDI system of *B. thailandensis* excludes CDI-sensitive cells from developing pillars (101). Cells that produce the same CDI system, presumably siblings, are not killed by CDI due to their cognate immunity genes. This selective killing by CDI provides a kin discrimination mechanism for *B. thailandensis* biofilms and likely protects the biofilm from invaders. Taken together, the CDI functions of *B. thailandensis* demonstrate important competitive advantages that arise in close cellular proximity through direct inhibition of competitors and through construction of defensive biofilm structures.

Type VI secretion systems

The type VI secretion system (T6SS) was originally identified as a virulence factor produced by *V. cholerae* against amoebae and macrophages (102). Subsequently, genes encoding T6SS were found in roughly one-quarter of Proteobacteria with sequenced genomes (103) including, but not limited to, opportunistic pathogens such as *Acinetobacter baumannii* (104) and *Serratia marcescens* (105). The observation that many of the identified T6SS had no apparent effect on eukaryotic cells and that T6SS gene clusters occurred in non-pathogenic bacteria prompted investigation into potential antibacterial activities (105, 106).

The T6SS of Gram-negative bacteria have emerged as a powerful weapon in close-quarters interference competition between bacteria. The basic mechanism of function for T6SS is to inject toxic effector molecules directly into the cytoplasm of target cells. Structurally and functionally the T6SS apparatus is homologous to bacteriophage contractile tails (107). The T6SS apparatus is a cylindrical spiked-tipped inner tube that is surrounded by a sheath and anchored to the inner membrane (Figure 1E-F). When the cell is in physical contact with its target, the sheath contracts, and the inner tube is propelled outward and punctures the membrane of a target cell using its spiked tip. Within the target cell the spike disassociates from the tube and the toxic effectors are delivered. Common effectors characterized thus far include phospholipases (108–110), peptidoglycan hydrolases (111–113), and nucleases (114, 115).

In addition to T6SS being an effective delivery system for toxic payloads, one example demonstrates that the sharpened spike of the T6SS is a potent weapon even in the absence of toxic effectors. Using its TagQRST-PpkA-Fha1-PppA sensing system, *P. aeruginosa* detects cell envelope damage caused by the T6SS of other bacteria (116). This detection or "danger sensing" allows the cell to mount a response against its antagonist and minimize future damage to the cell or its siblings (117). In the case of *P. aeruginosa*, the cell retaliates against T6SS-mediated attacks, directing its own T6SS in the same direction as the initial attack in a behavior called "dueling" (118). Duels damage target cells and can cause membrane blebbing, plasmolysis, and even lysis. Strains of *P. aeruginosa* that are deficient in production of all known T6SS effectors still retaliate against T6S-mediated attacks and engage in dueling with effective killing activity (116). If *P. aeruginosa* cells lose their duels and are lysed by competitors, they release diffusible danger signals that stimulate T6SS activity and promote the survival of siblings (119).

Like CDI, The T6SS killing mechanism also functions to favor siblings in biofilm formation. Strains of *Proteus* sort self from non-self in mobile multicellular swarms. This kin-discrimination is observed as cell-free zones between swarms called Dienes lines (named for their discoverer Louis Dienes) on agar surfaces. In these zones, opposing swarms of *P. mirabilis* do not intermingle. The establishment of Dienes line formation was found to be due to T6SS (120). At the intersection between opposing swarms, *P. mirabilis* use their T6SS to kill, and in turn are killed by T6SS of

competitors, creating a demilitarized zone (DMZ) where the Dienes lines exist between mobile populations. As with *B. thailandensis*, strains join the beneficial swarm when they are not killed by the T6SS. An added benefit of this kin-discrimination arises because swarming provides increased resistance to antibiotics (80). Thus, entry into the swarm promotes competitive fitness of bacteria by excluding unrelated cells and from enhancing defense against antibiotics. Similar boundary formation has also been reported for *M. xanthus* (121) and *B. subtilis* (122). The observation of discrimination in *B. subtilis* demonstrates that CDI and T6SS are not the only mechanisms that bacteria use for kin-discrimination, as *B. subtilis* does not produce CDI or T6SS. The question remains whether *B. subtilis* demarcates Dienes lines through a contact-dependent or –independent mechanism, although evidence suggests combinatorial mechanisms are used (123).

Both the CDI and T6SS are analogous in that a toxin is delivered directly to a target cell. However, like many antibiotics, these toxins are typically soluble molecules. How then, are insoluble effectors delivered? In one case the T6SS toxin Tse6, produced by *P. aeruginosa*, contains transmembrane domains that are shielded from the aqueous environment by an associated chaperone. The chaperone, EagT6, protects Tse6 until delivery into the target's periplasm (124). This example appears to be the exception, where the majority of membrane-associated effectors lack a chaperone or other clear vectoring mechanism. As described previously, extracellular vesicles are another mechanism for delivery of otherwise insoluble cargo.

Outer membrane exchange

In addition to CDI, T6SS, and EVs, Gram-negative bacteria appear to use the outer membrane itself as an effective delivery system for otherwise insoluble toxins. Outer membrane exchange (OME) for *Myxobacteria*, for example, is a contact-dependent mechanism for cells to share membrane components, including phospholipids and insoluble lipoproteins, with other cells (125). OME has been demonstrated to extracellularly complement mutants deficient in production of particular outer membrane products. For example, via OME the gliding motility of non-motile *M. xanthus* mutants is stimulated when mutant cells are mixed with wild type cells (126). OME is also intertwined with colony swarming and sporulation (126). Furthermore, a recent report implicates OME as a powerful defensive mechanism to dilute membrane damage over a population of cells (127).

OME requires the production of an outer membrane protein complex TraAB in both the donor and recipient cell (126). TraAB appears to be the only component necessary to mediate OME (128) and, similarly to the BamA receptor in CDI systems, TraAB contains a polymorphic domain that limits OME to a narrow range of related targets (129). Given the functional similarities to CDI systems and the potential of OME to directly deliver toxic effectors into the envelope of target bacteria, it is not surprising that Myxobacteria use OME to mediate competition and engage in kin recognition. Motile cells of *M. xanthus* are killed when cultured with their non-motile siblings. Killing is dependent upon the presence of TraA in the target motile cell and a polyploid

prophage in the killer non-motile sibling (130). Currently, the effector delivered by OME is not known, but it is likely produced from toxin-antitoxin module encoded on the prophage (130). No further examples of OME-mediated competition have been reported thus far. However, as with EVs, new studies will likely uncover fascinating roles for these membrane-derived strategies in bacterial competition.

Conclusions

Bacteria use competitive mechanisms that are nearly as diverse as the competitors they encounter (Figure 2). Inherent in each competitive strategy are advantages and disadvantages. When bacteria use secreted effectors like antibiotics, enzymes, or vesicles, they are able to compete while minimizing the risks of direct damage during contact-mediated competition. Once a cell exports its competitive molecules across its envelope, those molecules are subject to diffusion, which diminishes their growth inhibitory effect on competitors at a distance. However, many of these metabolically expensive products operate between inactive and inhibitory concentrations and may possibly act as chemical cues for competitors (131). Exposure to subinhibitory antibiotic concentrations can induce resistant states (132–134), select for resistant competitors (135), stimulate biofilm formation (136–138), and motility (139). Activation of a resistant state allows a competitor unrestricted access into a previously protected niche. If potential prey senses a cue and escapes predation, then the producer loses nutrients in the form of that lysed cell. Thus, if a competitor senses a cue, the producer may suffer the consequences for competitive fitness. However it is important to

note that our current understanding of response to subinhibitory concentrations of antibiotics and other SMs in the context of bacterial communities is limited and requires further investigation. The direct delivery of toxins into a target cell by CDI or T6SS circumvents diffusion and the potential costs of subinhibitory antibiotic concentrations. The tradeoff is that contact-mediated competition puts a cell in direct contact with its competitor and allows the risk of retaliation such as in the dueling response (116) or from high concentrations of diffusible SMs.

We have emphasized the differences between competitive mechanisms that are contact-mediated and those that occur at-a-distance. However, bacteria are not mutually exclusive in the systems they employ. For example, *Pseudomonas* species use T6SS but are also prolific producers of SMs including antibiotics and siderophores (140). Bacteria also use direct contact to deliver secreted factors at high local concentration. Predatory *Bdellovibrio* species physically collide with target cells, pierce their cell envelope, and digest their prey from within using an impressive cocktail of secreted enzymes that includes nucleases and peptidoglycan hydrolases (141, 142). The differences between contact-mediated and distance approaches may reflect how bacteria use both systems in competition. A cell producing secreted molecules, like antibiotics, creates a chemical or enzymatic protective shell around itself. Within this shell the cell is also able to

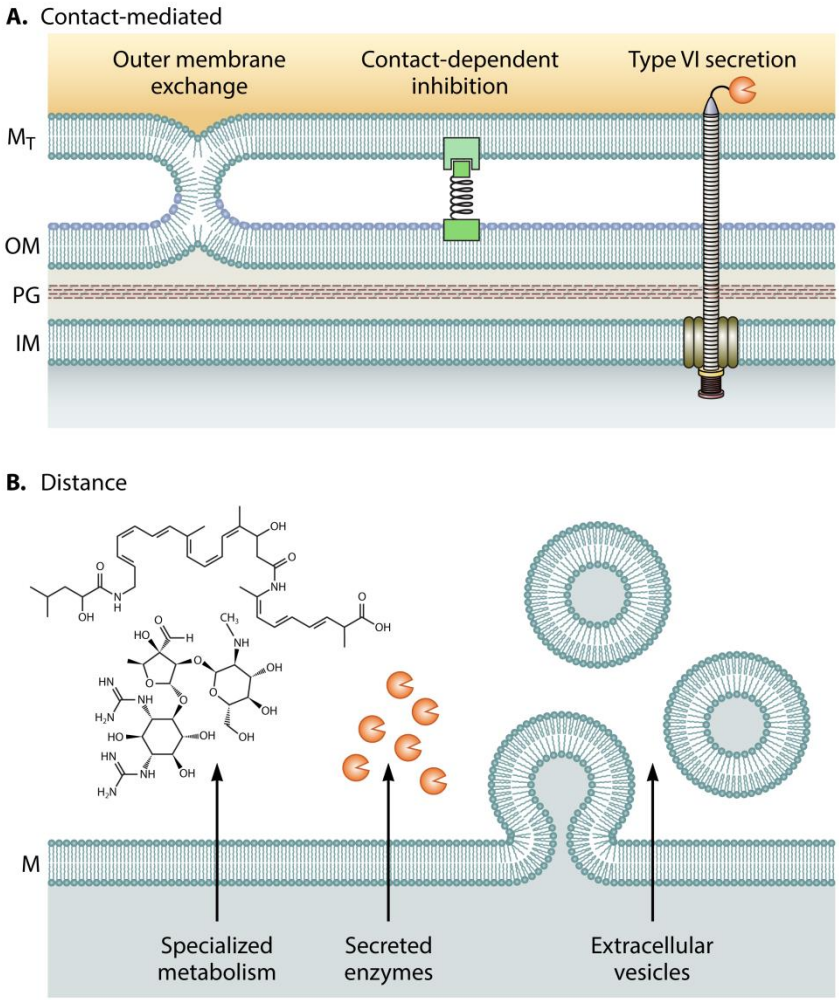

Figure 2. Summary of mechanisms used in bacterial competition

Contact-mediated mechanisms involve either direct contact between cell envelopes (OME) or are facilitated by protein complexes (CDI and T6SS). In the case of CDI and T6SS, toxic effectors (square or Pac-Man) are delivered into the target cell. Bacteria compete at-a-distance using SMs (examples shown are bacillaene and streptomycin), secreted enzymes, and extracellular vesicles. CDI, contact-dependent inhibition; EVs, extracellular vesicles; M, membrane; M_T, target cell membrane; IM, inner membrane; OM, outer membrane; PG, peptidoglycan; T6SS, type VI secretion system.

simultaneously engage in exploitative competition via its exclusive access to nearby nutrients. The spectrum of inhibitory activities, in concert with small size, low charge, and ease of entrance into target cells (143, 144), place antibiotics at the foundation of such protective chemical shells. However, if a competitor breaches the defenses, then the delivery of toxic effectors by CDI or T6SS directly into the target may stop the invasion. A remarkable balance of antibiotic resistance and contact-dependent mechanisms has been shown with *A. baumanii* (145). Several multi-drug resistant *A. baumannii* strains carry a plasmid that provides antibiotic resistance while also inhibiting expression of T6SS systems. However, the plasmid is unstable, and loss of the plasmid provides a mechanism to activate T6SS at the cost of losing antibiotic resistance in some cells. The net result is a population with shared functions in competitive fitness through defense and through close quarters exclusion of competitors. Perhaps contact-mediated mechanisms like CDI, T6SS, or OME are needed to selectively inhibit closely related competitors with the capacity to pass unharmed across a chemical defensive barrier (91, 129, 145).

Culture-based studies have revealed many mechanistic details of bacterial competition. However, we note that many of the studies highlighted in this introduction used simple, small-scale bacterial communities with minimal mixing. To gain a deeper understanding of bacterial competition in natural communities, systems are needed that combine the use of multiple approaches and expanded knowledge of diverse competitive mechanisms. Although beyond the scope of this introduction, mathematical modeling is

a powerful approach to understand how bacterial communities are formed and maintained (e.g. 146, 147). Mathematical approaches stand to become more powerful as they incorporate diverse competitive outcomes in addition to killing or survival. For instance, what effects does T6SS-mediated retaliation have in a modeled competition? How does SM-mediated developmental inhibition affect a community? What are the consequences of exposure for cells outside the inhibitory ranges of SMs? Using controlled experiments in the laboratory, new mechanistic details of competition are being identified, despite limitations to our understanding of these mechanisms in natural environments. The genomes of many antibiotic producing bacteria contain silent SM gene clusters that are not expressed under laboratory conditions (148). Likewise, many studies with CDI and T6SS require artificial expression conditions (149, 150). These obstacles are a central focus of current efforts to understand competitive mechanisms. Meanwhile, models that better mimic the native environment are being developed to provide a clearer view of bacterial interactions under natural conditions (e.g. 86, 115, 151) The examples above and many more innovative studies are expanding our views of the interactive interfaces between two bacterial cells. The emerging challenge is to build these interfaces into networks, which will represent the many facets of competition within microbial communities.

CHAPTER II

ESCAPE FROM LETHAL BACTERIAL COMPETITION THROUGH COUPLED ACTIVATION OF ANTIBIOTIC RESISTANCE AND A MOBILIZED SUBPOPULATION[2]

Summary

Bacteria have diverse mechanisms for competition that include biosynthesis of extracellular enzymes and antibiotic metabolites, as well as changes in community physiology, such as biofilm formation or motility. Considered collectively, networks of competitive functions for any organism determine success or failure in competition. How bacteria integrate different mechanisms to optimize competitive fitness is not well studied. Here we study a model competitive interaction between two soil bacteria: *Bacillus subtilis* and *Streptomyces* sp. Mg1 (*S.* Mg1). On an agar surface, colonies of *B. subtilis* suffer cellular lysis and progressive degradation caused by *S.* Mg1 cultured at a distance. We identify the lytic and degradative activity (LDA) as linearmycins, which are produced by *S.* Mg1 and are sufficient to cause lysis of *B. subtilis.* We obtained *B. subtilis* mutants spontaneously resistant to LDA (LDA^R) that have visibly distinctive morphology and spread across the agar surface. Every LDA^R mutant identified had a missense mutation in *yfiJK*, which encodes a previously uncharacterized two-component

[2]Reprinted from Stubbendieck RM, Straight PD. Escape from Lethal Bacterial Competition through Coupled Activation of Antibiotic Resistance and a Mobilized Subpopulation. PLoS Genet 11(12): e1005722. doi:10.1371/journal.pgen.1005722 under the Creative Commons Attribution License (https://creativecommons.org/licenses/by/4.0/), which permits unrestricted use, distribution, and reproduction in any medium, provided original work is cited. Copyright ©2015 Stubbendieck, Straight.

signaling system. We confirmed that gain-of-function alleles in *yfiJK* cause a combination of LDA^R, changes in colony morphology, and motility. Downstream of *yfiJK* are the *yfiLMN* genes, which encode an ATP-binding cassette transporter. We show that *yfiLMN* genes are necessary for LDA resistance. The developmental phenotypes of LDA^R mutants are genetically separable from LDA resistance, suggesting that the two competitive functions are distinct, but regulated by a single two-component system. Our findings suggest that a subpopulation of *B. subtilis* activate an array of defensive responses to counter lytic stress imposed by competition. Coordinated regulation of development and antibiotic resistance is a streamlined mechanism to promote competitive fitness of bacteria.

Introduction

Bacteria are communal organisms. As such, bacteria have mechanisms to interact with other species that range from cooperative to antagonistic. Antibiotics are a classic example of molecules produced by bacteria that probably function in shaping microbial communities due to their bioactive function, including growth inhibitory and stimulatory activities (3, 5, 152, 153). The study of antibiotics has revealed a great deal about the cellular functions they target, mechanisms of resistance, and uses in treating disease. The traditional approach to discovery of antibiotics typically begins with extraction of metabolites from culture media, followed by direct screening of culture extracts to identify growth inhibitory agents (19). While this approach has had tremendous success for antibiotic discovery, it has left great gaps in our understanding of competitive

dynamics between bacteria. Approaches to bacterial competition that rely on culture of two or more organisms together are emerging as a powerful tool to discover new bioactive molecules and reimagine mechanisms of competition between diverse species of bacteria (154, 155). For instance, microbial competitive functions include secreted enzymes, type VI secretion systems, and specialized metabolism, including developmental signals and antibiotics (152, 153, 156). In addition, changes in community functions such as biofilm formation or motility are recognized increasingly as important competitive strategies for bacteria (80, 157).

Specialized metabolism and developmental functions are common features among soil bacteria, including the actinomycetes, bacilli, and myxobacteria (34, 35, 158–162). In these bacteria, antibiotic production and cellular development are often intertwined and co-regulated processes, which is thought to provide fitness benefits to the organisms (31, 163, 164). For example, during typical development *Streptomyces* species differentiate and develop spores (35). During *Streptomyces* sporulation the substrate mycelium is cannibalized, which is thought to provide the cells with necessary nutrients to complete sporulation (165, 166). Cannibalization of the substrate mycelium is concurrent with production of many antibiotics, which are thought to protect the nutrient resources from opportunistic competitors (167). Use of simple, tractable assays of two or more competing bacteria is one approach to identify new specialized metabolites, enzymes, and bacterial functions that determine the outcomes of competitive interactions. Indeed, interaction assays reveal not only growth inhibitory

metabolites, but also changes in development and colony morphology that expose abundant and poorly understood survival mechanisms for bacteria. Dynamic patterns of interaction based on models of competition are producing new insights into bacterial competitive mechanisms (28, 31, 39, 40, 44, 157, 168).

As a model for competitive interactions, we use different species of *Bacillus* and *Streptomyces*. This competition model has led to identification of new functions for known molecules, including bacillaene and surfactin (31, 39). In the case of surfactin, a secreted hydrolase was identified from *Streptomyces* sp. Mg1 (*S.* Mg1) and shown to be a resistance mechanism that specifically degrades surfactin and plipastatin produced by *Bacillus subtilis* (40). The current study stems from observing colonies of *S.* Mg1 and *B. subtilis* placed side by side on agar media. In this format, cellular lysis occurs along with progressive degradation of the *B. subtilis* colony (47). Previously, imaging mass spectrometry revealed the loss of the polyglutamate component of colony extracellular matrix in the area of lysis, indicating degradation of both cellular and extracellular materials (169, 170). *Streptomyces* sp. Mg1 encodes production of many specialized metabolites with potential to participate in lysis and degradation (171). One gene cluster encodes the biosynthetic enzymes for chalcomycin A, which inhibits the growth of *B. subtilis* but does not cause lysis and colony degradation (47). Here we report both the identification of a lytic degradative activity (LDA) from *S.* Mg1, as well as a mechanism of resistance to LDA for *B. subtilis*. We show that resistant mutants of *B. subtilis* have a complex phenotype, which includes LDA resistance and visible changes in colony

morphology and motility. We show the LDA resistance and the changes in colony morphology and motility are genetically separable functions, all regulated by a two-component system of previously unknown function. Our results indicate that a subpopulation of *B subtilis* cells in a colony trigger a complex mechanism for competitive fitness when challenged by the streptomycete.

Results

Identification of the molecule responsible for LDA

When cultured next to *S.* Mg1, *Bacillus subtilis* colonies are progressively degraded and the underlying cells are lysed (Figure 3A) (47). Progressive degradation of the cells and the extracellular matrix is visible as a translucent patch that develops on a formerly opaque colony (Figure 3A). Our initial interest was to identify causes of lysis and colony degradation. To identify candidate lytic agents, we chose a direct approach to isolate *S.* Mg1 metabolites or enzymes that contribute to the lytic and degradative activity (LDA). Initially, we found active material present in whole plate butanol extracts from *S.* Mg1 grown on agar. To improve yields and decrease complexity of LDA extracts, we cultured *S.* Mg1 in liquid medium in the presence of non-polar HP-20 resin for adsorption of metabolites. Adsorbed metabolites were eluted using methanol to generate the crude extract. *Bacillus subtilis* colonies exposed to the crude extract lysed, indicating the presence of the activity. To isolate the active agent, we fractionated the crude extract, first using a stepwise (10%) methanol gradient followed by time-based HPLC fractionation, and tested for active fractions (see methods section for a detailed

description). The Δ*pksX* strain of *B. subtilis* was used for enhanced sensitivity in these assays, because the mutant is hypersensitive to lysis in co-culture with *S.* Mg1 (47). We isolated a single peak from a HPLC fraction that caused lysis and colony degradation similar to *S.* Mg1 (Figure 3A,C). The similarity between the effects of isolated LDA and a competing *S.* Mg1 colony suggested that lysis and colony degradation of *B. subtilis* may result from the action of a single compound.

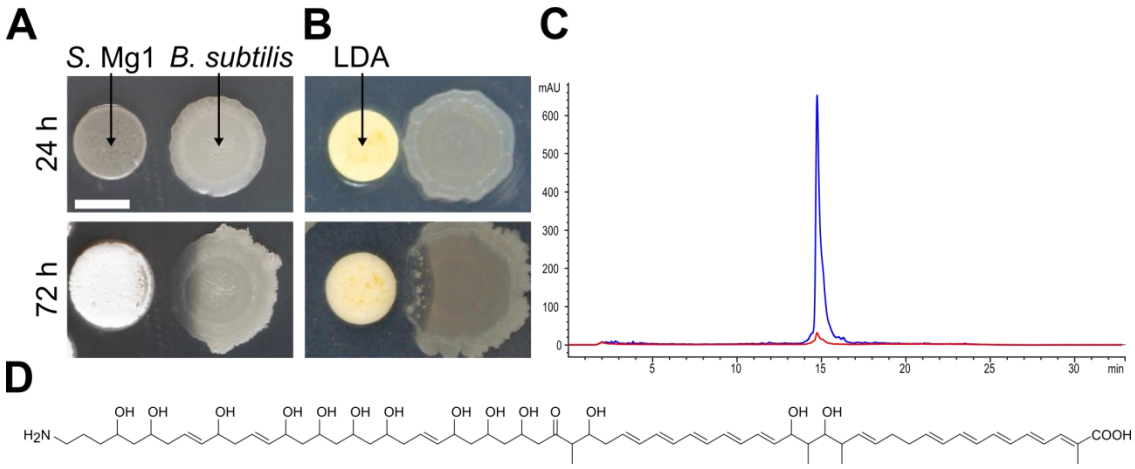

Figure 3. Identification of linearmycin B as the causative agent of LDA

(A) When co-cultured on MYM agar, *S.* Mg1 (left) releases molecule(s) that cause cellular lysis and colony degradation of *B. subtilis* (PDS0067) (right) at a distance. (B) We cultured *B. subtilis* (PDS0067) (right) alone on MYM7 agar for 24 h before adding isolated LDA onto a filter paper disc (left) adjacent to the colony, which subsequently lysed over 48 h similarly to co-culture with *S.* Mg1. (C) HPLC trace of the isolated LDA. The peak is detected by UV absorbance at 333 nm (blue). The background is shown by the 254 nm absorbing trace (red). (D) The structure of linearmycin B. Scale bar is 5 mm.

The linearmycins were originally identified as a pair of compounds, linearmycin A and B (172, 173). We examined the crude extracts and found them to also contain linearmycin A, which is also active for lysis of *B. subtilis* (*m/z* 1140) (Figure A2). Furthermore, the *S.* Mg1 genome (GenBank Accession CP011664) (171) includes a polyketide gene cluster predicted to be responsible for linearmycin biosynthesis. We tested a mutant strain, *S.* Mg1-Δ37, which contains a chromosome truncation that removes the linearmycin biosynthetic cluster, and found the mutant failed to lyse *B. subtilis* or produce linearmycins (Figure A2). In a parallel study, a targeted deletion of the acyl-transferase encoding gene in the linearmycin biosynthetic gene cluster disrupts linearmycin production specifically and blocks all lytic activity from the strain (personal communication, B. Chris Hoefler). Taken together, we conclude that *S.* Mg1 produces linearmycins, which are sufficient for LDA against *B. subtilis*. For simplicity, we collectively refer to these molecules as LDA.

No mechanism is known for either growth inhibition or the lytic effect that we observe with LDA. Linearmycin A was originally shown to inhibit growth of *Escherichia coli* and *Staphylococcus aureus* in addition to three fungal species, but no antibacterial mechanism of action was reported (172). Structurally related polyene antibiotics include antifungal agents such as amphotericin B (174), nystatin (175), and ECO-02301 (176). Amphotericin B and nystatin inhibit fungal growth specifically by interactions with ergosterol and the fungal plasma membrane (177–180). However, bacterial membranes lack ergosterol, suggesting a different mechanism of action against

bacteria for LDA. Nystatin was found to induce biofilm formation by *B. subtilis* grown in LB media (27), demonstrating that antifungal polyenes are biologically active in the absence of ergosterol. The lytic activity of LDA indicates a mechanism of action for the linearmycins that differs from nystatin. In the absence of a known target, we sought an approach to better understand the lysis and degradation of *B. subtilis*.

LDA resistance caused by activation of the YfiJK two-component system

When plated next to extracts of LDA or *S.* Mg1 colonies, small *B. subtilis* colonies emerge in the region of lysis and appear to be resistant to LDA (47). We wanted to identify mechanisms of resistance as an approach to better understand the lytic process caused by LDA (181). Direct comparison of Δ*pks* and wild-type strains of *B. subtilis*, either in culture with *S.* Mg1 or when treated with LDA, showed that the Δ*pks* strain is hypersensitive to lysis but has no other observable phenotype in these assays (47). Therefore as before, we used the Δ*pks* strain of *B. subtilis* for these assays, because the LDA hypersensitivity provided an expanded area of lysis in which we could scan for potential resistant mutants. We challenged colonies of the Δ*pksX* strain of *B. subtilis* with extracts from *S.* Mg1 cultures and observed small colonies appearing in the degraded portion of the parent colony after lysis occurred (e.g. Figure 3B). We isolated 60 small colonies from several lysed colonies and tested them for resistance to LDA in co-culture with *S.* Mg1. The majority of the isolates lysed when cultured again with *S.* Mg1, indicating only transient resistance to LDA. However, ten isolates were stably resistant to LDA (LDA^R), potentially having acquired mutations leading to resistance

(Figure 4A). Notably, all of the stable LDA resistant colonies developed a rough, wrinkled colony morphology that is distinct from the parental strain (Figure 4A). Due to a biofilm-like appearance of the LDA^R colonies, we suspect the mutations have pleiotropic effects on growth mode and development, as well as resistance to LDA.

To identify the mutant alleles in the LDA^R isolates, we sequenced six of the ten mutant genomes and compared the sequences to the parental genome (Δ*pks* strain). Surprisingly, all six isolates had point mutations in either of the two genes in the *yfiJK* operon. In addition, eleven non-overlapping mutations occurred in a subset of the spontaneous LDA^R mutants (Table A2). Three spontaneous LDA^R mutants possessed point mutations only in *yfiJ,* which prompted our focus on the *yfiJK* operon. Using PCR and Sanger sequencing we found that the other four LDA^R isolates also contained point mutations in *yfiJ*. In total, nine of ten mutations were found in *yfiJ* and one in *yfiK* (Figure 4B, Table 1). The *yfiJ* gene encodes a membrane-bound sensor histidine kinase (HK), and the *yfiK* gene encodes its cognate cytoplasmic response regulator (RR) (182). Together these proteins comprise a two-component system (TCS). In a canonical TCS, a HK dimer senses a signal and autophosphorylates on a conserved histidine residue (183). The phosphate is subsequently transferred to the cognate RR, which then effects a response, most commonly through DNA binding and regulation of gene expression (183). In the case of YfiK, the effector domain is a helix-turn-helix domain that likely binds DNA to modulate changes in gene expression (182). A role in LDA resistance is the first indication of a native function for this two-component system.

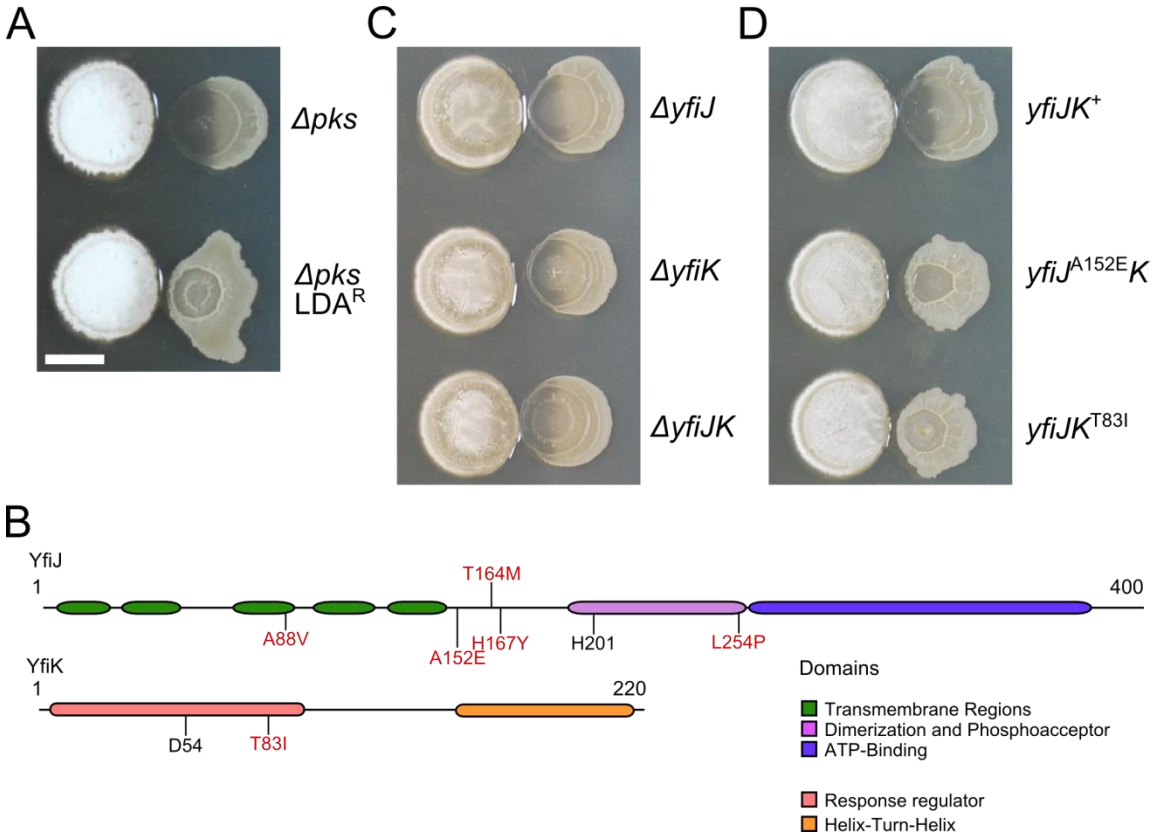

Figure 4. Point mutations in *yfiJK* are responsible for LDA resistance

(A) The parental strain of *B. subtilis*, Δ*pksX* (PDS0067, top), and a representative spontaneous LDA^R mutant (bottom). The colony formed by the parental strain is lysed but the mutant colony remains intact. The spontaneous LDA resistant mutant has a distorted shape and more wrinkled surface than its parental strain. (B) Diagrams of YfiJ and YfiK. The amino acid substitutions identified in spontaneous LDA^R mutants are shown in red. The predicted conserved phosphoacceptor residues are shown in black. (C) Strains of *B. subtilis* deleted for *yfiJ* (PDS0555) or *yfiK* (PDS0556) independently or *yfiJK* together (PDS0554) are lysed in co-culture with *S.* Mg1. (D) We complemented the *yfiJK* deletion strain by inserting at the non-essential *amyE* locus either wild-type *yfiJK* (PDS0627) or alleles identified in spontaneous resistant strains: *yfiJ*^{A152E}*K* (PDS0685) and *yfiJK*^{T83I} (PDS0628). In co-culture with *S.* Mg1, wild-type *yfiJK*$^+$ complement was lysed and degraded, but the strains complemented with LDA^R alleles of *yfiJK* were LDA resistant. The complementation strains reproducibly had a more wrinkled morphology than wild type, similar to the spontaneous LDA^R strain. All cultures place *S.* Mg1 on the left and *B. subtilis* on the right. Photographs were taken after 72 h co-incubation on MYM agar. Scale bar is 5 mm.

Table 1. Alleles of *yfiJK* identified in spontaneous LDA^R mutants

Allele	Nucleotide Change	Number Isolated	LDA Resistance
yfiJ$^+$	n/a	n/a	–
yfiJ^{A88V}	C257T	1	+
yfiJ^{A152E}	C455A	1	+
yfiJ^{T164M}	C491T	1	+
yfiJ^{H167Y}	C499T	6*	+
yfiJ^{L254P}	T761C	1†	+
yfiJK$^+$	n/a	n/a	–
yfiJK^{T83I}	C248T	1	+

Each allele is designated by the amino acid substitution. All numbering is with respect to the first amino acid or the first nucleotide of the start codon. Wild-type alleles are included to indicate LDA sensitivity and designated with a superscript $^+$ symbol. The – symbol indicates LDA sensitivity, and the + symbol indicates LDA resistance in co-culture with *S.* Mg1.
*We isolated C499T from three independent experiments.
†This resistant mutant was isolated from a transposon-mutagenized strain.

To determine whether LDA resistance requires active YfiJK, we deleted *yfiJ* and *yfiK* independently, or *yfiJK* together, in otherwise wild-type genetic backgrounds, and co-cultured these mutants with *S.* Mg1. In all three cases the mutants lysed and were indistinguishable from wild-type *B. subtilis* (Figure 4C). The absence of any observable phenotype for the *yfiJK* deletion mutations suggested that resistance arises from gain-of-function alleles that activate the two-component system. As a test for gain-of-function alleles, we genetically complemented the deletion strains of *yfiJ* or *yfiJK* with PCR-amplified alleles from the spontaneous LDA^R strains. Control strains complemented with native alleles were wild type with respect to lysis and colony morphology (Figure 2D). Conversely, complementation with the mutant alleles caused *B. subtilis* to be resistant to

LDA when cultured with *S.* Mg1, and the mutants developed a more wrinkled colony surface than wild type (Figure 4D, Table 1). Based on these observations, we concluded that each LDA^R allele is likely activating YfiJK to stimulate both abnormal colony development and LDA resistance.

We next investigated how YfiJK may relate to the mechanism of lysis and colony degradation. We considered the results of a previous microarray study to define the regulon of each known RR in *B. subtilis* (184). In that study, overexpression of *yfiK* repressed expression (≥ 4-fold) of 29 different genes, the majority involved in amino acid biosynthesis (184). The reported regulon also includes *skfF*, which encodes the ATP-binding cassette (ABC) transporter necessary for release of spore-killing factor (SKF), and *iseA*, a cell wall-associated protein that inhibits two major autolysins (185–187). We hypothesized that SKF and autolysis might be involved in linearmycin-induced lysis, and that *yfiJK* may regulate the expression of those functions. We tested sensitivity to LDA using four strains of *B. subtilis*. First, we tested a strain unable to produce SKF (Δ*skfA-H*) to determine if the cannibalism peptide functions as a lytic agent. Second, we tested whether a strain deficient in *iseA* would show enhanced lysis in the absence of an autolysin inhibitor. Third, because *iseA* regulates autolysins, we tested whether a strain deficient in production of three major autolysins (Δ*lytABC* Δ*lytD* Δ*lytF*) may show diminished lysis when exposed to LDA. Fourth, we tested a strain with a deletion of the major motility/autolysin regulator (Δ*sigD*) (188). All four strains lysed when cultured with *S.* Mg1, indicating that SKF and autolysis do not likely contribute to the lysis

mechanism (Figure A3). In a parallel approach, we used transposon mutagenesis to identify genes in *B. subtilis* that may cause lysis under linearmycin-induced stress. We obtained a single, stable LDA^R mutant, however LDA resistance was unlinked to the site of transposon insertion in this strain. We sequenced the mutant genome and identified an additional point mutation in *yfiJ* ($yfiJ^{L254P}$) (Table 1). Thus, using multiple approaches to identify functions conferring LDA resistance, we have found only apparent gain-of-function alleles in *yfiJK*.

LDA resistance requires YfiJK with active phosphotransfer function

Two-component signaling systems require conserved phosphoacceptor residues for activation and downstream signaling (183). We identified the phosphoacceptor histidine (H201) in YfiJ and the phosphoacceptor aspartate (D54) in YfiK using multiple sequence alignment to experimentally characterized TCS. Using site-directed mutagenesis we disrupted the phosphoacceptor residues and created the new alleles $yfiJ^{H201N}$ and $yfiK^{D54A}$. As anticipated based on the Δ*yfiJK* phenotype, both phosphoacceptor mutants were sensitive to LDA when cultured with *S.* Mg1 (Table 2). Next, we constructed new alleles that combined the phosphoacceptor disruptions with substitutions found in LDA^R alleles to generate the new, double mutant alleles $yfiJ^{A152E,\ H201N}$ and $yfiK^{D54A,\ T83I}$. When cultured with *S.* Mg1 these mutant strains lysed, which confirmed the disruption of the gain-of-function LDA^R phenotype in the absence of functional a TCS (Table 2). As a final test that LDA resistance results from specific downstream signaling of YfiJK, we constructed a pair of double mutants: (*i*) combining

the LDA^{R} allele *yfiJ*^{A152E} with the phosphoacceptor disruption *yfiK*^{D54A} and (*ii*) combining the phosphoacceptor disruption *yfiJ*^{H201N} with the LDA^{R} allele *yfiK*^{T83I}. When these strains were cultured with *S.* Mg1 they were sensitive to LDA (Table 2). These results suggest that LDA resistance is due to specific downstream signaling of YfiJK, leading us to conclude that LDA resistance is due specifically to activation of the TCS.

LDA^{R} alleles show specificity for linear polyene metabolites

Amphotericin B and nystatin are cyclic polyene antifungals (174, 175). The structurally related linear polyene, linearmycin A, is also antifungal but has also been shown to have antibacterial activity as well (172). We tested amphotericin B, nystatin, and ECO-02301, a polyene structurally related to the linearmycins (176), for activity against *B. subtilis*.

Table 2. LDA resistance requires phosphoacceptor residues

Allele	LDA Resistance
yfiJ^{A152E}	+
yfiJ^{H201N}	–
yfiJ$^{A152E, H201N}$	–
yfiJK^{T83I}	+
yfiJK^{D54A}	–
yfiJK$^{D54A, T83I}$	–
yfiJ^{A152E}*K*^{D54A}	–
yfiJ^{H201N}*K*^{T83I}	–

The conserved phosphoacceptor residues in YfiJ (H201) and YfiK (D54) were mutated to non-phosphorylatable residues. The + symbol indicates LDA resistance in co-culture with *S.* Mg1. The – symbol indicates LDA sensitivity. All numbering is relative to the first amino acid of the YfiJ and YfiK proteins.

ECO-02301 caused lysis similar to linearmycins, but the macrocyclic polyenes amphotericin B and nystatin were not lytic (Figure 5). When tested against purified ECO-02301, the LDA^{R} mutant (*yfiJ*^{A152E}) strain appeared to be partially resistant in this assay (Figure 5). We next sought a quantitative measure of the difference between LDA resistance and sensitivity to LDA and ECO-02301. First, we measured the minimum lytic concentration (MLC) for ECO-02301 using a quantitative agar diffusion assay and determined that a LDA^{R} strain of *B. subtilis* was 3.65-fold more resistant to ECO-02301 (Table 3). We applied the same assay to LDA, containing both linearmycin A and B, isolated from *S.* Mg1 cultures and quantified the fold difference in resistance between LDA^{R} and wild-type *B. subtilis*. The LDA^{R} mutant was nearly ten-fold more resistant to LDA compared to the sensitive strain (Table 3). The difference in relative resistance to ECO-02301 and LDA may be in part due to structural differences in the molecules. The synthesis of ECO-02301 includes tailoring reactions that glycosylate the polyketide backbone and condense an amidohydroxycyclopentenone moiety onto the terminal carboxylic acid group (176, 189). The structural differences may affect target affinity, solubility, or other properties of the molecule, leading to differences in overall activity.

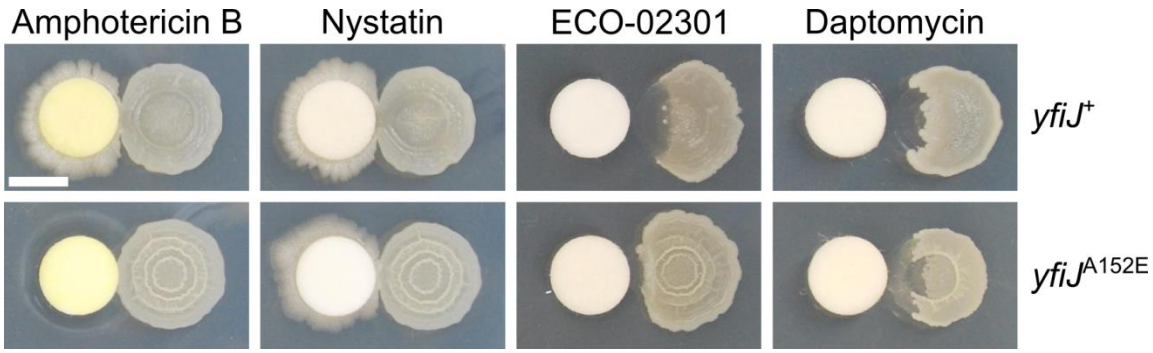

Figure 5. LDA^{R} alleles are specific to LDA caused by linear polyenes

Strains of B. subtilis (right) were pre-incubated for 24 h on MYM agar before exposure to the antibiotics on filter paper discs (left). Colonies were photographed 48 hours after antibiotic exposure. Amphotericin B (500 µg/filter disc) and nystatin (500 µg/filter disc) are not lytic to B. subtilis, which can grow around the filter paper disc. A *yfiJ*$^{+}$ strain of B. subtilis (PDS0571) is lysed by the linear polyene ECO-02301 (6.25 µg/filter disc) but a strain with the LDAR allele *yfiJ*^{A152E} (PDS0572) shows resistance to ECO-02301 at this concentration. However both *yfiJ*$^{+}$ and *yfiJ*^{A152E} strains are susceptible to daptomycin-induced lysis (250 µg/filter disk). Scale bar is 5 mm.

Table 3. Minimum lytic concentrations

Antibiotic	*yfiJ*$^{+}$ MLC (µg/mL)	*yfiJ*^{A152E} MLC (µg/mL)	Fold Difference (*yfiJ*^{A152E}/*yfiJ*$^{+}$)
Daptomycin	32.74	32.68	0.99
ECO-02301	0.40	1.46	3.65
LDA[*]	ND[†]	ND	9.58

[*]Linearmycins A and B extracted from *S.* Mg1 cultures.
[†]ND, not determined.

Because polyene antibiotics typically exert their effects on the cellular membrane, we wanted to determine if LDA resistant alleles of *yfiJK* provide *B. subtilis* with a generalizable cross resistance to membrane-active antibiotics. Daptomycin is a lipopeptide antibiotic that targets the cell membrane (177, 178, 190). The killing mechanism of daptomycin is not lytic, although lysis follows prolonged exposure (191). We found that daptomycin caused a morphologically similar lysis and degradation of *B. subtilis* when spotted on a filter paper disc adjacent to a colony (Figure 5). A LDA^R strain of *B. subtilis* also lysed when exposed to daptomycin. In comparison to the LDA sensitive strain, the LDA^R strain showed some residual opacity following lysis, suggesting that LDA^R alleles might provide cross-protection to daptomycin (Figure 5). However, we found the MLC of daptomycin was identical between the LDA resistant and sensitive strains (Table 3). Our results suggest that YfiJK signaling provides resistance either specifically to linear polyene molecules related to linearmycins, or commonly to the type of lytic cell damage caused by linearmycins.

The ABC transporter YfiLMN is necessary for LDA resistance

Immediately downstream of the *yfiJK* operon are three genes, *yfiLMN*, predicted to encode an ABC transporter (182, 192). This genetic architecture is similar to peptide-antibiotic resistance systems previously characterized in *B. subtilis* and other Firmicutes (193). In these systems, a TCS and an ABC transporter are functionally linked and required for antibiotic resistance. We hypothesized that YfiJK-LMN may function similarly to confer LDA resistance. Thus, we were interested in determining if YfiLMN

is necessary for LDA resistance. We engineered a strain with all five genes, *yfiJKLMN*, deleted. The Δ*yfiJKLMN* strain was lysed in co-culture with *S.* Mg1 (Figure 6). We inserted resistant alleles of *yfiJK* at the non-essential *amyE* locus to generate strains unable to produce YfiLMN but possessing LDA^R alleles of *yfiJK*. When cultured with *S.* Mg1, these strains were sensitive to LDA (Figure 6). We then complemented the loss of *yfiLMN* in these strains by inserting the *yfiLMN* genes, including the intergenic region between *yfiK* and *yfiL*, at the non-essential *lacA* locus. A predicted terminator exists downstream of *yfiK* (-8.9 kcal/mol) (genolist.pasteur.fr/SubtiList) (194). Our initial *yfiLMN* complementation construct included sequence immediately downstream of the terminator. However, this construct failed to complement the loss of resistance (Figure A4). Upon further investigation, we found no recognizable promoter elements in the intergenic region between the *yfiK* terminator and *yfiL* (143 bps). We hypothesized that *yfiJKLMN* may constitute a single operon with some level of terminator read-through resulting in *yfiLMN* expression. To circumvent the lack of an independent promoter, we placed the expression of *yfiLMN* under a constitutive $P_{spac(c)}$ promoter and inserted these constructs at the non-essential *yhdG* locus (195). Under constitutive expression, the *yfiLMN*-complementation strains were LDA resistant, showing only minimal lysis in co-culture with *S.* Mg1 (Figure 6). This effect was observed even in a strain complemented with wild-type *yfiJK* and in a strain lacking *yfiJK* entirely. These results demonstrate that YfiLMN is necessary for LDA resistance, and that constitutive expression bypasses the need for YfiJK. We speculate that YfiLMN either removes linearmycins from *B. subtilis* cells to provide resistance, or alternatively, functions in cell envelope processes or

regulatory functions that control LDA resistance. Determining the mechanism of YfiLMN-mediated LDA resistance will require further investigation.

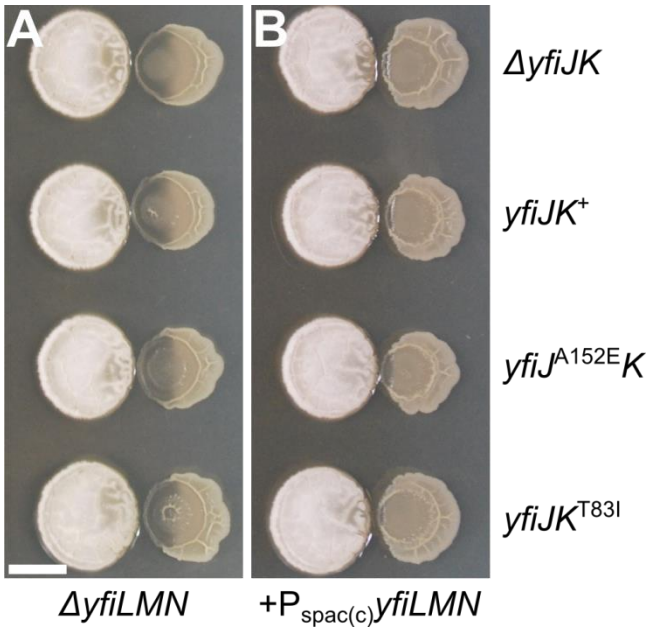

Figure 6. The ABC transporter YfiLMN is necessary for LDA resistance

(A) Strains with deletions of *yfiJKLMN* from *B. subtilis* (PDS0653) and *yfiJK* alleles inserted at the *amyE* locus as labeled on the right: *yfiJK*$^{+}$ (PDS0658), *yfiJ*^{A152E}*K* (PDS0686), or *yfiJK*^{T83I} (PDS0660). When cultured with *S.* Mg1, all *B. subtilis* Δ*yfiLMN* strains were lysed including those with a LDA^{R} allele of *yfiJK*. (B) Strains with the alleles of *yfiJK* as shown in (a), but containing $P_{spac(c)}$-*yfiLMN* inserted at the *yhdG* locus. All strains were resistant to LDA from *S.* Mg1 with minimal lysis visible next to the *S.* Mg1 colony. LDA resistance was observed in a strain lacking *yfiJK* (PDS0718), a strain with *yfiJK*$^{+}$ (PDS0719), and in strains with LDA^{R} alleles *yfiJ*^{A152E}*K* (PDS0720) and *yfiJK*^{T83I} (PDS0721). All cultures place *S.* Mg1 on the left and *B. subtilis* on the right. The cultures were photographed after 72 hours co-incubation on MYM agar plates. All images represent triplicate samples. Scale bar is 5 mm.

Intersection of colony developmental phenotypes and LDA resistance in LDA^R strains

In our study of the different LDA^R alleles, we observed some variation in the degree of wrinkled, motile phenotype in competition with *S.* Mg1 or under LDA exposure. To separate effects of the competitor from inherent LDA^R phenotypes, we plated colonies of LDA^R strains in isolation to view morphological features. All of the *yfiJK* mutant strains displayed a pattern of increased colony wrinkling and spreading across the agar surface and were distinct from the wild-type strain (Figure 7). We asked if differences in LDA^R morphology would be visible on the biofilm-inducing medium, MSgg (196). The mutant *B. subtilis* colonies developed a wrinkled appearance similar to wild type, indicating that traditional biofilm morphology and development are not disrupted in the mutant strains (Figure 7). We also noted that *B. subtilis* strains, either wild type or Δ*yfiJ,* formed smooth colonies in the absence of *S.* Mg1 when grown on rich media (Figure 7). In contrast, the same *B. subtilis* colonies in competition assays tend so show a somewhat wrinkled morphology, regardless of the *yfiJK* alleles present. Thus, the morphology of the *B. subtilis* colonies appears to be influenced by a combination of both the LDA alleles and the presence of the competitor species.

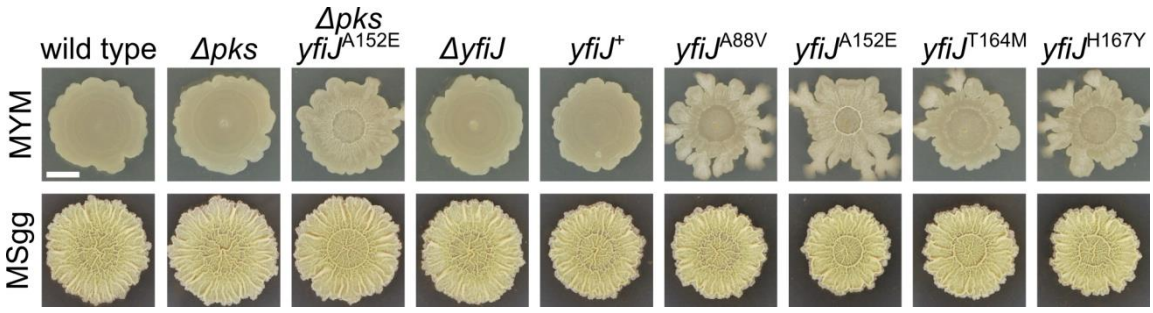

Figure 7. LDA^{R} mutants display aberrant wrinkled morphology

Representative colonies of *B. subtilis* with LDA^{R} alleles yfiJ^{A88V} (PDS0575), yfiJ^{A152E} (PDS0572), yfiJ^{T164M} (PDS0573), and yfiJ^{H167Y} (PDS0574) show architecturally complex colonies on MYM, while wild type (PDS0066), Δ*pks* (PDS0067), and Δ*yfiJ* (PDS0555) do not (top panels). The LDA^{R} colonies show both biofilm-like morphology and motile outgrowths at the colony periphery. When cultured on MSgg media, the LDA^{R} mutant strains develop biofilm colony morphology similar to control strains (lower panels). The Δ*pksX yfiJ*^{A152E} strain is a representative spontaneous LDA^{R} mutant. All photographs were taken after 72 h. Scale bar is 5 mm.

To directly compare colony morphology in isolation and with the competitor, the wild type and LDA^{R} strains were cultured at different distances to *S.* Mg1. We inoculated colonies of LDA^{R} *B. subtilis* and *S.* Mg1 in a perpendicular, cross-wise pattern on 1.5% agar MYM medium to provide a format for increasing distances between colonies of each species (Figure 8). The growth of *B. subtilis* with the wild-type *yfiJ* allele showed smooth colony formation with lysis proximal to the *S.* Mg1. In contrast, the *B. subtilis* strain with the *yfiJ*^{A152E} allele revealed different effects based on its proximity to *S.* Mg1 (Figure 8). The LDA^{R} colonies distant from *S.* Mg1 had the expected wrinkled morphology and spreading outgrowths, as was observed when cultured in isolation (Figure 7). However, the *S.* Mg1-proximal colonies were

morphologically different with a flattened surface and more uniform spreading pattern. The observed changes in colony morphology associated with LDA^R suggest that the YfiJK TCS regulates both specific resistance and developmental functions that coordinate a survival response to the competitor species.

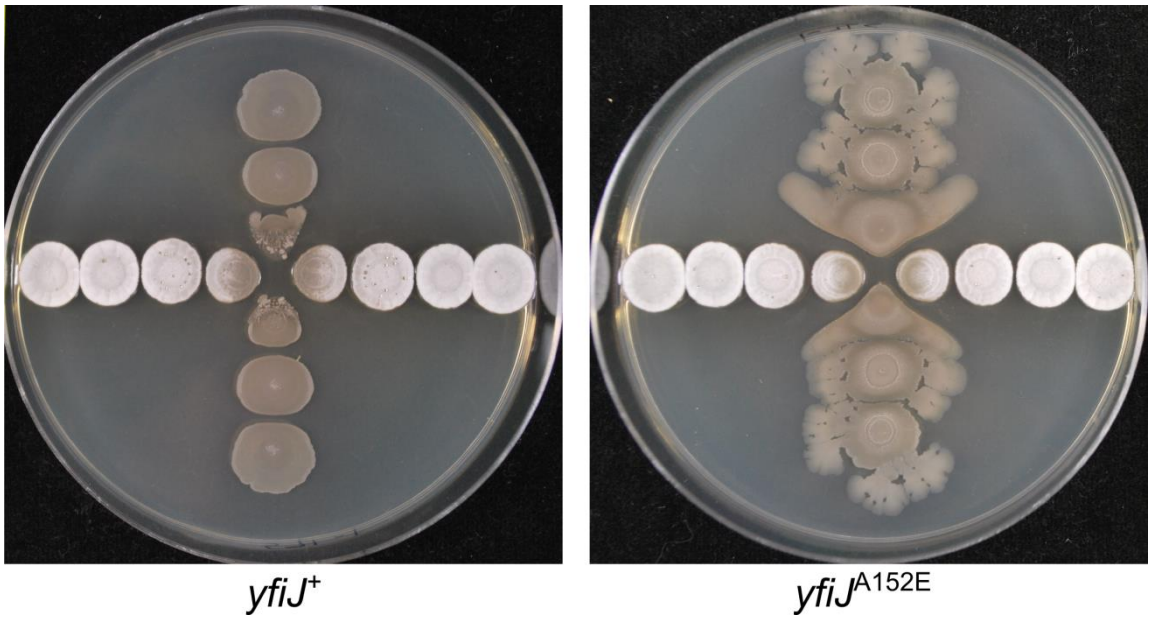

Figure 8. LDA^R mutants display a visible response to *S.* Mg1 in addition to inherent colony phenotypes

Wild type and LDA^R mutants were spotted in a perpendicular pattern, cross-wise to each other- *B. subtilis* (vertical) and *S.* Mg1 (horizontal). (Left) Strains of *B. subtilis* with $yfiJ^+$ (PDS0571) have flat, immotile colonies. Proximal to *S.* Mg1, the colonies are lysed and degraded. (Right) Strains of *B. subtilis* with the LDA^R allele $yfiJ^{A152E}$ (PDS0572) develop heterogeneous colonies, having wrinkled surfaces and motile outgrowths. Notably, the colonies of $yfiJ^{A152E}$ *B. subtilis* near *S.* Mg1 have a distinctive spreading morphology. Plates were photographed after 96 hours co-incubation on MYM + 1.5% agar. Plates represent duplicate experiments.

LDA^R and colony morphology phenotypes are genetically separable

To gain insight into possible connections between colony phenotypes and resistance to lysis, we considered that changes to extracellular matrix (ECM), the associated biofilm-like colony morphology, and changes in motility, may be responsible for LDA resistance (80, 98). For instance, the ECM may impede access of linearmycins to their target, possibly through overproduction of EPS or other matrix components (98). To test whether LDA resistance is dependent on known components of biofilm ECM, we sought to separate the two processes. We generated an ECM-defective strain, which was unable to produce exopolysaccharide (EPS) due to an *epsH* deletion (196), in an otherwise LDA resistant background (*yfiJ*^{A152E}). This strain developed as a flat, mucoid colony, but remained LDA resistant in co-culture with *S.* Mg1 (Figure 9). Based on this result, we concluded that, while EPS production is necessary for the wrinkled colony morphology, intact biofilm matrix in the LDA^R strains is not responsible for the LDA resistance mechanism. However, LDA resistance may require other biofilm matrix components (197). We asked whether hyperactivation of biofilm production would mimic the LDA resistance phenotype. We deleted the gene encoding *sinR*, the master biofilm repressor (198), in a LDA sensitive strain. When *sinR* is deleted, *B. subtilis* overproduces biofilm matrix and the colonies grow with a profoundly wrinkled appearance (198). If biofilm formation is responsible for LDA resistance, then a Δ*sinR* mutant should be resistant in co-culture with *S.* Mg1. However, the Δ*sinR* strain was sensitive to lysis (Figure 9). LDA resistance was observed in a Δ*sinR* strain only in the presence of the mutant *yfiJ* (*yfiJ*^{A152E}).

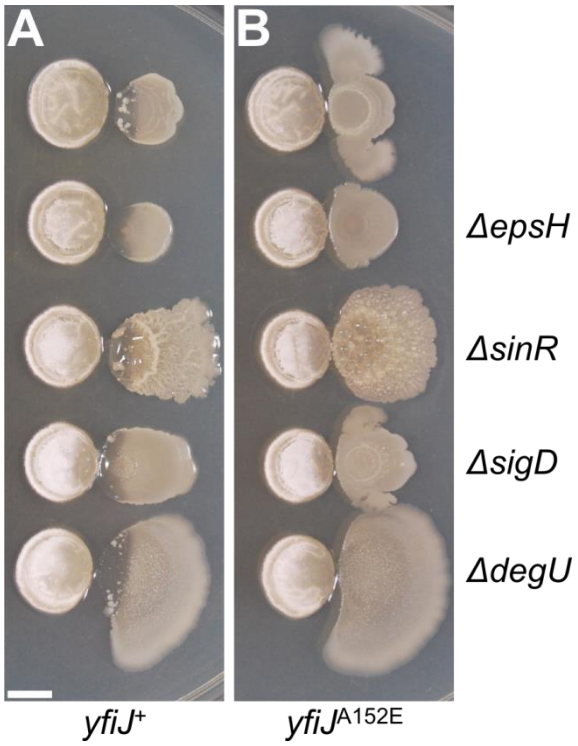

Figure 9. Colony morphology and LDA resistance are separable phenotypes

Genes involved in biofilm formation (*epsH*, *sinR*, and *degU*) and motility (*sigD*) were deleted from strains with either (A) *yfiJ*$^{+}$ (PDS0571) or (B) the LDA^{R} allele *yfiJ*^{A152E} (PDS0572). In all cases, the biofilm and motility mutant strains were sensitive to lysis with wild-type *yfiJ* and were resistant to lysis with *yfiJ*^{A152E}. All cultures place *S.* Mg1 on the left and *B. subtilis* on the right. Colonies were photographed after 72 hours co-incubation with *S.* Mg1 on MYM medium. Images are representative of triplicate samples. Scale bar is 5 mm.

Biofilm formation is controlled not only by SinR but also by the TCS DegSU. This TCS is responsible for control of the production of biofilm extracellular matrix components. Among these components are BslA and γ-poly-DL-glutamate (γ-PGA) (199–201). To test if matrix functions provided by DegU may contribute to LDA

resistance, we deleted *degU* in a LDA resistant background (*yfiJ*^{A152E}) and cultured the strain with *S.* Mg1. This mutant developed as a flat colony that was LDA resistant, suggesting that resistance to LDA does not require functions provided by DegU (Figure 9). Based on this finding and our SinR and EpsH experiments, we conclude that the changes in colony morphology of LDA^{R} mutants are not the principle cause of LDA resistance.

In addition to wrinkled colony morphology, the enhanced motility of LDA^{R} strains may be linked to resistance. For instance, swarming motility has been associated with elevated antibiotic resistance in multiple bacteria (80). Previously, we observed lysis in a Δ*sigD* strain, which is deficient in swarming and autolysin production (188, 202, 203) (Figure A3). We tested whether a Δ*sigD*, *yfiJ*^{A152E} double mutant strain would undergo lysis despite the presence of the LDA^{R} allele (Figure 9). This strain maintained both LDA resistance and morphological changes, including colony spreading. The spreading phenotype in the absence of *sigD* is consistent with LDA^{R} mutants exhibiting sliding motility when cultured with *S.* Mg1 (82). In sum, the combined phenotypes of LDA^{R} support a model wherein activation of YfiJK leads to LDA resistance through YfiLMN activation coordinated with separable changes in colony motility and morphology that promote survival during competition.

Genes identified by differential expression in a LDA^R strain

In an effort to identify a regulatory network for YfiJK, we sought to identify genes differentially expressed in a LDA^R mutant that may contribute to colony phenotypes. To perform differential expression analysis, we isolated and sequenced RNA from *yfiJK*$^+$ (PDS0627) and *yfiJ*^{A152E}*K* (PDS0685) strains cultured on agar plates. In our analysis, we identified six genes with statistically significant changes in expression between the two strains (Table 4). Expression of *yfiLMN* was increased on average ~18-fold in the LDA^R mutant. To corroborate this result we used qRT-PCR and observed a ~20-fold increase in *yfiL* expression from the *yfiJ*^{A152E}*K* strain (Figure A5). We did not observe a change in expression of *yfiJK* in our RNA-seq experiments, which is consistent with an additional control element between *yfiK* and *yfiL*. Three other differentially expressed genes were all decreased in the LDA^R mutant: *des*, which encodes a phospholipid desaturase responsible for cold shock adaptation (204, 205) and *yvfRS*, which encodes an ABC transporter of unknown function (192). Surprisingly, no genes in the *eps* operon or other known biofilm-related genes were identified as differentially expressed between the LDA sensitive and LDA^R strains. Also of note, we found no correspondence between the YfiJK-regulated genes we identified by RNA-seq and the regulon previously defined by microarray study of *yfiK* overexpression (184). In the absence of a clear connection to established biofilm and motility functions, the RNA-seq results suggest that the morphological changes observed in LDA^R colonies may arise directly from activation of YfiLMN function combined with repression of *des* (phospholipid content) and *yvfRS* (unknown function) by an unknown mechanism.

Alternatively, the morphological changes may occur only in a subpopulation of cells insufficient to be detected during our analysis.

YfiJK is required for transient LDA resistance and small colony formation

One of our initial goals was to identify mechanisms of resistance in an attempt to expose mechanistic aspects of linearmycin activity. We considered that LDA resistance may only exist under aberrant conditions, which arise through mutations that hyperactivate the YfiJK signaling system. In the absence of a clear phenotype for deletion of the genes, we sought an approach to identify wild-type YfiJK function in colony morphology and LDA resistance. We returned to an early observation that small colonies resistant to LDA emerge in the lysed region of a *B. subtilis* colony. The majority of the isolated LDA resistant colonies isolated were only transiently resistant

Table 4. Differential expression analysis between *yfiJ*^{A152E}*K* and *yfiJK*$^{+}$

Gene	Fold Difference (*yfiJ*^{A152E}*K*/*yfiJK*$^{+}$)	FDR
yfiN	21.28	2.02^{-22}
yfiM	19.15	1.70^{-20}
yfiL	14.14	3.59^{-17}
des	0.20	3.05^{-7}
yvfR	0.15	2.54^{-7}
yvfS	0.14	1.81^{-5}

Differential gene expression between a *yfiJ*^{152E}*K* strain (PDS0685) and a *yfiJK*$^{+}$ strain (PDS0627). Fold differences > 1 indicate increased expression in the *yfiJ*^{A152E}*K* strain relative to the *yfiJK*$^{+}$ strain.

(50/60). We reasoned that if the natural function of YfiJK is to provide temporary resistance to LDA-induced damage, the emergence of transient resistance would depend upon the function of YfiJK. Therefore, we tested 6 independent colonies, each in triplicate, of wild type and Δ*yfiJK* versus *S.* Mg1 to determine if resistant colonies would emerge in the absence of YfiJK (Figure 10, Figure A6). The resulting cultures showed many small colonies arising in the lysed areas of the wild-type *B. subtilis* colonies. By contrast, the few small colonies observed with the Δ*yfiJK* strain did not grow appreciably and lacked the morphological features of the *yfiJK*$^{+}$ colonies (Figure 10). This result is consistent with the natural function of YfiJK providing transient resistance to LDA-induced stress. In the case of *yfiJK* gain-of-function alleles, the substitutions in YfiJK may lock the TCS into an active state wherein every cell becomes resistant to LDA in contrast to the subpopulations observed among wild-type cells. Intriguingly, the transient resistance appears in only a subset of cells in the colony. Variable antibiotic resistance among a clonal population of cells has been described as heteroresistance, and is thought to be advantageous for survival of bacteria during antibiotic treatment (206–208). The ability to activate YfiJK in a subset of cells may constitute a mechanism of transient heteroresistance to linearmycins and related molecules, but defining the mechanism and limitation to a subpopulation of cells will require further investigation. The observed pattern of YfiJK-dependent LDA resistance highlights that this TCS, and possibly many TCS, may transiently serve a subset of cells in a population during times of competitive crisis.

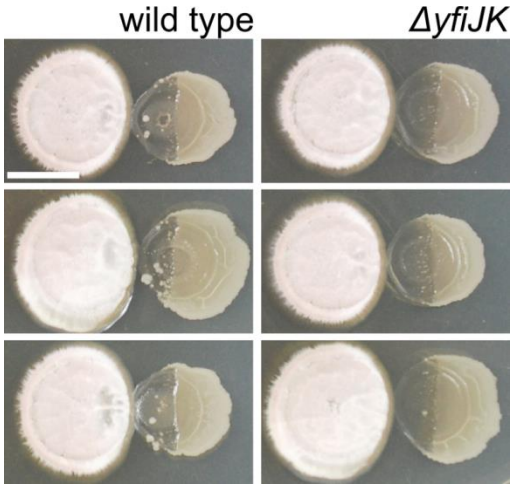

Figure 10. Small colonies among lysed cells in wild-type but not Δ*yfiJK* colonies

Eighteen wild-type and Δ*yfiJK* colonies of *B. subtilis* were cultured with *S.* Mg1. Many small, potentially LDA^R, colonies appeared in the region of lysis of wild-type colonies, while few could be seen in the Δ*yfiJK* strain. The few small colonies observed in the zone of lysis for Δ*yfiJK* did not have the morphological features of the wild-type colonies. Note, Figure A6 shows all eighteen replicate colonies for each strain. All cultures place *S.* Mg1 on the left and *B. subtilis* on the right. Photographs were taken after 96 hours co-incubation on MYM agar. Scale bar is 5 mm.

Discussion

In this study, we used a two-species culture model of bacterial competition to identify functions that contribute to bacterial competitive fitness. The present study stemmed from an earlier observation of lysis and degradation of *B. subtilis* colonies when cultured adjacent to *S.* Mg1 (47). Here, we first identified linearmycins, produced by *S.* Mg1, as the primary cause of progressive lysis and colony degradation. The culture format used for competition revealed small *B. subtilis* colonies spontaneously resistant to lysis. When isolated, the resistant colonies showed a biofilm-like appearance with increased wrinkled colony morphology and aberrant motility. We sequenced whole genomes of the resistant colonies and identified mutations that confer resistance. Genomic analysis revealed alleles of the *yfiJK* operon, which encodes a two-component

system of previously unknown function. Based on our observations, we define *yfiJK* as a regulator of *yfiLMN*, encoding an ABC transporter, and possibly other target genes that govern modes of colony growth and motility (Figure 11).

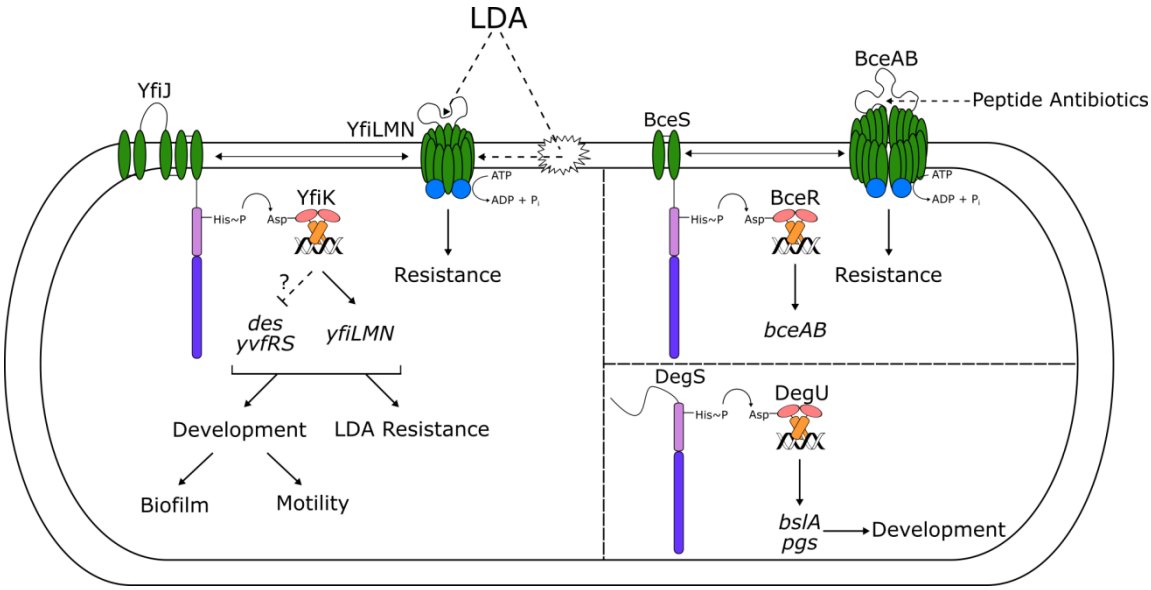

Figure 11. Model for YfiJK-LMN functions in LDA resistance and development

LDA is sensed either directly by the ABC transporter YfiLMN, similarly to the ABC transporter BceAB and peptide antibiotics, or indirectly as membrane damage. This signal is transferred to the histidine kinase YfiJ, which then activates YfiK via phosphorylation. YfiK~P then activates the transcription of *yfiLMN* and likely represses *des* and *yvfRS*, leading to LDA resistance, biofilm formation, and motility through an unknown mechanism. These functions promote survival of *B. subtilis* under competitive stress. The YfiJK system differs structurally and functionally from other TCS that control either antibiotic resistance, such as the BceRS-AB system, or development, such as the DegSU system. Interactions between HKs and ABC transporters are shown with double-headed arrows. Hypothesized interactions of molecules with ABC transporters or membranes are shown with dashed arrows.

We show that the LDA resistance is not dependent upon known biofilm-specific functions, suggesting that colony morphology and LDA^R are separable processes, unified under YfiJK regulation. Two-component systems are well established as regulators for cellular responses to environmental stresses, including antibiotics (209, 210). The significance of the current work is the use of model interspecies competition to reveal both the agent of aggression, linearmycins, and a multifaceted survival response from genes with no prior functional assignment, *yfiJKLMN*.

Only gain-of-function mutations in *yfiJK* were identified in this study to cause LDA resistance. The resistance alleles of *yfiJK* were due to missense mutations causing changes to four regions of YfiJK: *(i)* the third TM helix in YfiJ, *(ii)* the cytoplasmic linker between the fifth TM helix and the dimerization and histidine phosphotransfer (DHp) domain in YfiJ, *(iii)* the C-terminal end of the DHp, and *(iv)* the regulator domain in YfiK. We hypothesize that each of these amino acid substitutions are responsible for conformational changes in YfiJK, leading to a constitutively active state. A previous study described a similar phenotype caused by point mutations of *pmrAB* in *Pseudomonas aeruginosa*. Gain-of-function alleles in *pmrB* lead to polymyxin B resistance via increased signaling through the histidine kinase (211). We also considered an alternative mechanism, wherein point mutations in *yfiJK* could lead to non-cognate interactions of YfiJ or YfiK and aberrant signal transduction (212). However, we view this mechanism as unlikely because only one of the affected residues (L254) lies in the DHp domain, which is predicted to be involved in specificity (212), and LDA resistance

required the presence of the phosphoacceptor residue in the cognate partner. Thus, we conclude that gain-of-function alleles cause LDA resistance and changes in both colony morphology and motility, and that the signaling is specific to YfiJK. Although the specific defects caused by each allele will require further investigation, we note that many of the mutations we observed are responsible for amino acid changes in the cytoplasmic linker of YfiJ. The cytoplasmic linker domain of HKs has been best characterized in periplasmic-sensing histidine kinases. In these kinases, the linker may contain conserved PAS or HAMP domains that are necessary for signal transduction from the sensory machinery to the kinase domains (183, 213–215). YfiJ has neither of these conserved domains, suggesting that the short linker in this protein is the sole signal-transducing domain. The mutations in the *yfiJ* linker, through fixing the protein in activated state, may be very informative for determining the mechanism of signal transduction via the YfiJ intramembrane histidine kinase.

Two-component systems are commonly involved in sensing antibiotic and environmental stress (209, 210). Among Firmicutes, a conserved mechanism for resistance to peptide antibiotics pairs genes for two-component systems and ABC transporters (193, 216, 217). The identification of mutations in *yfiJK* suggests the cell envelope is the linearmycin target, based on comparison to other TCS-ABC transporter pairs in *B. subtilis* (193). Immediately downstream of *yfiJK* are three genes, *yfiLMN*, that are predicted to encode an ABC transporter. We found that when *B. subtilis* was unable to produce YfiLMN, the colonies were LDA sensitive and failed to develop altered

colony morphology, regardless of the presence of a LDA^R allele of *yfiJK*. Furthermore, expression of *yfiLMN* under a constitutive promoter resulted in LDA resistance, even in the absence of *yfiJK*. Thus, the YfiLMN transporter is necessary and sufficient for LDA resistance. We hypothesize that YfiLMN may act as an exporter either for linearmycin or for cell envelope remodeling factors that lead to LDA resistance.

We used RNA-seq to identify genes that may be regulated by YfiJK. As expected we identified that *yfiLMN* expression was increased in a LDA^R mutant. We also identified *yvfRS*, encoding an ABC transporter of unknown function, and *des* as genes downregulated by YfiJK. The *des* gene encodes a fatty acid desaturase that is responsible for altering membrane fluidity in response to cold shock (204, 205). Intriguingly, *B. subtilis* strains with *des* deletions are more susceptible to daptomycin-treatment, potentially due to their altered membrane fluidity (218). Antifungal polyenes structurally related to linearmycins target ergosterol in fungal membranes (177–180). The decreased expression of *des* in LDA^R mutants may contribute to resistance by affecting interactions between linearmycins and the cell membrane. Characterization of the cell envelopes of LDA sensitive and LDA^R strains may provide insight into the mechanism of linearmycin-induced lysis.

Mutants with LDA^R alleles of *yfiJK* grow as rugose colonies that resemble some aspects of biofilm development on rich media, which does not support traditional biofilm development. We demonstrated that we could functionally divorce this colony

morphology phenotype and LDA resistance by expressing *yfiLMN* constitutively and by introducing deletions of genes specifically required for biofilm development (*epsH*, *sinR*, *degU*). In so doing, we found that changes to the biofilm extracellular matrix are not responsible for resistance. LDA resistance may be modulated by specific matrix or cell envelope modifications activated by YfiJK-LMN, but such modifications remain to be identified. Although we found no obvious candidates in our RNA-seq data to explain colony morphological changes, the decreased expression of *des* or *yvfRS* may contribute to alterations in colony development. We also observed that LDA^R mutants respond to *S.* Mg1 by inducing motility, whereas wild type *B. subtilis* colonies are lysed. The pleiotropic phenotypes of *yfiJK* LDA^R alleles differentiate this coupled TCS-ABC transporter system from the BceRS-AB, PsdRS-AB, YxdJK-LM systems in *B. subtilis*, which appear to be dedicated antibiotic resistance systems (193, 219–222). To our knowledge, there are no phenotypes associated with development that have been attributed to these TCS-ABC transporter pairs, suggesting that YfiJK holds a specialized role in providing specific LDA resistance and in activating biofilm development and motility, both of which are known to increase resistance to antimicrobials (80, 98). We propose that activation of YfiJK-LMN promotes competitive fitness of *B. subtilis* by coupling a specific resistance mechanism (LDA^R) with generalized-resistance that occurs as a consequence of altered development and motility. A recent study using strains of *Pseudomonas aeruginosa* demonstrates that biofilm formation is stimulated in response to competition, as opposed to a cooperative function of different strains or cell types (157). The identification of YfiJK as a regulator of biofilm and motility functions

is consistent with a model wherein competition with *S.* Mg1 induces developmental responses, including biofilm and colony spreading, among a subpopulation of resistant cells of *B. subtilis*.

Using microbial competition we assigned resistance and developmental functions to a previously uncharacterized TCS in *B. subtilis*. Without imposing the conditions of competition on *B. subtilis*, these TCS functions may be difficult to identify, because the *yfiJ*, *yfiK*, and *yfiJK* deletion mutants have no phenotype when compared to wild type. The *B. subtilis* genome encodes 36 histidine kinases and 34 response regulators (223). The functions of at least 11 of these TCS are currently unknown. Bacteria use these systems to sense and respond to their environment, which include stresses and nutrient conditions, but also include other bacteria and their antagonistic enzymes and specialized metabolites. Many TCS of unknown function may have a role in the context of microbial competition, despite having no distinct phenotype under laboratory conditions. Thus, microbial competition studies provide an effective approach to identify functions for TCS and other genes that promote competitive fitness of bacteria. By expanding our knowledge of individual competitive functions, a more comprehensive view of bacterial competitive fitness will emerge.

Materials and methods

Bacterial strains, media, and general cloning

The strains of *B. subtilis* we used in this study are listed in Table A3. We cultured *B. subtilis* strains at 37 °C in lysogeny broth (LB) [1% tryptone (Bacto), 0.5% yeast extract (BBL), 0.5% sodium chloride (Sigma)] or on LB agar plates [1.5% Agar (Bacto)]. We maintained *Streptomyces* sp. Mg1 (PSK0558) as a spore stock in water at 4 °C. Unless otherwise stated all co-cultures were grown on MYM [0.4% malt extract (Bacto), 0.4% yeast extract (BBL), 0.4% D-(+)-maltose monohydrate (Sigma)] with 2% agar (Bacto). We used chloramphenicol (5 µg/mL), kanamycin (5 µg/mL), MLS (1 µg/mL erythromycin, 25 µg/mL lincomycin), spectinomycin (100 µg/mL), and tetracycline (20 µg/mL) as needed. The primers we used in this study are listed in Table A4. We used *Escherichia coli* DH5α or XL-1 blue for plasmid maintenance and manipulation. We prepared All *B. subtilis* genetic manipulations in either the 168 or PY79 strain background and then transduced them to NCIB3610 using SPP1 phage transduction as previously described (224).

LDA extraction and identification

We wetted 1 g Diaion HP-20 resin in 25 mL methanol (MeOH) followed by washes with 25 mL of water five times while shaking. Next, we removed the bulk liquid and resuspended the resin in 250 mL of MYM. We sterilized the media and resin by autoclaving the mixture. We inoculated cultures using 1 mL of *S.* Mg1 that was grown overnight (10^7 spores in 3% tryptone soy broth). We cultured the *S.* Mg1 for 6 d at 30 °C

while shaking at 225 RPM in the dark. We performed all culture growth and extractions in low ambient light, because the activity of extracts was diminished or lost if manipulated in the light. We separated the HP-20 resin from the bulk of the *S.* Mg1 by repeatedly washing the resin with water until all visible filaments were removed. To extract resin-bound molecules, we washed the resin with successive 25 mL volumes of MeOH until the solvent was clear. To generate our crude extract, we pooled the washes and removed MeOH using a rotary evaporator. The crude extract was dissolved to 100 mg/mL in 50% acetonitrile (ACN) and fractionated over a C_8 solid-phase extraction (SPE) column eluted with a MeOH/water stepwise gradient. We removed solvent from our fractions using a rotary evaporator and suspended the fractions to 50 mg/mL in 50% ACN. We tested the fractions for lytic activity against *B. subtilis* by spotting 10 µL on a filter paper disc adjacent to a *B. subtilis* colony that had been pre-grown for 24 h and observing lysis over a period of 48 h. The 70% and 80% MeOH fractions were active in the lysis assay and pooled for further fractionation.

Using an Agilent 1200 HPLC system, we further fractionated the active extract fractions over a semi-preparative (10 x 250 mm, 5 µm) Phenomenex Luna C_{18} column and eluted with an ACN/20 mM ammonium acetate pH 5 (NH_4OAc) gradient running at 5 mL/min. The elution program was as follows: 1) 5 min at 40% ACN then 2) a gradient up to 50% ACN over 10 min then 3) a gradient up to 75% ACN over 5 min, and 4) a gradient diminishing to 40% over 5 min. We injected 35 µL of pooled active fraction per injection. We collected time based fractions and tested them for lytic activity as above.

Active fractions were analyzed by mass spectrometry using a Bruker microTOF mass spectrometer. For NMR analysis, the sample was dried and resuspended in 300 µL deuterated dimethylsulfoxide (DMSO-d_6). We collected spectra on a Bruker Avance III 500 MHz spectrometer equipped with a cryoprobe.

LDA resistant mutant isolation and whole genome sequencing

We diluted overnight cultures inoculated with a single colony of *B. subtilis* Δ*pksX* (PDS0067) into 5 mL of LB at OD_{600} = 0.08 with no antibiotics. We cultured the cells to early stationary phase (OD_{600} = 0.9-1.5) at 37 °C and spotted 2 µL on MYM7 plates [as above with 100 mM MOPS and 25 mM potassium phosphate buffer pH 7, 1.5% agar (Bacto)]. After 24 h incubation, we placed 6 mm filter paper discs next to the *B. subtilis* colonies and added 10 µL of extract from *S.* Mg1. We returned the plates to the incubator and observed lysis and colony degradation over the next 48 h. After incubation, small colonies were observed in the region of lysis. We isolated 60 small colonies and passaged them on LB plates. We tested each isolate for LDA resistance using co-culture, as described below.

LDA^R mutants that were stable through passage in isolation and the parental Δ*pksX* strain were used for whole genome sequencing. Sequencing libraries were prepared using the PCR-free TrueSeq Kit from Illumina. 250 bp paired-end reads were sequenced using an Illumina MiSeq. We mapped reads from the LDA^R mutants onto the

parental Δ*pks* strain using MIRA and identified mutations by consensus discrepancy between the sequences (225, 226).

Transposon mutagenesis

We used a strain of *Bacillus subtilis* harboring the pMarA plasmid transposon mutagenesis system (227) (PDS0121) to identify genes that may cause lysis under linearmycin-induced stress. pMarA is a single copy plasmid that contains a *Himar1* transposase gene under control of the housekeeping sigma factor σ^A. Transposition occurs during growth and each cell should undergo a single transposition event. We diluted cultures of PDS0121 that were grown overnight at 22 °C to OD_{600} = 0.05 in 5 mL of LB with kanamycin (5 μg/mL). When the OD_{600} reached 0.3-0.4 we raised the temperature from 22 °C to 42 °C, which restricts replication of pMarA. When the culture reached OD_{600} = 1 (~10^9 cells/mL) we added 10 μL of LDA-containing and returned cultures to 42 °C. At this point the culture represented a library of transposon-insertion mutants. After ~3 hours of incubation, the OD_{600} decreased ≥ 10-fold upon cell lysis. We plated the surviving cells on LB containing LDA extract. Following incubation of the plates, we isolated ~200 survivors, which we subsequently passaged on LB without LDA extract. We then tested the passaged isolates for LDA resistance in culture with *S.* Mg1. Only a single stable LDA^R mutant passed through the selection. We mapped the transposon insertion to the *yopC* gene, which encodes a predicted membrane protein within the Spβ prophage sequence (228). A Δ*yopC* strain was not LDA resistant in culture with *S.* Mg1. We backcrossed the mutant strain to wild type and found the

transposon-associated marker was unlinked to LDA resistance. To locate the LDA^R-conferring allele, we sequenced this strain. The sequence revealed an additional point mutation in *yfiJ* (L254P substitution), which we confirmed for resistance to LDA (Table 1).

Construction of yfiJK and yfiJKLMN deletion mutants

We used long-flanking homology PCR to delete *yfiJK* and *yfiJKLMN*. Briefly, to delete *yfiJK* we amplified the upstream sequence using primers 13 and 14, the downstream sequence using primers 15 and 16, and the kanamycin resistance cassette from pDG780 using primers kn-fwd and kn-rev. We mixed the three PCR products together and used primers 13 and 16 to amplify a product, which we directly transformed into PDS0312 to generate PDS0546.

To delete *yfiJKLMN* we used primers 76 and 77 to amplify the upstream sequence of *yfiJ* and primers 78 and 79 to amplify the downstream sequence of *yfiN*. We combined these fragments with the kanamycin resistance cassette and amplified a product using primers 76 and 79, which we directly transformed into PDS0312 to generate PDS0652.

Complementation of yfiJ and yfiJK

To test alleles of *yfiJ,* we complemented the Δ*yfiJ* deletion. We amplified *yfiJ* with primers 25 and 26 from wild type and spontaneous LDA^R mutants. These primers include a BamHI and EcoRI site, which we used to clone the product into plasmid

pDR183 (*lacA::mls*). We transformed the plasmids into PDS0559 and verified insertion into the *lacA* locus by PCR. We moved these constructs into PDS0555 using SPP1 phage transduction.

We tested alleles of *yfiK* by complementing both *yfiJK* together into a Δ*yfiJK* strain. We complemented both genes together because *yfiK* is the second gene in the operon. We amplified *yfiJK* using primers 54 and 75 from wild-type or spontaneous LDA^R mutant and the plasmid backbone of pDR111 (*amyE::spc*, without the IPTG-inducible system) using primers 59 and 74. We combined these products together using Gibson assembly (229), transformed the plasmid into PDS0546, and verified insertion into the *amyE* locus by PCR. We moved these constructs into PDS0554 using SPP1 phage transduction.

Complementation with $P_{spac(c)}$yfiLMN

To complement *yfiLMN* we first amplified $P_{spac(c)}$ from BJH157 using primers 112 and 113. These primers included an EcoRI and SpeI site, which we used to clone the $P_{spac(c)}$ fragment into pBB275 to generate pRMS1. We amplified *yfiLMN* using primers 120 and 121 and the backbone of pRMS1 using primers 118 and 119. We assembled these fragments using Gibson assembly and transformed them directly into PDS0652 to generate PDS0717.

Site-directed mutagenesis

We used primer-mediated site-directed mutagenesis to generate phosphoacceptor residue changes. To generate *yfiJ*^{H201N} alleles we used primers 42 and 43. To generate *yfiK*^{D54A} alleles we used primers 50 and 51. Briefly, we PCR amplified plasmids containing *yfiJ* or *yfiJK* using overlapping primer pairs that included a single nucleotide change, DpnI-digested the reactions, and transformed *E. coli*. We isolated the plasmids and sequenced them to verify the mutation. We used plasmids containing the mutations to transform *B. subtilis* as above.

Lysis co-culture assays

To observe lysis, we grew cultures of *B. subtilis* as above and spotted 1 µL of *B. subtilis* on 20 mL MYM plates. We then spotted 5 µL of a 10^9 spores/mL stock of *S.* Mg1 ~6 mm from *B. subtilis*. These plates were incubated at 30 °C and monitored every 24 h.

Motility co-culture assays

To observe the effect of *yfiJ* alleles on motility we used a modified version of a motility assay we previously described (31). We plated 2.5 µL of a 10^7 spores/mL stock of *S.* Mg1 on a 25 mL MYM plate and incubated the plate at 30 °C. After 12 h of growth, we spotted 1.5 µL of *B. subtilis*, grown as above, perpendicularly to *S.* Mg1, returned the plates to the 30 °C incubator, and monitored the plates every 24 h.

Measuring minimum lytic concentrations

To measure MLC values we used an agar diffusion assay. We grew cultures of a LDA sensitive strain (PDS0571) and a LDA^R strain (PDS0572) in 25 mL of MYM to OD_{600} = 2. When the cultures reached this density, we centrifuged the cultures at 3220 x g for 5 min and resuspended the cell pellet in half the volume to reach OD_{600} = 4. We mixed 1.5 mL of resuspended cells with 4.5 mL of MYM agar (0.67%) and poured the layer over a MYM plate to generate an overlay with OD_{600} = 1 and 0.5% agar. We placed 6 mm filter paper discs onto the overlay and added 10 µL of 2-fold serial dilutions of daptomycin, ECO-02301, and LDA to the discs. Afterwards we incubated the plates for 4 h at 30 °C and then photographed the plates. We measured haloes of lysis using ImageJ and determined MLC values by plotting natural log-transformed antibiotic concentrations versus the area of lysis, and calculated the intercept to determine MLC values for the lytic agents (230).

RNA-seq

We grew two independent cultures each of *yfiJK*$^+$ (PDS0627) and *yfiJ*^{A152E}*K* (PDS0685) strains as above. When the cultures reached early stationary phase we diluted them 10^{-3} in LB and spread plated 100 µL on MYM plates. After 24 h we scraped the lawns of *B. subtilis* into RNAprotect Bacteria Reagent (Qiagen) and isolated RNA using an RNeasy mini kit (Qiagen). We removed trace DNA from the RNA samples using a Turbo DNA-free kit (Applied Biosystems). The ribosomal RNA was removed from RNA samples using a Ribo-Zero rRNA Removal Kit (Gram-Positive Bacteria)

(Illumina). 50-bp single-end reads libraries were prepared using a TruSeq Stranded Total RNA Kit (Illumina) and sequenced on an Illumina HiSeq 2500. We mapped reads to each open reading frame (ORF) in the *B. subtilis* 168 genome (GenBank: NC_000964.3) with kallisto (231) and used edgeR (232) for differential gene expression analysis. We filtered out lowly expressed ORFs (<1 count per million and only represented in one of the four samples) and used trimmed mean of M-value normalization to calculate effective library sizes before analysis [98]. We used the single-factor exact test and reported differentially expressed genes with a false discovery rate cutoff of $< 1^{-4}$ (233). The raw reads for this experiment are accessible from NCBI BioProject Accession PRJNA295934.

qRT-PCR

We isolated RNA from PDS0627 and PDS0685 as above and preformed qRT-PCR similarly as previously described (31). Briefly, we used 100 ng of total RNA as template for cDNA synthesis using a High-Capacity RNA-to-cDNA Kit (ThemoFisher Scientific). We used an SsoAdvanced Universal SYBR Green Supermix Kit (Bio-Rad) for and preformed quantitative PCR with a CFX96 Touch real-time PCR thermocycler (Bio-Rad). We used the following cycling parameters: denaturation at 95 °C for 30 s; 40 cycles of denaturation at 95 °C for 15 sec, annealing at 58 °C for 30 s, and extension at 72 °C for 30 s; and a final melting curve from 60 °C to 95 °C for 6 min. We used *gyrB* as our reference gene. We amplified *yfiL* using primers q1 and q2 and *gyrB* using primers *gyrB* qPCR-fwd and *gyrB* qPCR-rev (Table A4). We ran each reaction in

triplicate. Using LinReg (234) we calculated primer efficiency and quantification cycle values. We normalized *yfiL* abundance to *gyrB* and report fold difference relative to PDS0627.

CHAPTER III

LINEARMYCINS ACTIVATE A TWO-COMPONENT SIGNALING SYSTEM INVOLVED IN BACTERIAL COMPETITION AND BIOFILM FORMATION

Summary

The mechanisms that bacteria use in competition are numerous and differ among species. For instance, some bacteria produce chemically diverse specialized metabolites with numerous competitive activities including antibiosis. Meanwhile, other species of bacteria engage biofilm formation and motility mechanisms to survive and escape competition. While specialized metabolite production and biofilm formation are relatively well understood for bacterial species isolated in monoculture, how bacteria collectively employ and respond to these and other mechanisms during competitive interactions is not well studied. Within the context of bacterial communities, fitness is determined, in part, by success in competitive interspecies interactions. Therefore, to address fundamental questions relating to the competitive functions of different species, we have developed a model system using two species of soil bacteria: *Bacillus subtilis* and *Streptomyces* sp. Mg1 (*S.* Mg1). Using this system, we previously found that linearmycins produced by *S.* Mg1 cause lysis of *B. subtilis* cells and degradation of colony matrix. We identified linearmycin resistant mutants that activate the YfiJK two-component signaling system resulting constitutive expression of the *yfiLMN* operon, encoding an ATP-binding cassette transporter. Intriguingly, we observed that the linearmycin resistant mutants also form biofilms. Here, we determined that expression of

the *yfiLMN* operon, particularly *yfiM* and *yfiN*, is necessary for biofilm formation. Using transposon mutagenesis we identified highlight chaperone functions and other gene products that contribute to YfiLMN-mediated biofilm formation. To understand how YfiJ is activated we generated a transcriptional fusion of the *yfiLMN* promoter to *lacZ*. We found that YfiJ signaling is activated by linearmycins and other polyene metabolites. Finally, using a truncated YfiJ, we show that YfiJ requires its transmembrane domain and to activate downstream signaling. Taken together, our results suggest coordinated antibiotic resistance and biofilm formation by a single ABC transporter promotes competitive fitness of *B. subtilis*.

Introduction

Bacterial cells distribute themselves in the environment according to their individual metabolic and physiological needs. Though, neighboring cells may also cooperate with each other, competition is more likely to be the dominant mode of bacterial interaction in nature (1). Bacteria have evolved numerous mechanisms to engage in competition with their neighbors. Competitive mechanisms include production of specialized metabolites including antibiotics, contact-dependent inhibition systems, and type VI secretion systems that directly deliver toxins into cells, among others (reviewed in 235). As an outcome of competition, cells may be killed or displaced from favorable microenvironments, thus eliciting changes to the structure of the microbial community at large. As community dynamics change, other individuals or aggregates of cells may suffer fitness costs if they fail to adapt (236). Therefore, to avoid loss of

fitness and survive, bacteria integrate and respond to external signals that indicate changing environments.

The external signals bacteria sense include abiotic factors, such as nutrient and oxygen levels. In this way, bacteria can sense changes in these resources as a proxy for the presence of competitors. For example, when *Amycolatopsis* sp. AA4 and *Streptomyces coelicolor* are grown together, *A.* sp. AA4 downregulates the expression of its own siderophore biosynthesis genes and steals the siderophores produced by *S. coelicolor*. Subsequently, *S. coelicolor* induces expression of its siderophore biosynthesis genes to produce enough siderophores to capture the iron it requires (17). Bacteria also sense biotic factors that indicate the presence of microbial competitors. These factors include specialized metabolites. For instance, as populations of Vibrionales bacteria SWAT-3 grow they release extracellular metabolites, including the antibiotic andrimid, into their surrounding environment. When *Vibrio cholerae* is exposed to a gradient of andrimid, repulsive motility is induced and *V. cholerae* escapes competition (139). Finally, some bacteria are able to directly sense competitors by monitoring the integrity of their own cell envelopes. Such as the case of *Pseudomonas aeruginosa*, which responds to type VI secretion system-mediated attacks by directing the assembly and trigger of its own type VI secretion system directionally towards the offending competitor (116). As illustrated by these examples and others the ability to sense and respond to competitors and changing environmental conditions is essential for survival.

Two-component signaling (TCS) systems are among the primary mechanisms through which bacteria sense and respond to their external environments (223). The typical TCS system is comprised histidine kinase, which is generally membrane-bound, and its cognate, cytoplasmic response regulator, which is usually a DNA-binding protein. When the histidine kinase senses its corresponding signal, it undergoes ATP-dependent autophosphorylation on a conserved histidine residue. Next, this phosphate group is transferred onto an aspartic acid residue on the response regulator. After the phosphotransfer reaction, the response regulator changes its conformation, which affects its DNA-binding activity. The phosphorylated response regulator is a transcription factor and changes gene expression in response to the original signal (183). The *Bacillus subtilis* genome contains genes for 30 complete TCS pairs (223). Traditional laboratory approaches using genetic screens and mutational analyses have identified the signals and corresponding responses for many TCS signals. These TCS systems are responsible for sensing and maintaining metabolic homeostasis, nutrient uptake, and cell envelope structure, among other functions. However, many TCS system functions remain unknown because their corresponding deletion mutants have no phenotype under standard laboratory conditions. While many of these TCS systems are "non-essential" under laboratory conditions, their presence in the genome suggests this suite of signaling systems likely provides a selective advantage in a competitive environment.

The cell envelope is a common target for antibiotics and excessive damage to this important structure is lethal (237–239). Thus, it is important for bacterial cells to monitor

the condition of their envelopes in response to the environment and attack by other cells (240, 241). Accordingly, of the 30 complete TCS pairs encoded in the *B. subtilis* genome (223), currently ten are known to be involved in the regulation and maintenance of the membrane and/or cell wall and resistance to antibiotics that target these structures (193, 221, 222, 241–250). Typically, identifying the signals sensed by TCS systems is difficult. Of particular interest are signals that indicate damage to cells, as these signals may represent new therapeutic targets that would allow circumvention of adaptive cellular responses. The identities of many TCS system signals have been genetically inferred, with fewer signals having been experimentally demonstrated. For example, it has been demonstrated that the histidine kinase PhoR senses intermediates of wall teichoic acid synthesis as a proxy for cellular phosphate levels (249) and the histidine kinase KinC senses potassium ion leakage (27).

Streptomyces sp. Mg1 (*S.* Mg1) produces a family of linear polyketides known as linearmycins (248). The linearmycins induce progressive lysis and degradation of *B. subtilis* cultured next to *S.* Mg1 (47, 248). We previously identified point mutations in the *yfiJK*, encoding a TCS system, responsible for causing *B. subtilis* to become linearmycin resistant (248). Deletion of the *yfiJK* operon had no effect on competitive outcome when *B. subtilis* was cultured with *S.* Mg1, suggesting that the point mutations were gain-of-function. Indeed, we found that strains of *B. subtilis* with the *yfiJK* point mutations increased expression of the *yfiLMN* operon, encoding an ATP-binding cassette (ABC) transporter necessary for linearmycin resistance. We also observe that the

linearmycin resistant mutants form biofilm-like colonies on rich media, suggesting that the YfiJK system promotes biofilm formation.

In the present study, we investigated how *B. subtilis* linearmycin resistant mutants form biofilms. To investigate this phenotype, we started by reevaluating the genes in the YfiK regulon. We find that YfiK only regulates the expression of the *yfiLMN* operon. We show that the biofilm phenotype is dependent upon *yfiM* and *yfiN* but not *yfiL*. Using transposon mutagenesis, we identified additional genes that are not differentially regulated in linearmycin resistant mutants but are required for biofilm formation. Next, we sought to identify signals that the YfiJK-LMN system senses. We used a transcriptional fusion of the *yfiLMN* promoter to *lacZ* as a reporter for YfiJK activity. We show that *B. subtilis* responds to *S.* Mg1 during competition by inducing expression of the *yfiLMN* operon. Finally, we show that activation of the *yfiLMN* promoter is dependent upon linearmycins, which are sensed by YfiJ. Together, our data indicate that *B. subtilis* responds to competition with *S.* Mg1 by specifically regulating expression of a linearmycin resistance transporter, which also affects colony morphology. Our results provide new insight into the function of TCS systems and ABC transporters in *B. subtilis* and suggest that concerted activation of specific resistance and biofilm functions may promote *B. subtilis* fitness when faced with competitive challenge by *S.* Mg1.

Results

yfiJK complementation configuration influences colony phenotypes

In our previous study, we identified gain-of-function point mutations within the *yfiJK* operon that were responsible for causing *B. subtilis* to become resistant to linearmycins (248) (Figure 12A). Nine of these point mutations occurred within *yfiJ*, encoding a histidine kinase. We previously confirmed the *yfiJ* alleles by complementing a Δ*yfiJ* deletion strain at the ectopic *lacA* locus with monocistronic *yfiJ* under control of its native promoter and a plasmid-derived intrinsic terminator (Figure 12B). We also identified a single point mutation in *yfiK*, which encodes the cognate response regulator. Both open reading frames are part of a single transcript, as the *yfiJ* stop and *yfiK* start codons overlap and there are no putative promoter sequences for *yfiK* internal to the *yfiJ* sequence (Figure 12B). In addition, global expression profiles of *B. subtilis* confirm that *yfiJ* and *yfiK* are part of a bicistronic mRNA (251). Therefore, to test our *yfiK* allele, we complemented a Δ*yfiJK* deletion strain with bicistronic *yfiJK* at the ectopic *amyE* locus under the control of the native promoter and intrinsic terminator (Figure 12B). When complementing their respective deletion strains all identified point mutations resulted in linearmycin resistance, regardless of complementation configuration.

We noticed phenotypic variation for the *yfiJ*^{A152E} allele depending on the complementation configuration. When we complemented the Δ*yfiJ* deletion strain with monocistronic *yfiJ*^{A152E}, the *B. subtilis* colony reproducibly spreads out over the agar surface when cultured next to *S.* Mg1 (Figure 12A). However, when we complemented

the Δ*yfiJK* deletion strain with the bicistronic *yfiJ*^{A152E}*K*, the *B. subtilis* colony did not spread in response to *S.* Mg1. However, the bicistronic *yfiJ*^{A152E}*K* complement was linearmycin resistant and developed abnormal morphology (Figure 12A). We hypothesized the differences in phenotype observed for the two strain configurations may result from effects of the complementation configuration. For example, the expression levels from the complementation loci (*amyE* vs. *lacA*), the relative strength of the native (-9.30 kcal/mol) and plasmid-derived (-13.20 kcal/mol) intrinsic terminators we used, or simply disruption of regulatory functions dependent on the bicistronic arrangement of *yfiJK* could explain the differences between the *yfiJ*^{A152E} monocistronic and *yfiJ*^{A152E}*K* bicistronic complements. Though we currently do not know what factor(s) are responsible for the phenotypic variation we observe, we wanted to determine if complementation configuration affects YfiJK signaling.

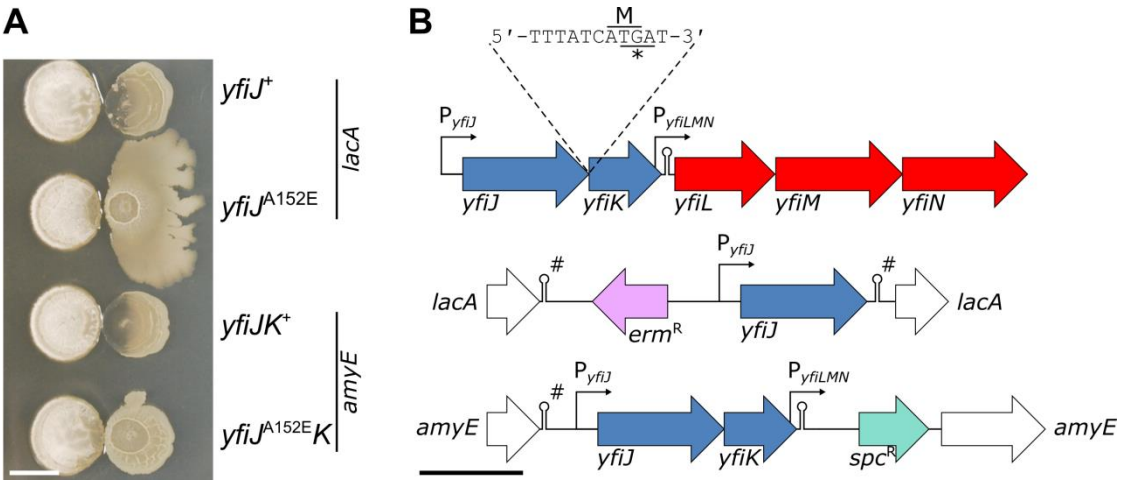

Figure 12. *yfiJ* complementation configuration influences competitive outcomes with *S.* Mg1

(A) Wild type *S.* Mg1 (PDS0543) colonies (left) were spotted with *B. subtilis* colonies (right). The different genotypes of the *B. subtilis* colonies are labeled on the right. The strains of *B. subtilis* with *yfiJ*$^{+}$ (PDS0571) and *yfiJ*^{A152E} (PDS0572) were complemented at the *lacA* locus as monocistrons with its native promoter and a plasmid-derived terminator. The strains of *B. subtilis* with *yfiJK*$^{+}$ (PDS0627) and *yfiJ*^{A152E}*K* (PDS0685) were complemented at the *amyE* locus with their native operon structure including the promoter and terminator. The labels on the right indicate complementation locus. The strains with wild-type *yfiJ* or *yfiJK* suffer lysis and colony degradation. Both strains with *yfiJ*^{A152E} alleles are resistant to linearmycin-induced lysis, but the *yfiJ*^{A152E} monocistron strain displays a motile response to *S.* Mg1 that is absent in the *yfiJ*^{A152E}K strain. The photograph was taken after 72 h co-incubation on MYM agar. The photograph is representative of triplicate samples. Scale bar is 5 mm. **(B)** (*top*) The configuration for *yfiJKLMN* at the native chromosome locus. The overlapping stop codon in *yfiJ* and start codon in *yfiK* are marked with * and M, respectively. (*middle*) The monocistronic complementation construct for *yfiJ* inserted at *lacA*. (*bottom*) The bicistronic complementation construct for *yfiJK* inserted at *amyE*. Open-reading frames are shown as block arrows, promoters are shown as arrows, and intrinsic terminators are shown as hairpins. Plasmid-derived terminators marked with a # symbol. The scale bar is 1 kb. *erm*^{R}, erythromycin resistance cassette. *spc*^{R}, spectinomycin resistance cassette.

The YfiJK system regulates a single operon

Previously, we used RNA-seq to compare the transcriptomes of the *yfiJ*^{A152E}*K* and the *yfiJK*$^{+}$ bicistronic complement strains. We found that expression of only the downstream *yfiLMN* operon was significantly upregulated (248) (Figure A7A). We identified a single active promoter within 150 bp upstream of *yfiL* and predicted no promoter sequences within *yfiL*, *yfiM*, or *yfiN* (Figure 12B). Therefore, to identify differential regulatory effects of the *yfiJ*^{A152E} monocistronic and *yfiJ*^{A152E}*K* bicistronic complements, we used quantitative reverse transcription PCR (qRT-PCR) to compare the relative fold expression of *yfiL* between the strains. In the *yfiJ*^{A152E} monocistronic complement, we found that the expression of *yfiL* was ~135 fold higher than *yfiJ*$^{+}$. For comparison, the expression of *yfiL* in the *yfiJ*^{A152E}*K* bicistronic complement was ~20 fold higher than *yfiJK*$^{+}$ (248). This suggests that the increased colony spreading exhibited by the monocistronic complement may be due, in part, to increased expression of the *yfiLMN* operon.

Given our interest in understanding the downstream functions of YfiJK, we decided to use the monocistronic complements as our strain background for all following experiments. The results from both colony morphology assays and qRT-PCR for *yfiL* demonstrated that this strain background would enhance the contrast between expression differences from the wild-type *yfiJ*$^{+}$ and mutant *yfiJ*^{A152E} complement strains. In addition to the *yfiLMN* operon, we identified the gene *des* and the *yvfRS* operon as significantly downregulated by YfiK (248) (Figure A7A). Because *yfiL* fold expression was much

higher in the monocistronic complement, we returned to our previous transcriptomic data to determine if expression of other genes, putatively repressed by YfiK, might be more extremely downregulated when comparing expression levels from the *yfiJ*^{A152E} and *yfiJ*$^{+}$ monocistronic complements. However, using qRT-PCR we found no change in *yvfS* expression and increased expression of *des*, which is inconsistent with our previous results (Figure A8). Furthermore, artificial overexpression of *des* from a xylose-inducible promoter had no impact on linearmycin resistance or colony morphology in *yfiJK*$^{+}$ or *yfiJ*^{A152E}*K* bicistronic complements (Figure A9). All taken together, given the magnitude of the difference of *yfiL* expression compared to *des* and *yvfS*, these results suggest that the *yfiLMN* operon is the only target directly regulated by YfiK.

Expression of the yfiLMN operon leads to biofilm formation

In monoculture, strains with the *yfiJ*^{A152E} allele develop colonies with a rough texture and a characteristic circular wrinkle in the center of the colony. In contrast, strains expressing a wild-type *yfiJ*$^{+}$ allele develop relatively flat and featureless colonies (Figure 13). We reasoned that production of the YfiLMN ABC transporter would be responsible promoting biofilm formation. To test this hypothesis, we constructed a deletion of the *yfiLMN* operon in both the *yfiJ*$^{+}$ and *yfiJ*^{A152E} strain backgrounds. In addition to rendering *B. subtilis* sensitive to linearmycin, the *yfiJ*^{A152E} Δ*yfiLMN* strain forms a colony that is indistinguishable from the wild type (Figure 13,Table 5). When we complemented the *yfiLMN* deletion with a constitutively expressed copy of the

yfiLMN operon from the $P_{spac(C)}$ promoter, both resistance and biofilm formation were restored, regardless of *yfiJ* allele (Figure 13, Table 5).

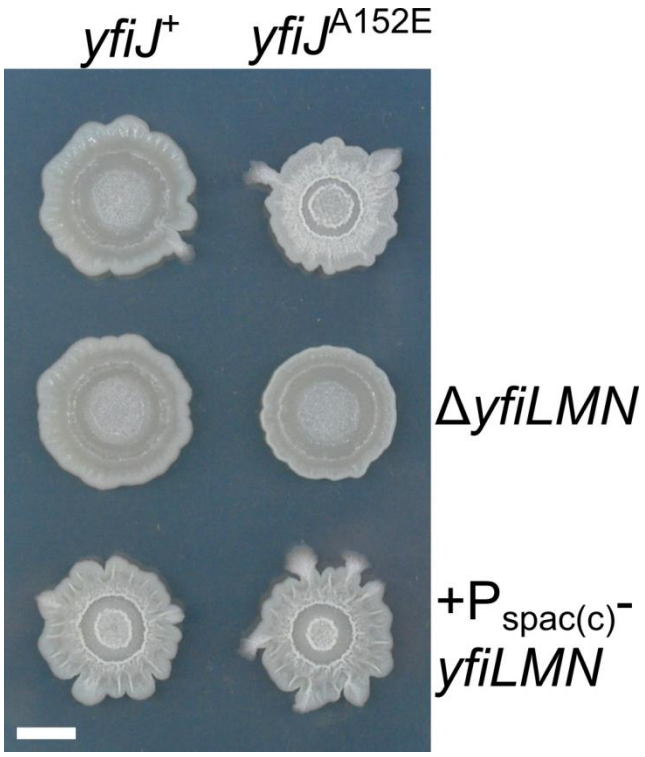

Figure 13. The biofilm morphology of linearmycin resistant mutants is dependent upon *yfiLMN*

The *yfiJ* allele is indicated on the top and the *yfiLMN* status is indicated on the right. The *B. subtilis yfiJ*$^{+}$ strain (PDS0571) develops as a smooth colony but the *yfiJ*^{A152E} strain (PDS0572) develops a biofilm structure. Introduction of the Δ*yfiLMN* deletion has no phenotypic effect on a *yfiJ*$^{+}$ strain (PDS0798) and causes the *yfiJ*^{A152E} strain (PDS0799) to develop as a smooth colony. Complementation of the Δ*yfiLMN* deletion with constitutively expressed *yfiLMN* ($P_{spac(c)}$-*yfiLMN*) results in both the *yfiJ*$^{+}$ strain (PDS0801) and the *yfiJ*^{A152E} strain (PDS0802) developing as biofilms. The photograph was taken after 48 h incubation on MYM agar. The photograph is representative of duplicate samples. Scale bar is 5 mm.

Table 5. YfiLMN functions in linearmycin resistance and biofilm development

	Linearmycin Resistance		Biofilm Development	
	yfiJ^{+}	*yfiJ*^{A152E}	*yfiJ*$^{+}$	*yfiJ*^{A152E}
yfiLMN^{+}	-	+	-	+
Δ*yfiLMN*	-	-	-	-
Δ*yfiLMN* + $P_{spac(c)}$-*yfiLMN*	+	+	+	+
Δ*yfiL*	-	-	-	+
Δ*yfiM*	-	-	-	-
Δ*yfiN*	-	-	-	-

Wild-type alleles are designated with a superscript $^{+}$ symbol. The $P_{spac(c)}$-*yfiLMN* strains constitutively express *yfiLMN* regardless of *yfiJ* allele. The + and - symbols indicate presence or absence, respectively, of linearmycin resistance in co-culture with *S*. Mg1 or biofilm formation in monoculture on MYM media.

We asked if a functional ABC transporter is necessary for both linearmycin resistance and biofilm formation. ABC transporters are typically comprised of two copies of a cytoplasmic nucleotide-binding domain protein, which provides energy through ATP hydrolysis, and two membrane-spanning domains that form the pore (252). In the case of YfiLMN, the nucleotide-binding domain is encoded by *yfiL* and the membrane-spanning domains are encoded by *yfiM* and *yfiN* (192). We constructed strains with single deletions of *yfiL*, *yfiM*, and *yfiN*. Surprisingly, the Δ*yfiL* strain was still able to form a biofilm, whereas the Δ*yfiM* and Δ*yfiN* single deletion mutant colonies

developed wild-type, non-biofilm morphologies (Table 5). While the Δ*yfiL* strain was still able to form a biofilm, it was sensitive to lysis when cultured with *S.* Mg1 (Table 5). This observation indicates that biofilm formation and linearmycin resistance are separable phenotypes, and that resistance likely requires a functional ABC transporter while biofilm formation does not. Consistent with our previous results, deletion of genes encoding important developmental regulators and structural components of biofilms had no effect on linearmycin resistance (248). Further, the wrinkled morphology of the *yfiJ*^{A152E} strains is reminiscent to that of *P. aeruginosa* mutants that are unable to produce the alternative electron acceptor phenazine. In phenazine-deficient mutants, wrinkling increases surface area but can be suppressed by supplementation with an alternative electron acceptor, such as nitrate (253). We hypothesized that overexpression of the *yfiLMN* operon may similarly affect redox homeostasis in *B. subtilis*. However, while we found nitrate supplementation caused *B. subtilis* to form smaller colonies, the *yfiJ*^{A152E} strain remained wrinkled indicating that biofilm formation is not likely caused by redox stress (Figure A10).

Transposon mutagenesis identifies additional genes involved in YfiLMN-mediated biofilm formation

Expression of the *yfiLMN* operon alone was sufficient to cause *B. subtilis* to form biofilms (Figure 13, Table 5). This observation is particularly provocative because canonical *B. subtilis* biofilm development requires numerous changes in gene expression (197). Therefore, we asked how YfiLMN causes biofilm formation. Based on protein

sequence alignments, YfiLMN belongs to the class of ABC exporters (192). However, based on the ability of the *yfiJ*^{A152E} Δ*yfiL* strain to form biofilms (Table 5), active transport is likely not required for this process. Therefore, we sought to use transposon mutagenesis to identify genes whose products are necessary for the biofilm formation but are not transcriptionally regulated by YfiK.

We introduced pMarA, a transposon mutagenesis plasmid (227) into the *yfiJ*^{A152E} strain background. Next, we screened colonies for aberrant morphology, when compared to the parental *yfiJ*^{A152E} strain. In total we screened 13,577 colonies. Initially we identified 97 isolates with abnormal colony morphology (0.71% of total colonies screened). Of the 97 isolates, 19 (0.14% total) were of particular interest because, the colonies developed non-biofilm morphologies typical of *yfiJ*$^{+}$ strains. To confirm linkage to the transposon insertion, we prepared SPP1 phage lysates from the 19 isolates and transduced a fresh *yfiJ*^{A152E} strain. The non-biofilm morphology was linked in 11 transposon-mutagenized strains (0.08% total). We extracted genomic DNA from the 11 linked transposon mutants and identified the position of each transposon insertion (Table 6).

Table 6. Transposon insertion loci identified in morphology screen

Insertion Position*	Identity	Gene Product	Annotated Function
76954(-)	IGR$_{hprT\text{-}ftsH}$	*hprT*: hypoxanthine phosphoribosyltransferase *ftsH*: ATP-dependent metalloprotease	purine salvage and interconversion, control of *ftsH* expression cell-division protein and general stress protein (class III heat-shock)
423837(+)	*gerKB*	subunit of GerK germination receptor	spore germination
1525015(+)†	IGR$_{rpoY\text{-}yrkA}$	*rpoY*: RNA polymerase ε subunit *yrkA*: putative membrane associated protein	control of RNA polymerase activity unknown
1866388(-)	IGR$_{ymaF\text{-}miaA}$	*ymaF*: unknown *miaA*: tRNA isopentenylpyrophosphate transferase	unknown tRNA modification
2300897(+)‡	*ilvD*	dihydroxy-acid dehydratase	biosynthesis of branched-chain amino acids
2328299(+)	*ypvA*	similar to ATP-dependent helicase	unknown
2625166(+)	*dnaJ*	heat-shock protein (activation of DnaK)	protein quality control
2627755(+)	*dnaK*	class I heat-shock protein (molecular chaperone)	protein quality control
2729794(+)	*azlB*	Lrp family repressor of the *azlBCD-brnQ-yrdK* operon	regulation of branched-chain amino acid transport
2887777(+)	IGR$_{tig\text{-}ysoA}$	*tig*: trigger factor (prolyl isomerase) *ysoA*: putative hydrolase	nascent polypeptide folding unknown
3856278(+)	BSU_MISC_RNA_57	T-box upstream of *thrZ*	regulation of *thrZ* expression

*Insertion nucleotide number and strand orientation is with respect to a sequenced genome of *B. subtilis* (GenBank accession: AL009126.3). †This insertion was identified in two independent isolates. ‡This insertion has a phenotype in *yfiJ*^{A152E} but not *yfiJ*$^{+}$ but does not lead to non-biofilm colony morphology. IGR, intergenic region

The gene functions identified in the screen do not fall into any known *B. subtilis* colony development pathways. However, we note a pattern for transposon insertions in and near genes associated with protein folding and quality control. We identified transposon insertions in *dnaJ*, *dnaK*, in the intergenic region between *hprT* and *ftsH*, and upstream of *tig* (Table 6). DnaJ and DnaK are components of a molecular chaperone complex involved in class I heat shock response (254, 255). FtsH is a membrane-anchored metalloprotease with diverse functions that include biofilm formation, heat shock response and chaperone activity (256–258). Tig is a ribosome-associated chaperone that promotes the proper folding of nascent polypeptides (259). The transposon insertions we identified in *dnaJ* and *dnaK* occur near the 3′ end and 5′ of the coding sequences, respectively, and likely disrupt the function of both proteins. It is known that the expression of *ftsH* is regulated by a complex formed by HprT and TilS (260). Therefore the transposon insertion may have polar effects on *ftsH* expression. Likewise, the transposon insertion upstream of *tig* may influence *tig* expression, which could lead to a change in biofilm formation through loss of chaperone activity.

We also identified branched chain amino acids as a possible biofilm-related function. First, we identified an insertion in *azlB*, which encodes a Lrp family repressor of *azlB*CD-*brnQ-yrdK* operon. This operon encodes genes involved in transport of branched chain amino acids (261). Second, we also identified a transposon insertion in *ilvD*, which encodes a dihydroxy-acid dehydratase involved in branched chain amino acid biosynthesis (262). Disruption of *ilvD* in a *yfiJ*^{A152E} background results in colonies

with lobate edges but otherwise had no visible phenotype in a *yfiJ*$^{+}$ background (Figure A11). In addition to protein synthesis, *B. subtilis* uses branched chain amino acids as precursors for anteiso-branched-chain fatty acid biosynthesis. Supplementation of isoleucine into culture medium can cause *B. subtilis* to produce more anteiso-branched-chain fatty acids (246), which influences membrane fluidity and may affect membrane protein dynamics. However, we found that isoleucine supplementation had no effect on either *yfiJ*$^{+}$ or *yfiJ*^{A152E} strains (Figure A12). Additional characterization is required to determine how *alzB*, *ilvD*, and the other identified transposon insertions influence YfiLMN-mediated biofilm formation.

The YfiJK system responds to linearmycins

We were interested in identifying the signal(s) that naturally activate the YfiJK system and lead to expression of the *yfiLMN* operon. To identify patterns of *yfiLMN* operon expression, we first analyzed results from a large scale transcriptional analysis of *B. subtilis* grown under 269 different conditions (251). In that study, under all conditions tested expression of the *yfiLMN* operon was low and did not appreciably change (Figure A7B-C). These transcriptional profiling experiments suggest that the YfiJK system is not activated under monoculture growth conditions. Because activating *yfiJK* mutations caused *B. subtilis* to become linearmycin resistant due to expression of the *yfiLMN* operon (248), we reasoned that YfiJ may sense linearmycins and become activated during competition with *S.* Mg1. To test this hypothesis, we cultured a *B. subtilis* strain with a transcriptional fusion of the *yfiLMN* promoter to *lacZ* (P_{yfiLMN}-*lacZ*) with *S.* Mg1.

We found that the P_{yfiLMN}-*lacZ* reporter was only active in the portion of the colony immediately adjacent to *S.* Mg1 (Figure 14A). To determine if the YfiJK system responds to linearmycins, we cultured the reporter strain with *S.* Mg1 Δ*lnyI*, a strain that is unable to produce linearmycins (Hoefler BC, Stubbendieck RM, Josyula NK, Moisan SM, Schulze EM, and Straight PD; in preparation). We found that the P_{yfiLMN}-*lacZ* was not induced by *S.* Mg1 Δ*lnyI* (Figure 14A). As a direct test that the YfiJK system responds to linearmycins, we spotted isolated linearmycins on top of a pre-grown *B. subtilis* colony. Over the following day, we observed that the *B. subtilis* colony was lysed from the inside out. We observed strong activation of the reporter on the periphery of the lysed region of the colony (Figure 14B). Together these results demonstrate that the YfiJK system responds to linearmycins directly and not some other factor produced by *S.* Mg1.

Expression of the yfiLMN operon is induced by multiple polyenes

A characteristic feature of the linearmycin family is the presence of multiple conjugated double bonds (172, 173). The polyene moiety is also present in several structurally related molecules that target the cytoplasmic membrane of fungi. These polyene antibiotics interact with ergosterol, which leads to membrane permeabilization and cell death (177–180). Because YfiJ is a membrane-anchored histidine kinase, we hypothesized that linearmycins may be sensed directly or as a secondary consequence of perturbation to the *B. subtilis* membrane. Therefore, we first asked if other polyenes activate YfiJK signaling or if activation is due to lytic stresses. First, we tested a linear

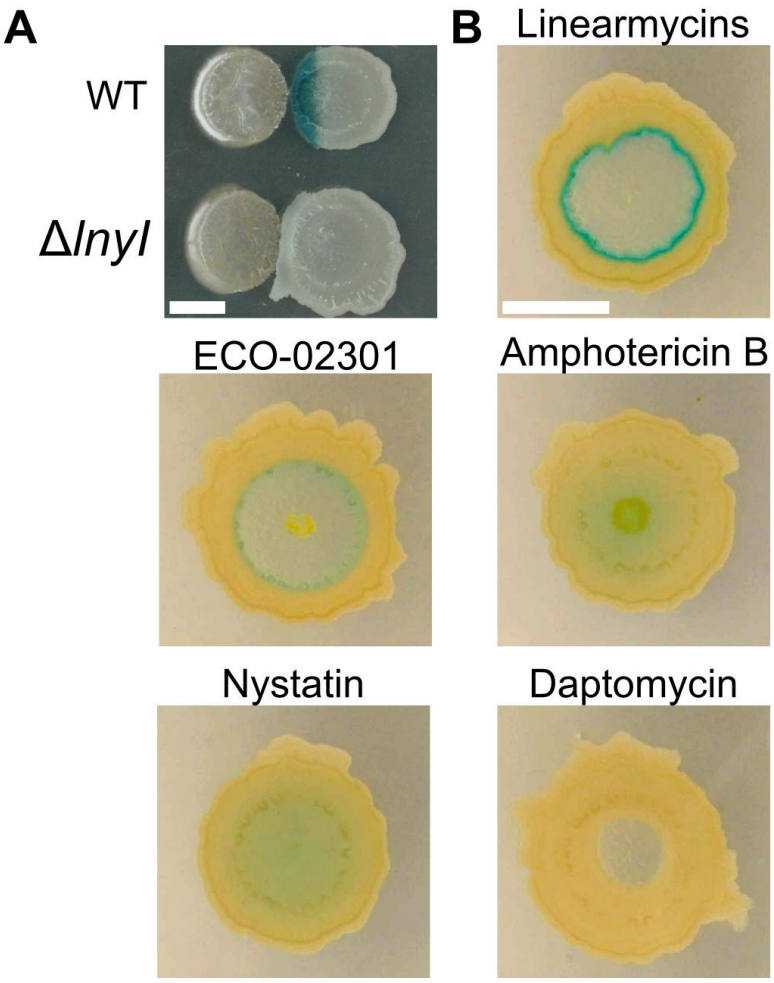

Figure 14. YfiJK signaling is activated by linearmycins and other polyenes

(A) A strain of *B. subtilis* (right) with a transcriptional fusion of *lacZ* to the *yfiLMN* promoter (P_{yfiLMN}-*lacZ*) (PDS0838) was cultured with either *S.* Mg1 (left) wild type (WT) (PDS0543) or Δ*lnyI* (PDS0755), which does not produce linearmycins. The *B. subtilis* colony cultured with wild type *S.* Mg1 suffers lysis and colony degradation in addition to activation of the P_{yfiLMN}-*lacZ* reporter. The *B. subtilis* colony cultured with *S.* Mg1 Δ*lnyI* is not lysed and does not activate the reporter. The photograph was taken after 72 h co-incubation of MYM agar with X-gal. The photograph is representative of quadruplicate samples. **(B)** The indicated molecules were spotted on top of pre-grown *B. subtilis* colonies. Exposure to linearmycins caused the *B. subtilis* colony to lyse inside-out and activate the P_{yfiLMN}-*lacZ* reporter on the periphery of the lysed region. Likewise, ECO-02301 also lyses *B. subtilis* and activates the P_{yfiLMN}-*lacZ* reporter. Amphotericin B and nystatin activate the P_{yfiLMN}-*lacZ* reporter without causing lysis. Daptomycin lyses *B. subtilis* without activating the P_{yfiLMN}-*lacZ* reporter. The photographs were taken after *B. subtilis* colonies were exposed to the molecules for 24 h. The *B. subtilis* colonies were photographed from the bottom. The brightness and contrast were evenly adjusted across the panels to better show the blue color on the amphotericin B and nystatin-treated colonies. Scale bar is 5 mm.

polyene ECO-02301 that also causes lysis of *B. subtilis* (176, 248). Similar to linearmycin exposure, we observed that ECO-02301 lyses *B. subtilis* and activates the P_{yfiLMN}-*lacZ* reporter on the periphery of the lysed region (Figure 14B). However, activation of the P_{yfiLMN}-*lacZ* reporter by ECO-02301 was much weaker than activation by linearmycins. Next, we tested the cyclic polyenes amphotericin B and nystatin. While the cyclic polyenes do not lyse *B. subtilis*, they do weakly activate the P_{yfiLMN}-*lacZ* reporter and demonstrate that activation of YfiJK signaling is not dependent upon lysis (Figure 14B). As a control, we also tested daptomycin, a structurally unrelated lipopeptide that lyses *B. subtilis* (248, 263). In contrast to the polyenes, lytic concentrations of daptomycin do not activate the P_{yfiLMN}-*lacZ* reporter (Figure 14B).

We observed that the strongest activation of the P_{yfiLMN}-*lacZ* reporter was caused by linearmycin exposure. We spotted 15 µg of amphotericin B (~16 nanomol), daptomycin (~9 nanomol), ECO-02301 (~12 nanomol), and nystatin (~16 nanomol) onto the *B. subtilis* colonies. Based on HPLC measurements, we estimate that we spotted between 3 – 6 µg of linearmycins (~3 – 5 nanomol). This estimation suggests that YfiJK signaling is most strongly activated specifically by linearmycins. Intriguingly, we previously found that a linearmycin resistant mutant was only weakly cross resistant to ECO-02301, despite their similar structures (248). Taken together, our results indicate that linearmycins and not lytic membrane stress stimulates YfiJK signaling. We note that exposure to amphotericin B and nystatin can cause potassium ion leakage in *B. subtilis*

(27). Therefore, it is possible that YfiJK signaling is activated by other membrane perturbations induced by polyene antibiotics.

Transposon mutagenesis suggests linearmycins are directly sensed

The known mechanisms for polyene sensing are indirect. For instance, in the budding yeast *Saccharomyces cerevisiae*, nystatin is sensed by SLN1, which is an osmosensing histidine kinase that senses changes in turgor pressure and detachment of the cytoplasmic membrane from the cell wall (264). Likewise, in *B. subtilis* nystatin is sensed as an effect of induced potassium leakage from the cell by the histidine kinase KinC (27). As a first approach to ask if linearmycins are indirectly sensed we used transposon mutagenesis. Specifically we asked if we could identify a mutant that activates the P_{yfiLMN}-*lacZ* reporter in the absence of an inducing polyene. We obtained four isolates (0.02% total) with spontaneous gain of blue color from a screen of 18,002 transposon-mutagenized colonies. After phage transduction we retested transductants for P_{yfiLMN}-*lacZ* reporter activation. We found that 2/3 transductants (0.01% total) were constitutively blue. For one isolate we never recovered transductants. In both positive transductants, we found that transposon insertion disrupted *lacR*. LacR is a transcriptional repressor for expression of *lacA*, which encodes an endogenous β-galactosidase. Thus, the blue color in these transductants resulted constitutive *lacA* expression and not activation of the P_{yfiLMN}-*lacZ* reporter construct (265). Assuming a Poisson distribution, we calculated the probability of screen saturation to be ~98.3%. Though inconclusive, the results and density of this transposon screen suggest that *B. subtilis* either senses linearmycin directly or that insertion mutants cannot reproduce the

effects of linearmycin exposure. To address these possibilities we first needed to determine the identity of the linearmycin sensor.

YfiLMN is not required for B. subtilis *to respond to linearmycins*

YfiJ has no canonical PAS sensing domains, which are often found in histidine kinases (266). Protein domain analysis predicted five to six transmembrane helices, with no substantial extracellular domain (≤ 17 residues) (Figure A14A). Otherwise, no apparent sensing domains were detected. We previously reported similarities between the YfiJK-LMN system and peptide sensing and detoxification (PSD) modules encoded in the *B. subtilis* genome. For instance, the genetic context for *yfiJKLMN*, with TCS system and related ABC transporter functions encoded side-by-side is identical to the organization of the PSD modules (182, 193) (Figure 12B). The bacitracin sensing and detoxification system BceAB-RS is currently the best characterized PSD system (222, 267–274). Similar to YfiJ, the histidine kinase BceS lacks PAS domains or a recognizable extracellular sensor sequence (Figure A14B). Instead, the ABC transporter BceAB is responsible for both sensing and detoxifying peptide antibiotics (271). Therefore Δ*bceAB* strains are unable to respond to bacitracin or induce expression of a P_{bceA}-*lacZ* transcriptional reporter (268).

Given the structural and genetic context similarities between YfiJ and BceS, we wanted to test if YfiLMN is required for *B. subtilis* to respond to linearmycins. We cultured Δ*yfiLMN* strains with *S.* Mg1 and found that the P_{yfiLMN}-*lacZ* reporter was still

activated during competition with *S.* Mg1 (Table 7). Thus, unlike the bacitracin sensing system, YfiLMN does not act as the linearmycin sensor for *B. subtilis*. Unexpectedly, we found that the P_{yfiLMN}-*lacZ* reporter was constitutively active in the *yfiJ*$^{+}$ Δ*yfiLMN* strain during monoculture but the *yfiJ*^{A152E} Δ*yfiLMN* strain responded identically to the *yfiJ*$^{+}$ strain (Table 7). We speculate that YfiLMN may have an additional regulatory function with respect to controlling activation of YfiJK signaling and the A152E substitution may affect this regulatory function.

Table 7. The YfiJ TMD is required for linearmycin sensing

	Activation of P_{yfiLMN}-*lacZ*	
Genotype	-*S.* Mg1	+*S.* Mg1
yfiJ^{+}	-	+
yfiJ^{A152E}	+	+
yfiJ^{+} Δ*yfiLMN*	+	+
yfiJ^{A152E} Δ*yfiLMN*	-	+
yfiJ$^{\Delta TMD}$	-	-
yfiJ$^{\Delta TMD, A152E}$	-	-
	Activation of P_{bceA}-*lacZ*	
Genotype	-*S.* Mg1	+*S.* Mg1
yfiJ^{TMD}-*bceS*^{cyto}	-	-
yfiJ$^{TMD\text{-}linker}$-*bceS*^{cyto}	TBD	TBD

Wild-type alleles are designated with a superscript $^{+}$ symbol. The + and - symbols indicate presence or absence, respectively, of blue color as an indication of reporter activation. TBD, to be determined.

YfiJ requires the transmembrane domain for B. subtilis *to respond to linearmycins*

The next most feasible identity of the linearmycin sensor was YfiJ. Specifically we hypothesized that the transmembrane domain in YfiJ ($YfiJ^{TMD}$) is responsible for sensing linearmycins. We generated a truncation of *yfiJ* by deleting the sequence that encodes the transmembrane helices ($yfiJ^{\Delta TMD}$). We cultured $yfiJ^{\Delta TMD}$ with *S.* Mg1 and found that there was no activation of the P_{yfiLMN}-*lacZ* reporter (Table 7). Unexpectedly, when we cultured a $yfiJ^{\Delta TMD,\ A152E}$ strain with *S.* Mg1 there was also no activation of the P_{yfiLMN}-*lacZ* reporter (Table 7). As $yfiJ^{A152E}$ strains constitutively express the *yfiLMN* operon, even in the absence of linearmycins, we hypothesize that membrane anchoring by the TMD is required for proper folding of YfiJ or additional regulatory functions such as phosphorylation of YfiK.

As the results of the TMD truncation were inconclusive we sought an alternative means to determine if the $YfiJ^{TMD}$ senses linearmycins. Chimeras are a powerful tool to determine which protein domains in histidine kinases are responsible for sensing and responding to external stimuli (e.g. 27, 264, 275–279). Therefore we generated a chimeric histidine kinase consisting of the $YfiJ^{TMD}$ fused to the cytoplasmic domain of BceS ($BceS^{Cyto}$). If the $YfiJ^{TMD}$ senses linearmycins, we hypothesized that linearmycin exposure would result in the $YfiJ^{TMD}$-$BceS^{Cyto}$ chimera phosphorylating BceR instead of YfiK. To test the output of the chimeric $YfiJ^{TMD}$-$BceS^{Cyto}$, we generated a transcriptional fusion of the *bceA* promoter to *lacZ* (P_{bceA}-*lacZ*) (222). We cultured a strain encoding both $yfiJ^{TMD}$-$bceS^{cyto}$ and the P_{bceA}-*lacZ* reporter with *S.* Mg1. However, we found that

competition with *S.* Mg1 did not activate the P_{bceA}-*lacZ* reporter (Table 7). Currently, we are building a construct that includes the $YfiJ^{TMD}$ and cytoplasmic linker fused to the BceS dimerization and phosphotransfer and ATP-binding domains. We will test this construct for activation of the P_{bceA}-*lacZ* reporter during competition with *S.* Mg1.

Nystatin exposure provides subsequent protection against linearmycins

We wanted to determine if there are functional consequences for activation of YfiJK signaling in response to polyenes other than linearmycins. We hypothesized that if *yfiLMN* expression is induced by polyenes then *B. subtilis* should become more resistant to subsequent linearmycin exposure. We pre-cultured wild type *B. subtilis* in increasing concentrations of nystatin and then exposed cells to serial dilutions of linearmycins. We found that as the pre-culture nystatin concentration increased, there was a concurrent decrease in *B. subtilis* lysis by linearmycins (Figure A13). We verified that the increased linearmycin resistance was due to YfiLMN by repeating the experiment with an isogenic Δ*yfiLMN* strain. Without pre-culture in nystatin, we observed no differences in lysis when comparing the $yfiJ^+$ and $yfiJ^+$ Δ*yfiLMN* strains (Figure 15A). As expected, when we cultured $yfiJ^+$ *B. subtilis* in nystatin we observed increased linearmycin resistance. Unexpectedly, pre-culture in nystatin also protected the $yfiJ^+$ Δ*yfiLMN* strain from linearmycins. However, this linearmycin protection was reduced in comparison to $yfiJ^+$ strain (Figure 15B). Nystatin alone can protect *B. subtilis* from linearmycin but expression of the *yfiLMN* operon by nystatin pre-culture contributes more protection

against linearmycin. Currently, the YfiLMN-independent mechanism of nystatin-mediated linearmycin protection is unknown.

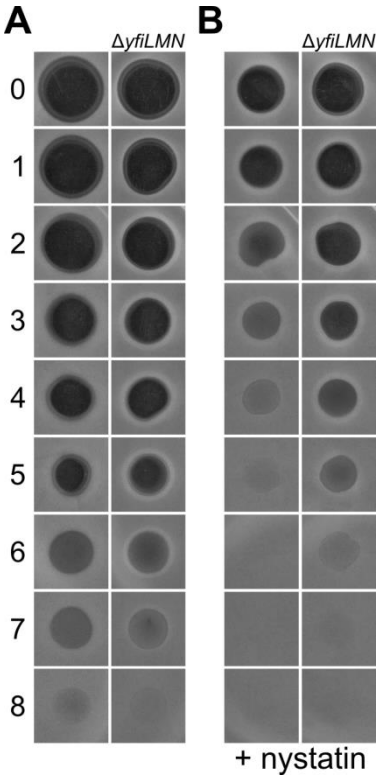

Figure 15. Preconditioning *B. subtilis* in nystatin enhances linearmycin resistance

Bacillus subtilis yfiJ$^+$ (PDS0571) and *yfiJ*$^+$ Δ*yfiLMN* (PDS0798) were preconditioned in **(A)** 0 or **(B)** 100 µg/mL nystatin then embedded in a soft agar overlay at equal cell density and spread over a MYM plate with the same concentration of nystatin. Two-fold serial dilutions of linearmycins were plated on top of the agar overlay. After 18 h incubation, the plates were photographed. Without the addition of nystatin, the lysis profiles are similar between the *yfiJ*$^+$ and the *yfiJ*$^+$ Δ*yfiLMN*. However, when *B. subtilis* was conditioned with nystatin both strains were more resistant to linearmycin but the *yfiJ*$^+$ strain is more resistant than the *yfiJ*$^+$ Δ*yfiLMN* strain. The numbers on the left indicate the dilution factor [$(1/2)^n$] for each panel.

Nystatin and KinC influence YfiLMN-mediated colony phenotypes

YfiJK signaling is activated by linearmycins and other polyenes. In addition, we showed that nystatin induces expression of the *yfiLMN* operon. Here, we return to our observation that expression of the *yfiLMN* operon leads to biofilm formation. We wanted to test if nystatin would induce YfiLMN-mediated morphological changes in *B. subtilis*. We cultured *yfiJ*$^{+}$ and *yfiJ*^{A152E} strains with and without nystatin. As expected, without nystatin we observed that the *yfiJ*^{A152E} strain forms a biofilm whereas the *yfiJ*$^{+}$ strain does not (Figure 16). However, when we cultured *yfiJ*$^{+}$ with nystatin (100 µg/mL), we observed biofilm formation. This *yfiJ*$^{+}$ biofilm was indistinguishable to a biofilm formed by *yfiJ*^{A152E} without nystatin supplementation. We tested the YfiLMN dependence of nystatin-induced biofilm formation by repeating the experiment with Δ*yfiLMN* strains. We found that a *yfiJ*$^{+}$ Δ*yfiLMN* strain only weakly formed biofilms at the highest concentration of nystatin. This observation suggests that nystatin activates expression of the *yfiLMN* operon and leads to biofilm formation.

We wanted to determine if KinC was required for nystatin-induced YfiLMN-mediated biofilm formation. We found that a *yfiJ*$^{+}$ Δ*kinC* strain is mucoid, consistent with defects in biofilm production (27, 258). Intriguingly, the *yfiJ*^{A152E} Δ*kinC* strain formed a colony that closely resembled a *yfiJ*$^{+}$ colony (Figure 16). Similarly, we found

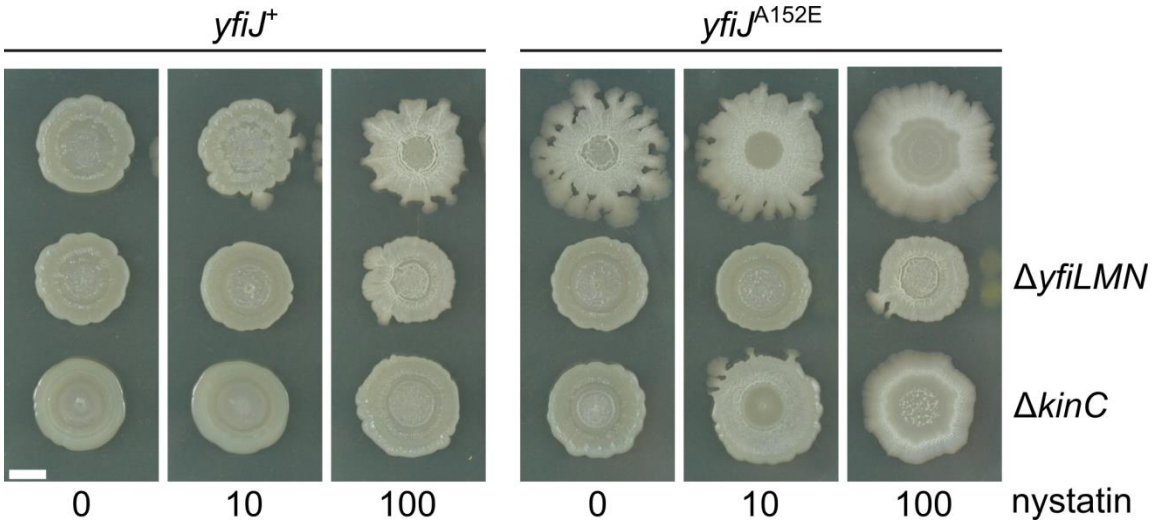

Figure 16. KinC is required for YfiLMN-mediated biofilm formation

The allele of *yfiJ* is indicated on the top. The *yfiLMN* and *kinC* status is indicated to the right. Without nystatin, the *yfiJ*$^{+}$ *B. subtilis* strain (PDS0571) produces a wild-type colony. At the highest concentration of nystatin, the *yfiJ*$^{+}$ strain forms a biofilm but the *yfiJ*$^{+}$ Δ*kinC* strain (PDS0914) does not. Without nystatin supplementation, the *yfiJ*^{A152E} strain (PDS0572) forms a biofilm but the *yfiJ*^{A152E} Δ*kinC* strain (PDS0915) does not. As the nystatin concentration increases the *yfiJ*^{A152E} strain begins to spread over the plate in a *yfiLMN*-dependent manner. Both Δ*yfiLMN* strains only form hints of a biofilm at the highest nystatin concentration. The photographs were taken after 48 h incubation on MYM agar with the nystatin concentration in µg/mL indicated under each panel. The photographs are representative of duplicate samples. Scale bar is 5 mm.

that at the highest nystatin concentrations that induce biofilm formation in *yfiJ*$^{+}$, the *yfiJ*$^{+}$ Δ*kinC* strain was unable to form a biofilm. Taken together, these results indicate that *kinC* is required for biofilm formation. The addition of nystatin caused the *yfiJ*^{A152E} strain to develop a new morphology. The *yfiJ*^{A152E} colonies flattened and spread out in a concentration-dependent manner. However, at the highest nystatin concentration, the Δ*kinC* deletion had only a small effect on the spreading morphology (Figure 16). As

both Δ*kinC* and Δ*yfiLMN* strains were unable to form biofilms under permissive media conditions or genetic backgrounds, we conclude that both gene products are required for YfiLMN-mediated biofilm formation.

Discussion

In this study, we used a model system to determine how one organism senses a competitor and elicits an appropriate response to bacterial competition. Here, we showed that the transmembrane domain of the histidine kinase YfiJ senses linearmycins produced by *S.* Mg1 and other polyenes. YfiJ then phosphorylates its cognate response regulator, which activates expression of the *yfiLMN* operon. *yfiL*, *yfiM*, and *yfiN* encode components of a linearmycin resistance ABC transporter that also induces biofilm formation. Further, we found that *yfiM* and *yfiN* but not *yfiL* are required for the biofilm phenotype of linearmycin resistant *B. subtilis* mutants. We identified other genes that are also required for YfiLMN-mediated biofilm formation including several chaperone-encoding genes. We also determine that *kinC* is required for YfiLMN-mediated biofilm formation.

In addition to YfiK acting as a transcriptional activator of the *yfiLMN* operon, we previously reported *des* and the *yvfRS* operon as putative candidates for repression by YfiK (Figure A7) (248). In the present study we took advantage of an observation that *B. subtilis* strains complemented with monocistronic $yfiJ^{A152E}$ exhibited a more extreme phenotype than strains complemented with bicistronic $yfiJ^{A152E}K$ (Figure 12). In our

previous study we focused on the latter strains for transcriptional analysis. Using the monocistronic complements, we determined that the YfiK only regulates *yfiLMN* operon, which is controlled by a single promoter.

We were interested in determining what factors cause linearmycin resistant *B. subtilis* to form biofilms. Because YfiK only regulates the *yfiLMN* operon, we targeted this operon to determine its effects on biofilm formation. We deleted the *yfiLMN* operon in a $yfiJ^{A152E}$ strain and found that the resulting colonies were indistinguishable from wild type. Further, we found that constitutive expression of the *yfiLMN* operon caused $yfiJ^{+}$ strains to form biofilms (Figure 13). We found that that *yfiM* and *yfiN* were required for the $yfiJ^{A152E}$ mutant to develop as a biofilm but *yfiL* was not. However, all three genes *yfiL*, *yfiM*, and *yfiN* were required for linearmycin resistance (Table 5). Taken together, the *yfiLMN* operon encodes a multifunctional ABC transporter that is involved in both biofilm formation and linearmycin resistance functions. This is in contrast to known ABC transporters that function solely in antibiotic resistance and to conventional *B. subtilis* biofilm development, which requires transcriptional regulation of many genes to affect colony development (197).

We hypothesize that the two functions of YfiLMN may result from the assembly of different hetero-oligomeric ABC transporter protein complexes. In the cytoplasm, the NBDs of ABC transporters form soluble dimers, which are thought to act as an initiation step in ABC transporter complex assembly (280). Certainly, incorporation of the NBDs

is necessary for proper ABC transporter function. The *yfiJ*^{A152E} Δ*yfiL* strain formed a biofilm but became sensitive to lysis by *S.* Mg1 (Table 5). This observation confirms that linearmycin resistance requires active ATP hydrolysis. However, in *E. coli* the maltose ABC transporter $MalFGK_2$ can form from multiple assembly pathways. All possible intermediate pairwise combinations of MalK (NBD), MalF (MSD), and MalG (MSD) were observed *in vivo* and found to be stable. This includes heterodimeric MalFG dimers (281). Further, MalFG dimers have been purified from *E. coli* and reassembled with $MalK_2$ *in vitro* to form functional ABC transporter complexes (282). Together, this suggests that ABC transporter complexes can form from convergent assembly pathways of different dimer composition (281). The *yfiJ*^{A152E} mutant expresses the *yfiLMN* operon ~135-fold over wild type (Figure A8). Perhaps these higher expression levels of *yfiM* and *yfiN* ultimately result in stable YfiMN heterodimers forming in the membrane. Though YfiMN heterodimers lack YfiL and ATPase activity, the heterodimer may facilitate biofilm formation as a secondary effect of membrane perturbation. Alternatively, formation of excess YfiLMN or YfiMN complexes in the membrane may generate pores that promote potassium ion leakage and trigger biofilm formation (27). In support of the latter model, we found that *kinC* is necessary for YfiLMN-mediated biofilm formation (Figure 16).

As an alternative approach to understanding the biofilm phenotype of YfiLMN, we used transposon mutagenesis and identified *yfiJ*^{A152E} mutants that failed to form biofilms. In 4/11 transposon mutants that we identified, there were transposon insertions

associated with genes encoding chaperone and protein quality control systems. Currently, we do not know how the YfiLMN transporter complex is formed. However, for the $MalFGK_2$ ABC transporter complex, MalK acts as a chaperone for assembly of MalFG (282, 283). Therefore, it is not unprecedented that the MSDs YfiM and YfiN may require chaperone activity to properly fold. We speculate that during overexpression of *yfiLMN* in $yfiJ^{A152E}$ strains chaperones promote the assembly of YfiMN complexes and lead to biofilm formation. We note that all transposon-mutagenized strains that we identified were linearmycin resistant, which indicates that some chaperone systems must be dispensable for assembly of functional YfiLMN. More work is required to determine how the YfiLMN transporter complex is naturally formed and if chaperones are required for its formation.

Using bacterial co-culture, we demonstrated that *B. subtilis* induces expression of the *yfiLMN* operon in response to *S.* Mg1. In particular, using a linearmycin biosynthesis deficient mutant and isolated linearmycins, we confirm that the YfiJK system responds to linearmycins (Figure 14A). With truncated variants of YfiJ, we show that the YfiJ transmembrane domain is required for activation of YfiJK signaling. As we currently do not know the mechanism of linearmycin-induced lysis of *B. subtilis*, we cannot rule out that linearmycin is sensed as a similar secondary effect. However, *B. subtilis* is similarly lysed by both linearmycins and daptomycin but does not induce *yfiLMN* expression in response to daptomycin (Figure 14B). Further, we were unable to identify any transposon mutants that spontaneously activated YfiJ signaling. Consequently, we

hypothesize that YfiJ act as a direct linearmycin sensor. Therefore, we rename *yfiJKLMN* to *lnrJKLMN* for linearmycin sensing and resistance.

Here we expand our understanding of a model system to include transcriptional regulation and biofilm formation as a response to bacterial competition. As we better understand model systems for interspecies interactions in the laboratory, we begin to piece together the rich and multifaceted suite of functions that bacteria use to survive and compete in the environment. By incorporating this information into models of bacterial communities, we will gain a more thorough understanding of community dynamics and their influence on the environment at large.

Materials and methods

Bacterial strains, media, and primers

The strains of *B. subtilis* used in this study are listed in Table A5. For general propagation and manipulation, we inoculated *B. subtilis* and *E. coli* strains in lysogeny broth (LB) [1% tryptone (Bacto), 0.5% yeast extract (BBL), 0.5% sodium chloride (Sigma)] or on LB agar plates [with 1.5% agar (Bacto)]. We maintained *S.* Mg1 strains as spore suspensions in water at 4 °C. All experiments used MYM [0.4% malt extract (Bacto), 0.4% yeast extract (BBL), 0.4% D-(+)-maltose monohydrate (Sigma), 1.5% agar (Bacto)]. We supplemented chloramphenicol (5 μg/mL), kanamycin (5 μg/mL), MLS (1 μg/mL erythromycin, 25 μg/mL lincomycin), and 5-bromo-4-chloro-3-indolyl-β-D-galactopyranoside (X-gal) (40 μg/mL) into media as needed. All primers are listed

in Table A6. We used *Escherichia coli* XL-1 blue or DH5α for plasmid maintenance and manipulation. We prepared *B. subtilis* genetic manipulations in the 168, PY79, or NCIB3610 Δ*comI* (284) strain backgrounds with one-step transformation. We used phage SPP1 to transduce our genetic manipulations into the NCIB3610 strain background as previously described (224).

Lysis co-culture assays

We performed all lysis co-culture assays as previously described (248).

RNA extraction and qRT-PCR

After 24 h of growth we scraped lawns of *B. subtilis* into RNAprotect Bacteria Reagent (Qiagen). We lysed 200 μL of fixed cells using lysozyme and Proteinase K digestion for 45 min at ambient temperature while vortexing. To extract RNA we used TRIreagent (Sigma) and standard procedures. We removed trace DNA from RNA samples using a Turbo DNA-free kit (Applied Biosystems). We performed qRT-PCR as previously described (248). All primers used for qRT-PCR are listed in Table A7.

Construction of yfiLMN, yfiL, yfiM, and yfiN deletion strains

To generate a *yfiLMN* deletion strain, we used long-flanking homology PCR. We used primers 11 and 75 to amplify an upstream sequence of *yfiL*, primers 79 and 155 to amplify a downstream sequence of *yfiN*, and primers 153 and 154 to amplify the MLS-resistance cassette from strain BKE08290. We mixed the three products together and

used primers 11 and 79 to amplify a LFH PCR product. We transformed the product directly into PDS0559 (Δ*yfiJ*) to generate PDS0795. We transduced the linked Δ*yfiJ* Δ*yfiLMN::mls* into wild type *B. subtilis* NCIB3610 (PDS0742) to generate strain PDS0796. We transduced pDR244 into PDS0796 to generate strain PDS0797 with markerless deletions Δ*yfiJ* Δ*yfiLMN*. To generate single deletions of *yfiL*, *yfiM*, and *yfiN*, we used primers 21 and 81 to amplify DNA containing the given deletions marked with a *mls* resistance cassette from strains BKE08310, BKE08320, and BKE08330, respectively. The PCR products were directly transformed into PDS0559 to generate Δ*yfiJ* Δ*yfiL::mls* (PDS0788), Δ*yfiJ* Δ*yfiM::mls* (PDS0810), and Δ*yfiJ* Δ*yfiN::mls* (PDS0811) strains. As above, we transduced the *mls* marked deletions into PDS0742 and used pDR244 to generate markerless deletions Δ*yfiJ* Δ*yfiL* (PDS0789), Δ*yfiJ* Δ*yfiM* (PDS0814), and Δ*yfiJ* Δ*yfiN* (PDS0815). To complement the *yfiJ* deletions, we transduced *lacA::yfiJ*$^{+}$ *(mls)* or *lacA::yfiJ*^{A152E} *(mls)* from PDS0562 and PDS0563, respectively.

In vivo transposon mutagenesis

We used plasmid pMarA for *in vivo* transposon mutagenesis of *B. subtilis*. The pMarA plasmid contains a Mariner element under control of the housekeeping sigma factor σ^{A} and a temperature-sensitive origin of replication (227). For our morphology screen, we transduced pMarA into PDS0572. For the spontaneous activation of P_{yfiLMN}-*lacZ* screen, we transduced pMarA into PDS0838. We selected transductants on kanamycin and MLS. We inoculated single colonies overnight in LB at 30 °C with both

antibiotics. After overnight growth, we diluted the cultures to OD_{600} = 0.08 and grew the cultures to OD_{600} = 0.3-0.4 at 30 °C, only under kanamycin selection. Afterwards, we raised the temperature to 42 °C to restrict pMarA replication. When the cultures reached OD_{600} = 1, we mixed 500 µL culture aliquots with 500 µL of 50% glycerol and froze the transposon libraries at -80 °C.

Colony morphology screen

To screen for *B. subtilis* mutants with altered colony morphology, we thawed an aliquot of the transposon library, serially diluted 100 µL 10^{-5} in LB, and plated 100-150 µL onto MYM plates containing kanamycin. After 2 d of growth, we screened the plates for colonies with altered morphology. Each plate, on average, contained ~38 colonies. At this stage, we considered colonies with abnormal morphology to have "passed" the first stage of the screen. We passaged each isolate on LB plates containing kanamycin. To verify altered morphology, we plated the isolates for single colonies on MYM plates. As before, after 2 d of growth we observed the isolates. At this stage, we classified isolates that retained altered morphology as passing the second stage of the screen. We prepared SPP1 phage lysates on the second stage isolates and transduced the transposon insertions into *yfiJ*$^{+}$ (PDS0571) and *yfiJ*^{A152E} (PDS0572) strain backgrounds. To pass the third and final stage of the screen, the abnormal morphology and kanamycin resistance markers must be linked through transduction. We extracted genomic DNA from the third stage transductants for insertion loci identification (see below).

Construction of P_{yfiLMN}- and P_{bceA}-lacZ transcriptional reporters

We used the PePPER webserver (285) to predict promoter sequences for *yfiL*, *yfiM*, and *yfiN*. We identified a single putative promoter that overlaps the stop codon and the predicted rho-independent terminator downstream of *yfiK*. Using primers 173 and 174 we amplified a 200 bp DNA sequence containing the putative *yfiLMN* promoter with EcoRI and HindIII restriction sites. Similarly, we used primers 180 and 181 to amplify P_{bceA} with EcoRI and HindIII restriction sites (286). To generate transcriptional fusions to *lacZ* we digested our PCR products and plasmid pDG1661 (*amyE::*RBS_{spoVG}-*lacZ cat spc bla*) (287) with EcoRI and HindIII. We ligated the digested products together using T4 DNA Ligase. We confirmed plasmid construction by restriction digest. We transformed the P_{yiLMN}-*lacZ* plasmid into DS7817 to generate PDS0838 in the NCIB 3610 strain background. We used SPP1 phage lysates from PDS0838 to introduce the P_{yiLMN}-*lacZ* reporter construct into other strain backgrounds. We transformed the P_{bceA}-*lacZ* plasmid into PDS0559 to generate PDS0917. We used SPP1 phage lysates from PDS0917 to introduce the P_{bceA}-*lacZ* reporter construct into PDS0555 and generate PDS0918 in the NCIB 3610 strain background.

Linearmycin and polyene assays

To test linearmycins and other polyenes for activation of the P_{yfiLMN}-*lacZ* reporter, we first diluted an overnight culture of PDS0838 to OD_{600} = 0.08 then grew the culture back to OD_{600} = 1 at 37 °C. We spotted 2 µL spots of the culture onto MYM plates containing X-gal and incubated the plates for 18 h at 30 °C. To test polyenes we spotted 3 µL containing 15 µg of amphotericin B, ECO-02301, or nystatin onto the pre-

grown colony and allowed the spot to dry before returning the plate to the incubator. Likewise, we spotted 15 µg of daptomycin. We isolated linearmycins from *S.* Mg1 and spotted a fraction onto a *B. subtilis* colony as above.

Constitutive activation of P_{yfiLMN}-lacZ screen

To screen for mutants with constitutive activation of the P_{yfiLMN}-*lacZ* reporter, we thawed an aliquot of our transposon library, serially diluted 100 µL 10^{-4} in LB, and plated 150 µL onto MYM plates containing kanamycin and X-gal. After 2 d of growth, we screened the plates for colonies with blue color. Each plate, on average, contained ~120 colonies. We passaged each blue isolate on MYM plates containing kanamycin and X-gal. After 2 d of growth, we scored the passaged isolates for the presence of blue color. We prepared SPP1 phage lysates from each positive isolate and transduced the transposon insertions into the fresh PDS0838 strain background. We extracted genomic DNA from the blue transductants for insertion loci identification (see below).

Identification of transposon insertion loci

TnYLB-1-insertion loci from pMarA were identified using degenerate primer PCR, inverse PCR, or single primer PCR. For degenerate primer PCR we used primers oIPCR-2 and Degen3 with the following cycling conditions: 98 °C for 5 min, followed by 25 cycles of 98 °C for 45 s, 60 °C for 45 s (decreasing by 0.5 °C/cycle), and 72 °C for 2 min. Next, we used 25 cycles of 98 °C for 45 s, 50 °C for 45 s, and 72 °C for 2 min. For inverse PCR we digested 5 µg of genomic DNA with AluI, Taq^{α}I, or Sau3AI. We

ligated the digested DNA using T4 DNA ligase for 16 h at 16 °C at a DNA concentration of 5 ng/µL. We used the outward facing primers oIPCR-1 and oIPCR-2 to amplify a linear product from the ligated circular DNA using Phusion polymerase with the following cycling conditions: 98 °C for 2 min, followed by 30 cycles of 98 °C for 10 s, 57 °C for 20 s, and 72 °C for 15 sec. For insertion loci that could not be identified by either degenerate or inverse PCR, we used single primer PCR. For single primer PCR we used primer oIPCR-2 with the following conditions to generate single stranded DNA: 98 °C for 2 min, followed by 30 cycles of 98 °C for 30 s, 57 °C for 10 s, and 72 °C for 2 min. Subsequently, we used 20 cycles of 98 °C for 30 s, 30 °C for 10 s, and 72 °C for 2 min, which allows for inward facing non-specific primer pairing. Finally, we used 30 cycles of 98 °C for 30 s, 57 °C for 10 s, and 72 °C for 2 min with a final extension of 2 min. We confirmed the presence of PCR products on 1% agarose gels and purified products before sequencing. All sequencing was performed using nested primer oIPCR-3. In all cases we clearly identified the boundary between the insertion element and genomic sequence.

Construction of yfiJ$^{\Delta TMD}$ truncation and yfiJ^{TMD}-bceS^{Cyto} strains

We amplified the *yfiJ* promoter (P_{yfiJ}) using primers 46 and 60, which includes a BamHI restriction site on the 5′ end. We used TMHMM (288) and Phobius (289) to predict the transmembrane helices in YfiJ, respectively. In both cases, predictions indicate that the transmembrane domain of YfiJ ends at residue 146. To generate a variant of *yfiJ* with a transmembrane domain truncation, we amplified *yfiJ* from codon

146 onward using primers 62 and 26. The forward primer includes an in frame ATG to serve as the start codon. The reverse primer contains an EcoRI restriction site on the 3′ end. Subsequently, we used joining PCR to fuse the P_{yfiJ} and $yfiJ^{\Delta TMD}$ fragments together. Briefly, we mixed the two DNA fragments together in an equimolar ratio in a standard PCR mix without primers for 10 cycles of amplification. Next, we added primers 46 and 26 and continued amplification for 30 cycles. We digested the fusion PCR product and the plasmid pDR183 (*lacA*::*mls bla*) (290) with BamHI and EcoRI. We ligated the digested products together using T4 DNA Ligase. To generate the $yfiJ^{\Delta TMD,\ A152E}$ allele, we used PCR-mediated site-directed mutagenesis with primers 92 and 93. We verified both constructs with Sanger sequencing. We transformed both plasmids into PDS0559 to generate PDS0910 and PDS0911, respectively. We used SPP1 phage transduction to introduce the constructs into PDS0909 and generate strains PDS0912 and PDS0913 in the NCIB 3610 strain background.

To construct the $yfiJ^{TMD}$-$bceS^{Cyto}$ chimera, we first amplified P_{yfiJ} and the first 146 codons of *yfiJ* using primers 175 and 176. Next, we amplified the cytoplasmic portion of *bceS* using primers 177 and 178. We used joining PCR as above to generate a $yfiJ^{TMD}$-$bceS^{Cyto}$ fusion fragment with SacI and SacII restriction sites. We digested the fusion PCR product and pDR183 with SacI and SacII. We ligated the digested products together using T4 DNA Ligase. We confirmed plasmid construction by restriction digest. We transformed the plasmid into PDS0559 to generate PDS0919. We used SPP1 phage

transduction to introduce the construct into PDS0918 to generate PDS0920 in the NCIB 3610 strain background.

CHAPTER IV

GROWTH PHASE-DEPENDENT REGULATION OF LINEARMYCIN BIOSYNTHESIS: EVIDENCE FOR AN AUTOLYTIC MECHANISM OF EXTRACELLULAR VESICLE BIOGENESIS

Summary

In addition to their primary metabolism, bacteria and other microbes produce numerous specialized metabolites. The structures of specialized metabolites differ as widely as their biological functions. These functions include roles in competition, development, nutrient acquisition, and stress response. *Streptomyces* sp. Mg1 (*S.* Mg1) produces linearmycins, which are polyketides responsible for the lysis and degradation of competitor *Bacillus subtilis* in co-culture. Mutants of *S.* Mg1 that are unable to produce linearmycins have defects in extracellular vesicle production, suggesting that linearmycin biosynthesis is integrated with extracellular vesicle production. Here, we determined the pattern of expression for the linearmycin *lny* biosynthetic gene cluster and linearmycin biosynthesis over the *S.* Mg1 growth curve. We find that both *lny* gene expression and linearmycin biosynthesis are growth phase regulated. We also observe that the morphology of extracellular vesicles isolated from stationary phase *S.* Mg1 is consistent with an autolytic origin. As the linearmycin biosynthesis mutant is unable to produce extracellular vesicles, our results implicate linearmycins as inducers of autolysis that leads to extracellular vesicle production. We also find that surfactin, a specialized metabolite produced by *B. subtilis*, enhances the lytic activity of extracellular vesicles

produced by *S.* Mg1. Together, our findings suggest that linearmycin-mediated autolysis is responsible for releasing linearmycin-laden vesicles from *S.* Mg1 and surfactin-mediated lysis is responsible for enhancing the activity of those same vesicles against *B. subtilis*.

Introduction

The capacity to engage in specialized metabolism is an attribute that is widely dispersed within the microbial world. Though once considered "secondary", many specialized metabolites play critical roles in bacterial competition, defense, development, physiology, signaling, and survival (5–10, 153). Our understanding of the functions of specialized metabolites is disproportionately focused on molecules with antibiotic activity. Though many specialized metabolites may intrinsically function as antibiotics, antibiotic activity in and of itself may a consequence when these molecules are divorced from their natural context and concentrations (7). To understand the ecological and physiological functions of specialized metabolites, we need to consider specialized metabolism within the context of the producing organism and its extracellular environment.

In our laboratory, we use models of bacterial interspecies interactions to identify specialized metabolites and their roles in competition. One particular model we use consists of two soil bacteria: *Bacillus subtilis* and *Streptomyces* sp. Mg1 (*S.* Mg1). When colonies of *B. subtilis* and *S.* Mg1 are cultured together on an agar surface, the *B. subtilis*

colony undergoes progressive degradation with concurrent cellular lysis (47). We identified linearmycins A and B as the causative agents of this lytic degradative activity (248). Linearmycins are long, linear polyketides with reported antibacterial and antifungal activities (172, 173). We identified the ~180 kb, type I polyketide synthase (PKS) *lny* gene cluster responsible for encoding the linearmycin biosynthesis machinery using the sequenced genome of *S.* Mg1 (171). Using mass spectral molecular networking, we have identified over 50 additional linearmycin variants (which we collectively refer to as "linearmycins"). From the *S.* Mg1 genome we identified the *lnyI* gene, which encodes the acyltransferase responsible for loading the starter unit onto the first PKS module (291). We found that deletion of *lnyI* results in loss of production of all linearmycins, and *B. subtilis* is not lysed by this deletion mutant. Intriguingly, the Δ*lnyI* strain also has a defect in the production of extracellular vesicles (EVs). We found that the linearmycins co-migrate with EVs during isolation, indicating that linearmycins may be a constituent or cargo of *S.* Mg1 EVs (Hoefler BC, Stubbendieck RM, Josyula NK, Moisan SM, Schulze EM, and Straight PD; in preparation).

Here we report the relationship between growth phase, *lny* gene expression, and linearmycin biosynthesis in *S.* Mg1. We find that expression of the *lny* gene cluster is dependent upon growth phase, reaching peak expression after a period of growth arrest. Thereupon, we find the highest concentrations of linearmycins within the cell-free supernatants associated with EVs. We show that linearmycins continue to accumulate in the EV fractions well past the transition into stationary phase. The morphology of EVs

isolated from stationary phase cultures is consistent with biogenesis resulting from cellular autolysis. Strikingly, we did not observe morphologically similar EVs from the Δ*lnyI* strain. Our results suggest a role for linearmycins in programmed cell death of *S.* Mg1, which results in EV release. We also find that surfactin, produced by *B. subtilis,* enhances the lytic activity of EVs isolated from *S.* Mg1 and indicates a new competitive interface for these specialized metabolites.

Results

Growth phase, lny gene expression, and linearmycin biosynthesis are coordinated processes

We hypothesized that *S.* Mg1 coordinates linearmycin biosynthesis with production of EVs over the course of its life cycle. We inoculated cultures with *S.* Mg1 spores and measure the growth of *S.* Mg1 over time. At specified time points, we collected the cell mycelium for growth measurement and RNA extraction, and the culture supernatant for EV isolation. As a control, we also inoculated a set of cultures with *S.* Mg1 Δ*lnyI*, which does not produce linearmycins and has an EV production defect (Hoefler BC, Stubbendieck RM, Josyula NK, Moisan SM, Schulze EM, and Straight PD; in preparation). The growth curve of *S.* Mg1 is similar to growth curves obtained from other streptomycetes grown in rich media (e.g. 292, 293). Over the first 12 h, there is little to no growth, which is consistent with spore germination. Following germination, the cultures grow for an additional 12 h, before growth pauses for the next 48 h. A pause period is characteristic for streptomycetes grown in rich media (e.g. 292,

293). When growth resumes, the *S.* Mg1 culture grows for an additional 24 h before reaching a plateau, indicating the entrance to stationary phase. We do not observe any significant differences in growth between the wild type and Δ*lnyI* strains of *S.* Mg1 (Figure 17).

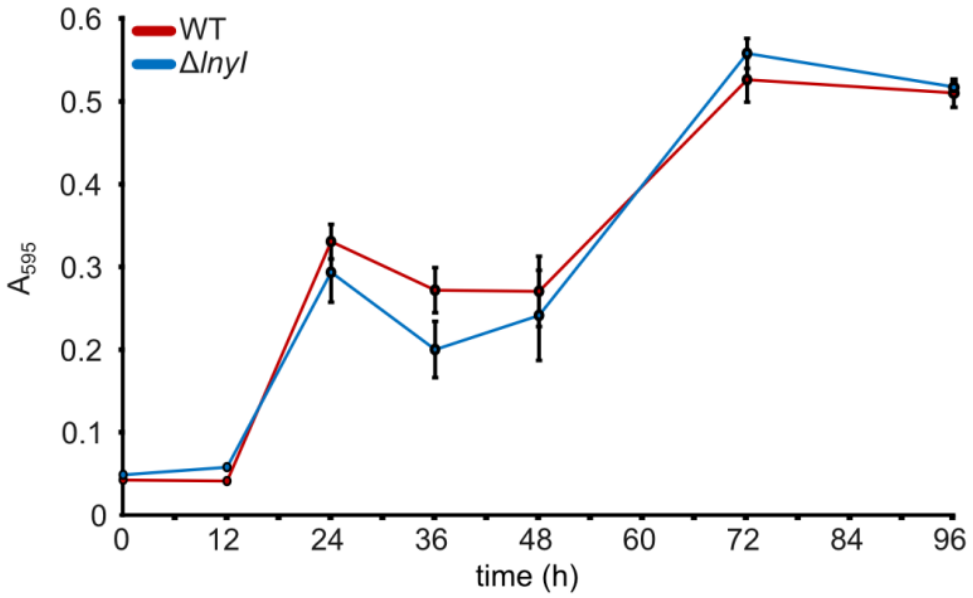

Figure 17. Growth curve of *S.* Mg1 in liquid MYM7 media

Growth curve of S. Mg1 wild type and Δ*lnyI* mutant measured by diphenylamine colorimetric assay. Each time point was measured ≥ 3 times and the error bars represent the standard deviation of the measurements.

We chose to monitor expression of *lnyHA* and *lnyHI* as representatives of the *lny* biosynthetic gene cluster. *lnyHA* and *lnyHI* encode the first and last PKS, respectively, with nearly ~117 kb of sequence between the two open-reading frames (171). We extracted RNA from each post-germination time point, synthesized cDNA, and used quantitative PCR to measure relative gene expression, normalized to the 24 h time point. We found that the expression of *lnyHA* and *lnyHI* increased over time and peaked at 48 h, coincident with the end of the pause period (Figure 18). Afterwards, expression levels decreased to near the initial level. Note, we synthesized cDNA from equal inputs of RNA and we report expression levels without reference to an internal housekeeping gene. Typically for *Streptomyces*, the *hrdB* gene is used as an internal control for expression normalization (294). We found that normalization of *lny* expression to *hrdB* maintains the same pattern of expression, except at 96 h where *lny* expression is inflated (Figure A15). The *hrdB* gene encodes the primary σ factor and its expression decreases during the transition to stationary phase (Figure A16) (295, 296). Therefore, the expression inflation observed at 96 h is likely a normalization artifact.

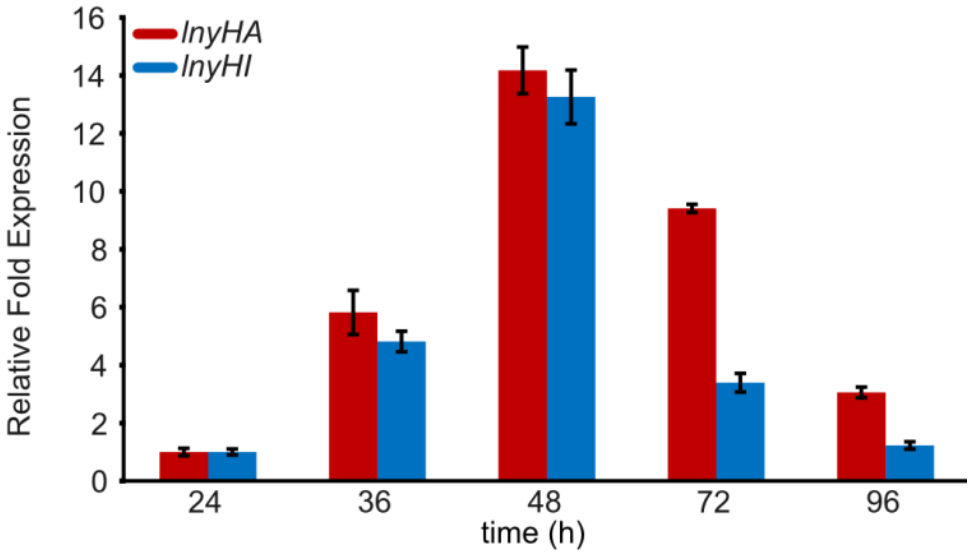

Figure 18. Expression of *lny* gene cluster during *S.* Mg1 growth

qRT-PCR was used to determine the relative fold expression in wild type *S.* Mg1 of the first (*lnyHA*) and last (*lnyHI*) PKS-encoding open-reading frame in the *lny* biosynthetic gene cluster. The error bars represent the standard deviation of the fold difference.

We wanted to determine how EV production is controlled over the course of *S.* Mg1 growth and its relation to *lny* gene expression. At each time point, we isolated EVs from cell-free supernatants using ultracentrifugation. We resuspended crude pellets containing EVs with other membranous debris and used differential gradient ultracentrifugation to separate the EVs from the other material. We isolated fractions from the top (Fraction 1) to the bottom (Fraction 10) of the density gradient. We observed a yellow-pigmented band (Fractions 5 and 6) present in samples derived from wild type *S.* Mg1 but absent in the Δ*lnyI* strain. Note that purified linearmycins are also

yellow due to the presence of the polyene moiety (297). Thus, we hypothesized that fractions 5 and 6 contain the highest concentrations of linearmycins.

Direct assay of fractions for vesicle number requires enumeration via electron microscopy from large numbers of biological replicates. Instead, based upon the presence of linearmycins and lysis of *B. subtilis*, we developed an indirect assay for EVs. We reasoned that measurement of the linearmycins content in EVs could serve as a proxy for EV number. To test fractions for lytic activity, we spotted each fraction onto a high-density lawn of *B. subtilis* embedded in agar. After incubation, we visualized lysis as clear zones in an otherwise opaque lawn. We observed lytic activity from wild type *S.* Mg1 in the 24 h sample and all subsequent time points. As expected, no lytic activity was ever observed from the Δ*lnyI* strain. From the 24 h sample, we observed that fractions 5 and 6 had the highest lytic activity. This finding accords with our observation of the yellow-pigmented band in these fractions. We also observed some, albeit lower, activity in fractions 4, 7, 8, 9, and 10 (Figure 19). At subsequent time points, the fractions were saturated with lytic activity, which enabled us to measure the relative activity at each time. Because fractions 5 and 6 contained the most activity, we chose these fractions as our focus for subsequent analysis.

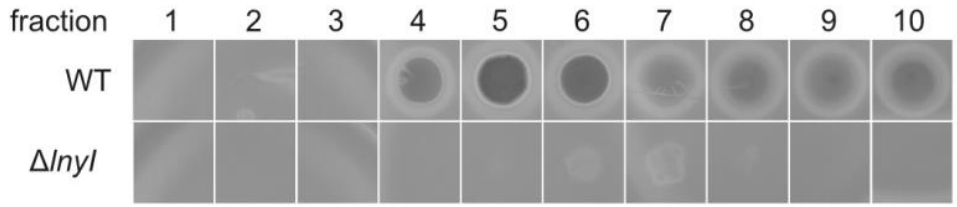

Figure 19. Plate assay used to detect the presence of linearmycins in extracellular vesicle fractions

Example activity assay used to detect the presence of linearmycin-containing vesicles from a culture of *S.* Mg1 grown for 24 h. Lysis is indicated by a zone of clearing when 3 µL of a vesicle fraction was spotted onto a high-density lawn of *B. subtilis.* Fraction number is indicated above each panel and ranges from 0% to 50% iodixanol in a continuous gradient. Fractions 5 and 6 were the most active and used for subsequent experiments.

We detected linearmycin content in the vesicle fractions using HPLC and by monitoring the UV absorbance at 333 nm (248). We observed no signal in the 12 h sample, consistent with an absence of lytic activity (Figure 20). We observed increasing linearmycin content over time. Intriguingly, we observed the largest increase in linearmycins between 48 and 72 h (Figure 20). This is the same period of time when *S.* Mg1 reinitiates growth after the pause period (Figure 17). The increase in linearmycin content is also concurrent with the peak in expression from the *lny* gene cluster (Figure 18). Taken together, this suggests that *S.* Mg1 constantly synthesizes linearmycins and produces EVs during its growth but that the total output regulated by the growth phase.

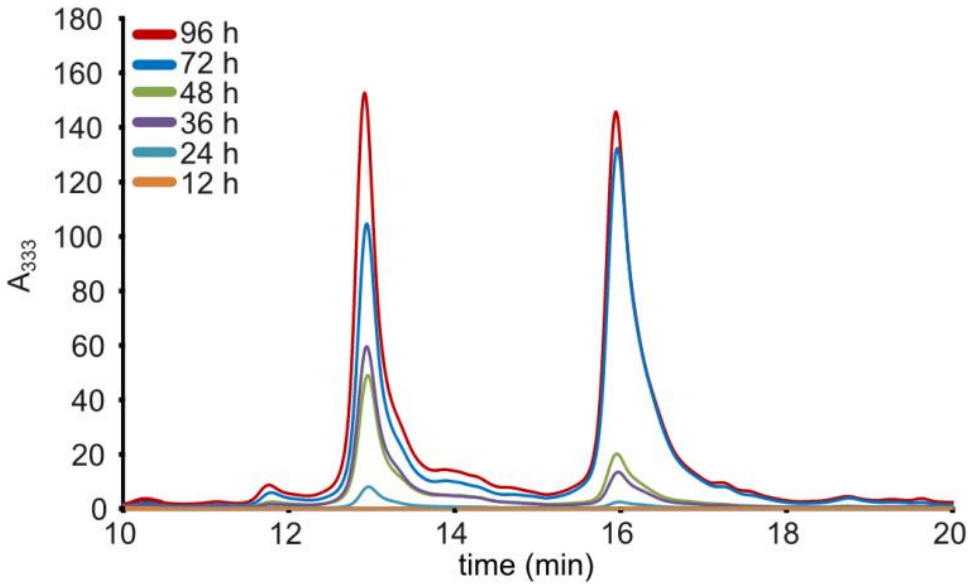

Figure 20. Detection of linearmycins in extracellular vesicle fractions by HPLC

Equal volumes of fractions 5 and 6 were pooled and extracted with methanol before injection onto an HPLC. Linearmycins were monitored by absorbance at 333 nm.

To quantitate lytic activity in the EV fractions, we returned to our plate assay. We spotted serial dilutions of pooled EV fractions 5 and 6 onto *B. subtilis* lawns, as above. At lower dilution factors, the EVs caused total lysis of *B. subtilis*. As we diluted the vesicles, we observed that the extent of lysis diminished as evidenced by the increased haziness of the lysed spots. For the earlier time points we diluted lytic activity below detectable levels. We measured the mean pixel intensity (MPI) of each lysed spot as a quantitative measure of *B. subtilis* lysis. There was a linear relationship between the dilution factor and the normalized MPIs of each lysed spot (Figure 21). Using this linear

relationship, we calculated the half maximal lytic concentration (LC_{50}) for pooled EV fractions extracted at each time point (Table 8). We also report fold lytic activity relative to the 24 h samples (Figure 22). As expected, the lytic activity measurements are in agreement with the linearmycin quantification by HPLC (Figure 20). Coincident with the end of the growth pause period, lytic activity rapidly increases.

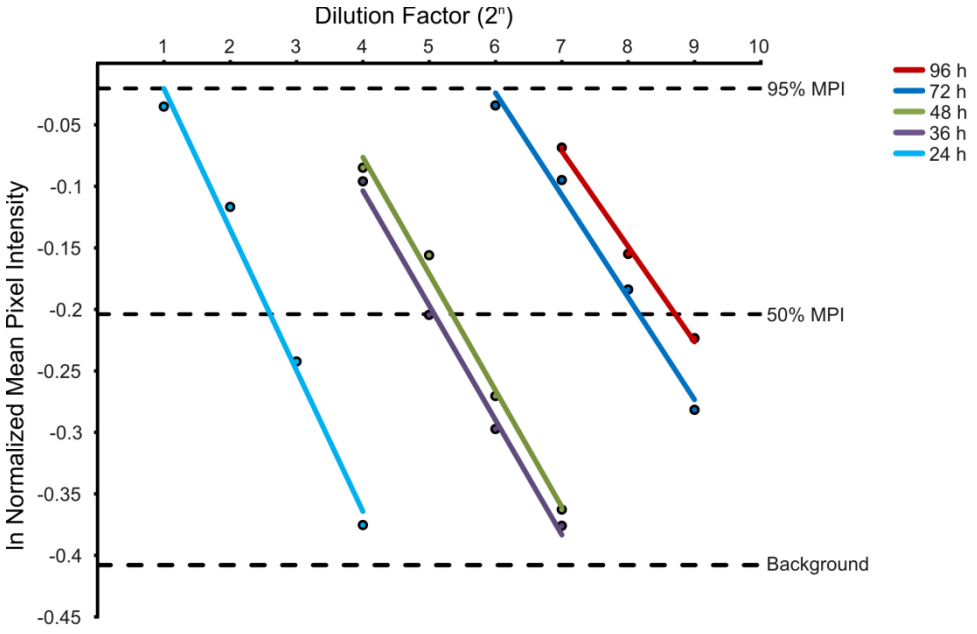

Figure 21. Measurement of LC_{50} values from extracellular vesicle fractions

Serial dilutions of pooled EV fractions isolated from *S.* Mg1 at specified time points were plated against lawns of *B. subtilis*. After 18 h of incubation, the plates were scanned. The MPI of each lysed spot was determined using ImageJ, normalized to MPI of the undiluted EV spot, and plotted against the dilution factor. The LC_{50} value is calculated from where each line crosses 50% MPI.

Table 8. LC_{50} measurements for EV fractions

Time Point (h)	LC_{50}
24	10.5
36	33.7
48	40.6
72	287.1
96	417.8

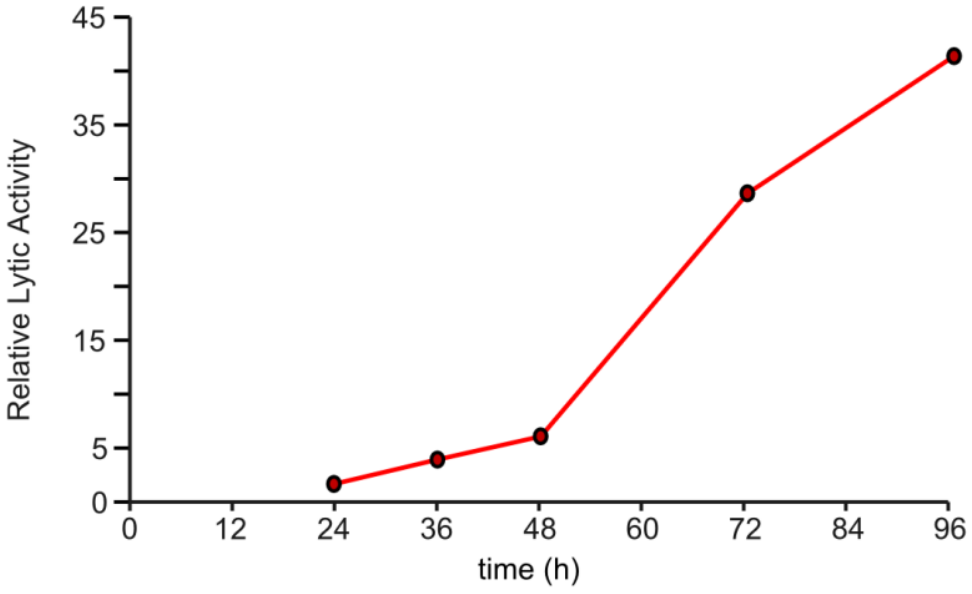

Figure 22. Relative lytic activity of pooled extracellular vesicle fractions

Visualization of the values in Table 8. LC_{50} values were normalized to the 24 h sample and reported as relative lytic activity.

Stationary phase EV morphology is distinct

The growth of *S.* Mg1 halts between 72 and 96 h (Figure 17). Concurrently, the expression of *hrdB* decreases (Figure A16), indicating that the culture is entering stationary phase. However, though the culture did not grow, we observed an increase in the lytic activity between 72 and 96 h (Figure 22, Table 8). To better understand this apparent discrepancy, we used electron microscopy and observed pooled EV fractions from wild type *S.* Mg1 isolated at both 72 and 96 h. From the 72 h sample, we observe a number of spherical vesicles that are morphologically consistent with vesicles previously isolated from *S.* Mg1 in our laboratory (Figure 23). However, the morphology of vesicles we isolated at 96 h is different. These vesicles are not uniform in size. Further, many of the vesicles are not spherical but are chained, clustered, or elongated in appearance (Figure 24). As a control, we examined equivalent fractions isolated from the Δ*lnyI* strain and found few vesicles, consistent with our previous results (Hoefler BC, Stubbendieck RM, Josyula NK, Moisan SM, Schulze EM, and Straight PD; in preparation).

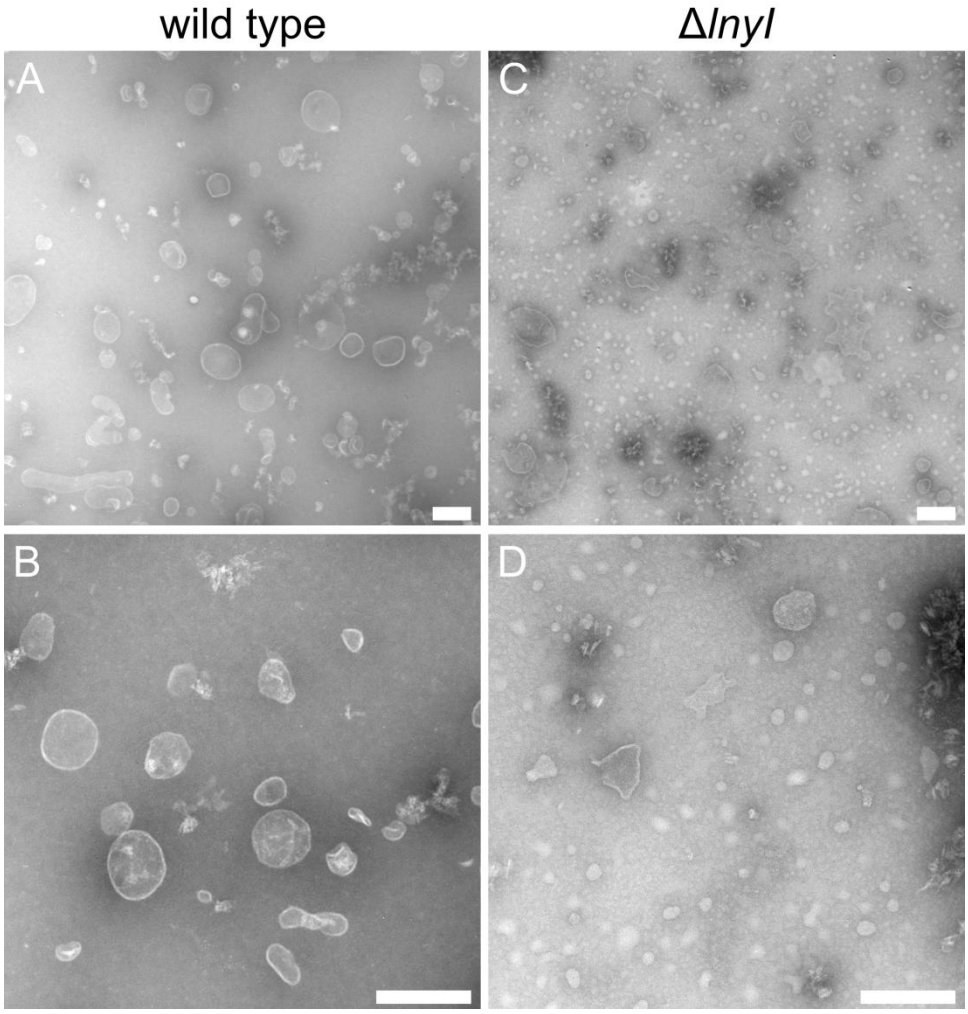

Figure 23. Electron micrographs of extracellular vesicle fractions isolated from *S.* Mg1 cultured for 72 h

Fractions 5 and 6 were pooled together and imaged using electron microscopy with negative staining. Spherical EVs are present in the wild-type sample (A-B) and mostly absent in the Δ*lnyI* mutant (C-D). The scale bar is 0.2 µm.

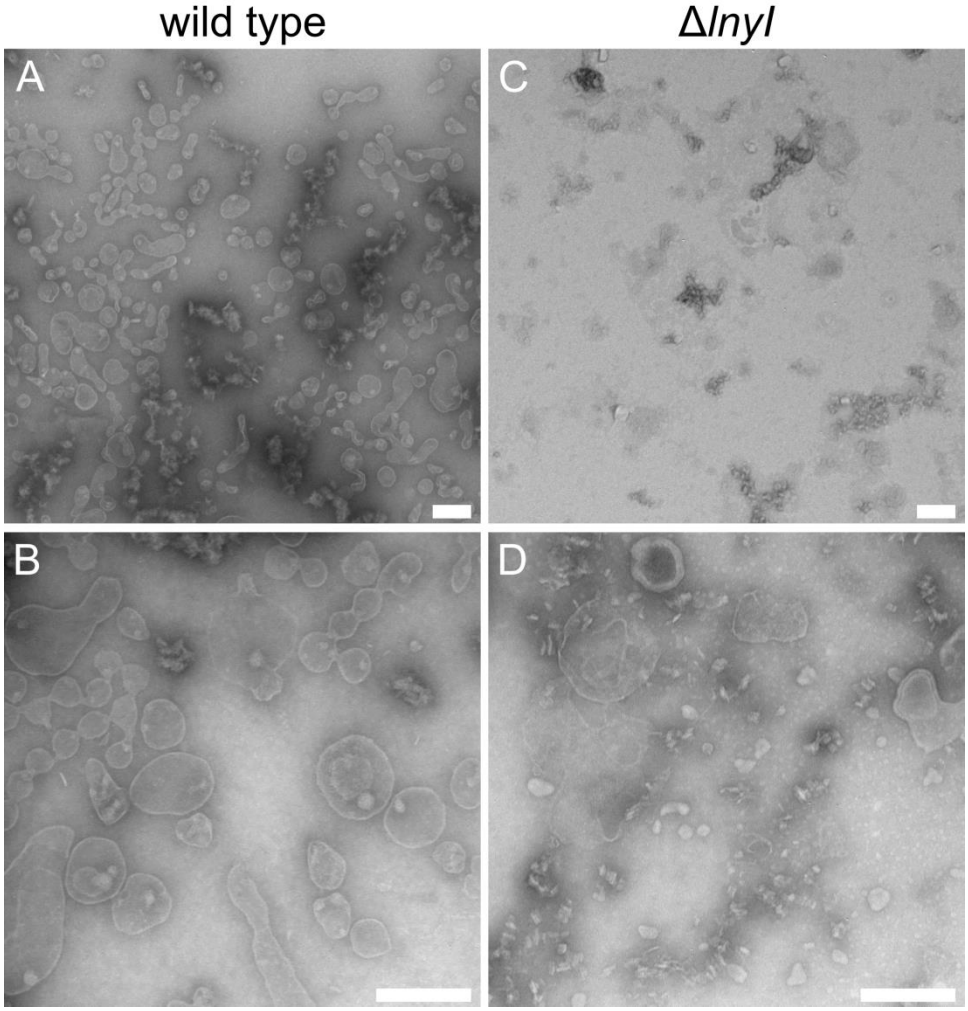

Figure 24. Electron micrographs of extracellular vesicle fractions isolated from S. Mg1 cultured for 96 h

Fractions 5 and 6 were pooled together and imaged using electron microscopy with negative staining. EVs with varying morphology including chains, clusters, and spheres are present in the wild-type sample (A-B) and mostly absent in the Δ*lnyI* mutant (C-D). The scale bar is 0.2 µm.

Surfactin enhances linearmycin sensitivity of B. subtilis

The focus of the current study has been to understand the control of linearmycin biosynthesis and EV production by *S.* Mg1. Among Gram-positive bacteria, EV production is not limited to the streptomycetes. Strains of *B. subtilis* are also reported to produce EVs (79). Biogenesis of EVs from *B. subtilis* has primarily been studied in laboratory strains or mutants that are unable to produce surfactin. This is because surfactin, a lipopeptide surfactant, self-produced lyses vesicles from *B. subtilis* (79). Therefore, we asked if surfactin would destabilize EVs from *S.* Mg1 and influence their lytic activity toward *B. subtilis*. We applied serial dilutions of *S.* Mg1 EVs onto high density, embedded lawns of *B. subtilis* wild type and Δ*srfAA*, which is unable to produce surfactin (39). We found that the Δ*srfAA* strain is largely resistant to lysis by *S.* Mg1 EVs (Figure 25A). However, when we pretreated the EVs with purified surfactin, then their lytic activity towards the Δ*srfAA* strain was restored and even enhanced (Figure 25B). We speculate that disruption of linearmycin-laden vesicles by surfactin increases their lytic activity due to increased solubilization of linearmycins.

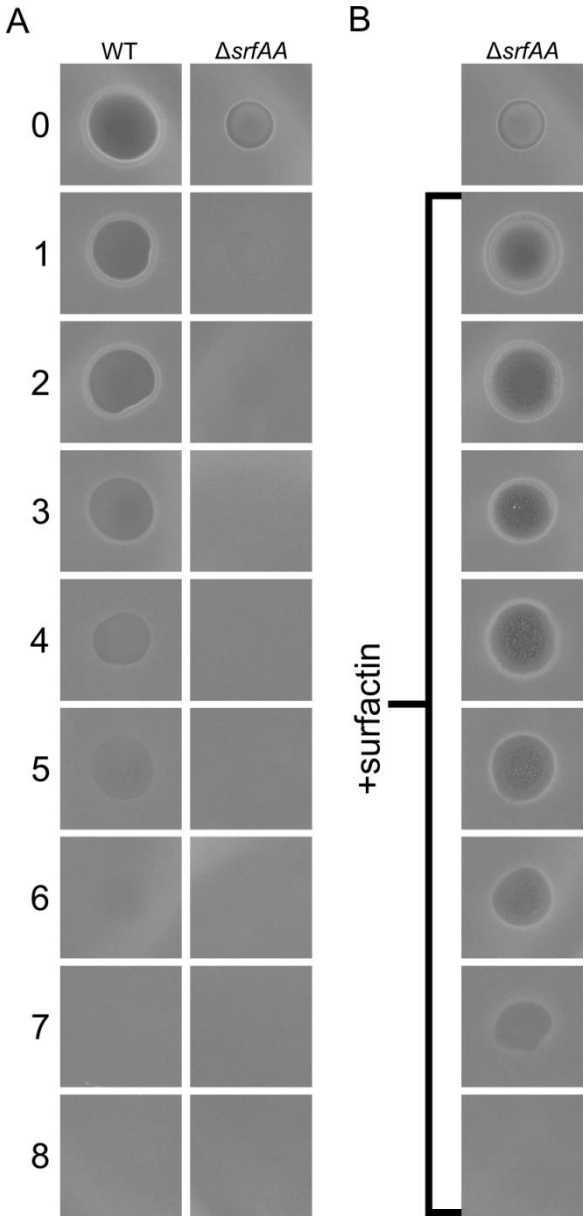

Figure 25. Surfactin enhances linearmycins sensitivity of *B. subtilis*

(A) High-density lawns of both wild type and Δ*srfAA B. subtilis* were treated with serial dilutions of pooled EV fractions 5 and 6 containing linearmycin from a culture of *S.* Mg1 grown for 24 h. Lysis is indicated by a zone of clearing. **(B)** High-density lawns of the Δ*srfAA* strain of *B. subtilis* were treated with serial dilutions of the same EV fractions from **(A)** but after pre-treatment with 2.5 mg/ml of surfactin before being spotted. The numbers on the left indicate the dilution factor [$(1/2)^n$] for each panel.

Discussion

In this study we identified growth phase-dependent regulation of *lny* biosynthetic gene cluster expression and linearmycin biosynthesis in *S.* Mg1. This study stemmed from previous work showing that *S.* Mg1 produces EVs and that linearmycins co-migrate with vesicles as potential cargo (Hoefler BC, Stubbendieck RM, Josyula NK, Moisan SM, Schulze EM, and Straight PD; in preparation). Here we first correlated *S.* Mg1 growth phase with expression of the *lny* biosynthetic gene cluster and linearmycin production. We observed that expression of the *lny* gene cluster peaks at the end of the pause period, which is followed by an increase in linearmycin content isolated from cell-free supernatants. We also noticed that after the transition of the *S.* Mg1 culture into stationary phase, there was a marked increase in lytic activity from EV fraction preparations. We also observed that the morphology of EVs isolated from stationary phase *S.* Mg1 cultures were markedly different from EVs isolated before stationary phase. The significance of the current work is in understanding how an organism controls production of a specialized metabolite that is involved in critical physiological processes (e.g. vesicle production) and bacterial competition.

In nutrient rich liquid culture, streptomycete growth follows five phases: *(i)* germination, *(ii)* initial growth, *(iii*) pause, *(iv)* second growth, and *(v)* stationary and death phase (e.g. 292, 293). As expected, we find that *S.* Mg1 conforms to this growth regimen (Figure 17). We hypothesized that linearmycin biosynthesis, and therefore EV production, is associated with culture growth phase. Indeed, we found that expression of

the *lny* genes increases through the initial growth phase, peaks during the pause period, and diminishes during the second growth and stationary phases (Figure 18). In addition, we found that expression of *lnyHI* decreases at a faster rate than *lnyHA*. This is consistent with the presence of a major promoter that is responsible for driving expression of all downstream PKS-encoding genes, as is the case for the ~74 kb *pks* operon in *B. subtilis* (31). After the pause period, we observe that the linearmycin content of the cell-free supernatant increases ~5 fold as measured by both HPLC and lytic activity (Figure 20, Figure 22). Together our data suggest that expression of the *lny* biosynthetic gene cluster is followed by translation of the PKS assembly machinery during pause period and a subsequent burst of linearmycin biosynthesis.

Streptomycetes are unique among bacteria due to their cell morphology and development. Like filamentous fungi, streptomycete growth initiates from spores. During germination a germ tube emerges from the spore to form the first hyphae. As the hyphae grows it lengthens and, at branch points, new hyphal growth is initiated (35). Given sufficient time to grow, streptomycetes become intertwined, and multinucleate mycelial mats. Similar to biofilms, access to nutrients and oxygen becomes limiting at increasing depths within the mycelium. The most interior cells in the mat starve and die over time (292, 298). Between 72 and 96 h, the expression of *hrdB* decreases, which indicates that the *S.* Mg1 culture has entered stationary phase (Figure A16). Concurrent with this transition is an apparent paradoxical increase in the lytic activity in cell-free supernatants without a concurrent increase in cell density (Figure 17, Figure 22). These

observations suggest that more EVs are produced after the culture reaches stationary phase.

Little is known about the biogenesis of EVs from Gram-positive bacteria. One major challenge is reconciling the inherent difficulties in vesicle formation and release through the peptidoglycan cell wall (64). We propose that the increased lytic activity, and therefore EV production, is due to autolysis of *S.* Mg1 releasing vesiculated membranes. An autolytic mechanism for vesicle biogenesis circumvents the need for Gram-positive bacteria to use a controlled vesicle release system. Further, the multinucleate and filamentous growth mode of streptomycetes ensures that fitness costs for autolysis are low. We speculate that after 72 h the *S.* Mg1 culture enters death phase and increased numbers of EVs are released by autolysis. This mechanism is not unprecedented. Indeed, within biofilms of the Gram-negative bacteria *Pseudomonas aeruginosa*, explosive cell lysis produces EVs (63). Using electron microscopy, we observed vesicles from both 72 and 96 h cultures, representing early and late stationary phase time points. Unlike the 72 h vesicles, the 96 h vesicles vary widely in their morphologies (Figure 23, Figure 24). We propose that EV biogenesis results from autolysis and subsequent vesiculation of *S.* Mg1 membranes. In support of this model, cryo-electron microscopy of *S.* Mg1 revealed the presence of vesicles near cracked *S.* Mg1 filaments (Straight PD, unpublished data). In addition, the lipid composition of vesicles and the *S.* Mg1 cytoplasmic membrane are identical (Josyula NK, unpublished data). However, most intriguingly is that we observe very few, if any, vesicles from the

Δ*lnyI* strain. Presumably, these cells are also in stationary phase, but the Δ*lnyI* strain does not undergo a substantial degree of autolysis. Given the capacity of linearmycins to lyse *B. subtilis*, perhaps these molecules are also responsible for mediating programmed cell lysis in *S.* Mg1. By sacrificing some of its filamentous mass, *S.* Mg1 is able to release a competitive molecule and associated vehicle into an aqueous environment where the molecule would otherwise be relatively insoluble. Future work is necessary to determine if there is a differential extent of death that occurs within the mycelial mats of wild type and Δ*lnyI* strains of *S.* Mg1.

Much of this study was focused on determining the dynamics of *lny* biosynthetic gene cluster expression linearmycin biosynthesis in monocultures of *S.* Mg1. However, our primary interest is in understanding how *S.* Mg1 uses EVs as agents for bacterial competition. In this study we did not directly co-culture *S.* Mg1 and *B. subtilis* together, but we observed that the efficacy of linearmycin-laden vesicles was largely diminished against a mutant of *B. subtilis* that is unable to produce surfactin. We also observed that treatment of vesicles with surfactin enhances the lytic activity of their linearmycin cargo against the *B. subtilis* Δ*srfAA* strain (Figure 25B). Though the enhanced lysis may be due to a secondary effect of exogenous application of surfactin onto the Δ*srfAA* strain (27, 299). We propose a direct effect. Previous studies have shown that surfactin lyses natural vesicles produced by *B. subtilis* and *Bacillus anthracis* (79), artificial vesicles (300), and membranes (301). Therefore, we propose that surfactin directly interacts with vesicles produced by *S.* Mg1 and that vesicle lysis or solubilization of linearmycins by surfactin

is responsible for increased lytic activity. Surfactin is involved in multiple important functions for *B. subtilis* including biofilm formation, motility, and bacterial competition (27, 37, 38). By interacting with a critical metabolite produced by *B. subtilis*, linearmycin-laden vesicles may counteract selective pressures for *B. subtilis* to adaptively lose surfactin biosynthesis genes.

In summary, the present study expands the interface of specialized metabolism, bacterial developmental physiology, and competitive functions. Beyond acting simply as antibiotics, many specialized metabolites function in crucial cellular processes. As mentioned above, surfactin is necessary for *B. subtilis* motility and biofilm formation (27, 37, 38). In addition, phenazines produced by *P. aeruginosa* are involved in redox balance and have roles in biofilm formation (6, 253, 302, 303). Autolysis is another process critical for bacterial development that intersects with specialized metabolism. For instance, during *P. aeruginosa* biofilm formation phenazine and pyocyanin contribute to hydrogen peroxide-mediated cell lysis and release of extracellular DNA, an important biofilm constituent (304, 305). Likewise, linearmycins may be responsible for autolysis of *S.* Mg1 and release of EVs. When taken out of their native context, many specialized metabolites act simply as inhibitory antibiotics. Only through careful consideration of the natural functions of these once "secondary" metabolites, we will uncover more interesting interfaces between bacterial development and specialized metabolism and garner new insight into bacterial physiology.

Materials and methods

Bacterial strains and media

The strains of *S.* Mg1 used in this study were wild type (PDS0543) or Δ*lnyI*::*apr* (PDS0755). The strains of *B. subtilis* used in this study were wild type (PDS0742) or Δ*srfAA*::*mls* (PSK0049). We used MYM media [0.4% malt extract (Bacto), 0.4% yeast extract (BBL), 0.4% D-(+)-maltose monohydrate (Sigma)] for all experiments. For culturing *S.* Mg1, we buffered liquid MYM with 100 mM MOPS (Chem-Impex) and 5 mM potassium phosphate at pH 7 (MYM7).

Time course experiment

To observe growth, *lny* biosynthetic gene cluster expression, and linearmycin biosynthesis over time, we inoculated independent 25 mL MYM7 cultures with a 100 µL suspension containing 5 x 10^7 spores of *S.* Mg1 wild type or Δ*lnyI*. At 12, 24, 36, 48, 72, and 96 h we harvested one culture each of wild type and Δ*lnyI*. At the specified collection time, we shook the culture flask to resuspend the mycelia. We removed three 1 mL aliquots from the culture. We centrifuged the aliquots at 21,130 x g for 10 min to pellet the mycelia, which we dried and stored at -20 °C for later growth measurements. After collecting aliquots for growth measurements, we centrifuged the remainder of the cultures at 12,000 x g for 10 min at 4 °C. We fixed the mycelial pellets with RNA-protect Bacteria Reagent (Qiagen). We stored the fixed pellets at -80 °C for later RNA extraction. We immediately processed culture supernatants for vesicle purification, as described below.

S. *Mg1 growth measurements*

The growth of *S.* Mg1 was determined using a diphenylamine colorimetric method (306). Briefly, we washed mycelial pellets twice with phosphate-buffered saline and resuspended each pellet in 1 mL of diphenylamine reagent [1.5% w/v diphenylamine, 1.5% v/v sulfuric acid, and 0.008% v/v aqueous acetaldehyde in glacial acetic acid]. We incubated the resuspended pellets at 60 °C for 1 h. After incubation, we centrifuged the samples at 21,130 x g for 5 min and measured the absorbance at 595 nm from 200 µL of the supernatant. We used ungerminated spores, at an identical density used to inoculate the cultures, to measure the 0 h time point.

EV isolation and preparation

To isolate EVs from culture supernatants, we first treated each supernatant with 0.1 mg of DNase I for 15 min while rotating at ambient temperature. We removed cells and large debris by filtering the supernatant through a 0.22 µm PES filter. We ultracentrifuged the filtrate in a Beckman Type 45 Ti rotor at 235,000 x g at 4 °C for 3 h. We resuspended the crude pellets in 200 µL of a 50% w/v iodixanol solution in Buffer A [10 mM HEPES, 0.85% w/v NaCl, pH 7.4]. We overlaid the resuspended pellet with lower-density iodixanol solutions [50 (200 µL), 40 (400 µL), 30 (400 µL), 20 (400 µL), 10 (400 µL), and 0% (100 µL) each in Buffer A] to form a step gradient (2.1 mL total). We ultracentrifuged the gradients to equilibrium in a TLS55 rotor at 120,000 x g at 4 °C for 16-18 h. Fractions (200 µL) were recovered from the top (fraction 1) to the bottom (fraction 10) of the tube and stored at 4 °C.

Plate overlay lysis assay and LC_{50} measurement

We adapted a previously described plate assay to assay EV fractions for lytic activity (248). Briefly, overnight cultures of *B. subtilis* were diluted to OD_{600} = 0.08 in 25 mL of MYM. When the cultures reached stationary phase, we concentrated the cells to OD_{600} = 4 by centrifugation at 3220 x g for 5 min and resuspension in a reduced volume of MYM. For each plate, we mixed 1.5 mL of concentrated *B. subtilis* with 4.5 mL of MYM agar (0.67% w/v agar) and spread the suspension evenly over a 25 mL MYM plate. Once the plates solidified, we spotted 3 µL of each vesicle fraction directly onto the overlay. After the spots dried, we incubated the plates at 30 °C. After 18 h we photographed or scanned the plates.

To compare lytic activity from vesicles extracted at different time points, we pooled equal volumes of EV fractions 5 and 6, made two-fold serial dilutions, and spotted each dilution onto plates. After incubation, we scanned the plates and measured the MPI of each lysed spot using ImageJ (307). We calculated the ratio of MPI of each lysed spot relative to the fully concentrated sample. This value was natural log-transformed and plotted against the dilution factor. Data points whose MPI ratios were $\geq$ 0.95 or $\leq$ 0.39 were not plotted because these values indicate assay saturation and background, respectively. For each EV preparation, the LC_{50} value was determined by calculating the dilution where the ratio of mean pixel intensity = 0.67, which represents the middle point between saturation and background intensity ratio. All linear regressions used 3 or 4 data points and the LC_{50} values were within the interpolable

range. All R^2 values were ≥ 0.99. We report all values as fold difference compared to the 24 h sample.

Quantification of linearmycin from EV preparations

To quantify linearmycins in EV fractions, we pooled 3 µL each of fractions 5 and 6 and extracted linearmycins with 6 µL of methanol. We injected a 6 µL sample of extracted linearmycins onto an Agilent 1200 HPLC system with a Phenomenex Luna C_{18} column (4.6 x 250 mm, 5 µm) and eluted with an ACN/20 mM ammonium acetate pH 5 gradient running at 1 mL/min. The elution program was as follows: 1) 5 min at 40% ACN then 2) a gradient up to 50% ACN over 10 min then 3) a gradient up to 75% ACN over 5 min, and 4) a gradient diminishing to 40% ACN over 5 min (248). Peaks primarily consisting of linearmycins A and B were detected by UV absorbance at 333 nm with retention times of 13 and 16 min, respectively.

RNA extraction and cleanup

We added five 3 mm glass beads and 2 mL of ice-cold lysis buffer [4 M guanidine thiocyanate, 25 mM trisodium citrate, 0.5% (w/v) sodium N-lauroyl sarcosinate, and 0.8% (v/v) β-mercaptoethanol) to each fixed mycelial pellet. After 2 min of vortexing, we added 2 mL of TRI Reagent (Sigma-Aldrich) to each sample. We vortexed each sample with four cycles of 30 s on vortex and 30 s on ice. After the addition of chloroform, we extracted RNA following standard procedures. We removed DNA from the RNA samples using a Turbo DNA-free kit (Applied Biosystems). We did

not extract RNA from the 0 and 12 h time points because the starting biomass was too low.

qRT-PCR of lny genes

We reverse transcribed cDNA from 100 ng of total RNA using a High-Capacity RNA-to-cDNA Kit (Thermo Fisher Scientific). We performed quantitative PCR using a Sso Advanced Universal SYBR Green Supermix Kit (Bio-Rad) and a CFX96 Touch real-time PCR thermocycler (Bio-Rad) with the following cycling parameters: denaturation at 95 °C for 30 s; 40 cycles of denaturation at 95 °C for 15 s, annealing at 58 °C for 30 s, and extension at 72 °C for 30 s; followed by a final melting curve from 60 °C to 95 °C for 6 min. We amplified *lnyHA* and *lnyHI*, the first and last PKS-encoding open-reading frames, respectively using the primers listed in Table A8. Each reaction was run in triplicate. Using LinReg (234), we calculated the primer efficiency and quantification cycle values. We report all values are as fold difference compared to the 24 h sample.

Electron microscopy of EV fractions

To remove iodixanol for electron microscopy, we pooled 100 µL each of fractions 5 and 6 and diluted the samples to 2.1 mL with Buffer A. We ultracentrifuged the diluted samples at 120,000 x g at 4 °C for ≥ 6 h. We resuspended the vesicle-containing pellet in 30 µL of Buffer A. To image vesicles with EM, we adsorbed 3 µL of the resuspended vesicles onto freshly glow-discharged carbon-coated Formvar grids. We

washed the vesicles washed briefly with water and followed by a negative stain with 2% w/v ammonium molybdate. We imaged samples with a JEOL 1200 EX transmission electron microscope operated at an acceleration voltage of 100 kV. We collected electron micrographs at calibrated magnifications using a 3k slow-scan CCD camera (model 15C, SIA). We processed images using ImageJ (307).

Surfactin EV lysis assay

To test the effect of surfactin on vesicle preparations, we extracted vesicles from a 24 h old culture of S. Mg1. We pooled equal volumes of vesicle fractions 5 and 6, and made two-fold serial dilutions in Buffer A containing a 2.5 mg/mL mixture of surfactins in ethanol (Sigma). We assayed lysis as above.

CHAPTER V

CONCLUSIONS AND FUTURE DIRECTIONS[3]

Bacterial communities vary in their species composition, niches occupied, and influence on different environments. Based on these complexities, communities defy a single fundamental definition. Rather, they represent fascinating examples of interactive processes that differ with ecological scale. The complications in defining and characterizing communities are reflected in the early history of microbiology. In the late 1800s Robert Koch revolutionized the field of microbiology by pioneering his methods to establish causality between a microorganism and disease (308). Even to this day Koch's postulates remain the "gold standard" to associate microbes to disease or any other phenomenon of interest. Inspired by Koch's reductionist approach, the vast majority of research over the past one hundred years has investigated the growth and physiology of microbes grown in pure culture. Studying single species of bacteria axenically was essential for birth of modern biochemistry and molecular biology and remains important to this day. However, even as early as the 1870s microbiologists including Louis Pasteur reported phenomena resulting from interactions of bacteria existing in multispecies communities (309). Bacteria are social organisms that interact extensively within and between species all while responding to external stimuli from

[3]Some text adapted from Stubbendieck RM, Vargas-Bautista C, and Straight PD. Bacterial Communities: Interactions to Scale. Front Microbiol. 2016 Aug 8;7:1234. doi: 10.3389/fmicb.2016.01234 under the Creative Commons Attribution License (https://creativecommons.org/licenses/by/4.0/), which permits unrestricted use, distribution, and reproduction in any medium, provided original work is cited. Copyright ©2016 Stubbendieck, Vargas-Bautista, and Straight.

their environments. Indeed, the ability to perceive neighboring cells and the environment is often reflected in the content of bacterial genomes. Recently, the construction of *Mycoplasma mycoides* JCVI-syn3.0, a bacterium with a minimal genome containing only 531 kilobase pairs and 473 genes was reported (310). When compared to the genome of a natural, soil bacterium *Myxococcus xanthus,* which contains 9.14 megabase pairs and 7388 protein coding genes (52) the genome of *M. mycoides* JCVI-syn3.0 is miniscule. While JCVI-syn3.0 inhabits rich, complete media in the laboratory, *M. xanthus* competes in its environment and requires a large number of genes for signaling systems to interpret changing environmental conditions and the presence of competitors. In fact, many organisms, including two of our best studied model species *Bacillus subtilis* and *Escherichia coli*, contain large numbers of genes deemed "non-essential". However, many of these genes may be absolutely critical to survival when bacteria are faced with competitors. As an old adage states: "no microbe is an island". Thus, to truly understand a bacterial species it must be placed within its ecological context including the other members of its community.

To understand a bacterial species, it must be placed into an ecological context, but doing so is challenging. Consequently, we use complementary biological and computational approaches to study bacterial communities. Commonly used computational approaches include metagenomic analysis and mathematical modeling. In typical metagenomic approaches, total DNA is isolated from environmental samples, sequenced, and different species are identified as determined by the sequence of their

ribosomal RNA genes (311–313). Metagenomic analyses have the potential to uncover the composition and connectivity of species in a bacterial community. However, by only using single snapshot binary comparisons of two community states, it is not possible to ascertain how members of the community interact. To infer interactions from metagenomic data it is necessary to following the composition of a community over a sufficiently long period of time with high temporal resolution (314, 315). In addition, inferences of interspecies interactions do not reveal the pertinent mechanistic details underlying interaction mechanisms. Likewise, mathematical models are used to predict bacterial community dynamics over time. In general, models attempt to capture many biological variables and place them into well-defined rules that govern how systems behave. Though models are incredibly powerful tools to investigate biological phenomena, they are limited by our current understanding of individual systems. By wedding models generated from metagenomic and mathematical approaches to complementary cultured-dependent experiments we gain deeper insights into the specific interactions that undergird community function

Though a bacterial community may be comprised of large number of cells, bacteria likely interact at the scale of single cells or multicellular aggregates (100, 316–319). The dynamics of the community at large are thus determined by interactions that occur between pairs of individual cells residing within the community. Using models of bacterial competition, often taking the form of macroscopic bacterial colonies competing on an agar plate, is a proven approach to address fundamental questions regarding

competitive mechanisms. Though artificial, by observing macroscopic colonies we gain insight into competitive mechanisms that bacteria use at single cell levels. For instance, Alexander Fleming's famous laboratory observation that *Penicillium chrysogenum* inhibited *Staphylococcus aureus* growth may be one of the first examples of interference competition investigated by this method (320). The agar plate was subsequently adopted for screening antibiotic compounds and it remains an invaluable tool for investigating competition (19). The outcomes of competition on an agar plate are often manifested in visible phenotypes including developmental defects, growth inhibition, lysis, motility, and pigment production (e.g. 17, 22, 26, 28, 32, 120, 151, 154, 321–326)

Our own experience using *Bacillus subtilis* and *Streptomyces* spp. in different formats reveals variable patterns and functions of bacterial competition. Importantly, changing the competitive dynamics between these organisms by using different species or mutants of *Bacillus* and *Streptomyces*, or changing plating formats has continued to uncover new mechanistic insights into functions of secreted enzymes and specialized metabolites in bacterial competition. For example the *B. subtilis* produced specialized metabolite bacillaene, originally identified as a translation inhibitor (29), is involved in a suite of functions with respect to different competitors. Bacillaene also inhibits the growth of *Streptomyces avermitilis* (327), interferes with production of pigmented prodigiosin *Streptomyces coelicolor* (30) and *Streptomyces lividans* (31), and is involved in defense against consumption by *Myxococcus xanthus* (44) and lysis by *Streptomyces* sp. strain Mg1 (*S.* Mg1) (47). *Bacillus subtilis* also produces surfactin, a lipopeptide

surfactant (27, 37, 38). Surfactin also inhibits sporulation of many *Streptomyces* species by antagonizing a morphogenetic peptide SapB, which is visually striking on an agar plate (39, 41). Imaging mass spectrometry of competitions between *B. subtilis* and *S.* Mg1 revealed that *S.* Mg1 produces a secreted hydrolase (SfhA) that specifically degrades surfactin and plipastatin produced by *B. subtilis* (40). Additionally, MALDI-TOF-IMS of competitions between these same two organisms led to the identification of chalcomycin A produced by *S.* Mg1 and revealed patterns of many unknown specialized metabolites that may also be involved in competition (47).

In this dissertation, I studied the interaction between *S.* Mg1 and *B. subtilis* that results in lysis of *B. subtilis*. First, I found that *S.* Mg1 produces linearmycins that cause lysis of *B. subtilis* (Chapter II). Using linearmycins, I identified mutants of *B. subtilis* that are spontaneously resistant to lysis. The linearmycin-resistant *B. subtilis* mutants revealed competitive functions for YfiJK, a previously uncharacterized two-component signaling system (Chapter II). I found genetic evidence that the histidine kinase YfiJ is a linearmycin sensor (Chapter III) and its cognate response regulator YfiK controls expression of the *yfiLMN* operon (Chapter II). We find that YfiLMN is an ATP-binding cassette transporter complex that is involved in linearmycin resistance and causes morphological changes in *B. subtilis* with regard colony development (Chapters II, III). Finally, I uncovered growth phase-dependent regulation of expression of the *lny* biosynthetic gene cluster and linearmycin biosynthesis in *S.* Mg1, consistent with an

autolytic model for extracellular vesicle biogenesis (Chapter IV). In this final chapter, I will discuss the conclusions and highlight future directions of this research.

Linearmycins are specialized metabolites involved in a suite of competitive functions

Offensive and defensive roles for linearmycins in competition

In this dissertation study I found that linearmycins are involved in multiple facets of bacterial competition. In particular, exposure to linearmycins causes subsequent lysis of *B. subtilis* (Chapter II). One interpretation of this observation is that *S.* Mg1 produces linearmycins as a means to lyse *B. subtilis* prey for consumption. However, though some species such as *Streptomyces scabies* are known plant pathogens (328), streptomycetes are typically considered to be saprophytic organisms (35). In addition, streptomycetes are mostly non-motile, unlike known predatory myxobacteria (53). An alternative interpretation is that linearmycins may function as a defense mechanism against motile competitors, such as *B. subtilis*. Coordinated antibiotic production and sporulation of streptomycetes are hypothesized to protect nutrients released by cannibalized substrate mycelium from motile competitors (165–167). Consistent with this defensive role, we have observed on agar plates that *B. subtilis* overruns the linearmycin biosynthesis deficient mutant *S.* Mg1 Δ*lnyI* (Figure A17). Finally, it is possible that the distinction between the offensive and defensive properties of linearmycins is simply due to constraints in our laboratory models. A provocative hypothesis is that release of nutrients from the cannibalized substrate mycelia may function as a lure to ensnare nutrient-

seeking motile microbes, akin to a Venus flytrap or a spider in a web. Determining the natural functions of linearmycin will require subsequent study under conditions that better mimic a natural soil environment.

Linearmycins as effectors of autolysis

In addition to their competitive functions, the linearmycins may also be involved in *S.* Mg1 programmed cell death. Using *S.* Mg1 Δ*lnyI*, we observed a connection between extracellular vesicle production and linearmycins. In particular, we noted a marked defect in vesicle production by the Δ*lnyI* strain. Subsequently, activity assays and mass spectrometry confirmed the presence of linearmycins in extracellular vesicles fractions (Hoefler BC, Stubbendieck RM, Josyula NK, Moisan SM, Schulze EM, and Straight PD; in preparation). When we profiled linearmycin biosynthesis and *lny* biosynthetic gene cluster expression over the course of *S.* Mg1 growth, we observed growth phase-dependent regulation of both of these processes (Figure 18, Figure 20). In particular, during stationary phase we observed an increase in linearmycin-associated lytic activity, without a concurrent increase in cell density (Figure 17). Instead of uniform spherical vesicles, we observed that the morphology of extracellular vesicles varied in size and shape that often were chained or clustered (Figure 24). We suspect that these extracellular vesicles are derived from *S.* Mg1 autolysis. Importantly, we note the absence of morphologically similar particles in the Δ*lnyI* strain. Given the capacity for linearmycins to lyse *B. subtilis*, we currently speculate that linearmycins may function in an autolytic process in *S.* Mg1. Our current model is that linearmycins build

up to a critical concentration in the *S.* Mg1 cytoplasmic membrane until autolysis occurs. Through autolysis, the cytoplasmic membrane of *S.* Mg1 undergoes vesiculation, which allows linearmycins to be released into the environment. Extracellular vesicles may be a necessary vehicle to deliver linearmycins under environmental conditions. On their own, linearmycins are relatively insoluble and tend to form aggregates under aqueous conditions. Thus, by intertwining linearmycins, autolysis, and vesicle biogenesis *S.* Mg1 is able to release a competitive molecule into the environment that would otherwise likely be diffusion limited. Further work is necessary to determine how linearmycins trigger autolysis and the precise mechanism of extracellular vesicle biogenesis.

The mechanism of linearmycin-induced lysis

We currently do not know the mechanism of linearmycin-induced lysis of *B. subtilis*. However, preliminary results indicate that DNA replication, transcription, translation, and active metabolism are not required for lysis of *B. subtilis* by linearmycins (Figure A18). An understanding of the lysis mechanism will also inform our efforts to determine how linearmycins mediate autolysis in *S.* Mg1.

Linearmycin variants may have different biological activities in competition

Through mass spectral molecular networking we have observed >50 structural variants of linearmycins. The tandem MS/MS spectra for some of these variants indicate the presence of alternative polyketide starter units, glycosylations, and other modifications (Hoefler BC, Stubbendieck RM, Josyula NK, Moisan SM, Schulze EM,

and Straight PD; in preparation). Perhaps specific linearmycin variants will have alternative functions in competition. For instance, the polyketide ECO-02301 is structurally similar to the linearmycins (176). However, after polyketide synthesis ECO-02301 is glycosylated and an amidohydroxycyclopentenone moiety is condensed onto the terminal carboxylic acid group (176, 189). Linearmycin resistant mutants of *B. subtilis* are weakly cross resistant to lysis by ECO-02301 (Table 3). This suggests that different modifications to the linearmycin backbone can result in different biological activities. Currently, isolation and characterization of each linearmycin variant is not feasible as the abundances are low and linearmycins are unstable through extended purification. Further characterization of the *lny* biosynthetic gene cluster may result in identification of mutants that produce particular variants at higher abundances, which will allow us to identify specific activities for specific linearmycin variants.

Linearmycins interface with specialized metabolites produced by B. subtilis

Under the context of bacterial competition, we have observed functional associations of linearmycins with specialized metabolites produced by *B. subtilis*. In addition to providing defense against *M. xanthus*, bacillaene is also important for defense against *S.* Mg1. The bacillaene biosynthesis deficient mutant *B. subtilis* Δ*pks* is hypersensitive to lysis caused by linearmycins (47). The mechanism of bacillaene-mediated protection against linearmycins is not known. Bacillaene is a known translation inhibitor (29). Therefore, during competition with *S.* Mg1, *B. subtilis* may produce bacillaene and partially inhibit translation by *S.* Mg1. The Δ*pks* mutant may be

hypersensitive to lysis by *S.* Mg1 because the latter is uninhibited by bacillaene and better able to synthesize and release linearmycins. Accordingly, in the case of *M. xanthus* predation of *B. subtilis*, it is thought that bacillaene transiently delays *M. xanthus* development. By delaying *M. xanthus* development, *B. subtilis* has time to form spore-filled megastructures and escape consumption by the predator (44, 329). We have also observed an intersection between linearmycin and surfactin. We found that a surfactin biosynthesis deficient mutant *B. subtilis* Δ*srfAA* is mostly resistant to lysis by *S.* Mg1 extracellular vesicles. Pretreatment of *S.* Mg1 vesicles with surfactin before application to *B. subtilis* Δ*srfAA* restored lytic activity (Figure 25). We hypothesize that surfactin may lyse the vesicles produced by *S.* Mg1 or that surfactin may solubilize linearmycins and cause increased lytic activity. As we expand our interaction models to include competitors other than *B. subtilis* we may find new functions of linearmycins.

Bacterial competition identifies multiple functions for an uncharacterized two-component signaling system and an ATP-binding cassette transporter

The YfiJK system senses and responds to linearmycins

After the identification of linearmycins, we became interested in determining their mechanism of lysis against *B. subtilis*. Our initial efforts involved the identification of mutated loci in spontaneous resistant mutants. However, instead of identifying the target of linearmycin, we implicated the YfiJK two-component signaling (TCS) system in linearmycin resistance. Previously, there was no indication of function for this particular TCS system. Subsequently, we became interested in characterizing YfiJK and

its effects on *B. subtilis* as a means to understand signal transduction systems in bacterial competition. We found that the histidine kinase YfiJ acts as a linearmycin sensor (Figure 14, Table 7), which triggers autophosphorylation of a conserved histidine residue. The phosphate is transferred to an aspartate residue on the cognate response regulator YfiK (Table 2). Phosphorylation of response regulators triggers a conformational change that, in the case of YfiK, activates a helix-turn-helix DNA-binding domain (182, 183). The phosphorylated YfiK then binds to the *yfiLMN* promoter and activates expression of the *yfiLMN* operon (Table 4, Figure A7A). YfiLMN is an ATP-binding cassette (ABC) transporter that is both necessary and sufficient for linearmycin resistance (Figure 6).

The ABC transporter YfiLMN is involved in linearmycin resistance and biofilm formation

Previous work in *B. subtilis* has identified three peptide antibiotic-sensing and detoxification (PSD) systems. In PSD systems, the TCS system and ABC transporter genes are encoded together and the TCS system regulates expression of the ABC transporter-encoding genes (193). Currently, only resistance functions have been ascribed to the PSD systems. However, based on the morphology of colonies of linearmycin resistant *B. subtilis*, we have identified additional functions for the YfiJK-LMN system that extend beyond resistance. We found that expression of *yfiLMN* alone is sufficient to causes *B. subtilis* colonies to form biofilms (Figure 13). Intriguingly, unlike canonical biofilm formation in *B. subtilis* that requires many regulators and differential expression of many genes, increased expression from a single operon results

in a morphological similar colony structure (Table 4, Figure A7A). In addition, we found that biofilm formation requires *yfiM* and *yfiN* but not *yfiL* (Table 5). *yfiM* and *yfiN* each encode a membrane spanning domain of the ABC transporter complex. However, *yfiL* encodes the nucleotide-binding domain, which hydrolyzes ATP and provides energy to the complex (192). One hypothesis is that overloading the *B. subtilis* cytoplasmic membrane with membrane proteins may trigger a non-specific biofilm response. We have used transposon mutagenesis to obtain biofilm formation deficient mutants of linearmycin resistant strains as a first step to identify if any additional factors are required to act with YfiM and YfiN. We have identified several candidate genes, with an emphasis on chaperone related functions, and are currently attempting to understand how each candidate influences biofilm formation (Table 6). We also found that the potassium ion leakage sensor KinC is required for YfiLMN-mediated biofilm formation (Figure 16). We hypothesize that YfiLMN causes potassium ion leakage, which KinC senses as part of the mechanism for biofilm formation (27).

Biofilms formed by *B. subtilis* and other bacteria are structures wherein the underlying cells are protected from environmental stresses and insults, including antibiotic exposure (98). We speculate that by coupling specific linearmycin resistance to biofilm formation through YfiLMN, *B. subtilis* may survive competition and prime a protective response against subsequent stresses. For instance, the small and transient linearmycin resistant colonies that we observed in regions of lysis required *yfiJK*, and thus *yfiLMN* expression, to form (Figure 10, Figure A6). Perhaps each small colony was

also in a biofilm state and protected from additional stress, akin to spore-filled megastructures that *B. subtilis* forms when it is exposed to predation by *M. xanthus* (168). Additional work is required to what, if any, environmental stresses YfiLMN-mediated biofilms are protected from. Importantly, the *yfiL* deletion divorces the biofilm and linearmycin resistance functions for the YfiLMN system. Indeed, while *yfiL* is still required for linearmycin resistance, the nucleotide-binding domain is not required for biofilm formation (Table 5). The *yfiL* deletion mutant suggests that active transport is necessary to detoxify *B. subtilis* cells exposed to linearmycin. Further study is necessary to determine how YfiLMN exports linearmycin from the cell.

YfiLMN enables B. subtilis to respond to a motility inducer produced by S. *Mg1*

In addition to biofilm formation, we observed a colony motility phenotype when we cultured linearmycin resistant strains of *B. subtilis* with *S.* Mg1. We find that the portion of *B. subtilis* colonies exposed to *S.* Mg1 undergo a transition from an immotile to a spreading state (Figure 8). Using deletion mutants, we confirmed that this colony motility is dependent upon exopolymeric substances and surfactin, consistent with a type of motility known as sliding (Figure A19). Initially, we hypothesized that induction of sliding motility results as another function of YfiJK. However, when we cultured wild type *B. subtilis* with *S.* Mg1 Δ*lnyI* we found that motility was induced in *B. subtilis* (Figure A17). This observation indicated that motility of *B. subtilis* is induced by *S.* Mg1 but inhibited by linearmycins. Other work from our laboratory has indicated that chloramphenicol and some other ribosome-targeting antibiotics induce *B. subtilis*

motility at subinhibitory concentrations (Liu Y, unpublished results). The *S.* Mg1 genome encodes biosynthetic machinery for only a single recognizable translation inhibitor, chalcomycin A (47, 171). We find that a chalcomycin A biosynthesis mutant of *S.* Mg1 still induces *B. subtilis* motility during competition (Figure A20), which indicates chalcomycin A is either not the motility inducer or *S.* Mg1 may produce multiple motility inducers. Indeed, we have been able to extract a molecule(s) with motility inducing activity from *S.* Mg1, which are currently under investigation (Figure A21).

Conclusions

In summary, this dissertation contributes to our knowledge of a model of bacterial competition by ascribing functions to a previously uncharacterized family of specialized metabolites produced by *S.* Mg1 and a TCS system and ABC transporter complex in *B. subtilis*. The results of this dissertation are summarized in Figure 26. We find that the linearmycins likely trigger an autolytic process in *S.* Mg1 that results in release of linearmycin-laden vesiculated membrane particles as extracellular vesicles. Subsequent exposure to linearmycins then causes the lysis of *B. subtilis*. However, *B. subtilis* senses and responds to the presence of linearmycins with the YfiJK TCS system by activating expression of *yfiLMN*. The YfiLMN ABC transporter complex then prevents *B. subtilis* lysis by presumably detoxifying or pumping linearmycins out of the cytoplasmic membrane.

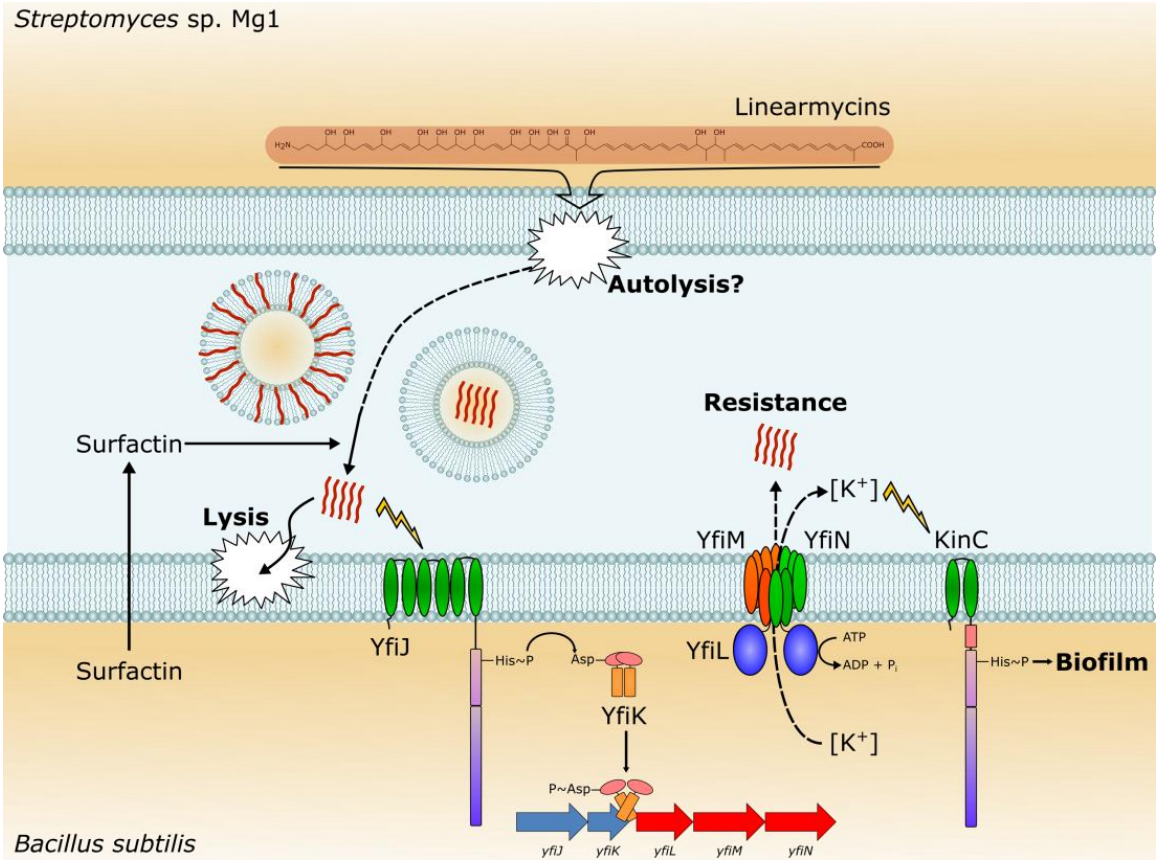

Figure 26. Model of linearmycin-mediated bacterial competition between *B. subtilis* and *S.* Mg1

Linearmycins (red squiggles) are released from *S.* Mg1 through an autolytic process, which also causes the formation of extracellular vesicles, containing linearmycins either within the membrane or as cargo. Surfactin lyses the extracellular vesicles or solubilizes linearmycins. Exposure to linearmycins results in lysis of *B. subtilis*. However, the histidine kinase YfiJ can sense linearmycins, which triggers a signaling cascade that activates the response regulator YfiK and leads to expression of the *yfiLMN* operon. The ABC transporter YfiLMN is responsible for *B. subtilis* linearmycin resistance and biofilm formation through KinC.

Currently, bacterial competition between *B. subtilis* and *S.* Mg1 is one of the best studied models of interspecies interactions. Our laboratory has identified roles for the *B. subtilis* produced specialized metabolites bacillaene and surfactin in bacterial competition. We have also identified competitive functions for chalcomycin A and linearmycins produced by *S.* Mg1. In addition, we identified a hydrolase produced by *S.* Mg1 that is specific against surfactin and plipastatin, another lipopeptide produced by *B. subtilis*. Our current efforts are focused on identifying the motility inducer(s) produced by *S.* Mg1. Concurrently, our laboratory is also undergoing efforts to systematically disrupt genes encoding biosynthetic machinery for every predicted specialized metabolite gene cluster encoded in the *S.* Mg1 genome (Zhang C, unpublished data). By combining chemical, biochemical, and genetic approaches, we will continue to characterize specialized metabolites and enzymes to understand their effects on bacterial competition. Eventually, we can combine and apply this information, along with information garnered from other studies, to train new models of interspecies interactions. Through application of this knowledge we will understand how interactions between two species change dynamics in microbial communities over time.

REFERENCES

1. **Foster KR**, **Bell T**. 2012. Competition, not cooperation, dominates interactions among culturable microbial species. Curr Biol **22**:1845–50.
2. **Birch LC.** 1957. The Meanings of Competition. Am Nat **91**:5–18.
3. **Hibbing ME**, **Fuqua C**, **Parsek MR**, **Peterson SB**. 2010. Bacterial competition: surviving and thriving in the microbial jungle. Nat Rev Microbiol **8**:15–25.
4. **Ling LL**, **Schneider T**, **Peoples AJ**, **Spoering AL**, **Engels I**, **Conlon BP**, **Mueller A**, **Schäberle TF**, **Hughes DE**, **Epstein S**, **Jones M**, **Lazarides L**, **Steadman V a**, **Cohen DR**, **Felix CR**, **Fetterman KA**, **Millett WP**, **Nitti AG**, **Zullo AM**, **Chen C**, **Lewis K**. 2015. A new antibiotic kills pathogens without detectable resistance. Nature **517**:455–9.
5. **Davies J**. 2013. Specialized microbial metabolites: functions and origins. J Antibiot (Tokyo) **66**:361–4.
6. **Price-Whelan A**, **Dietrich LEP**, **Newman DK**. 2006. Rethinking "secondary" metabolism: physiological roles for phenazine antibiotics. Nat Chem Biol **2**:71–8.
7. **Davies J**. 2006. Are antibiotics naturally antibiotics? J Ind Microbiol Biotechnol **33**:496–9.
8. **Yim G**, **Wang HH**, **Davies J**. 2006. The truth about antibiotics. Int J Med Microbiol **296**:163–70.
9. **Yim G**, **Wang HH**, **Davies J**. 2007. Antibiotics as signalling molecules. Philos Trans R Soc Lond B Biol Sci **362**:1195–200.
10. **Romero D**, **Traxler MF**, **López D**, **Kolter R**. 2011. Antibiotics as signal

molecules. Chem Rev **111**:5492–505.

11. **Park T**. 1954. Experimental Studies of Interspecies Competition II. Temperature, Humidity, and Competition in Two Species of Tribolium. Physiol Zool **27**:177–238.

12. **Hider RC**, **Kong X**. 2010. Chemistry and biology of siderophores. Nat Prod Rep **27**:637–57.

13. **Winkelmann G**. 2002. Microbial siderophore-mediated transport. Biochem Soc Trans **30**:691–6.

14. **Lee KH**, **Ruby EG**. 1994. Competition between Vibrio fischeri strains during initiation and maintenance of a light organ symbiosis. J Bacteriol **176**:1985–91.

15. **Harrison F**, **Paul J**, **Massey RC**, **Buckling A**. 2008. Interspecific competition and siderophore-mediated cooperation in Pseudomonas aeruginosa. ISME J **2**:49–55.

16. **Andrews SC**, **Robinson AK**, **Rodríguez-Quiñones F**. 2003. Bacterial iron homeostasis. FEMS Microbiol Rev **27**:215–37.

17. **Traxler MF**, **Seyedsayamdost MR**, **Clardy J**, **Kolter R**. 2012. Interspecies modulation of bacterial development through iron competition and siderophore piracy. Mol Microbiol **86**:628–44.

18. **Galet J**, **Deveau A**, **Hôtel L**, **Frey-Klett P**, **Leblond P**, **Aigle B**. 2015. Pseudomonas fluorescens pirates both ferrioxamine and ferricoelichelin siderophores from Streptomyces ambofaciens. Appl Environ Microbiol **81**:3132–41.

19. **Lewis K**. 2013. Platforms for antibiotic discovery. Nat Rev Drug Discov **12**:371–87.

20. **Davies J**, **Ryan KS**. 2012. Introducing the parvome: bioactive compounds in the microbial world. ACS Chem Biol **7**:252–9.

21. **Bernier SP**, **Surette MG**. 2013. Concentration-dependent activity of antibiotics in natural environments. Front Microbiol **4**:20.

22. **Wang W**, **Ji J**, **Li X**, **Wang J**, **Li S**, **Pan G**, **Fan K**, **Yang K**. 2014. Angucyclines as signals modulate the behaviors of Streptomyces coelicolor. Proc Natl Acad Sci U S A **111**:5688–93.

23. **Jones C**, **Allsopp L**, **Horlick J**, **Kulasekara H**, **Filloux A**. 2013. Subinhibitory concentration of kanamycin induces the Pseudomonas aeruginosa type VI secretion system. PLoS One **8**:e81132.

24. **Davies J**, **Spiegelman GB**, **Yim G**. 2006. The world of subinhibitory antibiotic concentrations. Curr Opin Microbiol **9**:445–53.

25. **Haas D**, **Défago G**. 2005. Biological control of soil-borne pathogens by fluorescent pseudomonads. Nat Rev Microbiol **3**:307–19.

26. **Powers MJ**, **Sanabria-Valentín E**, **Bowers A a.**, **Shank E a.** 2015. Inhibition of Cell Differentiation in Bacillus subtilis by Pseudomonas protegens. J Bacteriol **197**:2129–38.

27. **López D**, **Fischbach M a**, **Chu F**, **Losick R**, **Kolter R**. 2009. Structurally diverse natural products that cause potassium leakage trigger multicellularity in Bacillus subtilis. Proc Natl Acad Sci U S A **106**:280–5.

28. **Bleich R**, **Watrous JD**, **Dorrestein PC**, **Bowers A a.**, **Shank E a.** 2015. Thiopeptide antibiotics stimulate biofilm formation in Bacillus subtilis. Proc Natl Acad Sci U S A **112**:3086–91.

29. **Patel PS**, **Huang S**, **Fisher S**, **Pirnik D**, **Aklonis C**, **Dean L**, **Meyers E**, **Fernandes P**, **Mayerl F**. 1995. Bacillaene, a novel inhibitor of procaryotic protein synthesis produced by Bacillus subtilis: production, taxonomy, isolation, physico-chemical characterization and biological activity. J Antibiot (Tokyo) **48**:997–1003.

30. **Straight PD**, **Fischbach M a**, **Walsh CT**, **Rudner DZ**, **Kolter R**. 2007. A singular enzymatic megacomplex from Bacillus subtilis. Proc Natl Acad Sci U S A **104**:305–10.

31. **Vargas-Bautista C**, **Rahlwes K**, **Straight P**. 2014. Bacterial competition reveals differential regulation of the pks genes by Bacillus subtilis. J Bacteriol **196**:717–28.

32. **Teasdale ME**, **Liu J**, **Wallace J**, **Akhlaghi F**, **Rowley DC**. 2009. Secondary metabolites produced by the marine bacterium Halobacillus salinus that inhibit quorum sensing-controlled phenotypes in gram-negative bacteria. Appl Environ Microbiol **75**:567–72.

33. **Kwan JC**, **Meickle T**, **Ladwa D**, **Teplitski M**, **Paul V**, **Luesch H**. 2011. Lyngbyoic acid, a "tagged" fatty acid from a marine cyanobacterium, disrupts quorum sensing in Pseudomonas aeruginosa. Mol Biosyst **7**:1205–16.

34. **Chater KF**. 2006. Streptomyces inside-out: a new perspective on the bacteria that

provide us with antibiotics. Philos Trans R Soc Lond B Biol Sci **361**:761–8.

35. **Flärdh K**, **Buttner MJ**. 2009. Streptomyces morphogenetics: dissecting differentiation in a filamentous bacterium. Nat Rev Microbiol **7**:36–49.

36. **Kodani S**, **Hudson ME**, **Durrant MC**, **Buttner MJ**, **Nodwell JR**, **Willey JM**. 2004. The SapB morphogen is a lantibiotic-like peptide derived from the product of the developmental gene ramS in Streptomyces coelicolor. Proc Natl Acad Sci U S A **101**:11448–53.

37. **Kearns DB**, **Losick R**. 2003. Swarming motility in undomesticated Bacillus subtilis. Mol Microbiol **49**:581–90.

38. **López D**, **Vlamakis H**, **Losick R**, **Kolter R**. 2009. Paracrine signaling in a bacterium. Genes Dev **23**:1631–8.

39. **Straight PD**, **Willey JM**, **Kolter R**. 2006. Interactions between Streptomyces coelicolor and Bacillus subtilis: Role of surfactants in raising aerial structures. J Bacteriol **188**:4918–25.

40. **Hoefler BC**, **Gorzelnik K V.**, **Yang JY**, **Hendricks N**, **Dorrestein PC**, **Straight PD**. 2012. Enzymatic resistance to the lipopeptide surfactin as identified through imaging mass spectrometry of bacterial competition. Proc Natl Acad Sci U S A **109**:13082–7.

41. **Gaskell AA**, **Giovinazzo JA**, **Fonte V**, **Willey JM**. 2012. Multi-tier regulation of the streptomycete morphogenetic peptide SapB. Mol Microbiol **84**:501–15.

42. **Wright GD**. 2005. Bacterial resistance to antibiotics: enzymatic degradation and modification. Adv Drug Deliv Rev **57**:1451–70.

43. **Basler M**, **Pilhofer M**, **Henderson GP**, **Jensen GJ**, **Mekalanos JJ**. 2012. Type VI secretion requires a dynamic contractile phage tail-like structure. Nature **483**:182–6.

44. **Müller S**, **Strack SN**, **Hoefler BC**, **Straight PD**, **Kearns DB**, **Kirby JR**. 2014. Bacillaene and sporulation protect Bacillus subtilis from predation by Myxococcus xanthus. Appl Environ Microbiol **80**:5603–10.

45. **Mootz HD**, **Finking R**, **Marahiel M a.** 2001. 4'-phosphopantetheine transfer in primary and secondary metabolism of Bacillus subtilis. J Biol Chem **276**:37289–98.

46. **McLoon AL**, **Guttenplan SB**, **Kearns DB**, **Kolter R**, **Losick R**. 2011. Tracing the domestication of a biofilm-forming bacterium. J Bacteriol **193**:2027–34.

47. **Barger SR**, **Hoefler BC**, **Cubillos-Ruiz A**, **Russell WK**, **Russell DH**, **Straight PD**. 2012. Imaging secondary metabolism of Streptomyces sp. Mg1 during cellular lysis and colony degradation of competing Bacillus subtilis. Antonie Van Leeuwenhoek **102**:435–45.

48. **Kang BR**, **Lee JH**, **Ko SJ**, **Lee YH**, **Cha JS**, **Cho BH**, **Kim YC**. 2004. Degradation of acyl-homoserine lactone molecules by Acinetobacter sp. strain C1010. Can J Microbiol **50**:935–41.

49. **Park S**, **Kang H**, **Jang H**, **Lee J**, **Koo B**, **Yum D**. 2005. Identification of extracellular N-acylhomoserine lactone acylase from a Streptomyces sp. and its application to quorum quenching. Appl Environ Microbiol **71**:2632–41.

50. **Sio CF**, **Otten LG**, **Cool RH**, **Diggle SP**, **Braun PG**, **Bos R**, **Daykin M**,

Cámara M, **Williams P**, **Quax WJ**. 2006. Quorum quenching by an N-acyl-homoserine lactone acylase from Pseudomonas aeruginosa PAO1. Infect Immun **74**:1673–82.

51. **Medina-Martínez MS**, **Uyttendaele M**, **Rajkovic A**, **Nadal P**, **Debevere J**. 2007. Degradation of N-acyl-L-homoserine lactones by Bacillus cereus in culture media and pork extract. Appl Environ Microbiol **73**:2329–32.

52. **Goldman BS**, **Nierman WC**, **Kaiser D**, **Slater SC**, **Durkin a S**, **Eisen JA**, **Eisen J**, **Ronning CM**, **Barbazuk WB**, **Blanchard M**, **Field C**, **Halling C**, **Hinkle G**, **Iartchuk O**, **Kim HS**, **Mackenzie C**, **Madupu R**, **Miller N**, **Shvartsbeyn A**, **Sullivan S a**, **Vaudin M**, **Wiegand R**, **Kaplan HB**. 2006. Evolution of sensory complexity recorded in a myxobacterial genome. Proc Natl Acad Sci U S A **103**:15200–5.

53. **Berleman JE**, **Kirby JR**. 2009. Deciphering the hunting strategy of a bacterial wolfpack. FEMS Microbiol Rev **33**:942–57.

54. **Sudo S**, **Dworkin M**. 1972. Bacteriolytic enzymes produced by Myxococcus xanthus. J Bacteriol **110**:236–45.

55. **Lina G**, **Boutite F**, **Tristan A**, **Bes M**, **Etienne J**, **Vandenesch F**. 2003. Bacterial competition for human nasal cavity colonization: role of Staphylococcal agr alleles. Appl Environ Microbiol **69**:18–23.

56. **Iwase T**, **Uehara Y**, **Shinji H**, **Tajima A**, **Seo H**, **Takada K**, **Agata T**, **Mizunoe Y**. 2010. Staphylococcus epidermidis Esp inhibits Staphylococcus aureus biofilm formation and nasal colonization. Nature **465**:346–9.

57. **Chen C**, **Krishnan V**, **Macon K**, **Manne K**, **Narayana SVL**, **Schneewind O**. 2013. Secreted proteases control autolysin-mediated biofilm growth of Staphylococcus aureus. J Biol Chem **288**:29440–52.

58. **Laufer AS**, **Metlay JP**, **Gent JF**, **Fennie KP**, **Kong Y**, **Pettigrew MM**. 2011. Microbial communities of the upper respiratory tract and otitis media in children. MBio **2**:e00245-10.

59. **Bomar L**, **Brugger SD**, **Yost BH**, **Davies SS**, **Lemon KP**. 2016. Corynebacterium accolens Releases Antipneumococcal Free Fatty Acids from Human Nostril and Skin Surface Triacylglycerols. MBio **7**:e01725-15.

60. **Speert DP**, **Wannamaker LW**, **Gray ED**, **Clawson CC**. 1979. Bactericidal effect of oleic acid on group A streptococci: mechanism of action. Infect Immun **26**:1202–10.

61. **Berleman J**, **Auer M**. 2013. The role of bacterial outer membrane vesicles for intra- and interspecies delivery. Environ Microbiol **15**:347–54.

62. **Schwechheimer C**, **Sullivan CJ**, **Kuehn MJ**. 2013. Envelope control of outer membrane vesicle production in Gram-negative bacteria. Biochemistry **52**:3031–40.

63. **Turnbull L**, **Toyofuku M**, **Hynen AL**, **Kurosawa M**, **Pessi G**, **Petty NK**, **Osvath SR**, **Cárcamo-Oyarce G**, **Gloag ES**, **Shimoni R**, **Omasits U**, **Ito S**, **Yap X**, **Monahan LG**, **Cavaliere R**, **Ahrens CH**, **Charles IG**, **Nomura N**, **Eberl L**, **Whitchurch CB**. 2016. Explosive cell lysis as a mechanism for the biogenesis of bacterial membrane vesicles and biofilms. Nat Commun **7**:11220.

64. **Brown L**, **Wolf JM**, **Prados-Rosales R**, **Casadevall A**. 2015. Through the wall: extracellular vesicles in Gram-positive bacteria, mycobacteria and fungi. Nat Rev Microbiol **13**:620–30.

65. **Kadurugamuwa JL**, **Beveridge TJ**. 1996. Bacteriolytic effect of membrane vesicles from Pseudomonas aeruginosa on other bacteria including pathogens: conceptually new antibiotics. J Bacteriol **178**:2767–74.

66. **Schooling SR**, **Beveridge TJ**. 2006. Membrane vesicles: an overlooked component of the matrices of biofilms. J Bacteriol **188**:5945–57.

67. **Biller SJ**, **Schubotz F**, **Roggensack SE**, **Thompson AW**, **Summons RE**, **Chisholm SW**. 2014. Bacterial vesicles in marine ecosystems. Science **343**:183–6.

68. **Kuehn MJ**, **Kesty NC**. 2005. Bacterial outer membrane vesicles and the host-pathogen interaction. Genes Dev **19**:2645–55.

69. **Mashburn LM**, **Whiteley M**. 2005. Membrane vesicles traffic signals and facilitate group activities in a prokaryote. Nature **437**:422–5.

70. **Ciofu O**, **Beveridge TJ**, **Kadurugamuwa J**, **Walther-Rasmussen J**, **Høiby N**. 2000. Chromosomal beta-lactamase is packaged into membrane vesicles and secreted from Pseudomonas aeruginosa. J Antimicrob Chemother **45**:9–13.

71. **Lee J**, **Lee E-Y**, **Kim S-H**, **Kim D-K**, **Park K-S**, **Kim KP**, **Kim Y-K**, **Roh T-Y**, **Gho YS**. 2013. Staphylococcus aureus extracellular vesicles carry biologically active β-lactamase. Antimicrob Agents Chemother **57**:2589–95.

72. **Kulkarni HM**, **Nagaraj R**, **Jagannadham M V**. 2015. Protective role of E. coli

outer membrane vesicles against antibiotics. Microbiol Res **181**:1–7.

73. **Vasilyeva N V**, **Tsfasman IM**, **Suzina NE**, **Stepnaya O a**, **Kulaev IS**. 2008. Secretion of bacteriolytic endopeptidase L5 of Lysobacter sp. XL1 into the medium by means of outer membrane vesicles. FEBS J **275**:3827–35.

74. **Schrempf H**, **Koebsch I**, **Walter S**, **Engelhardt H**, **Meschke H**. 2011. Extracellular Streptomyces vesicles: amphorae for survival and defence. Microb Biotechnol **4**:286–99.

75. **Schrempf H**, **Merling P**. 2015. Extracellular Streptomyces lividans vesicles: composition, biogenesis and antimicrobial activity. Microb Biotechnol **8**:644–58.

76. **Berleman JE**, **Allen S**, **Danielewicz MA**, **Remis JP**, **Gorur A**, **Cunha J**, **Hadi MZ**, **Zusman DR**, **Northen TR**, **Witkowska HE**, **Auer M**. 2014. The lethal cargo of Myxococcus xanthus outer membrane vesicles. Front Microbiol **5**:474.

77. **Meiser P**, **Bode HB**, **Müller R**. 2006. The unique DKxanthene secondary metabolite family from the myxobacterium Myxococcus xanthus is required for developmental sporulation. Proc Natl Acad Sci U S A **103**:19128–33.

78. **Gerth K**, **Jansen R**, **Reifenstahl G**, **Höfle G**, **Irschik H**, **Kunze B**, **Reichenbach H**, **Thierbach G**. 1983. The myxalamids, new antibiotics from Myxococcus xanthus (Myxobacterales). I. Production, physico-chemical and biological properties, and mechanism of action. J Antibiot (Tokyo) **36**:1150–6.

79. **Brown L**, **Kessler A**, **Cabezas-Sanchez P**, **Luque-Garcia JL**, **Casadevall A**. 2014. Extracellular vesicles produced by the Gram-positive bacterium Bacillus subtilis are disrupted by the lipopeptide surfactin. Mol Microbiol **93**:183–98.

80. **Butler MT**, **Wang Q**, **Harshey RM**. 2010. Cell density and mobility protect swarming bacteria against antibiotics. Proc Natl Acad Sci U S A **107**:3776–81.

81. **Kearns DB**, **Chu F**, **Rudner R**, **Losick R**. 2004. Genes governing swarming in Bacillus subtilis and evidence for a phase variation mechanism controlling surface motility. Mol Microbiol **52**:357–69.

82. **van Gestel J**, **Vlamakis H**, **Kolter R**. 2015. From cell differentiation to cell collectives: Bacillus subtilis uses division of labor to migrate. PLoS Biol **13**:e1002141.

83. **Aoki SK**, **Pamma R**, **Hernday AD**, **Bickham JE**, **Braaten B a**, **Low D a**. 2005. Contact-dependent inhibition of growth in Escherichia coli. Science **309**:1245–8.

84. **Jacob-Dubuisson F**, **Locht C**, **Antoine R**. 2001. Two-partner secretion in Gram-negative bacteria: a thrifty, specific pathway for large virulence proteins. Mol Microbiol **40**:306–13.

85. **Aoki SK**, **Poole SJ**, **Hayes CS**, **Low DA**. 2011. Toxin on a stick: modular CDI toxin delivery systems play roles in bacterial competition. Virulence **2**:356–9.

86. **Aoki SK**, **Diner EJ**, **de Roodenbeke CT**, **Burgess BR**, **Poole SJ**, **Braaten BA**, **Jones AM**, **Webb JS**, **Hayes CS**, **Cotter PA**, **Low DA**. 2010. A widespread family of polymorphic contact-dependent toxin delivery systems in bacteria. Nature **468**:439–42.

87. **Aoki SK**, **Malinverni JC**, **Jacoby K**, **Thomas B**, **Pamma R**, **Trinh BN**, **Remers S**, **Webb J**, **Braaten BA**, **Silhavy TJ**, **Low DA**. 2008. Contact-dependent growth inhibition requires the essential outer membrane protein BamA (YaeT) as the

receptor and the inner membrane transport protein AcrB. Mol Microbiol **70**:323–40.

88. **Webb JS**, **Nikolakakis KC**, **Willett JLE**, **Aoki SK**, **Hayes CS**, **Low DA**. 2013. Delivery of CdiA nuclease toxins into target cells during contact-dependent growth inhibition. PLoS One **8**:e57609.

89. **Ruhe ZC**, **Nguyen JY**, **Beck CM**, **Low DA**, **Hayes CS**. 2014. The proton-motive force is required for translocation of CDI toxins across the inner membrane of target bacteria. Mol Microbiol **94**:466–81.

90. **Willett JLE**, **Gucinski GC**, **Fatherree JP**, **Low DA**, **Hayes CS**. 2015. Contact-dependent growth inhibition toxins exploit multiple independent cell-entry pathways. Proc Natl Acad Sci U S A **112**:11341–6.

91. **Ruhe ZC**, **Wallace AB**, **Low DA**, **Hayes CS**. 2013. Receptor polymorphism restricts contact-dependent growth inhibition to members of the same species. MBio **4**:529–542.

92. **Stewart PS**, **Franklin MJ**. 2008. Physiological heterogeneity in biofilms. Nat Rev Microbiol **6**:199–210.

93. **Kim W**, **Racimo F**, **Schluter J**, **Levy SB**, **Foster KR**. 2014. Importance of positioning for microbial evolution. Proc Natl Acad Sci U S A **111**:E1639-47.

94. **Anderson MS**, **Garcia EC**, **Cotter PA**. 2012. The Burkholderia bcpAIOB genes define unique classes of two-partner secretion and contact dependent growth inhibition systems. PLoS Genet **8**:e1002877.

95. **Garcia EC**, **Anderson MS**, **Hagar JA**, **Cotter PA**. 2013. Burkholderia BcpA

mediates biofilm formation independently of interbacterial contact-dependent growth inhibition. Mol Microbiol **89**:1213–25.

96. **Ruhe ZC**, **Townsley L**, **Wallace AB**, **King A**, **Van der Woude MW**, **Low DA**, **Yildiz FH**, **Hayes CS**. 2015. CdiA promotes receptor-independent intercellular adhesion. Mol Microbiol **98**:175–92.

97. **Mercy C**, **Ize B**, **Salcedo SP**, **de Bentzmann S**, **Bigot S**. 2016. Functional Characterization of Pseudomonas Contact Dependent Growth Inhibition (CDI) Systems. PLoS One **11**:e0147435.

98. **Mah TF**, **O'Toole G a.** 2001. Mechanisms of biofilm resistance to antimicrobial agents. Trends Microbiol **9**:34–9.

99. **Nadell CD**, **Bassler BL**. 2011. A fitness trade-off between local competition and dispersal in Vibrio cholerae biofilms. Proc Natl Acad Sci U S A **108**:14181–5.

100. **Rendueles O**, **Ghigo J**. 2015. Mechanisms of Competition in Biofilm Communities. Microbiol Spectr **3**:1–18.

101. **Anderson MS**, **Garcia EC**, **Cotter PA**. 2014. Kind discrimination and competitive exclusion mediated by contact-dependent growth inhibition systems shape biofilm community structure. PLoS Pathog **10**:e1004076.

102. **Pukatzki S**, **Ma AT**, **Sturtevant D**, **Krastins B**, **Sarracino D**, **Nelson WC**, **Heidelberg JF**, **Mekalanos JJ**. 2006. Identification of a conserved bacterial protein secretion system in Vibrio cholerae using the Dictyostelium host model system. Proc Natl Acad Sci U S A **103**:1528–33.

103. **Bingle LE**, **Bailey CM**, **Pallen MJ**. 2008. Type VI secretion: a beginner's guide.

Curr Opin Microbiol **11**:3–8.

104. **Carruthers MD**, **Nicholson P a**, **Tracy EN**, **Munson RS**. 2013. Acinetobacter baumannii utilizes a type VI secretion system for bacterial competition. PLoS One **8**:e59388.

105. **Murdoch SL**, **Trunk K**, **English G**, **Fritsch MJ**, **Pourkarimi E**, **Coulthurst SJ**. 2011. The opportunistic pathogen Serratia marcescens utilizes type VI secretion to target bacterial competitors. J Bacteriol **193**:6057–69.

106. **Hood RD**, **Singh P**, **Hsu F**, **Güvener T**, **Carl MA**, **Trinidad RRS**, **Silverman JM**, **Ohlson BB**, **Hicks KG**, **Plemel RL**, **Li M**, **Schwarz S**, **Wang WY**, **Merz AJ**, **Goodlett DR**, **Mougous JD**. 2010. A type VI secretion system of Pseudomonas aeruginosa targets a toxin to bacteria. Cell Host Microbe **7**:25–37.

107. **Leiman PG**, **Basler M**, **Ramagopal U a**, **Bonanno JB**, **Sauder JM**, **Pukatzki S**, **Burley SK**, **Almo SC**, **Mekalanos JJ**. 2009. Type VI secretion apparatus and phage tail-associated protein complexes share a common evolutionary origin. Proc Natl Acad Sci U S A **106**:4154–9.

108. **Russell AB**, **LeRoux M**, **Hathazi K**, **Agnello DM**, **Ishikawa T**, **Wiggins P a**, **Wai SN**, **Mougous JD**. 2013. Diverse type VI secretion phospholipases are functionally plastic antibacterial effectors. Nature **496**:508–12.

109. **Jiang F**, **Waterfield NR**, **Yang J**, **Yang G**, **Jin Q**. 2014. A Pseudomonas aeruginosa type VI secretion phospholipase D effector targets both prokaryotic and eukaryotic cells. Cell Host Microbe **15**:600–10.

110. **Flaugnatti N**, **Le TTH**, **Canaan S**, **Aschtgen M-S**, **Nguyen VS**, **Blangy S**,

Kellenberger C, **Roussel A**, **Cambillau C**, **Cascales E**, **Journet L**. 2016. A phospholipase A1 antibacterial Type VI secretion effector interacts directly with the C-terminal domain of the VgrG spike protein for delivery. Mol Microbiol **99**:1099–118.

111. **Russell AB**, **Hood RD**, **Bui NK**, **LeRoux M**, **Vollmer W**, **Mougous JD**. 2011. Type VI secretion delivers bacteriolytic effectors to target cells. Nature **475**:343–7.

112. **Russell AB**, **Singh P**, **Brittnacher M**, **Bui NK**, **Hood RD**, **Carl MA**, **Agnello DM**, **Schwarz S**, **Goodlett DR**, **Vollmer W**, **Mougous JD**. 2012. A widespread bacterial type VI secretion effector superfamily identified using a heuristic approach. Cell Host Microbe **11**:538–49.

113. **Chou S**, **Bui NK**, **Russell AB**, **Lexa KW**, **Gardiner TE**, **LeRoux M**, **Vollmer W**, **Mougous JD**. 2012. Structure of a peptidoglycan amidase effector targeted to Gram-negative bacteria by the type VI secretion system. Cell Rep **1**:656–64.

114. **Koskiniemi S**, **Lamoureux JG**, **Nikolakakis KC**, **t'Kint de Roodenbeke C**, **Kaplan MD**, **Low D a**, **Hayes CS**. 2013. Rhs proteins from diverse bacteria mediate intercellular competition. Proc Natl Acad Sci U S A **110**:7032–7.

115. **Ma L-S**, **Hachani A**, **Lin J-S**, **Filloux A**, **Lai E-M**. 2014. Agrobacterium tumefaciens deploys a superfamily of type VI secretion DNase effectors as weapons for interbacterial competition in planta. Cell Host Microbe **16**:94–104.

116. **Basler M**, **Ho BT**, **Mekalanos JJ**. 2013. Tit-for-tat: type VI secretion system counterattack during bacterial cell-cell interactions. Cell **152**:884–94.

117. **LeRoux M**, **Peterson SB**, **Mougous JD**. 2015. Bacterial danger sensing. J Mol Biol **427**:3744–53.

118. **Basler M**, **Mekalanos JJ**. 2012. Type 6 secretion dynamics within and between bacterial cells. Science **337**:815.

119. **LeRoux M**, **Kirkpatrick RL**, **Montauti EI**, **Tran BQ**, **Peterson SB**, **Harding BN**, **Whitney JC**, **Russell AB**, **Traxler B**, **Goo YA**, **Goodlett DR**, **Wiggins PA**, **Mougous JD**. 2015. Kin cell lysis is a danger signal that activates antibacterial pathways of Pseudomonas aeruginosa. Elife **4**:1–65.

120. **Alteri CJ**, **Himpsl SD**, **Pickens SR**, **Lindner JR**, **Zora JS**, **Miller JE**, **Arno PD**, **Straight SW**, **Mobley HLT**. 2013. Multicellular bacteria deploy the type VI secretion system to preemptively strike neighboring cells. PLoS Pathog **9**:e1003608.

121. **Vos M**, **Velicer GJ**. 2009. Social conflict in centimeter-and global-scale populations of the bacterium Myxococcus xanthus. Curr Biol **19**:1763–7.

122. **Stefanic P**, **Kraigher B**, **Lyons NA**, **Kolter R**, **Mandic-Mulec I**. 2015. Kin discrimination between sympatric Bacillus subtilis isolates. Proc Natl Acad Sci U S A **112**:14042–7.

123. **Lyons NA**, **Kraigher B**, **Stefanic P**, **Mandic-Mulec I**, **Kolter R**. 2016. A Combinatorial Kin Discrimination System in Bacillus subtilis. Curr Biol **26**:733–42.

124. **Whitney JC**, **Quentin D**, **Sawai S**, **LeRoux M**, **Harding BN**, **Ledvina HE**, **Tran BQ**, **Robinson H**, **Goo YA**, **Goodlett DR**, **Raunser S**, **Mougous JD**. 2015.

An interbacterial NAD(P)(+) glycohydrolase toxin requires elongation factor Tu for delivery to target cells. Cell **163**:607–19.

125. **Nudleman E**, **Wall D**, **Kaiser D**. 2005. Cell-to-cell transfer of bacterial outer membrane lipoproteins. Science **309**:125–7.

126. **Pathak DT**, **Wei X**, **Bucuvalas A**, **Haft DH**, **Gerloff DL**, **Wall D**. 2012. Cell contact-dependent outer membrane exchange in myxobacteria: genetic determinants and mechanism. PLoS Genet **8**:e1002626.

127. **Vassallo C**, **Pathak DT**, **Cao P**, **Zuckerman DM**, **Hoiczyk E**, **Wall D**. 2015. Cell rejuvenation and social behaviors promoted by LPS exchange in myxobacteria. Proc Natl Acad Sci U S A **112**:E2939-46.

128. **Dey A**, **Wall D**. 2014. A genetic screen in Myxococcus xanthus identifies mutants that uncouple outer membrane exchange from a downstream cellular response. J Bacteriol **196**:4324–32.

129. **Pathak DT**, **Wei X**, **Dey A**, **Wall D**. 2013. Molecular recognition by a polymorphic cell surface receptor governs cooperative behaviors in bacteria. PLoS Genet **9**:e1003891.

130. **Dey A**, **Vassallo CN**, **Conklin AC**, **Pathak DT**, **Troselj V**, **Wall D**. 2016. Sibling Rivalry in Myxococcus xanthus Is Mediated by Kin Recognition and a Polyploid Prophage. J Bacteriol **198**:994–1004.

131. **Goh E-B**, **Yim G**, **Tsui W**, **McClure J**, **Surette MG**, **Davies J**. 2002. Transcriptional modulation of bacterial gene expression by subinhibitory concentrations of antibiotics. Proc Natl Acad Sci U S A **99**:17025–30.

132. **Chen L**, **He S**, **Li C**, **Ryu J**. 2009. Sublethal kanamycin induced cross resistance to functionally and structurally unrelated antibiotics. J Exp Microbiol Immunol **13**:53–57.

133. **Han TH**, **Lee J-HJ**, **Cho MH**, **Wood TK**, **Lee J-HJ**. 2011. Environmental factors affecting indole production in Escherichia coli. Res Microbiol **162**:108–16.

134. **Roch M**, **Clair P**, **Renzoni A**, **Reverdy M-E**, **Dauwalder O**, **Bes M**, **Martra A**, **Freydière A-M**, **Laurent F**, **Reix P**, **Dumitrescu O**, **Vandenesch F**. 2014. Exposure of Staphylococcus aureus to subinhibitory concentrations of β-lactam antibiotics induces heterogeneous vancomycin-intermediate Staphylococcus aureus. Antimicrob Agents Chemother **58**:5306–14.

135. **Gullberg E**, **Cao S**, **Berg OG**, **Ilbäck C**, **Sandegren L**, **Hughes D**, **Andersson DI**. 2011. Selection of resistant bacteria at very low antibiotic concentrations. PLoS Pathog **7**:e1002158.

136. **Hoffman LR**, **D'Argenio DA**, **MacCoss MJ**, **Zhang Z**, **Jones RA**, **Miller SI**. 2005. Aminoglycoside antibiotics induce bacterial biofilm formation. Nature **436**:1171–5.

137. **Marr AK**, **Overhage J**, **Bains M**, **Hancock REW**. 2007. The Lon protease of Pseudomonas aeruginosa is induced by aminoglycosides and is involved in biofilm formation and motility. Microbiology **153**:474–82.

138. **Kaplan JB**, **Izano E a**, **Gopal P**, **Karwacki MT**, **Kim S**, **Bose JL**, **Bayles KW**, **Horswill AR**. 2012. Low levels of β-lactam antibiotics induce extracellular DNA

release and biofilm formation in Staphylococcus aureus. MBio **3**:e00198-12.

139. **Graff JR**, **Forschner-Dancause SR**, **Menden-Deuer S**, **Long R a**, **Rowley DC**. 2013. Vibrio cholerae Exploits Sub-Lethal Concentrations of a Competitor-Produced Antibiotic to Avoid Toxic Interactions. Front Microbiol **4**:8.

140. **Boruah HPD**, **Kumar BSD**. 2002. Biological activity of secondary metabolites produced by a strain of Pseudomonas fluorescens. Folia Microbiol (Praha) **47**:359–63.

141. **Lerner TR**, **Lovering AL**, **Bui NK**, **Uchida K**, **Aizawa S**, **Vollmer W**, **Sockett RE**. 2012. Specialized peptidoglycan hydrolases sculpt the intra-bacterial niche of predatory Bdellovibrio and increase population fitness. PLoS Pathog **8**:e1002524.

142. **Lambert C**, **Sockett RE**. 2013. Nucleases in Bdellovibrio bacteriovorus contribute towards efficient self-biofilm formation and eradication of preformed prey biofilms. FEMS Microbiol Lett **340**:109–16.

143. **Chopra I**. 1988. Molecular mechanisms involved in the transport of antibiotics into bacteria. Parasitology **96 Suppl**:S25-44.

144. **Livermore DM**. 1990. Antibiotic uptake and transport by bacteria. Scand J Infect Dis Suppl **74**:15–22.

145. **Weber BS**, **Ly PM**, **Irwin JN**, **Pukatzki S**, **Feldman MF**. 2015. A multidrug resistance plasmid contains the molecular switch for type VI secretion in Acinetobacter baumannii. Proc Natl Acad Sci U S A **112**:9442–7.

146. **Kurtz ZD**, **Müller CL**, **Miraldi ER**, **Littman DR**, **Blaser MJ**, **Bonneau RA**. 2015. Sparse and compositionally robust inference of microbial ecological

networks. PLoS Comput Biol **11**:e1004226.

147. **Coyte KZ**, **Schluter J**, **Foster KR**. 2015. The ecology of the microbiome: Networks, competition, and stability. Science **350**:663–6.

148. **Ochi K**, **Hosaka T**. 2013. New strategies for drug discovery: activation of silent or weakly expressed microbial gene clusters. Appl Microbiol Biotechnol **97**:87–98.

149. **Beck CM**, **Morse RP**, **Cunningham D a.**, **Iniguez A**, **Low D a.**, **Goulding CW**, **Hayes CS**. 2014. CdiA from Enterobacter cloacae delivers a toxic ribosomal RNase into target bacteria. Structure **22**:707–18.

150. **Mougous JD**, **Cuff ME**, **Raunser S**, **Shen A**, **Zhou M**, **Gifford C a**, **Goodman AL**, **Joachimiak G**, **Ordoñez CL**, **Lory S**, **Walz T**, **Joachimiak A**, **Mekalanos JJ**. 2006. A virulence locus of Pseudomonas aeruginosa encodes a protein secretion apparatus. Science **312**:1526–30.

151. **Koch G**, **Yepes A**, **Förstner KU**, **Wermser C**, **Stengel ST**, **Modamio J**, **Ohlsen K**, **Foster KR**, **Lopez D**. 2014. Evolution of resistance to a last-resort antibiotic in Staphylococcus aureus via bacterial competition. Cell **158**:1060–71.

152. **Straight PD**, **Kolter R**. 2009. Interspecies chemical communication in bacterial development. Annu Rev Microbiol **63**:99–118.

153. **Traxler MF**, **Kolter R**. 2015. Natural products in soil microbe interactions and evolution. Nat Prod Rep **32**:956–70.

154. **Traxler MF**, **Watrous JD**, **Alexandrov T**, **Dorrestein PC**, **Kolter R**. 2013. Interspecies interactions stimulate diversification of the Streptomyces coelicolor

secreted metabolome. MBio **4**:1–12.

155. **Derewacz DK**, **Covington BC**, **McLean J a.**, **Bachmann BO**. 2015. Mapping microbial response metabolomes for induced natural product discovery. ACS Chem Biol 150603152224005.

156. **Russell AB**, **Peterson SB**, **Mougous JD**. 2014. Type VI secretion system effectors: poisons with a purpose. Nat Rev Microbiol **12**:137–48.

157. **Oliveira NM**, **Oliveria NM**, **Martinez-Garcia E**, **Xavier J**, **Durham WM**, **Kolter R**, **Kim W**, **Foster KR**. 2015. Biofilm formation as a response to ecological competition. PLoS Biol **13**:1–23.

158. **Sansinenea E**, **Ortiz A**. 2011. Secondary metabolites of soil Bacillus spp. Biotechnol Lett **33**:1523–38.

159. **Weissman KJ**, **Müller R**. 2010. Myxobacterial secondary metabolites: bioactivities and modes-of-action. Nat Prod Rep **27**:1276–95.

160. **Lopez D**, **Vlamakis H**, **Kolter R**. 2009. Generation of multiple cell types in Bacillus subtilis. FEMS Microbiol Rev **33**:152–163.

161. **Claessen D**, **Rozen DE**, **Kuipers OP**, **Søgaard-Andersen L**, **van Wezel GP**. 2014. Bacterial solutions to multicellularity: a tale of biofilms, filaments and fruiting bodies. Nat Rev Microbiol **12**:115–124.

162. **Stein T**. 2005. Bacillus subtilis antibiotics: Structures, syntheses and specific functions. Mol Microbiol **56**:845–857.

163. **Nakano MM**, **Magnuson R**, **Myers a.**, **Curry J**, **Grossman a. D**, **Zuber P**. 1991. srfA is an operon required for surfactin production, competence

development, and efficient sporulation in Bacillus subtilis. J Bacteriol **173**:1770–1778.

164. **Miyake K**, **Kuzuyama T**, **Horinouchi S**, **Beppu T**. 1990. The A-factor-binding protein of Streptomyces griseus negatively controls streptomycin production and sporulation. J Bacteriol **172**:3003–3008.

165. **Méndez C**, **Braña AF**, **Manzanal MB**, **Hardisson C**. 1985. Role of substrate mycelium in colony development in Streptomyces. Can J Microbiol **31**:446–50.

166. **Manteca A**, **Fernandez M**, **Sanchez J**. 2006. Cytological and biochemical evidence for an early cell dismantling event in surface cultures of Streptomyces antibioticus. Res Microbiol **157**:143–152.

167. **Chater KF**, **Biró S**, **Lee KJ**, **Palmer T**, **Schrempf H**. 2010. The complex extracellular biology of Streptomyces. FEMS Microbiol Rev **34**:171–98.

168. **Müller S**, **Strack SN**, **Ryan SE**, **Kearns DB**, **Kirby JR**. 2015. Predation by Myxococcus xanthus induces Bacillus subtilis to form spore-filled megastructures. Appl Environ Microbiol **81**:203–10.

169. **Leenders F**, **Stein TH**, **Kablitz B**, **Franke P**, **Vater J**. 1999. Rapid typing of Bacillus subtilis strains by their secondary metabolites using matrix-assisted laser desorption/ionization mass spectrometry of intact cells. Rapid Commun Mass Spectrom **13**:943–949.

170. **Yang Y-L**, **Xu Y**, **Straight P**, **Dorrestein PC**. 2009. Translating metabolic exchange with imaging mass spectrometry. Nat Chem Biol **5**:885–7.

171. **Hoefler BC**, **Konganti K**, **Straight PD**. 2013. De Novo Assembly of the

Streptomyces sp. Strain Mg1 Genome Using PacBio Single-Molecule Sequencing. Genome Announc **1**:1–2.

172. **Sakuda S**, **Guce-Bigol U**, **Itoh M**, **Nishimura T**, **Yamada Y**. 1996. Novel linear polyene antibiotics: linearmycins. J Chem Soc Perkin Trans 1 2315–2319.

173. **Sakuda S**, **Guce-Bigol U**, **Itoh M**, **Nishimura T**, **Yamada Y**. 1995. Linearmycin A, a Novel Linear Polyene Antibiotic. Tetrahedron Lett **36**:2777–2780.

174. **Oura M**, **Sternberg TH**, **Wright ET**. 1955. A new antifungal antibiotic, amphotericin B. Antibiot Annu **3**:566–73.

175. **Sloane MB**. 1955. A new antifungal antibiotic, mycostatin (nystatin), for the treatment of moniliasis: a preliminary report. J Invest Dermatol **24**:569–71.

176. **McAlpine JB**, **Bachmann BO**, **Piraee M**, **Tremblay S**, **Alarco A-M**, **Zazopoulos E**, **Farnet CM**. 2005. Microbial genomics as a guide to drug discovery and structural elucidation: ECO-02301, a novel antifungal agent, as an example. J Nat Prod **68**:493–496.

177. **Odds FC**, **Brown AJP**, **Gow N a R**. 2003. Antifungal agents: mechanisms of action. Trends Microbiol **11**:272–9.

178. **Baginski M**, **Sternal K**, **Czub J**, **Borowski E**. 2005. Molecular modelling of membrane activity of amphotericin B, a polyene macrolide antifungal antibiotic. Acta Biochim Pol **52**:655–8.

179. **Gray KC**, **Palacios DS**, **Dailey I**, **Endo MM**, **Uno BE**, **Wilcock BC**, **Burke MD**. 2012. Amphotericin primarily kills yeast by simply binding ergosterol. Proc Natl Acad Sci U S A **109**:2234–9.

180. **Anderson TM**, **Clay MC**, **Cioffi AG**, **Diaz KA**, **Hisao GS**, **Tuttle MD**, **Nieuwkoop AJ**, **Comellas G**, **Maryum N**, **Wang S**, **Uno BE**, **Wildeman EL**, **Gonen T**, **Rienstra CM**, **Burke MD**. 2014. Amphotericin forms an extramembranous and fungicidal sterol sponge. Nat Chem Biol **10**:400–6.

181. **Azad M a.**, **Wright GD**. 2012. Determining the mode of action of bioactive compounds. Bioorganic Med Chem **20**:1929–1939.

182. **Yamamoto H**, **Uchiyama S**, **Sekiguchi J**. 1996. The Bacillus subtilis chromosome region near 78 ° contains the genes encoding a new two-component system, three ABC transporters and a lipase. Gene **181**:147–151.

183. **Stock AM**, **Robinson VL**, **Goudreau PN**. 2000. Two-component signal transduction. Annu Rev Biochem **69**:183–215.

184. **Kobayashi K**, **Ogura M**. 2001. Comprehensive DNA Microarray Analysis of Bacillus subtilis Two-Component Regulatory Systems. J Bacteriol **183**:7365–7370.

185. **González-Pastor JE**, **Hobbs EC**, **Losick R**. 2003. Cannibalism by sporulating bacteria. Science **301**:510–3.

186. **Salzberg LI**, **Helmann JD**. 2007. An antibiotic-inducible cell wall-associated protein that protects Bacillus subtilis from autolysis. J Bacteriol **189**:4671–80.

187. **Yamamoto H**, **Hashimoto M**, **Higashitsuji Y**, **Harada H**, **Hariyama N**, **Takahashi L**, **Iwashita T**, **Ooiwa S**, **Sekiguchi J**. 2008. Post-translational control of vegetative cell separation enzymes through a direct interaction with specific inhibitor IseA in Bacillus subtilis. Mol Microbiol **70**:168–82.

188. **Márquez LM**, **Helmann JD**, **Ferrari E**, **Parker HM**, **Ordal GW**, **Chamberlin MJ**. 1990. Studies of sigma D-dependent functions in Bacillus subtilis. J Bacteriol **172**:3435–43.

189. **Zhang W**, **Bolla ML**, **Kahne D**, **Walsh CT**. 2010. A Three Enzyme Pathway for 2-Amino-3-hydroxycyclopent-2-enone Formation and Incorporation in Natural Product Biosynthesis. J Am Chem Soc **132**:6402–6411.

190. **Robbel L**, **Marahiel M a.** 2010. Daptomycin, a bacterial lipopeptide synthesized by a nonribosomal machinery. J Biol Chem **285**:27501–27508.

191. **Pogliano J**, **Pogliano N**, **Silverman JA**. 2012. Daptomycin-mediated reorganization of membrane architecture causes mislocalization of essential cell division proteins. J Bacteriol **194**:4494–504.

192. **Quentin Y**, **Fichant G**, **Denizot F**. 1999. Inventory, assembly and analysis of Bacillus subtilis ABC transport systems. J Mol Biol **287**:467–484.

193. **Staroń A**, **Finkeisen DE**, **Mascher T**. 2011. Peptide antibiotic sensing and detoxification modules of Bacillus subtilis. Antimicrob Agents Chemother **55**:515–25.

194. **de Hoon MJL**, **Makita Y**, **Nakai K**, **Miyano S**. 2005. Prediction of transcriptional terminators in Bacillus subtilis and related species. PLoS Comput Biol **1**:e25.

195. **Fujita M**, **Losick R**. 2002. An investigation into the compartmentalization of the sporulation transcription factor sigmaE in Bacillus subtilis. Mol Microbiol **43**:27–38.

196. **Branda SS**, **González-Pastor JE**, **Ben-Yehuda S**, **Losick R**, **Kolter R**. 2001. Fruiting body formation by Bacillus subtilis. Proc Natl Acad Sci U S A **98**:11621–6.

197. **Vlamakis H**, **Chai Y**, **Beauregard P**, **Losick R**, **Kolter R**. 2013. Sticking together: building a biofilm the Bacillus subtilis way. Nat Rev Microbiol **11**:157–68.

198. **Kearns DB**, **Chu F**, **Branda SS**, **Kolter R**, **Losick R**. 2005. A master regulator for biofilm formation by Bacillus subtilis. Mol Microbiol **55**:739–749.

199. **Verhamme DT**, **Murray EJ**, **Stanley-Wall NR**. 2009. DegU and Spo0A jointly control transcription of two loci required for complex colony development by Bacillus subtilis. J Bacteriol **91**:100–108.

200. **Ostrowski A**, **Mehert A**, **Prescott A**, **Kiley TB**, **Stanley-Wall NR**. 2011. YuaB functions synergistically with the exopolysaccharide and TasA amyloid fibers to allow biofilm formation by Bacillus subtilis. J Bacteriol **193**:4821–4831.

201. **Stanley NR**, **Lazazzera B a.** 2005. Defining the genetic differences between wild and domestic strains of Bacillus subtilis that affect poly-gamma-dl-glutamic acid production and biofilm formation. Mol Microbiol **57**:1143–58.

202. **Fredrick KL**, **Helmann JD**. 1994. Dual chemotaxis signaling pathways in Bacillus subtilis: a sigma D-dependent gene encodes a novel protein with both CheW and CheY homologous domains. J Bacteriol **176**:2727–35.

203. **Calvio C**, **Osera C**, **Amati G**, **Galizzi a.** 2008. Autoregulation of swrAA and Motility in Bacillus subtilis. J Bacteriol **190**:5720–5728.

204. **Aguilar PS**, **Cronan JE**, **de Mendoza D**. 1998. A Bacillus subtilis gene induced by cold shock encodes a membrane phospholipid desaturase. J Bacteriol **180**:2194–200.

205. **Weber MH**, **Klein W**, **Müller L**, **Niess UM**, **Marahiel MA**. 2001. Role of the Bacillus subtilis fatty acid desaturase in membrane adaptation during cold shock. Mol Microbiol **39**:1321–9.

206. **Kayser FH**, **Benner EJ**, **Hoeprich PD**. 1970. Acquired and native resistance of Staphylococcus aureus to cephalexin and other beta-lactam antibiotics. Appl Microbiol **20**:1–5.

207. **Wang X**, **Kang Y**, **Luo C**, **Level S**, **Stress A**, **Strategy P**, **Coordination GI**, **Feeds RSS**, **Journal a SM**. 2014. Heteroresistance at the Single-Cell Level : Adapting to Antibiotic Stress through a Population-Based Strategy and Growth-Controlled **5**:1–9.

208. **El-Halfawy OM**, **Valvano MA**. 2015. Antimicrobial heteroresistance: an emerging field in need of clarity. Clin Microbiol Rev **28**:191–207.

209. **Laub MT**. 2011. The Role of Two-Component Signal Transduction Systems in Bacterial Stress Responses, p. 45–58. *In* Hengge, R, Storz, G (eds.), Bacterial Stress Responses, 2nded. ASM Press, Washington, DC.

210. **Poole K**. 2012. Bacterial stress responses as determinants of antimicrobial resistance. J Antimicrob Chemother **67**:2069–2089.

211. **Moskowitz SM**, **Brannon MK**, **Dasgupta N**, **Pier M**, **Sgambati N**, **Miller AK**, **Selgrade SE**, **Miller SI**, **Denton M**, **Conway SP**, **Johansen HK**, **Høiby N**. 2012.

PmrB mutations promote polymyxin resistance of Pseudomonas aeruginosa isolated from colistin-treated cystic fibrosis patients. Antimicrob Agents Chemother **56**:1019–1030.

212. **Podgornaia AI**, **Laub MT**. 2013. Determinants of specificity in two-component signal transduction. Curr Opin Microbiol **16**:156–62.

213. **Aravind L**, **Ponting CP**. 1999. The cytoplasmic helical linker domain of receptor histidine kinase and methyl-accepting proteins is common to many prokaryotic signalling proteins. FEMS Microbiol Lett **176**:111–116.

214. **Taylor BL**, **Zhulin IB**. 1999. PAS domains: internal sensors of oxygen, redox potential, and light. Microbiol Mol Biol Rev **63**:479–506.

215. **Mascher T**, **Helmann JD**, **Unden G**. 2006. Stimulus perception in bacterial signal-transducing histidine kinases. Microbiol Mol Biol Rev **70**:910–938.

216. **Dintner S**, **Staroń A**, **Berchtold E**, **Petri T**, **Mascher T**, **Gebhard S**. 2011. Coevolution of ABC transporters and two-component regulatory systems as resistance modules against antimicrobial peptides in Firmicutes bacteria. J Bacteriol **193**:3851–3862.

217. **Coumes-Florens S**, **Brochier-Armanet C**, **Guiseppi A**, **Denizot F**, **Foglino M**. 2011. A new highly conserved antibiotic sensing/resistance pathway in firmicutes involves an ABC transporter interplaying with a signal transduction system. PLoS One **6**:e15951.

218. **Hachmann A-B**, **Angert ER**, **Helmann JD**. 2009. Genetic analysis of factors affecting susceptibility of Bacillus subtilis to daptomycin. Antimicrob Agents

Chemother **53**:1598–1609.

219. **Joseph P**, **Guiseppi A**, **Sorokin A**, **Denizot F**. 2004. Characterization of the Bacillus subtilis YxdJ response regulator as the inducer of expression for the cognate ABC transporter YxdLM. Microbiology **150**:2609–2617.

220. **Joseph P**, **Fichant G**, **Quentin Y**, **Denizot F**. 2002. Regulatory relationship of two-component and ABC transport systems and clustering of their genes in the Bacillus/Clostridium group, suggest a functional link between them. J Mol Microbiol Biotechnol **4**:503–13.

221. **Mascher T**, **Zimmer SL**, **Smith T-AA**, **Helmann JD**. 2004. Antibiotic-inducible promoter regulated by the cell envelope stress-sensing two-component system LiaRS of Bacillus subtilis. Antimicrob Agents Chemother **48**:2888–96.

222. **Ohki R**, **Giyanto**, **Tateno K**, **Masuyama W**, **Moriya S**, **Kobayashi K**, **Ogasawara N**. 2003. The BceRS two-component regulatory system induces expression of the bacitracin transporter, BceAB, in Bacillus subtilis. Mol Microbiol **49**:1135–44.

223. **Fabret C**, **Feher V a**, **Hoch J a**. 1999. Two-component signal transduction in Bacillus subtilis: how one organism sees its world. J Bacteriol **181**:1975–83.

224. **Yasbin RE**, **Young FE**. 1974. Transduction in Bacillus subtilis by bacteriophage SPP1. J Virol **14**:1343–1348.

225. **Chevreux B**, **Wetter T**, **Suhai S**. 1999. Genome Sequence Assembly Using Trace Signals and Additional Sequence Information. Comput Sci Biol Proc Ger Conf Bioinforma 45–56.

226. **Chevreux B**, **Pfisterer T**, **Drescher B**, **Driesel AJ**, **Müller WEG**, **Wetter T**, **Suhai S**. 2004. Using the miraEST assembler for reliable and automated mRNA transcript assembly and SNP detection in sequenced ESTs. Genome Res **14**:1147–59.

227. **Le Breton Y**, **Mohapatra NP**, **Haldenwang WG**. 2006. In vivo random mutagenesis of Bacillus subtilis by use of TnYLB-1, a mariner-based transposon. Appl Environ Microbiol **72**:327–33.

228. **Lazarevic V**, **Düsterhöft A**, **Soldo B**, **Hilbert H**, **Mauël C**, **Karamata D**. 1999. Nucleotide sequence of the Bacillus subtilis temperate bacteriophage SPbetac2. Microbiology **145 (Pt 5**:1055–67.

229. **Gibson DG**, **Young L**, **Chuang R-Y**, **Venter JC**, **Hutchison C a**, **Smith HO**. 2009. Enzymatic assembly of DNA molecules up to several hundred kilobases. Nat Methods **6**:343–345.

230. **Bonev B**, **Hooper J**, **Parisot J**. 2008. Principles of assessing bacterial susceptibility to antibiotics using the agar diffusion method. J Antimicrob Chemother **61**:1295–1301.

231. **Bray NL**, **Pimentel H**, **Melsted P**, **Pachter L**. 2016. Near-optimal probabilistic RNA-seq quantification. Nat Biotech **34**:525–527.

232. **Robinson MD**, **McCarthy DJ**, **Smyth GK**. 2009. edgeR: A Bioconductor package for differential expression analysis of digital gene expression data. Bioinformatics **26**:139–140.

233. **Robinson MD**, **Smyth GK**. 2008. Small-sample estimation of negative binomial

dispersion, with applications to SAGE data. Biostatistics **9**:321–332.

234. **Ruijter JM**, **Ramakers C**, **Hoogaars WMH**, **Karlen Y**, **Bakker O**, **Van Den Hoff MJB**, **Moorman a. FM**. 2009. Amplification efficiency: Linking baseline and bias in the analysis of quantitative PCR data. Nucleic Acids Res **37**.

235. **Stubbendieck RM**, **Straight PD**. 2016. Multifaceted Interfaces of Bacterial Competition. J Bacteriol **198**:JB.00275-16.

236. **Stubbendieck RM**, **Vargas-Bautista C**, **Straight PD**. 2016. Bacterial Communities: Interactions to Scale. Front Microbiol **7**:1–19.

237. **Silhavy TJ**, **Kahne D**, **Walker S**. 2010. The bacterial cell envelope. Cold Spring Harb Perspect Biol **2**:a000414.

238. **Rashid R**, **Veleba M**, **Kline KA**. 2016. Focal Targeting of the Bacterial Envelope by Antimicrobial Peptides. Front cell Dev Biol **4**:55.

239. **Liu Y**, **Breukink E**. 2016. The Membrane Steps of Bacterial Cell Wall Synthesis as Antibiotic Targets. Antibiot (Basel, Switzerland) **5**.

240. **Jordan S**, **Hutchings MI**, **Mascher T**. 2008. Cell envelope stress response in Gram-positive bacteria. FEMS Microbiol Rev **32**:107–46.

241. **Radeck J**, **Fritz G**, **Mascher T**. 2017. The cell envelope stress response of Bacillus subtilis: from static signaling devices to dynamic regulatory network. Curr Genet **63**:79–90.

242. **Dubrac S**, **Bisicchia P**, **Devine KM**, **Msadek T**. 2008. A matter of life and death: cell wall homeostasis and the WalKR (YycGF) essential signal transduction pathway. Mol Microbiol **70**:1307–22.

243. **Serizawa M**, **Kodama K**, **Yamamoto H**, **Kobayashi K**, **Ogasawara N**, **Sekiguchi J**. 2005. Functional analysis of the YvrGHb two-component system of Bacillus subtilis: identification of the regulated genes by DNA microarray and northern blot analyses. Biosci Biotechnol Biochem **69**:2155–69.

244. **Mascher T**, **Margulis NG**, **Wang T**, **Ye RW**, **Helmann JD**. 2003. Cell wall stress responses in Bacillus subtilis: the regulatory network of the bacitracin stimulon. Mol Microbiol **50**:1591–604.

245. **Beckering CL**, **Steil L**, **Weber MHW**, **Völker U**, **Marahiel MA**. 2002. Genomewide transcriptional analysis of the cold shock response in Bacillus subtilis. J Bacteriol **184**:6395–402.

246. **Cybulski LE**, **Albanesi D**, **Mansilla MCMC**, **Altabe S**, **Aguilar PS**, **de Mendoza D**. 2002. Mechanism of membrane fluidity optimization: isothermal control of the Bacillus subtilis acyl-lipid desaturase. Mol Microbiol **45**:1379–88.

247. **Hyyryläinen H-L**, **Pietiäinen M**, **Lundén T**, **Ekman A**, **Gardemeister M**, **Murtomäki-Repo S**, **Antelmann H**, **Hecker M**, **Valmu L**, **Sarvas M**, **Kontinen VP**. 2007. The density of negative charge in the cell wall influences two-component signal transduction in Bacillus subtilis. Microbiology **153**:2126–36.

248. **Stubbendieck RM**, **Straight PD**. 2015. Escape from Lethal Bacterial Competition through Coupled Activation of Antibiotic Resistance and a Mobilized Subpopulation. PLoS Genet **11**:e1005722.

249. **Botella E**, **Devine SK**, **Hubner S**, **Salzberg LI**, **Gale RT**, **Brown ED**, **Link H**, **Sauer U**, **Codée JD**, **Noone D**, **Devine KM**. 2014. PhoR autokinase activity is

controlled by an intermediate in wall teichoic acid metabolism that is sensed by the intracellular PAS domain during the PhoPR-mediated phosphate limitation response of Bacillus subtilis. Mol Microbiol **94**:1242–59.

250. **Fukushima T**, **Furihata I**, **Emmins R**, **Daniel RA**, **Hoch JA**, **Szurmant H**. 2011. A role for the essential YycG sensor histidine kinase in sensing cell division. Mol Microbiol **79**:503–22.

251. **Nicolas P**, **Mäder U**, **Dervyn E**, **Rochat T**, **Leduc A**, **Pigeonneau N**, **Bidnenko E**, **Marchadier E**, **Hoebeke M**, **Aymerich S**, **Becher D**, **Bisicchia P**, **Botella E**, **Delumeau O**, **Doherty G**, **Denham EL**, **Fogg MJ**, **Fromion V**, **Goelzer A**, **Hansen A**, **Härtig E**, **Harwood CR**, **Homuth G**, **Jarmer H**, **Jules M**, **Klipp E**, **Le Chat L**, **Lecointe F**, **Lewis P**, **Liebermeister W**, **March A**, **Mars RAT**, **Nannapaneni P**, **Noone D**, **Pohl S**, **Rinn B**, **Rügheimer F**, **Sappa PK**, **Samson F**, **Schaffer M**, **Schwikowski B**, **Steil L**, **Stülke J**, **Wiegert T**, **Devine KM**, **Wilkinson AJ**, **van Dijl JM**, **Hecker M**, **Völker U**, **Bessières P**, **Noirot P**. 2012. Condition-dependent transcriptome reveals high-level regulatory architecture in Bacillus subtilis. Science **335**:1103–6.

252. **Davidson AL**, **Dassa E**, **Orelle C**, **Chen J**. 2008. Structure, function, and evolution of bacterial ATP-binding cassette systems. Microbiol Mol Biol Rev **72**:317–64, table of contents.

253. **Dietrich LEP**, **Okegbe C**, **Price-Whelan A**, **Sakhtah H**, **Hunter RC**, **Newman DK**. 2013. Bacterial community morphogenesis is intimately linked to the intracellular redox state. J Bacteriol **195**:1371–1380.

254. **Schröder H**, **Langer T**, **Hartl FU**, **Bukau B**. 1993. DnaK, DnaJ and GrpE form a cellular chaperone machinery capable of repairing heat-induced protein damage. EMBO J **12**:4137–44.

255. **Szabo A**, **Langer T**, **Schröder H**, **Flanagan J**, **Bukau B**, **Hartl FU**. 1994. The ATP hydrolysis-dependent reaction cycle of the Escherichia coli Hsp70 system DnaK, DnaJ, and GrpE. Proc Natl Acad Sci U S A **91**:10345–9.

256. **Deuerling E**, **Mogk A**, **Richter C**, **Purucker M**, **Schumann W**. 1997. The ftsH gene of Bacillus subtilis is involved in major cellular processes such as sporulation, stress adaptation and secretion. Mol Microbiol **23**:921–33.

257. **Schumann W**. 1999. FtsH--a single-chain charonin? FEMS Microbiol Rev **23**:1–11.

258. **Yepes A**, **Schneider J**, **Mielich B**, **Koch G**, **García-Betancur J-C**, **Ramamurthi KS**, **Vlamakis H**, **López D**. 2012. The biofilm formation defect of a Bacillus subtilis flotillin-defective mutant involves the protease FtsH. Mol Microbiol **86**:457–71.

259. **Hoffmann A**, **Bukau B**, **Kramer G**. 2010. Structure and function of the molecular chaperone Trigger Factor. Biochim Biophys Acta **1803**:650–61.

260. **Lin T-H**, **Hu Y-N**, **Shaw G-C**. 2014. Two enzymes, TilS and HprT, can form a complex to function as a transcriptional activator for the cell division protease gene ftsH in Bacillus subtilis. J Biochem **155**:5–16.

261. **Belitsky BR**, **Gustafsson MC**, **Sonenshein AL**, **Von Wachenfeldt C**. 1997. An lrp-like gene of Bacillus subtilis involved in branched-chain amino acid transport.

J Bacteriol **179**:5448–57.

262. **Mäder U**, **Hennig S**, **Hecker M**, **Homuth G**. 2004. Transcriptional organization and posttranscriptional regulation of the Bacillus subtilis branched-chain amino acid biosynthesis genes. J Bacteriol **186**:2240–52.

263. **Müller A**, **Wenzel M**, **Strahl H**, **Grein F**, **Saaki TN V**, **Kohl B**, **Siersma T**, **Bandow JE**, **Sahl H-G**, **Schneider T**, **Hamoen LW**. 2016. Daptomycin inhibits cell envelope synthesis by interfering with fluid membrane microdomains. Proc Natl Acad Sci U S A.

264. **Reiser V**, **Raitt DC**, **Saito H**. 2003. Yeast osmosensor Sln1 and plant cytokinin receptor Cre1 respond to changes in turgor pressure. J Cell Biol **161**:1035–40.

265. **Errington J**, **Vogt CH**. 1990. Isolation and characterization of mutations in the gene encoding an endogenous Bacillus subtilis beta-galactosidase and its regulator. J Bacteriol **172**:488–90.

266. **Galperin MY**, **Nikolskaya AN**, **Koonin E V**. 2001. Novel domains of the prokaryotic two-component signal transduction systems. FEMS Microbiol Lett **203**:11–21.

267. **Bernard R**, **Joseph P**, **Guiseppi A**, **Chippaux M**, **Denizot F**. 2003. YtsCD and YwoA, two independent systems that confer bacitracin resistance to Bacillus subtilis. FEMS Microbiol Lett **228**:93–7.

268. **Bernard R**, **Guiseppi A**, **Chippaux M**, **Foglino M**, **Denizot F**. 2007. Resistance to bacitracin in Bacillus subtilis: unexpected requirement of the BceAB ABC transporter in the control of expression of its own structural genes. J Bacteriol

189:8636–42.

269. **Rietkötter E**, **Hoyer D**, **Mascher T**. 2008. Bacitracin sensing in Bacillus subtilis. Mol Microbiol **68**:768–85.

270. **Kingston AW**, **Zhao H**, **Cook GM**, **Helmann JD**. 2014. Accumulation of heptaprenyl diphosphate sensitizes Bacillus subtilis to bacitracin: implications for the mechanism of resistance mediated by the BceAB transporter. Mol Microbiol **93**:37–49.

271. **Dintner S**, **Heermann R**, **Fang C**, **Jung K**, **Gebhard S**. 2014. A sensory complex consisting of an ATP-binding cassette transporter and a two-component regulatory system controls bacitracin resistance in Bacillus subtilis. J Biol Chem **289**:27899–910.

272. **Fritz G**, **Dintner S**, **Treichel NS**, **Radeck J**, **Gerland U**, **Mascher T**, **Gebhard S**. 2015. A New Way of Sensing: Need-Based Activation of Antibiotic Resistance by a Flux-Sensing Mechanism. MBio **6**:e00975.

273. **Radeck J**, **Gebhard S**, **Orchard PS**, **Kirchner M**, **Bauer S**, **Mascher T**, **Fritz G**. 2016. Anatomy of the bacitracin resistance network in Bacillus subtilis. Mol Microbiol **100**:607–20.

274. **Fang C**, **Nagy-Staroń A**, **Grafe M**, **Heermann R**, **Jung K**, **Gebhard S**, **Mascher T**. 2016. Insulation and wiring specificity of BceR-like response regulators and their target promoters in Bacillus subtilis. Mol Microbiol.

275. **Dartois V**, **Djavakhishvili T**, **Hoch JA**. 1997. KapB is a lipoprotein required for KinB signal transduction and activation of the phosphorelay to sporulation in

Bacillus subtilis. Mol Microbiol **26**:1097–108.

276. **Ganesh I**, **Ravikumar S**, **Lee SH**, **Park SJ**, **Hong SH**. 2013. Engineered fumarate sensing Escherichia coli based on novel chimeric two-component system. J Biotechnol **168**:560–6.

277. **Ward SM**, **Delgado A**, **Gunsalus RP**, **Manson MD**. 2002. A NarX-Tar chimera mediates repellent chemotaxis to nitrate and nitrite. Mol Microbiol **44**:709–19.

278. **Heermann R**, **Lippert M-L**, **Jung K**. 2009. Domain swapping reveals that the N-terminal domain of the sensor kinase KdpD in Escherichia coli is important for signaling. BMC Microbiol **9**:133.

279. **Yoshida T**, **Phadtare S**, **Inouye M**. 2007. The design and development of Tar-EnvZ chimeric receptors. Methods Enzymol **423**:166–83.

280. **Kennedy KA**, **Traxler B**. 1999. MalK forms a dimer independent of its assembly into the MalFGK2 ATP-binding cassette transporter of Escherichia coli. J Biol Chem **274**:6259–64.

281. **Kennedy KA**, **Gachelet EG**, **Traxler B**. 2004. Evidence for multiple pathways in the assembly of the Escherichia coli maltose transport complex. J Biol Chem **279**:33290–7.

282. **Sharma S**, **Davis JA**, **Ayvaz T**, **Traxler B**, **Davidson AL**. 2005. Functional reassembly of the Escherichia coli maltose transporter following purification of a MalF-MalG subassembly. J Bacteriol **187**:2908–11.

283. **Traxler B**, **Beckwith J**. 1992. Assembly of a hetero-oligomeric membrane protein complex. Proc Natl Acad Sci U S A **89**:10852–6.

284. **Konkol MA**, **Blair KM**, **Kearns DB**. 2013. Plasmid-encoded ComI inhibits competence in the ancestral 3610 strain of Bacillus subtilis. J Bacteriol **195**:4085–93.

285. **de Jong A**, **Pietersma H**, **Cordes M**, **Kuipers OP**, **Kok J**. 2012. PePPER: a webserver for prediction of prokaryote promoter elements and regulons. BMC Genomics **13**:299.

286. **Kallenberg F**, **Dintner S**, **Schmitz R**, **Gebhard S**. 2013. Identification of regions important for resistance and signalling within the antimicrobial peptide transporter BceAB of Bacillus subtilis. J Bacteriol **195**:3287–97.

287. **Guérout-Fleury AM**, **Frandsen N**, **Stragier P**. 1996. Plasmids for ectopic integration in Bacillus subtilis. Gene **180**:57–61.

288. **Krogh A**, **Larsson B**, **von Heijne G**, **Sonnhammer EL**. 2001. Predicting transmembrane protein topology with a hidden Markov model: application to complete genomes. J Mol Biol **305**:567–80.

289. **Käll L**, **Krogh A**, **Sonnhammer ELL**. 2007. Advantages of combined transmembrane topology and signal peptide prediction--the Phobius web server. Nucleic Acids Res **35**:W429-32.

290. **Doan T**, **Marquis KA**, **Rudner DZ**. 2005. Subcellular localization of a sporulation membrane protein is achieved through a network of interactions along and across the septum. Mol Microbiol **55**:1767–81.

291. **Moore BS**, **Hertweck C**. 2002. Biosynthesis and attachment of novel bacterial polyketide synthase starter units. Nat Prod Rep **19**:70–99.

292. **Manteca A**, **Alvarez R**, **Salazar N**, **Yagüe P**, **Sanchez J**. 2008. Mycelium differentiation and antibiotic production in submerged cultures of Streptomyces coelicolor. Appl Environ Microbiol **74**:3877–3886.

293. **McArthur M**, **Bibb MJ**. 2008. Manipulating and understanding antibiotic production in Streptomyces coelicolor A3(2) with decoy oligonucleotides. Proc Natl Acad Sci U S A **105**:1020–5.

294. **Li S**, **Wang W**, **Li X**, **Fan K**, **Yang K**. 2015. Genome-wide identification and characterization of reference genes with different transcript abundances for Streptomyces coelicolor. Sci Rep **5**:15840.

295. **Shiina T**, **Tanaka K**, **Takahashi H**. 1991. Sequence of hrdB, an essential gene encoding sigma-like transcription factor of Streptomyces coelicolor A3(2): homology to principal sigma factors. Gene **107**:145–8.

296. **Shinkawa H**, **Hatada Y**, **Okada M**, **Kinashi H**, **Nimi O**. 1995. Nucleotide sequence of a principal sigma factor gene (hrdB) of Streptomyces griseus. J Biochem **118**:494–9.

297. **Hamilton-Miller JM**. 1973. Chemistry and biology of the polyene macrolide antibiotics. Bacteriol Rev **37**:166–96.

298. **Beites T**, **Oliveira P**, **Rioseras B**, **Pires SDS**, **Oliveira R**, **Tamagnini P**, **Moradas-Ferreira P**, **Manteca Á**, **Mendes M V**. 2015. Streptomyces natalensis programmed cell death and morphological differentiation are dependent on oxidative stress. Sci Rep **5**:12887.

299. **Uttlová P**, **Pinkas D**, **Bechyňková O**, **Fišer R**, **Svobodová J**, **Seydlová G**. 2016.

Bacillus subtilis alters the proportion of major membrane phospholipids in response to surfactin exposure. Biochim Biophys Acta **1858**:2965–2971.

300. **Heerklotz H**, **Seelig J**. 2007. Leakage and lysis of lipid membranes induced by the lipopeptide surfactin. Eur Biophys J **36**:305–14.

301. **Buchoux S**, **Lai-Kee-Him J**, **Garnier M**, **Tsan P**, **Besson F**, **Brisson A**, **Dufourc EJ**. 2008. Surfactin-triggered small vesicle formation of negatively charged membranes: a novel membrane-lysis mechanism. Biophys J **95**:3840–9.

302. **Wang Y**, **Kern SE**, **Newman DK**. 2010. Endogenous phenazine antibiotics promote anaerobic survival of Pseudomonas aeruginosa via extracellular electron transfer. J Bacteriol **192**:365–9.

303. **Glasser NR**, **Kern SE**, **Newman DK**. 2014. Phenazine redox cycling enhances anaerobic survival in Pseudomonas aeruginosa by facilitating generation of ATP and a proton-motive force. Mol Microbiol **92**:399–412.

304. **Das T**, **Manefield M**. 2012. Pyocyanin promotes extracellular DNA release in Pseudomonas aeruginosa. PLoS One **7**:e46718.

305. **Das T**, **Manefield M**. 2013. Phenazine production enhances extracellular DNA release via hydrogen peroxide generation in Pseudomonas aeruginosa. Commun Integr Biol **6**:e23570.

306. **Zhao Y**, **Xiang S**, **Dai X**, **Yang K**. 2013. A simplified diphenylamine colorimetric method for growth quantification. Appl Microbiol Biotechnol **97**:5069–5077.

307. **Schindelin J**, **Rueden CT**, **Hiner MC**, **Eliceiri KW**. 2015. The ImageJ

ecosystem: An open platform for biomedical image analysis. Mol Reprod Dev **in press**:DOI: 10.1002/mrd.22489.

308. **Koch R**. 1876. Untersuchungen ueber Bakterien V. Die Aetiologie der Milzbrand-Krankheit, begruendent auf die Entwicklungsgeschichte des Bacillus Anthracis. Beitrage zur Biol der Pflanz 277–310.

309. **Pasteur L**. 1877. Charbon et septicémie. [Paris] :, [Paris] :

310. **Hutchison CA**, **Chuang R-Y**, **Noskov VN**, **Assad-Garcia N**, **Deerinck TJ**, **Ellisman MH**, **Gill J**, **Kannan K**, **Karas BJ**, **Ma L**, **Pelletier JF**, **Qi Z-Q**, **Richter RA**, **Strychalski EA**, **Sun L**, **Suzuki Y**, **Tsvetanova B**, **Wise KS**, **Smith HO**, **Glass JI**, **Merryman C**, **Gibson DG**, **Venter JC**. 2016. Design and synthesis of a minimal bacterial genome. Science **351**:aad6253.

311. **Clavel T**, **Lagkouvardos I**, **Hiergeist A**. 2016. Microbiome sequencing: challenges and opportunities for molecular medicine. Expert Rev Mol Diagn **16**:795–805.

312. **Moore-Connors JM**, **Dunn KA**, **Bielawski JP**, **Van Limbergen J**. 2016. Novel Strategies for Applied Metagenomics. Inflamm Bowel Dis **22**:709–18.

313. **Human Microbiome Project Consortium**. 2012. Structure, function and diversity of the healthy human microbiome. Nature **486**:207–14.

314. **Trosvik P**, **de Muinck EJ**. 2015. Ecology of bacteria in the human gastrointestinal tract--identification of keystone and foundation taxa. Microbiome **3**:44.

315. **Trosvik P**, **de Muinck EJ**, **Stenseth NC**. 2015. Biotic interactions and temporal

dynamics of the human gastrointestinal microbiota. ISME J **9**:533–41.

316. **Alldredge AL**, **Silver MW**. 1988. Characteristics, dynamics and significance of marine snow. Prog Oceanogr **20**:41–82.

317. **Stoodley P**, **Hall-Stoodley L**, **Lappin-Scott HM**. 2001. Detachment, surface migration, and other dynamic behavior in bacterial biofilms revealed by digital time-lapse imaging. Methods Enzymol **337**:306–19.

318. **Stoodley P**, **Wilson S**, **Hall-Stoodley L**, **Boyle JD**, **Lappin-Scott HM**, **Costerton JW**. 2001. Growth and detachment of cell clusters from mature mixed-species biofilms. Appl Environ Microbiol **67**:5608–13.

319. **Kragh KN**, **Hutchison JB**, **Melaugh G**, **Rodesney C**, **Roberts AEL**, **Irie Y**, **Jensen PØ**, **Diggle SP**, **Allen RJ**, **Gordon V**, **Bjarnsholt T**. 2016. Role of Multicellular Aggregates in Biofilm Formation. MBio **7**:e00237-16.

320. **Fleming A**. 1929. On the Antibacterial Action of Cultures of a Penicillium, with Special Reference to their Use in the Isolation of B. influenzæ. Br J Exp Pathol **10**:226.

321. **Be'er A**, **Zhang HP**, **Florin E-L**, **Payne SM**, **Ben-Jacob E**, **Swinney HL**. 2009. Deadly competition between sibling bacterial colonies. Proc Natl Acad Sci U S A **106**:428–33.

322. **Cude WN**, **Mooney J**, **Tavanaei A a**, **Hadden MK**, **Frank AM**, **Gulvik C a**, **May AL**, **Buchan A**. 2012. Production of the antimicrobial secondary metabolite indigoidine contributes to competitive surface colonization by the marine roseobacter Phaeobacter sp. strain Y4I. Appl Environ Microbiol **78**:4771–80.

323. **Garbeva P**, **Silby MW**, **Raaijmakers JM**, **Levy SB**, **Boer W De**. 2011. Transcriptional and antagonistic responses of Pseudomonas fluorescens Pf0-1 to phylogenetically different bacterial competitors. ISME J **5**:973–85.

324. **Hol FJH**, **Galajda P**, **Woolthuis RG**, **Dekker C**, **Keymer JE**. 2015. The idiosyncrasy of spatial structure in bacterial competition. BMC Res Notes **8**:245.

325. **Kerr B**, **Riley MA**, **Feldman MW**, **Bohannan BJM**. 2002. Local dispersal promotes biodiversity in a real-life game of rock-paper-scissors. Nature **418**:171–4.

326. **Shank E a**, **Klepac-Ceraj V**, **Collado-Torres L**, **Powers GE**, **Losick R**, **Kolter R**. 2011. Interspecies interactions that result in Bacillus subtilis forming biofilms are mediated mainly by members of its own genus. Proc Natl Acad Sci U S A **108**:E1236-43.

327. **Butcher RA**, **Schroeder FC**, **Fischbach M a**, **Straight PD**, **Kolter R**, **Walsh CT**, **Clardy J**. 2007. The identification of bacillaene, the product of the PksX megacomplex in Bacillus subtilis. Proc Natl Acad Sci U S A **104**:1506–9.

328. **Lerat S**, **Simao-Beaunoir A-M**, **Beaulieu C**. 2009. Genetic and physiological determinants of Streptomyces scabies pathogenicity. Mol Plant Pathol **10**:579–85.

329. **Muller S**, **Strack SN**, **Ryan SE**, **Kearns DB**, **Kirby JR**. 2014. Predation by Myxococcus xanthus Induces Bacillus subtilis To Form Spore-Filled Megastructures. Appl Environ Microbiol **81**:203–210.

330. **Omasits U**, **Ahrens CH**, **Müller S**, **Wollscheid B**. 2014. Protter: interactive protein feature visualization and integration with experimental proteomic data.

Bioinformatics **30**:884–6.

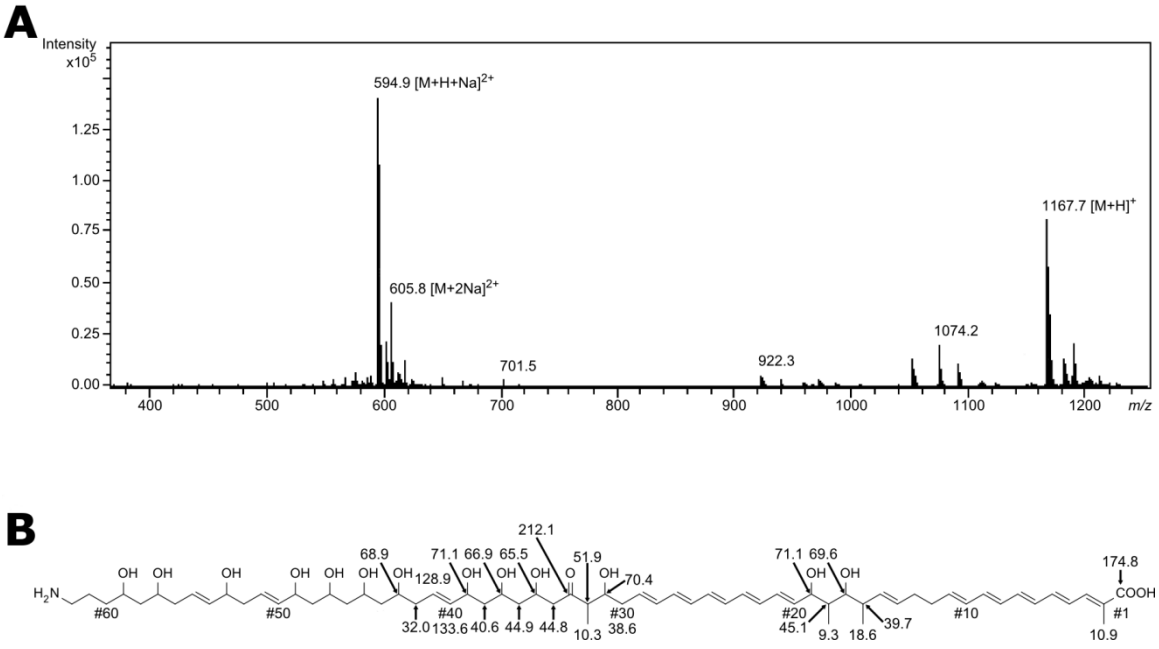

Figure A1. Characterization of the molecule responsible for LDA

(A) Mass spectrum of the isolated peak with lytic activity against *B. subtilis*. The prominent masses detected in the experiment match those of linearmycin B, *m/z* 594.9 $[M+H+Na]^{2+}$, 605.8 $[M+2Na]^{2+}$ and 1167.7 $[M+H]^{+}$ (B) Structure of linearmycin B with ^{13}C NMR chemical shift assignments obtained in DMSO-d_6. Carbons are numbered linearly starting with the carbonyl carbon of the carboxylic acid group.

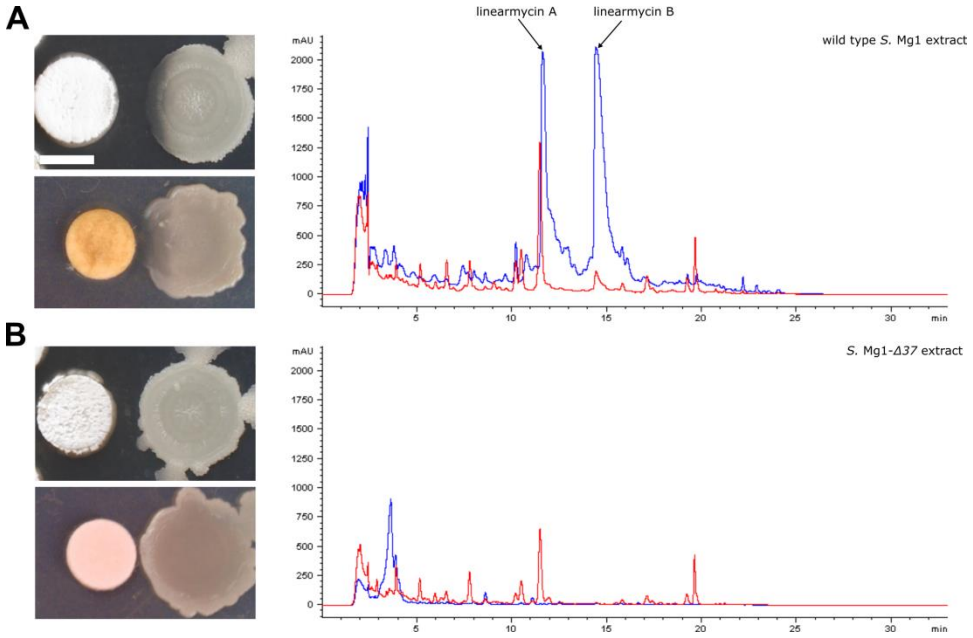

Figure A2. Disruption of the linearmycin biosynthetic gene cluster abolishes LDA

The *S.* Mg1 wild type strain (A) and a strain with a chromosome arm deletion (Δ*37*) that includes the linearmycin biosynthetic gene cluster (B) were co-cultured with *B. subtilis* Δ*pksX* (PDS0067) (top left panels). *Bacillus subtilis* is not lysed by *S.* Mg1 Δ*37*. Extracts from each streptomycete were spotted on filter paper discs adjacent to a *B. subtilis* Δ*pksX* colony (lower left panels). The *B. subtilis* colony challenged with the *S.* Mg1 Δ*37* extract was not lysed. The extracts were analyzed by HPLC (right panels). Linearmycins are detected by UV absorbance at 333 nm (blue) while the background is shown by the 254 nm absorbing trace (red). The predominant difference in the extracts is the presence or absence of linearmycins A and B. Linearmycin A (*m/z* 1140) and B (*m/z* 1166) identities were confirmed by mass spectrometry. Colonies were photographed after 72 h of co-incubation or after 48 h exposure to extract. Scale bar is 5 mm.

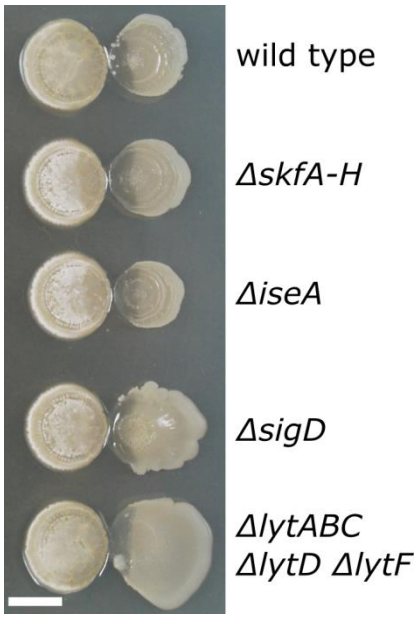

Figure A3. Genes predicted to be repressed by YfiK are not responsible for LDA

Spore-killing factor (SKF) and autolysis were predicted to be regulated by YfiK. Strains of *B. subtilis* (right) with deletions in genes responsible for SKF biosynthesis (Δ*skfA-H*) (DL598), an autolysin inhibitor (Δ*iseA*) (PDS0785), deletions in the major autolysin regulator σ^D (Δ*sigD*) (DS323), and deletions in three major autolysins (Δ*lytABC*, Δ*lytD*, Δ*lytF*) (DS2483) were tested for resistance to LDA in co-culture with *S.* Mg1 (left). All strains lysed similarly to wild type (PDS0066). Cultures were photographed after 72 h co-incubation on MYM agar plates. Scale bar is 5 mm. These results were consistent across six replicates.

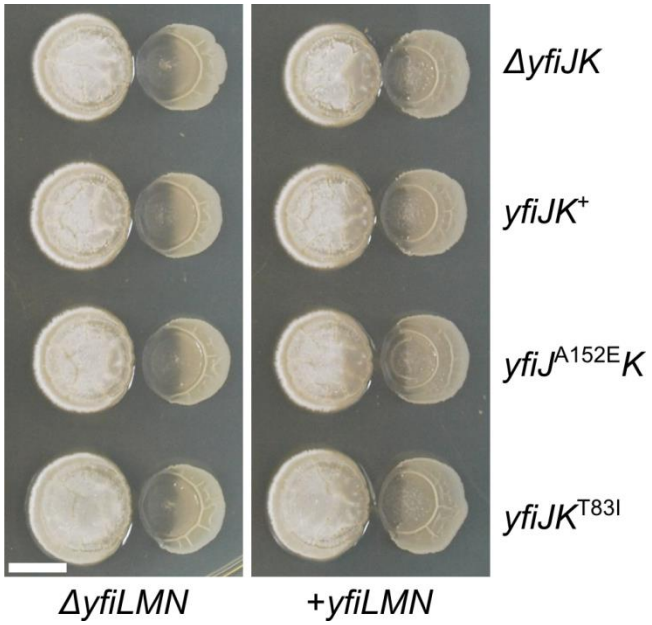

Figure A4. Complementation of *yfiLMN* with *yfiK* terminator-*yfiL* intergenic sequence fails to restore LDA resistance

The *yfiLMN* deletion was complemented at *lacA* using the intergenic sequence between the terminator downstream of *yfiK* and the first coding nucleotide of *yfiL* as upstream sequence (143 bp). Lysis was observed in a strain lacking *yfiJK* (PDS0687), a strain with *yfiJK*$^{+}$ (PDS0688), and in strains with LDA^{R} alleles *yfiJ*^{A152E}*K* (PDS0689) and *yfiJK*^{T83I} (PDS0690). All cultures place *S.* Mg1 on the left and *B. subtilis* on the right. Cultures were photographed after 72 h co-incubation on MYM agar plates. Scale bar is 5 mm. These results were consistent across three replicates.

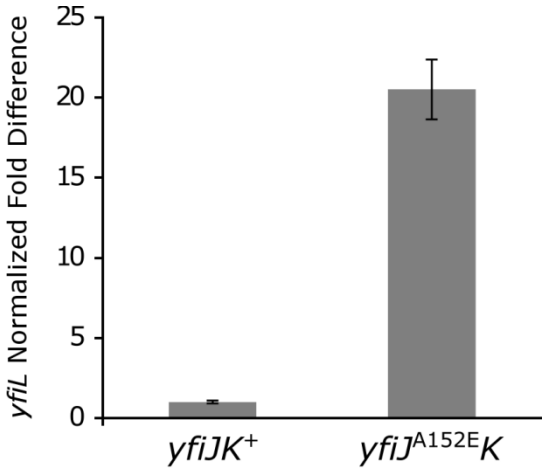

Figure A5. *yfiL* expression is increased in a LDA^{R} mutant

qRT-PCR was used to quantify expression of *yfiL* in strains with *yfiJK*$^{+}$ (PDS0627) or *yfiJ*^{A152E}*K* (PDS0685). Expression was normalized relative to *gyrB.* The fold difference relative to expression in the *yfiJK*$^{+}$ strain is reported. The error bars represent the standard deviation of the fold difference.

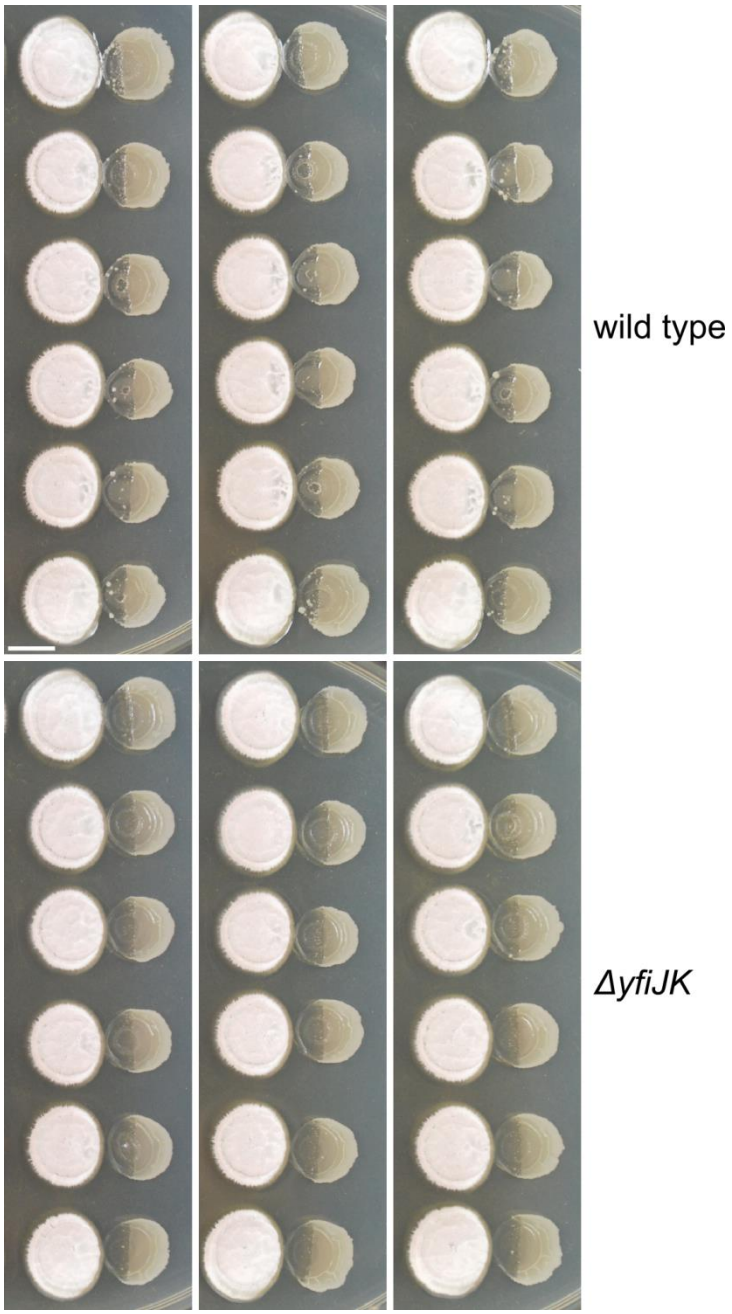

Figure A6. Small colony formation requires *yfiJK*

We cultured eighteen wild type (PDS0066) and Δ*yfiJK* (PDS0554) colonies of *B. subtilis* with *S.* Mg1. Many small, potentially LDA^R, colonies appeared in the region of lysis of wild type colonies. A few small colonies appeared in the zone of lysis of two Δ*yfiJK* colonies, but these did not grow similarly and lacked the morphological features of the $yfiJK^+$ small colonies. All cultures place *S.* Mg1 on the left and *B. subtilis* on the right. Colonies were photographed after 96 hours co-incubation on MYM agar plates. The scale bar is 5 mm.

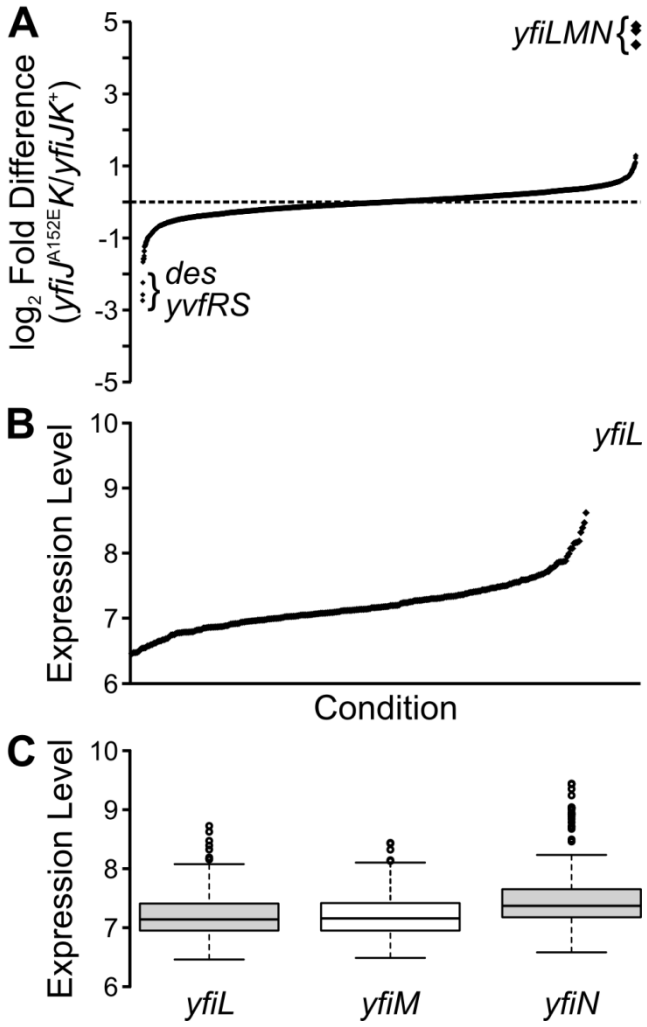

Figure A7. *yfiLMN* expression profiles

(A) Differential gene expression in *yfiJ*^{A152E}*K* (PDS0685) compared to *yfiJK*$^{+}$ (PDS0627). Each open reading frame in the *B. subtilis* genome is represented as a diamond and are plotted from lowest to highest fold difference between *yfiJ*^{A152E}*K* and *yfiJK*$^{+}$. The dashed line represents no difference in mRNA abundance. **(B)** Expression data for *yfiL* from 269 different conditions. Each diamond represents one condition and is plotted from lowest to highest expression level. **(C)** Expression data for *yfiL*, *yfiM*, and *yfiN* from 269 different conditions. The center lines of the box plots show the media of expression level. The upper and lower box limits indicate the 25th and 75th percentiles, respectively. The whiskers extend 1.5 times the interquartile range from the 25th and 75th percentiles. Outliers are shown as open circles.

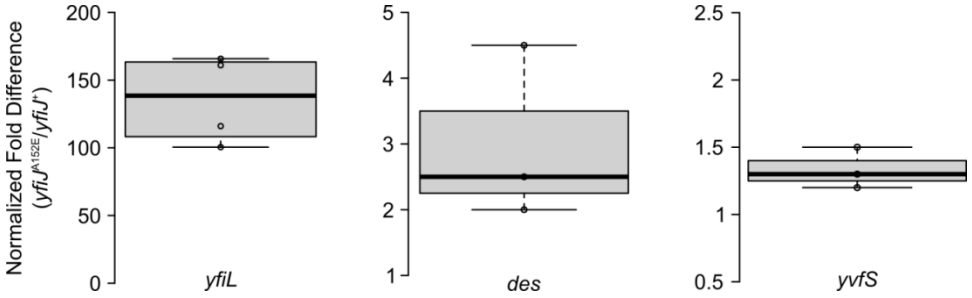

Figure A8. qRT-PCR of putative genes in the YfiK regulon previously predicted by RNA-seq.

qRT-PCR was used to quantify expression of *yfiL*, *des*, and *yvfS* in *yfiJ*$^{+}$ strains (PDS0571) and *yfiJ*^{A152E} strains (PDS0572). Expression was normalized to *gyrB*. The fold difference relative to expression in the *yfiJ*$^{+}$ strain is reported. Each biological replicates is shown as an open circle. The center lines of the box plots show the median of the fold differences. The upper and lower box limits indicate the 25th and 75th percentiles, respectively. The whiskers extend 1.5 times the interquartile range from the 25th and 75th percentiles. Note, the reported scales are different for each gene.

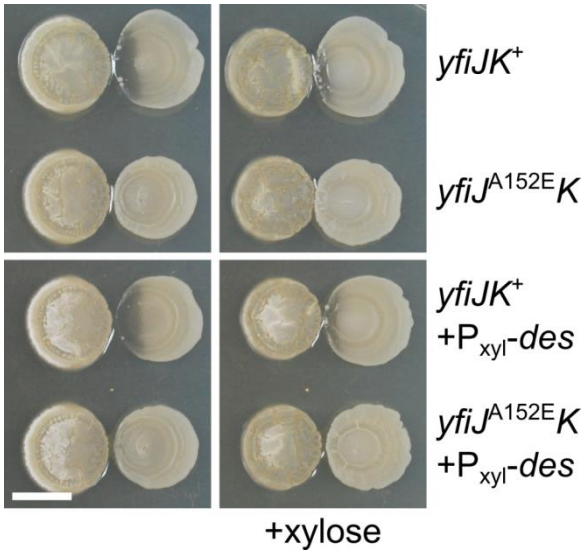

Figure A9. Overexpression of *des* does not affect linearmycin resistance or colony morphology

(*top* panels) *Bacillus subtilis* (right) *yfiJK*$^{+}$ (PDS0627) is lysed by *S.* Mg1 (left) while *yfiJ*^{A152E}*K* (PDS0685) is linearmycin resistant. (*bottom* panels) Artificial overexpression of *des* from a xylose-inducible promoter has no effect on *B. subtilis* lysis or colony morphology, when compared to the above strains. The photograph was taken after 72 h co-incubation on MYM agar with or without 0.3% w/v xylose. The photograph is representative of duplicate samples. Scale bar is 5 mm.

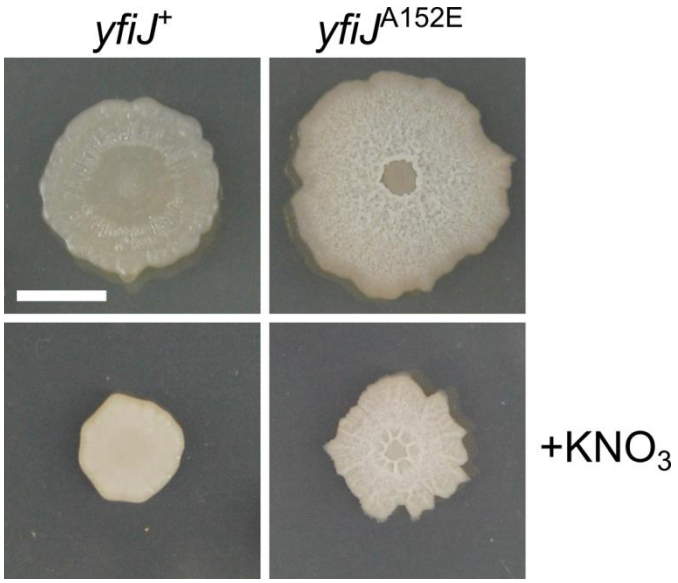

Figure A10. Nitrate supplementation does not affect the wrinkled phenotype of *yfiJ*^{A152E}

When grown from single cells, the *B. subtilis yfiJ*$^{+}$ (PDS0571) colony develops as a relatively flat and featureless colony whereas the *yfiJ*^{A152E} colony (PDS0572) spreads and forms a wrinkled colony. The addition of 40 mM potassium nitrate (+KNO_3) causes both strains to form smaller, lighter pigmented colonies but the *yfiJ*^{A152E} colony remains wrinkled. The photograph was taken after 48 h incubation on MYM agar. Scale bar is 5 mm.

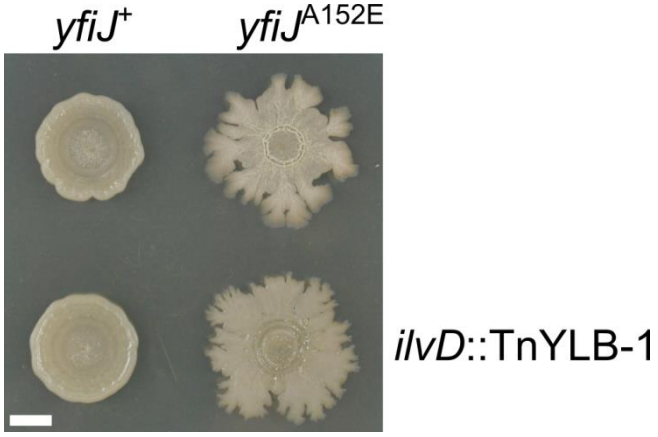

Figure A11. Disruption of *ilvD* affects *yfiJ*^{A152E} colony morphology

The *B. subtilis yfiJ*$^{+}$ colony (PDS0571) develops as a smooth colony but the *yfiJ*^{A152E} colony (PDS0572) forms a biofilm. Disruption of *ilvD* by the transposable element TnYLB-1 has no effect on *yfiJ*$^{+}$ colony morphology but results in the *yfiJ*^{A152E} colony edges becoming lobate and the colony center to become more mucoid. The photograph was taken after 48 h incubation on MYM agar. The photograph is representative of duplicate samples. Scale bar is 5 mm.

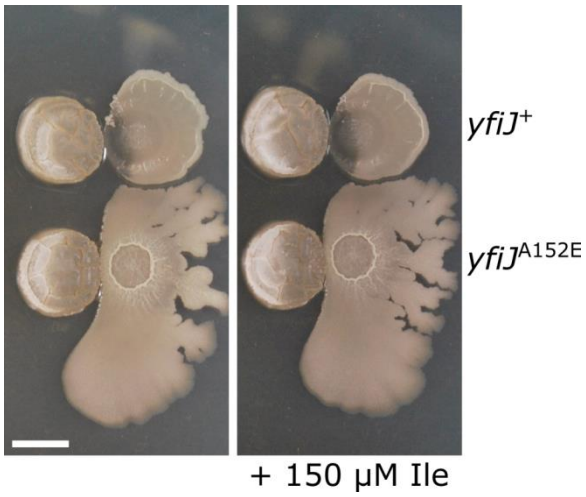

Figure A12. Isoleucine supplementation has no effect on linearmycin resistance or colony morphology

Wild type *S.* Mg1 (PDS0543) colonies (left) was co-spotted with *B. subtilis* colonies (right). The different genotypes of the *B. subtilis* colonies are labeled on the right. (*left*) Co-culture on media without isoleucine (Ile) supplementation. (*right*) Co-culture on media supplemented with 150 µM Ile. There are no visible differences between the two conditions. The photograph was taken after 72 h co-incubation on MYM agar. The photograph is representative of quadruplicate samples. Scale bar is 5 mm.

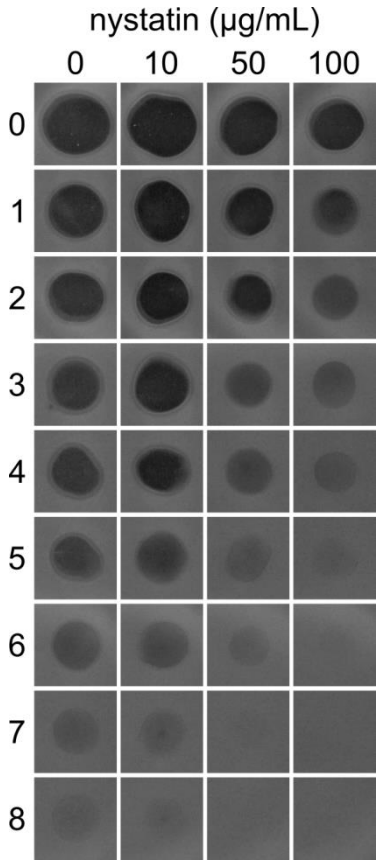

Figure A13. Preconditioning *B. subtilis* in increasing concentrations of nystatin enhances linearmycin resistance

Wild type *B. subtilis* (PDS0742) was preconditioned in 0, 10, 50, or 100 µg/mL nystatin then embedded in a soft agar overlay at equal cell density and spread over a MYM plate with the same concentration of nystatin. Two-fold serial dilutions of linearmycins were plated on top of the agar overlay. After 18 h incubation, the plates were photographed. As the preconditioned concentration of nystatin increases, *B. subtilis* becomes more resistant to subsequent nystatin exposure. The numbers on the left indicate the dilution factor [$(1/2)^n$] for each panel.

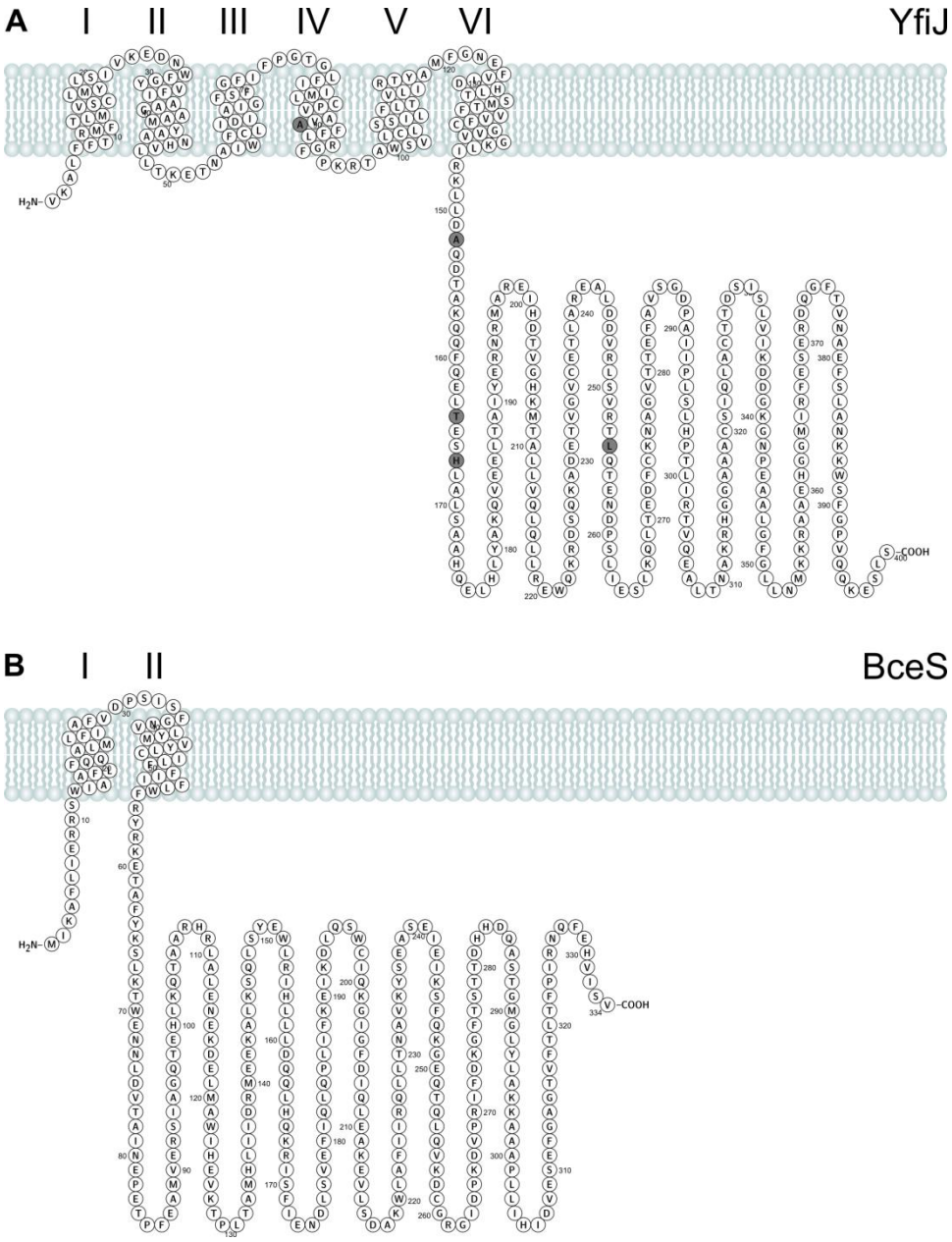

Figure A14. Predicted transmembrane topology for YfiJ and BceS

The transmembrane topologies for YfiJ **(A)** and BceS **(B)** were predicted using Protter (330). Residues changed in linearmycin resistant *B. subtilis* are shown in gray.

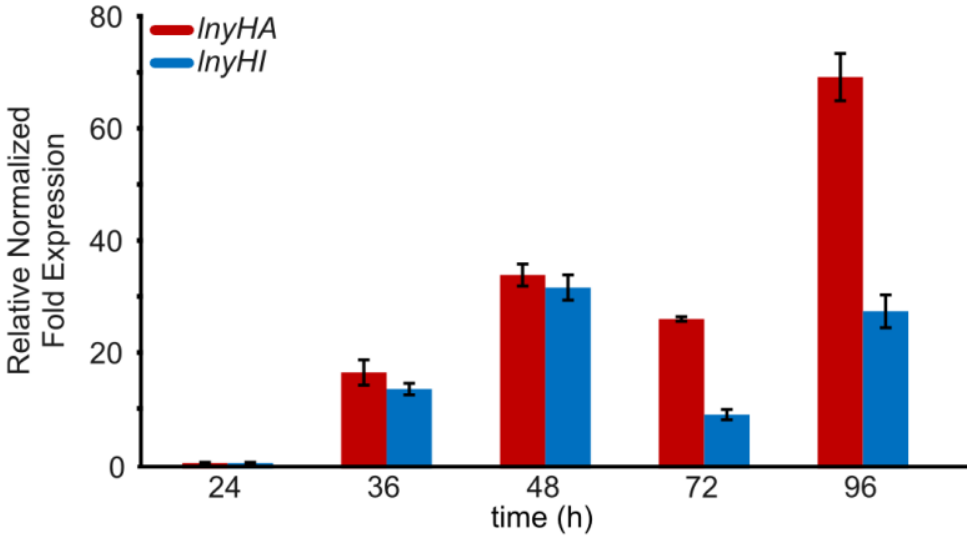

Figure A15. Expression of *lny* gene cluster during *S.* Mg1 growth normalized to *hrdB*

qRT-PCR was used to determine the relative fold expression in wild type *S.* Mg1 of the first (*lnyHA*) and last (*lnyHI*) PKS-encoding open-reading frame in the *lny* biosynthetic gene cluster. Expression was normalized to *hrdB*. The error bars represent the standard deviation of the fold difference.

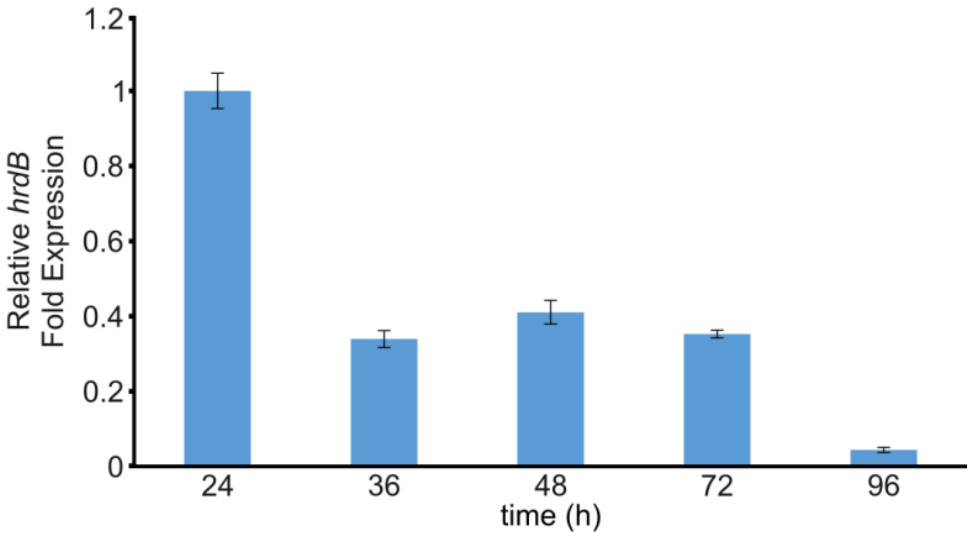

Figure A16. Expression of *hrdB* during *S.* Mg1 growth

qRT-PCR was used to determine the relative fold expression in wild type *S.* Mg1 of *hrdB*. The error bars represent the standard deviation of the fold difference.

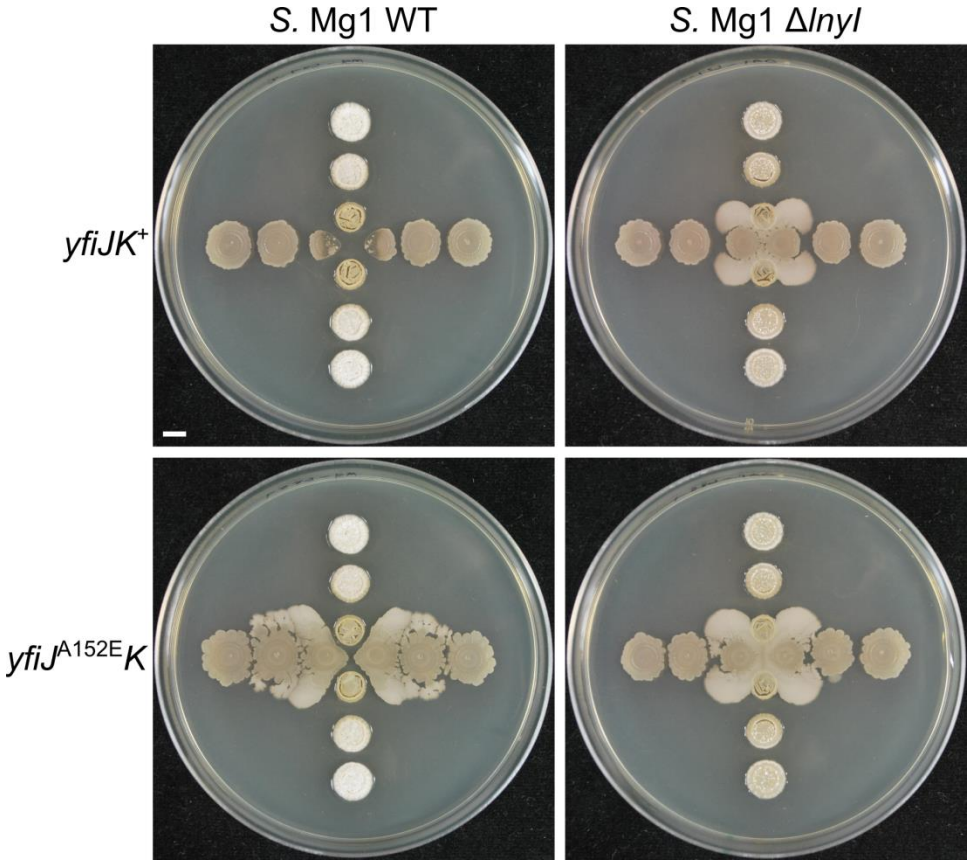

Figure A17. Linearmycins inhibit *B. subtilis* motility

Strains of *B. subtilis* (horizontal) were cross-plated with strains of *S.* Mg1 (vertical). The genotype of *B. subtilis* is indicated on the left and the genotype of *S.* Mg1 is indicated on the top. The *yfiJK*$^{+}$ strain of *B. subtilis* (PDS0627) is lysed by wild type (WT) *S.* Mg1 (PDS0543) but the *yfiJ*^{A152E}*K B. subtilis* strain (PDS0685) resists lysis and exhibits induced motility. If either *B. subtilis* strain is plated with the *S.* Mg1 linearmycin biosynthesis mutant Δ*lnyI* (PDS0755) then both strains are motile. Photographs were taken after 72 h co-incubation on GYM7 agar. Scale bar is 5 mm.

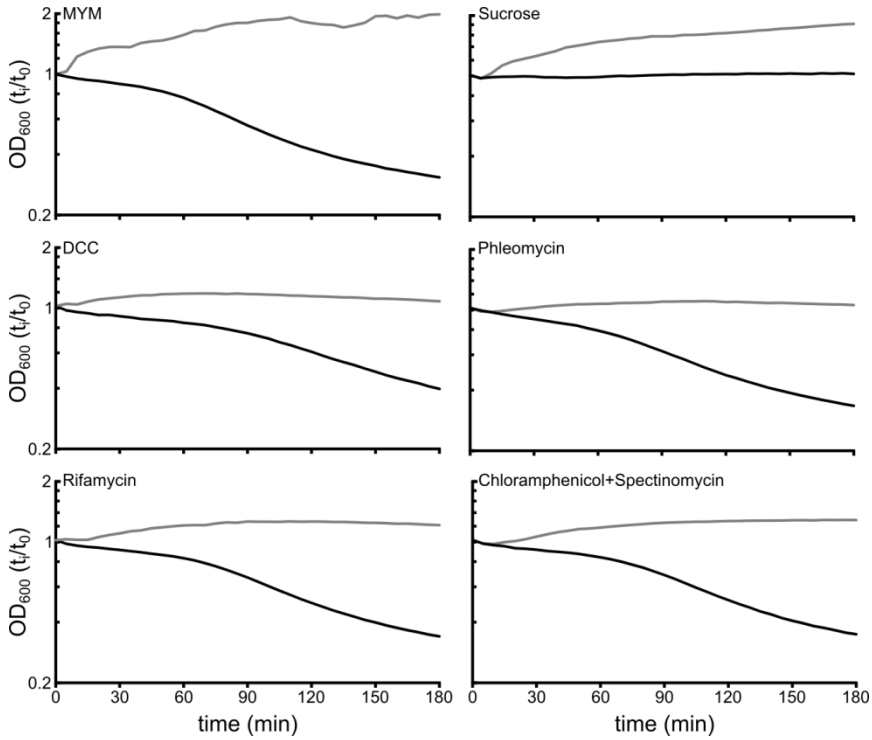

Figure A18. Lysis of *B. subtilis* by linearmycins occurs independent of major cellular pathways

Wild type *B. subtilis* (PDS0742) was grown in liquid MYM to OD_{600} = 1. The cells were washed and resuspended in MYM containing 0.25 M sucrose (osmoprotectant), 2.5 mM DCC (ATPase inhibitor), 200 µg/mL phleomycin (DNA replication inhibitor), 1 µg/mL rifamycin (transcription inhibitor), or 250 and 100 µg/mL chloramphenicol and spectinomycin (translation inhibitor), or plain MYM with and without linearmycins (400 units). The linearmycin treated samples (black lines) were lysed similarly, except with sucrose stabilization, whereas the control treated samples (gray lines) halted growth. The data points were sampled at 5 min intervals in a plate reader and the average of triplicates is reported here.

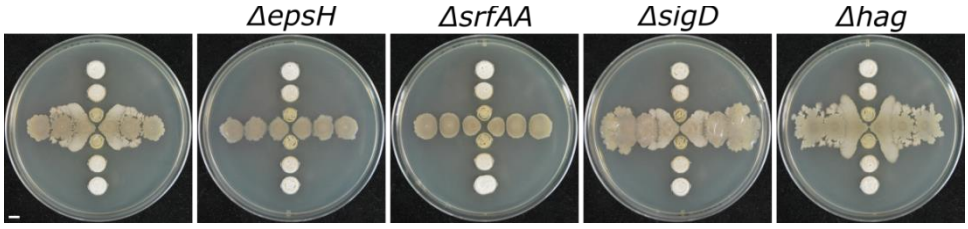

Figure A19. Linearmycin resistant *B. subtilis* motility is consistent with sliding

Linearmycin resistant *B. subtilis yfiJ*^{A152E}*K* (PDS0685, horizontal) was cross-plated with wild type *S.* Mg1 (PDS543, vertical). The genotype of *B. subtilis* is indicated on the top. The *yfiJ*^{A152E}*K* strains with deletions in *epsH* or *srfAA* are immotile whereas strains with deletions in *sigD* and *hag* are motile when cultured with *S.* Mg1. Photographs were taken after 72 h co-incubation on GYM7 agar. Scale bar is 5 mm.

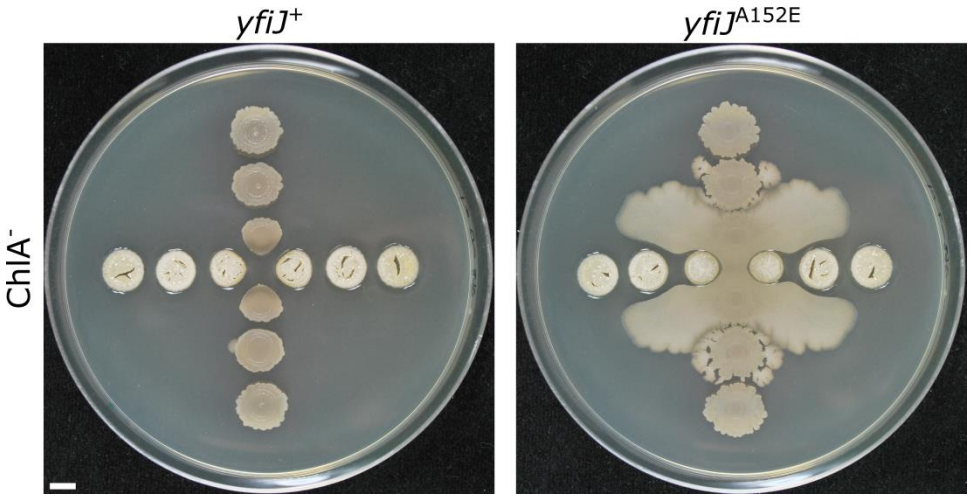

Figure A20. Chalcomycin is not required to induce motility of linearmycin resistant *B. subtilis*

Strains of *B. subtilis* (vertical) were cross-plated with chalcomycin biosynthesis deficient (ChlA$^-$) *S.* Mg1 (horizontal). The genotype of *B. subtilis* is indicated on the top. The *yfiJ*$^+$ (PDS0067) strain of *B. subtilis S.* Mg1 but the *yfiJ*^{A152E} *B. subtilis* strain (RM7) resists lysis and exhibits induced motility. Photographs were taken after 72 h co-incubation on GYM7 agar. Scale bar is 5 mm.

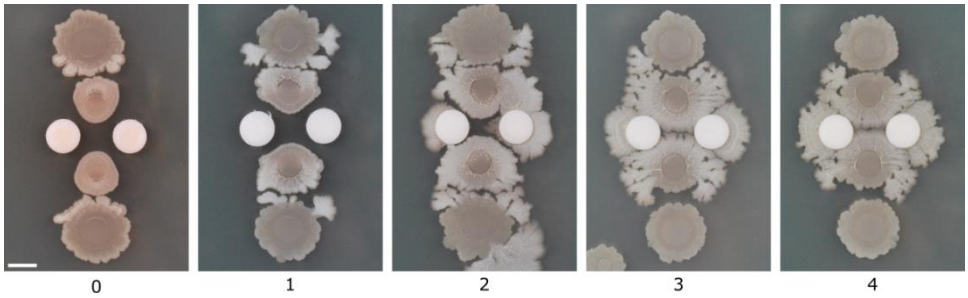

Figure A21. Motility inducing fraction extracted from *S.* Mg1

Wild type *B. subtilis* (PDS0742) was spotted vertically. Extracts from a *S.* Mg1 (PDS0543) culture were spotted onto the paper discs next to *B. subtilis*. The numbers below each panel indicate the dilution factor [$(1/2)^n$]. At lower dilutions the extract is inhibitory for *B. subtilis* growth. After two dilutions *B. subtilis* motility is induced by the extract. All photographs were taken after 72 h co-spotting on GYM7 agar. Scale bar is 5 mm.

Table A1. ^{13}C Chemical Shifts for Linearmycin B

C-No.	δ_C	C-No.	δ_C	C-No.	δ_C	C-No.	δ_C	C-No.	δ_C
33	212.07		132.40		75.13		45.83		24.27
1	174.78		132.09	39	71.12	18	45.11		24.18
	138.52		131.75	19	71.09	36	44.98	16-Me	18.55
	136.85		131.29	31	70.41	34	44.88	2-Me	10.91
	135.69		131.24	17	69.58	38	40.64	32-Me	10.26
	135.32		131.10	43	68.90	16	39.65	18-Me	9.25
	135.25		130.02		68.76	30	38.58		
	134.97		128.98		68.48		34.45		
40	133.62	41	128.91		67.75		32.68		
	133.56		128.75	37	66.86	42	31.91		
	133.22		126.72	35	65.49		31.39		
	132.93		126.65		63.83		29.91		
	132.86		126.38		63.65		29.13		
	132.80		125.06	32	51.86		28.82		
	132.74		125.01		48.70		28.47		

Spectra were collected in DMSO-d6 on a Bruker Avance 500 MHz spectrometer equipped with a cryoprobe. Chemical shifts (δ) are reported in ppm with reference to the residual solvent peak. Designated carbons are listed. The carbon number (C-No.) is with reference to the numbering in Figure A1B.

Table A2. Mutations in spontaneous LDA^{R} mutants not related to *yfiJK*

Gene	Nucleotide change	Effect	Annotation
fosB	G57T	none	bacillithiol-S-transferase, fosfomycin resistance protein
rnc	C299T	P100L	RNase III
nrdEB[*]	A622G	K208E	SPβ phage ribonucleoside-diphosphate reductase, alpha subunit
yodT[*]	C582T	none	putative aminovalerate aminotransferase
yozT[*]	A66G	none	unknown
ypzE[*]	A124G	K42E	unknown
nadD[†]	T392A	V131E	nicotinate-nucleotide adenylyltransferase
recJ[†]	C499T	A150V	single-strand DNA-specific exonuclease
tpx[†]	A209G	E70G	putative peroxiredoxin
yhgB[†]	32_33insG	frame shift	unknown
yopC[†]	*yopC*::TnYLB-1	disruption	unknown membrane protein

All numbering is with respect to the first amino acid or the first nucleotide of the start codon. [*]Mutations identified in the same spontaneous mutant. [†]Mutations identified in a transposon-mutagenized strain.

Table A3. Strains of *Bacillus subtilis* used in Chapter II

Strain	Genotype	Source
PDS0066	NCIB3610 undomesticated wild type strain	Laboratory collection
PDS0067	NCIB3610 Δ*pksX::spc*	Laboratory collection
PDS0121	NCIB3610 pMarA	Laboratory collection
PDS0312	PY79 wild type	Laboratory collection
PDS0540	PY79 pDR244	Laboratory collection
PDS0546	PY79 Δ*yfiJK::kn*	This study
PDS0547	NCIB3610 Δ*yfiJ::mls*	This study
PDS0548	NCIB3610 Δ*yopC::mls*	This study
PDS0553	NCIB3610 Δ*yfiK::mls*	This study
PDS0554	NCIB3610 Δ*yfiJK::kn*	This study
PDS0555	NCIB3610 Δ*yfiJ*	This study
PDS0556	NCIB3610 Δ*yfiK*	This study
PDS0559	168 Δ*yfiJ*	This study
PDS0562	168 Δ*yfiJ lacA::yfiJ* (*mls*)	This study
PDS0563	168 Δ*yfiJ lacA::yfiJ*^{A152E} (*mls*)	This study
PDS0564	168 Δ*yfiJ lacA::yfiJ*^{T164M} (*mls*)	This study
PDS0565	168 Δ*yfiJ lacA::yfiJ*^{H167Y} (*mls*)	This study
PDS0566	168 Δ*yfiJ lacA::yfiJ*^{A88V} (*mls*)	This study
PDS0567	168 Δ*yfiJ lacA::yfiJ*^{H201N} (*mls*)	This study
PDS0571	NCIB3610 Δ*yfiJ lacA::yfiJ* (*mls*)	This study
PDS0572	NCIB3610 Δ*yfiJ lacA::yfiJ*^{A152E} (*mls*)	This study
PDS0573	NCIB3610 Δ*yfiJ lacA::yfiJ*^{T164M} (*mls*)	This study
PDS0574	NCIB3610 Δ*yfiJ lacA::yfiJ*^{H167Y} (*mls*)	This study
PDS0575	NCIB3610 Δ*yfiJ lacA::yfiJ*^{A88V} (*mls*)	This study
PDS0576	NCIB3610 Δ*yfiJ lacA::yfiJ*^{H201N} (*mls*)	This study
PDS0594	168 Δ*yfiJ lacA::yfiJ*$^{A152E, H201N}$ (*mls*)	This study
PDS0604	NCIB3610 Δ*yfiJ lacA::yfiJ*$^{A152E, H201N}$ (*mls*)	This study
PDS0608	NCIB3610 Δ*yfiJ* Δ*epsH::kn lacA::yfiJ*^{A152E} (*mls*)	This study
PDS0623	PY79 Δ*yfiJK::kn amyE::yfiJK* (*spc*)	This study
PDS0624	PY79 Δ*yfiJK::kn amyE::yfiJK*^{T83I} (*spc*)	This study
PDS0625	PY79 Δ*yfiJK::kn amyE::yfiJK*^{D54A} (*spc*)	This study
PDS0626	PY79 Δ*yfiJK::kn amyE::yfiJK*$^{D54A, T83I}$ (*spc*)	This study
PDS0627	NCIB3610 Δ*yfiJK::kn amyE::yfiJK (spc)*	This study
PDS0628	NCIB3610 Δ*yfiJK::kn amyE::yfiJK*^{T83I} *(spc)*	This study
PDS0629	NCIB3610 Δ*yfiJK::kn amyE::yfiJK*^{D54A} *(spc)*	This study
PDS0630	NCIB3610 Δ*yfiJK::kn amyE::yfiJK*$^{D54A, T83I}$ *(spc)*	This study

PDS0652	PY79 Δ*yfiJKLMN::kn*	This study
PDS0653	NCIB3610 Δ*yfiJKLMN::kn*	This study
PDS0658	NCIB3610 Δ*yfiJKLMN::kn amyE::yfiJK (spc)*	This study
PDS0660	NCIB3610 Δ*yfiJKLMN::kn amyE::yfiJK*^{T83I} *(spc)*	This study
PDS0685	NCIB3610 Δ*yfiJK::kn amyE::*yfiJ^{A152E}*K (spc)*	This study
PDS0686	NCIB3610 Δ*yfiJKLMN::kn amyE::yfiJ*^{A152E}*K (spc)*	This study
PDS0687	NCIB3610 Δ*yfiJKLMN::kn lacA::yfiLMN (mls)*	This study
PDS0688	NCIB3610 Δ*yfiJKLMN::kn amyE::yfiJK (spc) lacA::yfiLMN (mls)*	This study
PDS0689	NCIB3610 Δ*yfiJKLMN::kn amyE::yfiJ*^{A152E}*K (spc) lacA::yfiLMN (mls)*	This study
PDS0690	NCIB3610 Δ*yfiJKLMN::kn amyE::yfiJK*^{T83I} *(spc) lacA::yfiLMN (mls)*	This study
PDS0691	PY79 Δ*yfiJKLMN::kn lacA::yfiLMN (mls)*	This study
PDS0717	PY79 Δ*yfiJKLMN::kn yhdG::*P$_{spac(c)}$*yfiLMN (cm)*	This study
PDS0718	NCIB3610 Δ*yfiJKLMN::kn yhdG::*P$_{spac(c)}$*yfiLMN (cm)*	This study
PDS0719	NCIB3610 Δ*yfiJKLMN::kn amyE::yfiJK (spc) yhdG::*P$_{spac(c)}$*yfiLMN (cm)*	This study
PDS0720	NCIB3610 Δ*yfiJKLMN::kn amyE::yfiJ*^{152E}*K (spc) yhdG::*P$_{spac(c)}$*yfiLMN (cm)*	This study
PDS0721	NCIB3610 Δ*yfiJKLMN::kn amyE::yfiJK*^{T83I} *(spc) yhdG::*P$_{spac(c)}$*yfiLMN (cm)*	This study
PDS0731	NCIB3610 Δ*yfiJ* Δ*epsH::kn lacA::yfiJ (mls)*	This study
PDS0732	NCIB3610 Δ*yfiJ* Δ*sinR::spc lacA::yfiJ (mls)*	This study
PDS0733	NCIB3610 Δ*yfiJ* Δ*sigD::tet lacA::yfiJ (mls)*	This study
PDS0734	NCIB3610 Δ*yfiJ* Δ*degU::tet lacA::yfiJ (mls)*	This study
PDS0735	NCIB3610 Δ*yfiJ* Δ*sinR::spc lacA::yfiJ*A^{152E} *(mls)*	This study
PDS0736	NCIB3610 Δ*yfiJ* Δ*sigD::tet lacA::yfiJ*A^{152E} *(mls)*	This study
PDS0737	NCIB3610 Δ*yfiJ* Δ*degU::tet lacA::yfiJ*A^{152E} *(mls)*	This study
PDS0738	NCIB3610 Δ*yfiJ lacA::yfiJ*^{L254P} (*mls*)	This study
PDS0739	NCIB3610 Δ*yfiJK::kn amyE::yfiJ*^{A152E}*K*^{D54A} *(spc)*	This study
PDS0740	NCIB3610 Δ*yfiJK::kn amyE::yfiJ*^{H201N}*K*^{T83I} *(spc)*	This study
PDS0785	NCIB3610 Δ*iseA::mls*	This study
BKE18380	168 Δ*iseA::mls*	*Bacillus* Genetic Stock Center
BKE20940	168 Δ*yopC::mls*	*Bacillus* Genetic Stock Center
BKE08290	168 Δ*yfiJ::mls*	*Bacillus* Genetic Stock Center
BKE08300	168 Δ*yfiK::mls*	*Bacillus* Genetic Stock Center
DL598	NCIB3610 Δ*skfABCDEFGH::cm*	R. Kolter Laboratory
DS323	NCIB3610 Δ*sigD::tet*	D. Kearns Laboratory
DS2483	NCIB3610 Δ*lytABC::kn* Δ*lytD::mls* Δ*lytF::tet*	D. Kearns Laboratory

Table A4. Primers used in Chapter II

Primer	Sequence (5′ - 3′)
kn-Fwd	CAGCGAACCATTTGAGGTGATAGG
kn-Rev	CGATACAAATTCCTCGTAGGCGCTCGG
13	GGCAGGAAATCAAAGCGCTC
14	GCGCCTACGAGGAATTTGTATCGCCATCAAGGTGAACATTCTCGT
15	CCTATCACCTCAAATGGTTCGCTGAGAACCCAAGCCGCCATTTA
16	TTTCATTGCCGTCCCTCCTC
25	CCATGGATCCATTGATGCAGGGATCGAGGG
26	TCATGAATTCGATGCCAGCCCTTCTCTGAC
42	GGCGCGTGAAATCAATGATACAGTGGGG
43	CCCCACTGTATCATTGATTTCACGCGCC
50	GGATATCGTGTTAATGGCCATCCGCATGCCGGTTTC
51	GAAACCGGCATGCGGATGGCCATTAACACGATATCC
54	GCGACCGGCGCTCAGGATCCATTGATGCAGGGATCGAGGG
59	CCCTCGATCCCTGCATCAATGGATCCTGAGCGCCGGTCGC
74	TATGTTCTATCTGCCGCTACGAATTCCTGCAGCCCTGGCG
75	GTAGCGGCAGATAGAACATA
76	GGCCGCCCGCGGTAGGATCCTTGTAAGGCGGCGCTTGAAG
77	CCTACGAGGAATTTGTATCGGCTCATCACTCCCGATACCC
78	TCACCTCAAATGGTTCGCTGAAAACATCTGCCGTTTAGGC
79	CCCGGGGAGCTCATGAATTCACGACAGGATTATGTACTGACTC
112	ATGCGAATTCTACACAGCCCAGTC
113	ATGCACTAGTAACCGGATTCCACACATTATGCCAC
118	ACTAGTAACCGGATTCCACA
119	GGATCCCATACGGCAATAGT
120	TGTGGAATCCGGTTACTAGTAGGAGTGAGACGACGTGCTG
121	ACTATTGCCGTATGGGATCCTTAGGCTCGGAGCGCTTTCA
q1: *yfiL*-F	AAGCGTTTCTTGTGGCGATC
q2: *yfiL*-R	TGATGAGCCGCAGAAATGTC
gyrB-F	GGGCAACTCAGAAGCACGGACG
gyrB-R	GCCATTCTTGCTCTTGCCGCC

Table A5. Strains of *Bacillus subtilis* used in Chapter III

Strain	Genotype	Source
BKE08310	168 Δ*yfiL*::*mls*	*Bacillus* Genetic Stock Center
BKE08320	168 Δ*yfiM*::*mls*	*Bacillus* Genetic Stock Center
BKE08330	168 Δ*yfiN*::*mls*	*Bacillus* Genetic Stock Center
BKE14490	168 Δ*kinC*::*mls*	*Bacillus* Genetic Stock Center
DS7817	NCIB3610 Δ*comI*	W. Winkler
PDS0555	NCIB3610 Δ*yfiJ*	(248)
PDS0559	168 Δ*yfiJ*	(248)
PDS0562	168 Δ*yfiJ lacA*::*yfiJ*$^{+}$ (*mls*)	(248)
PDS0563	168 Δ*yfiJ lacA*::*yfiJ*^{A152E} (*mls*)	(248)
PDS0571	NCIB3610 Δ*yfiJ lacA*::*yfiJ*$^{+}$ (*mls*)	(248)
PDS0572	NCIB3610 Δ*yfiJ lacA*::*yfiJ*^{A152E} (*mls*)	(248)
PDS0627	NCIB3610 Δ*yfiJK*::*kn amyE*::*yfiJK*$^{+}$ (*spc*)	(248)
PDS0685	NCIB3610 Δ*yfiJK*::*kn amyE*::*yfiJ*^{A152E}*K* (*spc*)	(248)
PDS0742	NCIB3610 undomesticated wild type strain	Laboratory Collection
PDS0788	NCIB3610 Δ*yfiJ* Δ*yfiL*::*mls*	This Study
PDS0789	NCIB3610 Δ*yfiJ* Δ*yfiL*	This Study
PDS0790	NCIB3610 Δ*yfiJ* Δ*yfiL lacA*::*yfiJ*$^{+}$ (*mls*)	This Study
PDS0791	NCIB3610 Δ*yfiJ* Δ*yfiL lacA*::*yfiJ*^{A152E} (*mls*)	This Study
PDS0795	168 Δ*yfiJ* Δ*yfiLMN*::*mls*	This Study
PDS0796	NCIB3610 Δ*yfiJ* Δ*yfiLMN*::*mls*	This Study
PDS0797	NCIB3610 Δ*yfiJ* Δ*yfiLMN*	This Study
PDS0798	NCIB3610 Δ*yfiJ* Δ*yfiLMN lacA*::*yfiJ*$^{+}$ (*mls*)	This Study
PDS0799	NCIB3610 Δ*yfiJ* Δ*yfiLMN lacA*::*yfiJ*^{A152E} (*mls*)	This Study
PDS0801	NCIB3610 Δ*yfiJ* Δ*yfiLMN lacA*::*yfiJ*$^{+}$ (*mls*) *yhdG*::$P_{spac(c)}$-*yfiLMN* (*cm*)	This Study
PDS0802	NCIB3610 Δ*yfiJ* Δ*yfiLMN lacA*::*yfiJ*^{A152E} (*mls*) *yhdG*::$P_{spac(c)}$-*yfiLMN* (*cm*)	This Study
PDS0810	168 Δ*yfiJ* Δ*yfiM*::*mls*	This Study
PDS0811	168 Δ*yfiJ* Δ*yfiN*::*mls*	This Study
PDS0812	NCIB3610 Δ*yfiJ* Δ*yfiM*::*mls*	This Study
PDS0813	NCIB3610 Δ*yfiJ* Δ*yfiN*::*mls*	This Study
PDS0814	NCIB3610 Δ*yfiJ* Δ*yfiM*	This Study
PDS0815	NCIB3610 Δ*yfiJ* Δ*yfiN*	This Study
PDS0816	NCIB3610 Δ*yfiJ* Δ*yfiM lacA*::*yfiJ*$^{+}$ (*mls*)	This Study
PDS0817	NCIB3610 Δ*yfiJ* Δ*yfiM lacA*::*yfiJ*^{A152E} (*mls*)	This Study
PDS0818	NCIB3610 Δ*yfiJ* Δ*yfiN lacA*::*yfiJ*$^{+}$ (*mls*)	This Study
PDS0819	NCIB3610 Δ*yfiJ* Δ*yfiN lacA*::*yfiJ*^{A152E} (*mls*)	This Study
PDS0838	NCIB3610 *amyE*::P_{yfiLMN}-RBS_{spoVG}-*lacZ* (*cm*) Δ*comI*	This Study
PDS0840	NCIB3610 Δ*yfiJ lacA*::*yfiJ*$^{+}$ (*mls*) *amyE*::P_{yfiLMN}-RBS_{spoVG}-*lacZ* (*cm*)	This Study

PDS0841	NCIB3610 Δ*yfiJ lacA*::*yfiJ*^{A152E} (*mls*) *amyE*::P$_{yfiLMN}$-RBS$_{spoVG}$-*lacZ* (*cm*)	This Study
PDS0842	NCIB3610 Δ*yfiJ* Δ*yfiLMN lacA*::*yfiJ*$^{+}$ (*mls*) *amyE*::P$_{yfiLMN}$-RBS$_{spoVG}$-*lacZ* (*cm*) (cm)	This Study
PDS0843	NCIB3610 Δ*yfiJ* Δ*yfiLMN lacA*::*yfiJ*^{A152E} (mls) *amyE*::P$_{yfiLMN}$-RBS$_{spoVG}$-*lacZ* (*cm*)	This Study
PDS0909	NCIB3610 Δ*yfiJ amyE*::P$_{yfiLMN}$-RBS$_{spoVG}$-*lacZ* (*cm*)	This Study
PDS0910	168 Δ*yfiJ lacA*::*yfiJ*$^{\Delta TMD}$ (*mls*)	This Study
PDS0911	168 ΔyfiJ *lacA*::*yfiJ*$^{\Delta TMD,\ A152E}$ (*mls*)	This Study
PDS0912	NCIB3610 Δ*yfiJ lacA*::*yfiJ*$^{\Delta TMD}$ (*mls*) *amyE*::P$_{yfiLMN}$-RBS$_{spoVG}$-*lacZ* (*cm*)	This Study
PDS0913	NCIB3610 Δ*yfiJ lacA*::*yfiJ*$^{\Delta TMD,\ A152E}$ (*mls*) *amyE*::P$_{yfiLMN}$-RBS$_{spoVG}$-*lacZ* (*cm*)	This Study
PDS0914	NCIB3610 Δ*yfiJ* Δ*kinC lacA*::*yfiJ*$^{+}$ (*mls*)	This Study
PDS0915	NCIB3610 Δ*yfiJ* Δ*kinC lacA*::*yfiJ*^{A152E} (*mls*)	This Study
PDS0916	NCIB3610 Δ*yfiJ* Δ*kinC*	This Study
PDS0917	PY79 *amyE*::P$_{bceA}$-RBS$_{spoVG}$-*lacZ* (*cm*)	This Study
PDS0918	NCIB 3610 Δ*yfiJ amyE*::P$_{bceA}$-RBS$_{spoVG}$-*lacZ* (*cm*)	This Study
PDS0919	168 ΔyfiJ *lacA*::*yfiJ*^{TMD}-*bceS*^{cyto} (*mls*)	This Study
PDS0920	NCIB3610 Δ*yfiJ lacA*::*yfiJ*^{TMD}-*bceS*^{cyto} (*mls*) *amyE*::P$_{bceA}$-RBS$_{spoVG}$-*lacZ* (*cm*) (cm)	This Study

Table A6. Primers used in Chapter III

Primer	Sequence (5′ - 3′)
Degen3	TAGAGTTATTAATGGAATTGCTGATNNNNNNNNNNN
oIPCR-1	GCTTGTAAATTCTATCATAATTG
oIPCR-2	AGGGAATCATTTGAAGGTTGG
oIPCR-3	GCATTTAATACTAGCGACGCC
11	AGGCAGCACTTGGTTTTGGT
26	TCATGAATTCGATGCCAGCCCTTCTCTGAC
46	GGCCGCCCGCGGTAGGATCCATTGATGCAGGGATCGAGGG
60	GCATCCAACAGCTTGCGCATGCTCATCACTCCCGATACCC
62	ATGCGCAAGCTGTTGGATGC
75	GTAGCGGCAGATAGAACATA
79	CCCGGGGAGCTCATGAATTCACGACAGGATTATGTACTGACTC
81	AGCACAGCCAGATTTACCCT
92	CGCAAGCTGTTGGATGAGCAGGATACGGCAAAAC
93	GTTTTGCCGTATCCTGCTCATCCAACAGCTTGCG
153	TATGTTCTATCTGCCGCTACGCAGGCGAGAAAGGAGAG
154	CGAGGCTCCTGTCACTGC
155	GCAGTGACAGGAGCCTCGAAAACATCTGCCGTTTAGGC
173	ATGCAAGCTTTTTTTTGATCCATTGCCATTG
174	ATGCGAATTCAGAACCCAAGCCGCCATTTA
175	GGCCGCCCGCGGTAGGATCCATTGATGCAGGGATCGAGGG
176	GATTAATTTGCCCACGACACC
177	GTGTCGTGGGCAAATTAATCCGCTATCGGAAAGAAACAGC
178	CCCGGGGAGCTCATGAATTCTCACACGCTTATGACATGTTC
180	ATGCGAATTCGAACATGTCATAAGCGTGTG
181	ATGCAAGCTTTATCGATGCCCTTCAGCACTTCC

Table A7. qRT-PCR primers used in Chapter III

Primer	Sequence (5′ - 3′)
q1: *yfiL*-F	AAGCGTTTCTTGTGGCGATC
q2: *yfiL*-R	TGATGAGCCGCAGAAATGTC
q7: *des*-F	TGGTGCAAGGCCCGATATTT
q8: *des*-R	GCCTGAACGTAGCTCCAGTT
q11: *yvfS*-F	TTCTGTTCGGCGCAATCATC
q12: *yvfS*-R	GCGCCAAACAAAATCCACAG
gyrB-F	GAAGGATTGGAAGCTGTTCG
gyrB-R	GCGAGGGCTTCGTCAATACT

Table A8. qRT-PCR primers used in Chapter IV

Primer	Sequence (5′ - 3′)
q21: *lnyHA*-F	GTGCCTTCGTACCCGTCATG
q22: *lnyHA*-R	TGCGACCAGTTCACCTTCAG
q23: *lnyHI*-F	CCTCGTCGACATCTACTCGC
q24: *lnyHI*-R	AGTCGAAGAACTGCTCCTGC
q27: *hrdB*-F	CTGGCCAAGGAACTCGACAT
q28: *hrdB*-R	CTGGAGGAGGGTGAAGGAGA